ITORIAL STAFF
IL V. KING, *Editor*
RMAN HACKERMAN, *Technical Editor*
TH G. STERNS, *Managing Editor*
B. THOMAS, *News Editor*
TALIE MICHALSKI, *Assistant Editor*
ANOR BLAIR, *Assistant Editor*

VISIONAL EDITORS
C. VOSBURGH, *Battery*
E. DRALEY, *Corrosion*
N J. CHAPMAN, *Electric Insulation*
NER BRENNER, *Electrodeposition*
C. FROELICH, *Electronics*
H. BAIRD, *Electronics—Semiconductors*
ERLOCK SWANN, JR., *Electro-Organic*
N M. BLOCHER, JR., *Electrothermics and Metallurgy, I*
U. SEYBOLT, *Electrothermics and Metallurgy, II*
C. GARDINER, *Industrial Electrolytic*
W. TOBIAS, *Theoretical*

EGIONAL EDITORS
OWARD T. FRANCIS, *Chicago*
SEPH SCHULEIN, *Pacific Northwest*
C. SCHUMACHER, *Los Angeles*
W. HEISE, *Cleveland*
H. FETTERLEY, *Niagara Falls*
IVER OSBORN, *Houston*
ARL A. GULBRANSEN, *Pittsburgh*
C. HOLM, *Canada*
W. CUTHBERTSON, *Great Britain*
L. RAMA CHAR, *India*

DVERTISING OFFICE
ACK BAIN, *Advertising Manager*
5 Fifth Avenue, New York 17, N. Y.

CS OFFICERS
ANS THURNAUER, *President*
Minnesota Mining & Mfg. Co., St. Paul, Minn.
ORMAN HACKERMAN, *Vice-President*
University of Texas, Austin, Texas
HERLOCK SWANN, JR., *Vice-President*
University of Illinois, Urbana, Ill.
. C. GARDINER, *Vice-President*
Olin Mathieson Chemical Corp., Niagara Falls, N. Y.
YLE I. GILBERTSON, *Treasurer*
Air Reduction Co., Murray Hill, N. J.
ENRY B. LINFORD, *Secretary*
Columbia University, New York, N. Y.

Journal of the
Electrochemical Society

MARCH 1957 VOL. 104 · NO. 3

CONTENTS

Editorial

The Future of Mankind 50C

Technical Papers

Supercooling, Preferred Orientation, and Inverse Segregation in Lead-Antimony Alloys. *A. C. Simon and E. L. Jones* .. 133

The Question of Space Charge in Anodic Ta_2O_5 Films. *D. A. Vermilyea* 140

Low-Pressure Solubility and Diffusion of Hydrogen in Zirconium. *M. W. Mallett and W. M. Albrecht* 142

Mechanisms of Aqueous Corrosion of Aluminum at 100°C. *K. M. Carlsen* 147

Rates of Oxidation of Germanium. *J. T. Law and P. S. Meigs* 154

Electrolytic Reduction of Cyanamide. *K. Odo and K. Sugino* . 160

The Voltage of Sodium Chlorate Cells. *V. de Valera* 162

Influence of Impurities in the Electrolyte in Chlorine-Caustic Electrolysis by the Mercury Cell Process, VI. Investigation of the Influence of Graphite Particles on Amalgam Decomposition and Cathodic Current Efficiency. *G. Angel, R. Brännland, and S. Dahlerus* 167

Streaming Potential in Spherical-Grain Sands. *W. Schriever and C. E. Bleil* 170

The Galvani Electrode Potential. *P. Rüetschi* 176

Hydrogen Evolution Reaction on Copper, Gold, Molybdenum, Palladium, Rhodium, and Iron. Mechanism and Measurement Technique under High Purity Conditions. *N. Pentland, J. O'M. Bockris, and E. Sheldon* 182

Kinetics of Silver-Silver Ion Exchange. *C. V. King and Ann-Mari Simonsen* 194

Current Affairs

Complete Washington Meeting Program 53C

Division News 78C
Section News 78C
New Members 80C
Personals 81C
News Items 81C
Book Reviews 84C
Announcements from Publishers 86C
Employment Situations ... 86C

Published monthly by The Electrochemical Society, Inc., Mount Royal and Guilford Aves., Baltimore 2, Md., combining the JOURNAL and TRANSACTIONS OF THE ELECTROCHEMICAL SOCIETY. Editorial offices: 216 West 102nd Street, New York 25, N. Y. Statements and opinions given in articles and papers in the JOURNAL OF THE ELECTROCHEMICAL SOCIETY are those of the contributors, and The Electrochemical Society assumes no responsibility for them. Nondeductible subscription to members $5.00; subscription to nonmembers $18.00. Single copies $1.25 to members, $1.75 to nonmembers. Copyright 1957 by The Electrochemical Society, Inc. Entered as second-class matter. November 15, 1947, at the Post Office at Baltimore, Md., under the act of August 24, 1912.

Editorial

The Future of Mankind

MAN-LIKE CREATURES roamed the earth 20 million years ago, and by the year 300,000 B.C. some tribes of man had attained a considerable degree of civilization and culture, as evidenced by relics and works of art which have been found in European caves. Barring the man-made catastrophe of a nuclear war which would make human life impossible because of radioactive residues, there is every reason to believe that man will exist on the earth for many more millions of years. Two outstanding books of prediction have appeared in recent years: "The Next Million Years" by Charles G. Darwin and "The Foreseeable Future" by Sir George Thomson. Darwin speaks of a million years because normally that is long enough to create a new species, i.e., *Homo Sapiens* might acquire a new second name. Sir George points out the directions in which modern technology and research seem to lead, discussing the limitations imposed by known laws of Nature. He refuses to be drawn into the prediction of new physical principles.

The present era is one of truly frantic struggle to increase the distributional entropy of all materials on the earth for which man can find any use. What will man's status be, say 100,000 years from now? His appearance and intelligence will change somewhat, but not drastically. It is safe to say that he will have searched out and destroyed or scattered all the coal, oil, natural gas, concentrated deposits of ores and minerals, including uranium and thorium. Will he then of necessity revert to a primarily agricultural economy, with very limited means of transportation, materials of construction, or goods for comfort and luxury?

The answer depends largely on the discovery and development of new sources of power, and on the economical use of energy. With abundant energy, ingenuity, and a high degree of automation, metals and chemicals can be extracted from sources of low concentration: aluminum from almost any earth, iron from red clay or shale. The oceans contain 1.5×10^8 tons of copper, at a concentration of 1 part in 10^{10}; the theoretical minimum energy of extraction is only a few hundred kwhr per ton. Man 100,000 years hence will have to concentrate his materials from such sources. He will most likely not wear a few ounces from a 3000-lb machine, then let the rest disintegrate in a dump. Further, many present industrial methods would seem like burning down the house to roast the pig.

With abundant energy, hydrocarbons for fuels and organics can be made from carbon dioxide secured from the air or carbonate rocks, and water. A great break-through in the energy problem may be in the control of nuclear fusion reactions. It is possible, but hardly probable, that atomic fuels and other materials will be imported from other parts of the solar system or of the universe. The heat of the earth's interior may be tapped, perhaps useful minerals discovered, by deep borings. It has been estimated[1] that, even now, the cost of drilling a slanting hole to a vertical depth of 10 miles would not be out of line with the cost of certain other exploratory endeavors.

The population which the earth can support in any era will depend on the relative attention paid to the problems of food and of material possessions and comforts. If man does not limit his numbers voluntarily, sporadic famine and catastrophe will.

In the past, man's cruelty to man has known no bounds. This may be an inheritance from the days when a man-creature of another clan was both a dangerous enemy and just another animal to be killed and eaten if possible. Until recent times torture and death were important religious rites, often accompanied by cannibalism. Today, torture and death are still common political and police rites in a large part of the world. The long-range tendency seems to be toward abolishment of cruelty, both private and official, but recurrence of barbarism is all too frequent and violent. There is reason and hope to believe that barbaric practices will be abandoned before the hypothetical year 101,957.

—CVK

[1] *Science*, October 12, 1956.

Plating Electrotype Shells

Plating Stereotypes

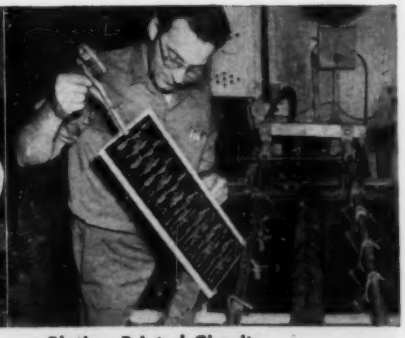

Plating Printed Circuits

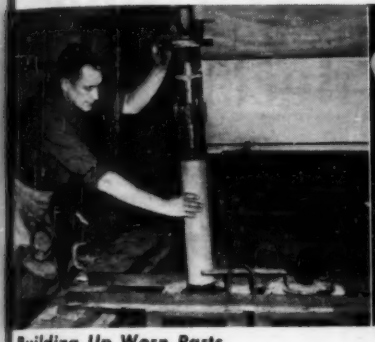

Building Up Worn Parts

Plating Versatile Lead-Tin Alloys

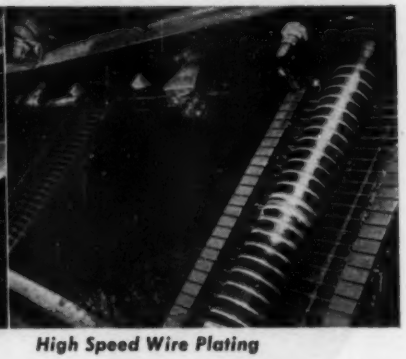

High Speed Wire Plating

You can electroplate 10 ways better

with B&A FLUOBORATE Plating Solutions

LEAD
TIN
IRON
COPPER
NICKEL
CADMIUM
INDIUM

1. No mixing or dissolving necessary . . . supplied in concentrated solution form
2. Easier bath preparation
3. Stability of bath composition
4. Ease of control
5. Practically 100% anode and cathode efficiencies
6. High conductivity
7. Good covering power
8. Fine-grained deposits of good color
9. Faster, high-speed operation
10. Readily adaptable for alloy deposits: lead-tin and lead-tin-copper alloys

FINE CHEMICALS
B&A
STANDARD OF PURITY
REAGENTS

AND MANY MORE ADVANTAGES . . .

. . . enabling you to increase production . . . lower your operating costs . . . get easier, simpler operations. In addition to the advantages listed, each fluoborate bath offers a number of special advantages for its particular applications.

Here is the *modern* way to electroplate. Mail the coupon now for complete information.

JE-3

BAKER & ADAMSON® *Fine Chemicals*
GENERAL CHEMICAL DIVISION
ALLIED CHEMICAL & DYE CORPORATION
40 Rector Street, New York 6, N. Y.

Please send me, without cost or obligation, complete technical data on the use of fluoborate solutions for the following plating applications

_____

Name_____

Title_____

Company_____

Address_____

City_____ Zone____ State_____

SARGENT POLAROGRAPH

Trademark Reg. U.S. Pat. Off.

MODEL XXI Visible Chart Recording

Indispensable Chemical Facility

Many Uses . . . Many Users

In 1937, eleven Polarographs were known to be located in the United States. Today there are many hundreds of Sargent Polarographs in use—employed for a wide variety of purposes.

From Australia to Sweden, and all over America, Sargent Polarographs are constantly at work for the progress of science.

Dozens of users have more than one Sargent Polarograph working for them. One industrial firm alone has already obtained sixteen.

Of the hundred universities, colleges and research institutes employing Sargent Polarographs, one operates seven and over twenty universities use two or more. The United States Government has already placed more than forty in service.

The Sargent Polarograph's uses are varied and many . . . . . .

1. For the routine analysis of non-ferrous alloys and ores when determining minor constituents including copper, lead, cadmium, zinc, manganese, iron and cobalt.
2. For the routine determination of lead, copper, nickel, manganese and cobalt in ferrous alloys.
3. For the analytical control of plating baths, notably in the field of precious metals.
4. For trace metal measurements in food products, in body fluids and in petroleum products.
5. For the analysis of source materials and processed products for a variety of hormones and vitamins.
6. For the identification and estimation of numerous substances of nutritional and biological regulatory function, supporting or replacing biological assay.
7. For the determination of halides and sulfate groups by titration with a polarized electrode.
8. For the analytical measurement of innumerable organic compounds containing reducible groups.
9. For specific industrial controls such as the estimation of aldehydes in alcoholic products, the quantitative differentiation of sugars and the control of aging quality in sugars.
10. For the measurement of dissolved oxygen, oxygen demand and metal ions in water and sewage.
11. For many uncommon analyses for which classical procedures are unavailable, less accurate and slower.
12. For the investigation and control of commercial reduction processes.
13. For thermodynamic investigations relating to states of ionic aggregations, mobilities and diffusion rates, solubilities, reaction rates and equilibrium constants.

For a complete description of the Sargent Polarograph Model XXI, write today.

S-29303 POLAROGRAPH—Model XXI Visible Chart Recording, Sargent. For operation from 115 Volt 50/60 cycle circuits.....**$2275.00**

SARGENT

SCIENTIFIC LABORATORY INSTRUMENTS • APPARATUS • SUPPLIES • CHEMICALS

Catalog No. 100 Now Available

E. H. SARGENT & COMPANY, 4647 W. FOSTER AVE., CHICAGO 30, ILLINOIS
MICHIGAN DIVISION, 8560 WEST CHICAGO AVENUE, DETROIT 4, MICHIGAN
SOUTHWESTERN DIVISION, 5915 PEELER STREET, DALLAS 35, TEXAS
SOUTHEASTERN DIVISION, 3125 SEVENTH AVE., N., BIRMINGHAM 4, ALA.

Supercooling, Preferred Orientation, and Inverse Segregation in Lead-Antimony Alloys

A. C. Simon and E. L. Jones

Naval Research Laboratory, Washington, D. C.

ABSTRACT

Experiments are described which confirm the previously reported inverse segregation of Sb in the Pb-Sb alloy castings. Supercooling of Sb at eutectic temperatures and a preferred orientation and growth direction for the Sb crystals are responsible for the excessively large coverage by Sb in the surface of the cast alloy. Interdendritic flow, previously claimed as a principal factor in this inverse segregation, is now found to be unnecessary. Preferred orientation with the [111] direction perpendicular to the surface and preferred directions of growth parallel to the (111) plane are shown to be caused by the strong covalent linkages within the (111) pairs of planes. This, plus a number of factors such as temperature gradient, surface tension, and Sb concentration in the surface film, favors the growth of those nuclei that originate with their (111) planes parallel to the surface. This preferred orientation of Sb can influence the tensile strength and ductility of hypereutectic Pb-Sb alloys.

An unusual concentration of Sb is found at the surface of hypoeutectic (below 11% Sb) Pb-Sb castings (1). The crystal form of this Sb indicates that it has solidified prior to the eutectic, contrary to the equilibrium phase diagram of the system.

The primary crystallization of Sb at the surface in excessive concentration was previously explained as being caused by an interdendritic flow of molten metal from the interior of the casting into the gap left between the semi-solid crust and the mold face during the solidification contraction. This satisfactorily explained the observed phenomena, but required the assumption of an unusual degree of supercooling to explain the large amount of Sb that froze as primary crystals.

Additional work and a reappraisal of the original observations have shown that supercooling of Sb takes place not only at the surface but throughout the interdendritic melt. In addition, excessive concentrations of Sb were also found at the surface of hypereutectic (above 11% Sb) alloy castings. A modification of the original explanation appears necessary. The following discussion shows that there is a preferred orientation of Sb at the surface with the [111] direction perpendicular to the surface, and that there is a preferred growth direction parallel to the surface. These factors influence not only the surface appearance of the as-cast Pb-Sb alloy series but the physical properties as well.

Experimental Procedure

The method of casting against polished mold walls in order to obtain a surface suitable for metallographic examination has been described (1) and criticized (2). Interpretation of the results, however, had been carefully verified by comparison with conventionally prepared metallographic cross sections for each of the alloys studied and by comparison with commercially prepared castings obtained from various sources. In addition, the presence of this Sb surface layer had been confirmed by x-ray analysis and chemical tests and additionally, as herein reported, by crystallographic measurement and identification of the actual crystals formed, so that the authors do not feel that such criticism is justified.

Alloy series were prepared in a concentration range of 3–21% Sb in increments of 2% under five casting conditions. The reasons for these conditions are brought out in the subsequent discussion.

1. Additional series of castings were made under the conditions reported previously (1).

2. Castings were made between highly polished parallel Al plates separated by 0.005-in. shim stock that acted as the narrow sides of the mold so that a 3 x 4 x 0.005-in. foil resulted. The mold was heavily insulated and suspended so that the parallel plates were vertical, with the width (3-in. dimension) and thickness (0.005-in. dimension) parallel to the base and with the height (4-in. dimension) vertical to the base. Heating was from the base, and controlled reduction of temperature began at the base. Cooling took place from the small, uninsulated top surface. The freezing therefore proceeded from top to bottom, and the cooling rate was approximately 5°/min.

3. Cast foils were made under the above conditions except that the top was heavily insulated immediately after casting, the source of heat was removed from the bottom, and a water-cooled Al plate was substituted. Freezing began at the bottom and cooling was at approximately the same rate as above. Series 2 and 3 were cast with the mold temperature initially slightly above the freezing point of the alloy since this was the only way in which such thin foils could be prepared.

4. Series 2 and 3 were duplicated except that the foil was made 0.125-in. thick.

5. Castings were made in a mold in which was suspended an Al sheet with both sides polished. This sheet was supported in the center of the mold by pointed Transite blocks so that heat transfer was at a minimum. The polished plate was 1-in.^{2} and 0.125-in. thick and was

FIG. 1. Etch pits left in Pb-Sb alloy surface by removal of primary Sb crystals; from the as-cast surface of a hypereutectic alloy containing 13% Sb. 500×.

surrounded on all sides by a 1-in. thick casting section. The mold was originally at a temperature above the melting point of the alloy and was held at this temperature a sufficient length of time after casting so that the interior plate reached the melt temperature before cooling began. By milling the edges of the resulting casting, the two halves of the casting could be separated at the interior Al surface.

To determine crystal orientation and habit, the following procedure was used: When a Pb-Sb alloy is corroded anodically in a H_2SO_4 solution, visible formation of lead oxides does not take place until the Sb present in the surface of the casting has been leached out (3). Specimens of the various castings that contained suitable Sb crystals were given this treatment, using a very low current density. Removal of Sb resulted in a negative replica of the crystal in the surrounding Pb (Fig. 1). Surface dimensions and angles of this depression, its depth, and the position of the deepest portion with relation to the surface outline were measured with various microscope accessories. With this information, the shape of the crystal was reconstructed, the angles that the sides made with one another calculated, and the crystal habit and the preferred directions of dendritic growth determined. Preferred directions of dendritic growth were then used to determine the orientation of the thin platelets which were not suitable for the above method of determination.

OBSERVATIONS AND CONCLUSIONS

Hypoeutectic Alloys

1. Primary crystallization of Sb and excessive amounts of Sb in the as-cast surface occur under all casting conditions for the hypoeutectic alloys. Whether the casting was large or small (relatively speaking, since the largest casting examined was only 5 in. long by 3 in. in diameter), rapidly or slowly cooled, or subjected to differential cooling, the surface always showed segregation of excess Sb and primary crystallization. As reported previously, the degree to which segregation occurred depended on the cooling rate and the amount of Sb in the alloy, but it was always present to some extent. This was true even at the internal surface formed by suspending a plate in the center of the mold. Repetition of the experiments reported previously led to the same conclusions as formerly. Castings made against Al, Fe, glass, Cr, Pb, and Transite and against Al and Fe surfaces under silicone oil all exhibited this same excessive Sb segregation at the surface.

2. The appearance of primary Sb crystals and excessive proportions of Sb at the casting surface of the hypoeutectic alloys is evidence of a larger than eutectic concentration of Sb and of supercooling. The eutectic concentration of Sb is reported to be about 11% by weight, and on that basis the eutectic structure would be expected to contain an Sb-to-Pb ratio of approximately 1:8 by weight or 1:5 by volume. Conditions that reverse this ratio in the surface cannot be explained by previous theories of inverse segregation.

A layer of eutectic composition and structure has been observed at the surface of many alloys. This has been proved to be caused by the natural enrichment of the remaining melt in solute as primary crystals of solvent precipitate. This melt, enriched to eutectic composition, may be extruded as a surface layer (4), or may only appear to be in excess at the surface because the roughly spherical or cylindrical primary crystals have a minimum area in the surface layer (5).

The term primary crystallization is used herein to mean the formation of an extensive dendritic crystal or a regular crystal of recognized form and habit, of a much larger size than would be associated with eutectic structure, and which has been precipitated prior to the eutectic in its immediate vicinity. For the hypoeutectic alloys, the real primary crystals are, of course, the Pb crystals that form the bulk of the solid. The primary crystallization of Sb in the surface layer of such an alloy depends on the melt in the immediate vicinity having some hypereutectic composition. The process of interdendritic flow, whereby molten metal flowing to the surface to compensate for shrinkage is enriched in Sb by the deposition of Pb on the colder walls of the interdendritic channels, cannot produce an Sb concentration greater than eutectic. The only process that suggests itself as a way out of this difficulty is that in which Sb supercools in the presence of Pb when the eutectic composition is reached. Just as one metal may supercool in a crucible made of another, so may Sb supercool in the interdendritic channels and at the surface of the primary Pb structure. But Pb can continue to precipitate, and so the remaining melt becomes enriched in Sb to a point where extensive primary crystallization of Sb occurs. The reasons that such supercooling is possible have been discussed previously (1).

3. The formation of a solid crust or extensive interdendritic flow is not necessary to produce the surface film of Sb. The possibility of a solid crust being formed and subsequently being partially remelted by heat from the interior as the heat transfer becomes interrupted by shrinkage from

the mold (4) was not considered likely from the evidence previously obtained, but such a possibility was advanced as a criticism (2) of the previous report.

Formation of a solid crust, made possible by normal eutectic freezing, not only would be evidence that supercooling of Sb did not occur but would leave no explanation of how Sb could occur in greater than eutectic amounts at the surface. For, if a solid crust is first formed and then remelted, the first portion to remelt would be of eutectic composition (lowest melting point), and any further remelting would cause enrichment of the melt in Pb. Enlargement of the surface pores by hotter material from the interior would aggravate this condition, so that the extruded material could not contain more than the eutectic amount of Sb and would probably contain less.

Thin alloy foils of 0.005 in. thickness cast as described were frozen so that the primary Pb dendritic crystals grew in one direction only, parallel to the mold faces. The thickness of the foil equaled the average diameter of one dendritic arm, and by proper control of cooling a row of parallel dendritic branches could be produced which were parallel to and between the foil surfaces. In other words, a foil was produced in which freezing had begun either at the upper or lower end and not from either foil surface. The resulting foil was not a single crystal, but the individual grains were large and their thickness equaled that of a single dendritic branch. The individual dendritic branches of each grain were parallel to the foil faces and roughly parallel to the long dimension of the foil which was also the vertical axis of the mold. This was checked by the preparation of chemical replicas (6), and by alternately etching and stripping the surface film with pressure-sensitive tape until the underlying dendritic structure was revealed.

In all of the foils, whether growth of the primary Pb dendritic crystals started from the bottom of the mold or from the top, the surface film of the casting showed excessive concentration and primary crystallization of Sb. The diameter of the individual dendritic branches was nearly the same as the thickness of the foil, and their length was many times their diameter. These crystals, the first solid to form in a given section, evidently had been able to grow to their final diameter in a medium that was still unfrozen.

In these circumstances there could be no formation of a solid crust with liquid center, nor any buildup of a higher concentration of Sb toward the center. Gravitational flow of still-molten metal through the interdendritic channels along the length of the foil maintained a liquid layer in contact with the mold surfaces during the shrinkage contraction so that the castings conformed closely to mold dimensions. For a mold of these dimensions, however, contraction of the solidifying metal would be small and movement of molten metal past any given point in the interdendritic channels would be small, far too small to cause any appreciable increase in concentration or the introduction of Sb-rich material at the surface in considerable quantity.

The argument might be made that a given section of the foil had been completely solid and, as shrinkage occurred, feeding had taken place from other regions through the gap between the metal and mold. That this is not true is attested to by the fact that the surface film of Sb was present regardless of whether freezing of the foil began at the bottom (which would favor gravitational flow) or from the top (which would preclude gravitational flow if the melt in a given section became completely solid).

Additional proof that there is no necessity for the formation of a solid crust or extensive interdendritic flow is given by the experiment wherein an Al plate was suspended in the interior of the mold. This plate, being well insulated from the exterior surfaces, centrally located, and at the temperature of the melt, would approximate conditions at the center of a casting that was being cooled through the exterior mold surfaces. The area around this plate then represents the last portion to freeze and cannot be supplied with liquid metal from any other region. Although the surface was always marred by many shrinkage cavities, freezing at this interior surface nevertheless took place with the formation of a surface layer of high-Sb concentration and primary crystallization, just as at the exterior surfaces.

The conclusion is reached, therefore, that this is a process that occurs in situ and does not depend on interdendritic flow. A completely solid crust was evidently not present at the time the surface film formed, but the main function of interdendritic flow is to maintain the liquid layer in contact with the mold face during solidification contraction.

4. For both hypoeutectic and hypereutectic Pb-Sb alloys there is a preferred orientation of Sb with the [111] direction perpendicular to the casting surface. Examination of the surface of castings made from hypoeutectic alloys revealed a host of elementary growth forms (Fig. 2), all of the same type, which on investigation were revealed as dendritic Sb crystals. In the most elementary form, these consisted of three needlelike or acicular dendritic branches parallel to the surface and meeting at a common center at angles of 120° to one another. As the concentration of Sb was increased or rate of cooling decreased, the dendritic crystals began to exhibit a center of regular crystal structure with the dendritic branches radiating from the corners (Fig. 3). This center was normally in the form of an equilateral triangle, although other forms appeared occasionally. These equilateral crystals were found to have

FIG. 2. Primary Sb crystals of primitive dendritic form, crystallized in the as-cast surface layer of a Pb-Sb alloy containing 9% Sb. 800×.

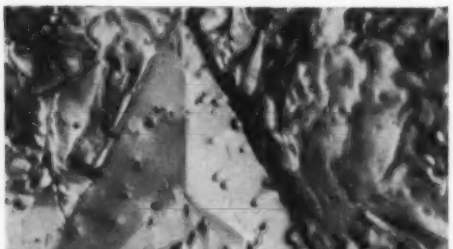

FIG. 3. Primary Sb crystals of regular form but with dendritic corner extensions, crystallized in the as-cast surface layer of a Pb-Sb alloy containing 11% Sb. 800×.

their (111) planes parallel to the surface. Cross sections revealed that for the hypoeutectic alloys these crystals had developed the (111) planes at the expense of all others, so that a very thin platy crystal was formed. For the hypereutectic alloys the equilateral triangle at the surface had developed into a tetrahedron with the (111) plane at the surface and the apex beneath the surface. The sides of this tetrahedron were made up of (110) planes. The tetrahedral crystals formed in the hypereutectic alloys did not exhibit dendritic growth from their corners or edges for reasons to be explained in a later section.

The hypoeutectic alloys showed a decided tendency toward dendritic growth from the corners of the equilateral triangles in the [11$\bar{1}$] and equivalent directions. As the cooling rate increased, these crystals began to exhibit

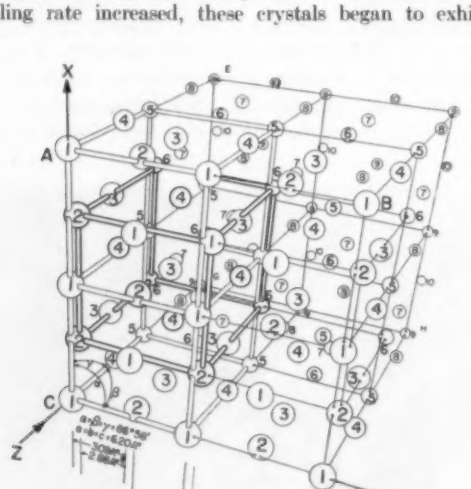

FIG. 4. Schematic representation of the interpenetrating lattice configuration of Sb. Similar numbers identify lattice points on the same plane, successively increasing numbers refer to planes at increasing depth behind plane ABCD. Note that the configuration forms a very slightly askew face-centered lattice.

additional directions of dendritic growth. While the dendritic growth usually originated at the corners of the triangle, and while dendrites at 120° to one another were the directions of principal growth, numerous other dendritic growths appeared at lesser angles, radiating from the corners like a diverging bundle of rays.

The occurrence of crystals with the (111) planes approximately parallel to the surface was estimated at about 95% of all the orientations that appeared. The crystals show a decided preferred orientation with the [111] direction at right angles to the surface, but the individual crystals appear to have no preferred orientation with respect to one another other than sharing a common axis in the [111] direction.

5. Preferential growth occurs at right angles to the direction of preferred orientation and causes a surface layer of Sb without the need for excessive supersaturation. In examining cross sections of the foils, the Sb particles in the matrix surrounding the primary dendritic branches of the Pb crystals were observed to have random orientation except at the as-cast surface, where they were almost invariably aligned with their long axis parallel to the surface. In addition, those crystals formed in the surface layer, when viewed from above the surface, showed extensive and continuous dendritic structure and even large crystals of regular structure but, when viewed in the cross section, were found to have grown very little in any direction away from the surface. This refusal of Sb crystals to grow into the interior, even when there was plenty of room to do so, was taken as evidence of a preferred direction of growth in the plane of the surface. Preferential growth direction is also indicated by the internal structure of Sb.

The lattice of Sb has been determined to have orthorhombic symmetry. As originally pictured (7), Sb atoms lie in two interpenetrating face-centered rhombohedral lattices (Fig. 4), and the unit rhombohedral cell is pictured as face-centered. The early literature reports the lattice constants on this basis, and some reports on crystal form and cleavage planes have been based on this notation.

But a primitive rhombohedron of the same height, but one-quarter of the volume of the original, can be outlined in the face-centered unit cell (Fig. 5), and it is the lattice constants of this cell that are reported in the recent literature. Since this change in cell also causes a transformation of axes and face indices, care is necessary in comparing reports on the habit, structure, orientation, and cleavage characteristics of Sb. Axes and face indices mentioned in the present report are based on the primitive cell of Fig. 5 and on the Miller system which employs three axes of reference.

Reported lattice constants (7–12) are in good agreement, but the exact positions of the atoms (the relative displacement of the two interpenetrating lattices) are still in doubt (7, 8).

The lattice structure of Sb is unusual, but this alone does not furnish the clue to the odd behavior of the surface film in alloy castings. As was shown for Ge (13), the preferred growth parallel to the metal surface is caused by its method of atom bonding. The (111) planes of the Sb lattice are arranged in double layers, with the two layers spaced at approximately 1.50Å apart and repeated at intervals of

about 2.25Å. The fourth layer is vertically over the first. In this arrangement, each atom has three close neighbors in the other plane of its double layer and three others at a somewhat greater distance in the next double layer (Fig. 6). Of the four covalent bonds associated with each atom, three appear to be bound with the three closest neighbors in the other half of the same double layer at a distance equivalent to the closest atom spacing. The remaining covalent bond could be considered to act through the next adjoining double layer on an atom at twice the above distance. Actually, each double layer might be regarded as a huge molecule held together by simple covalent bonds, while the layers themselves may be considered as held together by Van der Waals' forces or something like metallic bonds.

Atoms within a given double layer, therefore, attract each other strongly, being held together by the mutual attractions of three of their covalent linkages, while the attraction for atoms in other layers is much weaker. A strong tendency for approaching atoms to be drawn into an existing double layer rather than to begin another layer in the [111] direction would be expected to occur, and this effect would be strongest for the conditions favorable for dendritic growth. The evidence indicates that this is actually what does occur. The perfect cleavage parallel to the (111) planes is also explained by the bonding of the crystals.

Since the crystals show a preferred orientation with the [111] direction perpendicular to the surface and a preferred direction of growth parallel to the surface, there results an excessive coverage by Sb in the surface layer which appears to be caused by a large excess of Sb but, in reality, is the result of preferential growth of a comparatively small excess.

The cause of the preferred orientation is not obvious. In the case of those crystals which consist largely of the three dendritic arms meeting at 120° to one another, it appears that the nucleus itself must have been formed with this orientation or acquired it shortly after birth. The effect cannot be attributed to a thermal gradient extending into the interior because the same effect was observed at interior surfaces where the temperature differential was reversed. The effect does not appear to be caused by nucleation from the mold because, as was mentioned previously, various mold surfaces and air and silicone oil contact surfaces produce the same effect.

The phenomenon might be attributed to surface tension since it appears at all interfaces. The energy associated with the surface layer may have an influence on the formation of the nucleus or may influence the nucleus after its formation, since the effect of surface tension acting on an object becomes more and more important compared with its weight as the object becomes smaller.

As Gibbs has shown, if a substance lowers the surface tension of a liquid when dissolved in it, the concentration of the substance is greater in the surface film than in the bulk of the liquid. If this is true, the concentration of Sb in the interface will be higher than elsewhere. To be sure, the layer concerned may be only one or several atoms thick, but consideration is here being given only to the formation of a nucleus.

The supersaturated surface layer of the semisolid alloy may therefore be pictured as having an interface of high Sb concentration, a greater than eutectic concentration of Sb in the layer, a temperature gradient that produces the greatest supercooling at the interior mold surface or at the liquid-mold interface, and conditions that are ideal for

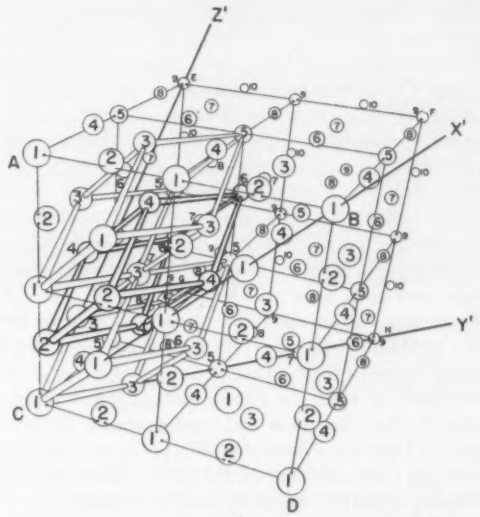

FIG. 5. Lattice configuration of Sb when a more primitive cell is used, same spatial distribution as before. For clearness only a portion of the new lattice has been drawn in. Note that an interpenetrating body-centered rhombohedral structure is produced. Observe also that the indices X′, Y′, Z′ are differently located than X, Y, Z of Fig. 4.

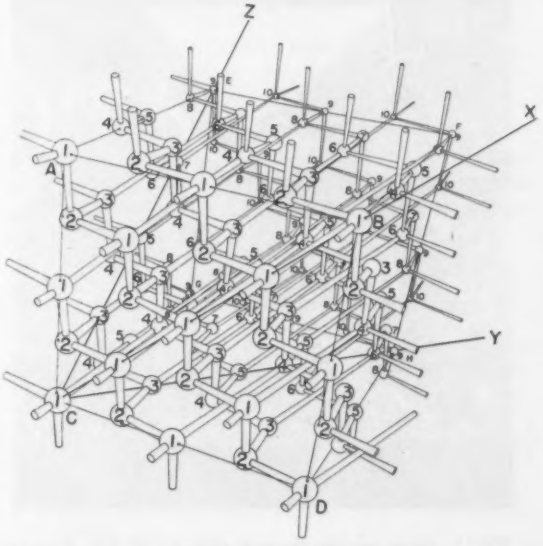

FIG. 6. Bonding configuration of Sb, same spatial arrangement as before. Covalent bonding forces are pictured as rigid bonds with maximum interaction shown in the closely grouped pair of (111) planes. Observe that the bonds operating within the closely grouped pairs are more numerous and act over shorter distances than those operating between paired planes.

dendritic-type crystal growth. Nucleation should logically occur at the interface with orientation as described. In addition, the heat associated with crystallization is radiated in all directions but is most readily transferred by the solid mold rather than by the liquid melt. Thus there exists briefly a more favorable condition along the mold face than into the molten material beneath the surface. Nuclei with an unfavorable orientation that causes them to grow away from the surface should be overwhelmed by those more favorably located with their (111) planes parallel to the surface. If this evaluation of the cause of preferred orientation is correct, the decease of the unfavorably located crystals must occur while they are yet very small, since very few crystals of other than the preferred orientation were found in the surface layer.

The surface of Pb-Sb alloys is not the only place where this preferred orientation of Sb occurs. A similar phenomenon has been reported for thin films of Sb, vacuum-evaporated upon a suitable support (14–16). These films are condensed as an amorphous layer and then spontaneously crystallize with the (111) planes parallel to the film surface. In one of these reports (15), the optical appearance is described in detail and photographs of the structure are included. The description and illustrations of the crystals obtained from the evaporated film apply equally well to the crystals obtained here in the surface film of the alloy, indicating a marked similarity in growth habit.

Another interesting observation has been reported concerning the orientation texture present at the cast surface of pure Cd and Zn (17). These metals, of hexagonal structure, had the basal (0001) planes oriented parallel to the surface, and this same texture was observed whether cast against air, Transite, Fe, or molten Pb.

FIG. 7. Cross section through thin Pb-Sb foil. Primary tetrahedral Sb crystal (bright triangle at right edge) is surrounded by an area in which Pb predominates. This dark area isolates the primary crystal and also outlines the shape of the dendritic Pb crystal. Remainder of Sb in picture represents "eutectic" structure formed upon relief of supercooling. 500×.

While the structure of Sb cannot be compared with that of Cd and Zn, the planes of maximum density are parallel to the surface in each case. This indicates that surface tension might be the largest single factor in determining orientation, whereas the solid-state conversion of an amorphous solid into an oriented crystal structure might require a different conclusion. In deposits condensed from the vapor, however, only materials having a high atomic mobility like Zn, Cd, Sb, Bi, and NaCl show a densely populated plane parallel to the surface (16).

Hypereutectic Alloys

The conclusions and observations pertaining to the hypereutectic alloys cover only that part of the alloy series containing between 11 and 21 % Sb, a small segment of the total series. In general, observations and conclusions are the same for the hypoeutectic range. There is the same excessive surface Sb, preferred orientation, and preferred growth direction as previously mentioned but there are also the following additional observations:

1. Since primary crystals of Sb precipitate first and at the surface, excess Sb at the surface cannot be explained by the usual explanation of inverse segregation. This must be considered as a special type of "normal" segregation.

2. In the hypereutectic alloys, the surface is made up of two kinds of crystals. Individual tetrahedra appear with preferred orientation with the [111] direction perpendicular to the surface, the basal (111) plane at the surface, and the apex beneath the surface. The remainder of the surface is covered with a thin, continuous, platy film of Sb in which neither dendritic structure nor individual crystals could be detected by the methods being used. For the reasons already given, this film was assumed to have the same preferred orientation with the [111] direction perpendicular to the surface. This was confirmed by x-ray analysis of a 15% Sb alloy foil which also verified the excessive amount of Sb in the surface layer (18).

3. Supercooling of Sb and preferred growth direction is responsible for the surface layer in the hypereutectic alloys just as in the hypoeutectic. When the amount of Sb in the alloy is increased beyond the eutectic composition, the surface is still covered with an Sb film, but the regular crystals of Sb in this film no longer have dendritic extensions from the edges or corners, and they are no longer platy but have become regular tetrahedra with the base at the surface.

The cross section of a thin Pb-Sb foil (Fig. 7) shows that each regular Sb crystal is surrounded by a region rich in Pb and in which there are no detectable particles of Sb. Beyond this lead envelope the so-called eutectic structure occurs. Examination shows that this Pb envelope around the regular Sb crystal sometimes is extended for considerable distances into the eutectic as dendritic prolongations. Although an effort was made to promote freezing of these alloys in a direction parallel to the foil faces as was done for the hypoeutectic alloys, the cross sections showed that all regular Sb crystals were formed at the foil surface (mold face) and grew inward. Dendritic Pb crystals had

completely random growth directions. If one mold face was intentionally made less well insulated, all the Sb crystals were found to have originated at this cooler mold face.

The evidence indicates that initial freezing of the melt occurs without supercooling. Under these conditions relatively few nuclei are formed, and the growth conditions favor regular rather than dendritic crystal growth. The crystals that do form naturally do so at the mold face and grow to a fairly large size in the tetrahedral form already described.

The Pb-rich area surrounding each crystal, in which no Sb appears, indicates that growth proceeds faster than diffusion can keep pace. The crystal thus becomes surrounded by a Pb-rich region which effectively prevents further growth and in which conditions are suitable for solidification of Pb. This permanently seals off the original Sb crystal and prevents it from nucleating any further precipitation of Sb. With all the original nuclei sealed off in this manner, the regular crystal growth of Sb crystals becomes a self-extinguishing process. The remainder of the Sb now supercools, for its most effective nucleation agents have been removed. Conditions are now the same as in the hypoeutectic alloys. The metal at the surface contains a greater than eutectic amount of Sb and is in a supercooled condition. Dendritic crystallization of Sb occurs with preferential growth in the surface plane. This is followed by eutectic-type crystallization throughout the remainder of the melt.

The relatively few regular crystals and their concentration at the surface suggests the possibility of heterogeneous nucleation. Their preferred orientation, however, indicates that the same combination of factors previously outlined is also responsible for this type of crystal. The thickness of the Pb envelope and the dendritic growth of Pb from it suggest that Pb also may have supercooled in the region surrounding each primary regular Sb crystal.

Under the conditions that encourage dendritic growth, such as supercooling, the crystallization of Sb does not become a self-extinguishing process because the rapid extension of dendritic filaments of relatively small cross section requires such a small removal of Sb from a given area that formation of a Pb-rich envelope does not occur until the tip of the growing dendrite has passed into an area as yet undepleted.

Effect of Preferred Orientation on Physical Properties

The preferred orientation of Sb and its excessive concentration in the surface film would be expected to exert some influence on the physical properties of the alloy concerned. Sb is an anisotropic material, and its physical properties vary with direction in the crystal. A preferred orientation at the surface of the crystal produces a maximum or minimum effect, depending on the property concerned.

One effect that was investigated was cleavage. Sections of the foil were bent at right angles and the result investigated. When hypoeutectic alloys were employed, no noticeable effect was obtained. When hypereutectic alloys were investigated, a significant difference was noted. When the bend occurred over the site of a regular tetrahedral Sb crystal, cleavage of the crystal occurred if the crystal was in the surface under tension (Fig. 8). Crystals in the surface under compression did not cleave. Cleavage of the crystal resulted in an open crack extending from the surface down through the crystal and well into the underlying lead. The brittle crystal, with its apex pointed at the center of the foil, was evidently acting much like a mechanical notch and causing failure in the underlying structure. This effect was either absent in the dendritic crystals or resulted in twinning, and no visible failure occurred through this type of crystal.

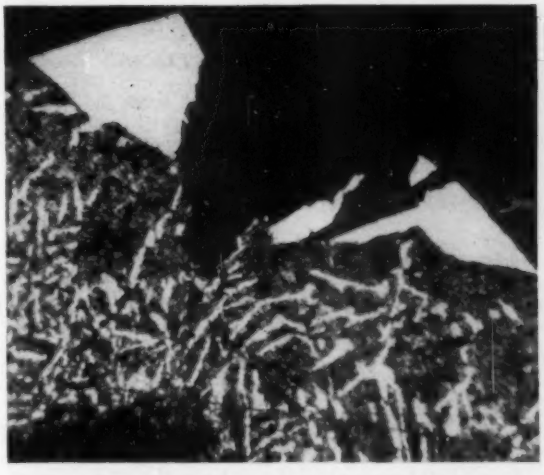

FIG. 8. Cross section of foil with 90° bend. Primary crystal of Sb has split, and crack has spread to eutectic portion of section. This effect is highly localized under site of crystal and does not represent an extensive crack across the foil. 500×.

As-cast Pb-Sb alloys show a sudden decrease in tensile strength near the eutectic concentration of Sb (19, 20); extruded and annealed specimens show no such decrease (21). Tetrahedral Sb crystals first make their appearance at this same point, and their demonstrated failure under tension would indicate that their presence is responsible for the sudden decrease of tensile strength at above eutectic concentrations.

Manuscript received July 17, 1956. This paper was prepared for delivery before the Cleveland Meeting, September 29 to October 3, 1956.

Any discussion of this paper will appear in a Discussion Section to be published in the December 1957 JOURNAL.

REFERENCES

1. A. C. SIMON AND E. L. JONES, *This Journal*, **101**, 536 (1954).
2. ANON., *Metal Ind. (London)*, **85**, 539 (1954).
3. J. B. BURBANK AND A. C. SIMON, *This Journal*, **100**, 11 (1953).
4. D. E. ADAMS, *J. Inst. Metals*, **75**, 809 (1949).
5. K. DETERT, *Z. Metallkunde*, **45**, 550 (1954).
6. J. BURBANK, *J. Metals*, **5**, 55 (1953).
7. R. W. JAMES, *Phil. Mag.*, **40**, 233 (1920).
8. A. OGG, *Phil. Mag.*, **42**, 163 (1921).
9. E. ROSA, *Nuovo cimento*, **12**, 448 (1935).
10. E. R. JETTE AND F. FOOTE, *J. Chem. Phys.*, **3**, 605 (1935).

11. J. E. Dorn and G. Glockler, *J. Phys. Chem.*, **41**, 499 (1937).
12. S. S. Lu and Y. L. Chang, *Proc. Phys. Soc (London)*, **53**, 517 (1941).
13. E. Billig, *Proc. Roy. Soc. (London)*, **A229**, 346 (1955).
14. J. E. Ruedy, *Phys. Rev.*, **59**, 926 (1941).
15. W. Lotmar, *Helv. Phys. Acta*, **18**, 232 (1945).
16. D. M. Evans and H. Wilman, *Acta Cryst.*, **5**, 731 (1952).
17. G. Edmunds, *Trans. Am. Inst. Mining and Met. Engrs.*, **161**, 114 (1945).
18. J. Burbank, Unpublished work.
19. A. M. Fairlee, *Metal Ind. (N. Y.)*, **9**, 24 (1911).
20. L. J. Gurevich and J. S. Hromatko, *Chem. & Met. Eng.*, **25**, 62 (1921).
21. R. S. Dean, L. Zickrick, and F. C. Nix, *Trans. Am. Inst. Mining and Met. Engrs.*, **73**, 505 (1926).

The Question of Space Charge in Anodic Ta_2O_5 Films

D. A. Vermilyea

Research Laboratory, General Electric Company, Schenectady, New York

Dewald (1) has extended the oxidation theory of Cabrera and Mott (2) to include the effect of an ionic space charge in the oxide film. Such a space charge will develop if, for example, the time required for an excess interstitial ion to move from one side of the film to the other is not very much smaller than the time required for the ion to cross the interface. Space charges do not develop in all types of film formation, since a mechanism involving the creation of pairs of defects within the film, rather than of single defects at an interface, leaves the film electrically neutral at all times. In a previous publication (3) an attempt was made to detect the presence of space charge in anodic Ta_2O_5 films. It was concluded that such space charges must be quite small. Recently Young (4) suggested that an ionic space charge would explain his measurements of the frequency and time dependence of the capacitance of niobium oxide films, and stated that behavior similar to that of niobium oxide is shown by Ta_2O_5 films "under certain conditions". In this paper the results of measurements of the capacitances of Ta_2O_5 films of various thicknesses are discussed. Measurements indicate there may be a charge in the film of such a density that the variation of electric field across a film 5000Å thick is about 1%.

Experimental

Oxide films were formed on chemically polished Ta sheet,[1] using a solution of 0.05% Na_2SO_4 in water as the electrolyte. The metal specimens were 2 in. x ½ in. x 0.005 in. and had a tab ½ in. x $\frac{1}{32}$ in. on one corner. They were cut from Ta sheet with a die and then chemically polished, so that the edges cut by the die and the rolled surfaces were smoothed and cleaned. It is known that chemical polishing leaves a film of unknown composition at the oxide-metal interface, and it is conceivable that such a film might have an effect on the results. However, the same results were obtained whether this film was kept in place or removed prior to formation by dipping the specimen in HF. It was necessary to have a very well-defined area on each specimen so that the current density of formation at all voltages would be constant and so that the capacitance would be measured on the same area. This was accomplished by applying a heavy coating of "Cello-Seal" (a semifluid substance which does not creep along the metal surface) to the specimen at the point where the tab joined the main part of the specimen, anodizing the tab up to the coating, and then removing the Cello-Seal. It was possible in this way to prevent the oxide film from creeping above the water line; a very sharp boundary between the anodized and clean part was produced.

Voltages applied to the specimens were measured by means of a voltage divider and a L&N type K potentiometer to a precision of 0.1%. The potential in the electrolyte near the Ta electrode was also measured with a calomel reference electrode so that changes in the cathode-solution potential could be compensated for.

The procedure employed was to apply a constant voltage across the forming cell and to allow the current to fall to 1.0 ma. The specimen was then removed from the bath, cleaned in H_2SO_4-$K_2Cr_2O_7$ cleaning solution, and placed in a cell containing 2% HNO_3 and a platinized-Pt electrode of 100 cm². The capacitance was measured using a General Radio impedance bridge which had been calibrated so that the capacitance could be measured with a precision of 0.5%.

It is known that a plot of oxide film thickness vs. voltage extrapolates to zero thickness at a voltage which is about 1 v negative. The value of the intercept cannot be calculated precisely, and hence some extrapolation method must be used to find it. For this purpose a plot of the measured capacitance times the measured voltage against the voltage was made for large voltages and extrapolated to zero voltage. Then, values of voltages required to make the results at small thicknesses fall on the extrapolated line were determined and compared to the measured voltages. It was found that a small constant voltage (about 0.9 v) added to all of the voltages would result in a smooth curve of C·V vs. film thickness. The constant to be added can be obtained by plotting the reciprocal of the capacitance against the voltage and extrapolating to zero voltage, but the accuracy is not as great. For an extrapolation of either type to be valid, it is necessary that there be no rapid change in either the density or the sign of any space charge in the film at very small distances from either electrode. Earlier measurements (5) at negative

[1] Obtained from Fansteel Metallurgical Corp.

applied voltages and film thicknesses down to a few angstrom units showed that a plot of reciprocal capacitance against voltage was still linear and was a continuation of the line obtained with positive voltages and larger thicknesses. Therefore, it appears that there is no sudden change of field in the oxide film close to either interface; hence the extrapolation used is valid.

Results and Discussion

Fig. 1 and 2 show plots of $C(V + k)$ against film thickness, where k is a small constant as shown. There is a slight decrease of this product with increasing film thickness for specimens held either at 19°C and a field of 0.067 v/Å or at 86°C and a field of 0.056 v/Å. Three specimens anodized under each set of conditions gave nearly identical results. For the 29°C specimens the decrease of the product $C(V + k)$ averaged 1.1%, while for the 86°C specimens the decrease averaged 1.4%.

There is a possible source of a decrease in $C(V + k)$ with thickness which makes the interpretation of these results difficult, that is that the area of the film could decrease as the film grew thicker. This might occur in two ways. First, a very thin film would follow the very small scale contours of the surface, while the outer surface of a thicker film would undoubtedly tend to be smoother and hence have a smaller area. Second, the metal surface itself would tend to become smoother as the film grew. An experiment was performed to see whether there was any permanent change of specimen area after formation by dissolving all but about 100Å of a film in HF and then repeating the measurement of capacitance vs. voltage. The second set of measurements shown in Fig. 1 was made in this way and it may be seen that the two sets of measurements agree very well. Thus there appears to be no permanent change in area, but it cannot be concluded that an effect of this type is entirely absent.

Therefore, it seems that there is some justification for interpreting these measurements as indicating that there is a small decrease in the average field across an oxide film during formation as the film thickness increases. If it is assumed that the space charge density is uniform, it can be shown that a density of 10^{16} electron charges/cm³ would result in a change of the average field in the film by 1%. It may be that a slightly higher field is required near one of the interfaces of the film to make the rates of ion transport in the film and at the interface equal. Because the effect is so small, however, it appears about equally justifiable to say that the field is essentially constant and that the small apparent decrease is the result of a change of effective area with film thickness or some other similar effect.

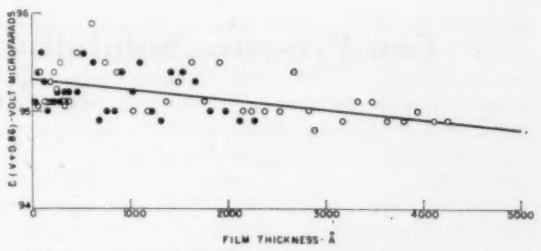

Fig. 1. Plot of $C(V + k)$ vs. film thickness for a specimen formed at 19°C. Closed circles represent the first run to about 150 v. All but about 100Å of the oxide film was then dissolved in HF and the second run (open circles) was made.

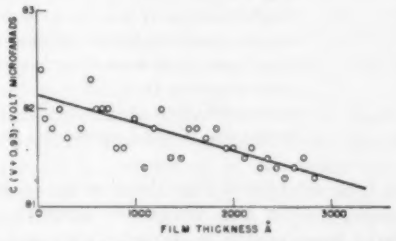

Fig. 2. Plot of $C(V + k)$ vs. film thickness for a specimen formed at 86°C.

Manuscript received March 23, 1956.
Any discussion of this paper will appear in a Discussion Section to be published in the December 1957 Journal.

REFERENCES

1. J. F. Dewald, *This Journal*, **102**, 1 (1955).
2. N. Cabrera and N. F. Mott, *Rep. Prog. Phys.*, **12**, 163 (1948–1949).
3. D. A. Vermilyea, *This Journal*, **102**, 655 (1955).
4. L. Young, *Trans. Faraday Soc.*, **51**, 1250 (1955).
5. D. A. Vermilyea, *This Journal*, **101**, 189 (1954).

Low-Pressure Solubility and Diffusion of Hydrogen in Zirconium

M. W. Mallett and W. M. Albrecht

Battelle Memorial Institute, Columbus, Ohio

ABSTRACT

Low-pressure solubilities were determined for H in α- and β-Zr and in two Zr-O alloys at 700°-1000°C and pressures of 0.1–4 μ Hg. The data followed Sieverts' law for each phase, and H solubility decreased with increasing temperature at a given pressure. Also, there was a slight increase in H solubility in α-Zr with increasing oxygen content. Diffusion coefficients for H in α-Zr were obtained in the range 300°–600°C by analysis of prepared concentration gradients. In the range 600°–800°C, degassing coefficients were determined from rate of H evolution from Zr cylinders. Degassing coefficients were much lower than expected from diffusion theory, and it was concluded that the degassing was not a pure diffusion phenomenon. Terminal solubilities obtained from the gradient analysis were in good agreement with those found by previous investigators.

It has been established that the presence of H has a deleterious effect on the mechanical properties of Zr, particularly those related to impact, creep, and fatigue (1–3).

H concentrations as low as 10 ppm can embrittle the metal, depending on previous heat treatment. Because arc-melted sponge Zr normally contains 25–100 ppm H, it must be vacuum annealed to 10 ppm or less H to eliminate brittleness.

Knowledge of optimum conditions for removal of H from Zr is commercially important. Therefore, determinations were made of low-pressure equilibrium solubilities and the diffusion coefficients of H in Zr. The resulting data indicate the effects of time, temperature, degree of vacuum, and section thickness on degassing of Zr.

Literature.—Early work (4) showed an abrupt change in H solubility at the allotropic transition of Zr. Later, a thorough investigation was made of the Zr-H system at pressures of 1–760 mm Hg from room temperature to 1050°C (5). Extrapolation of the data to low pressures, along with other solubilities calculated from diffusion studies in the range 400°–500°C, were reported in a discussion of the properties of Zr-H alloys (1). Gulbransen and Andrew (6) studied rather extensively the equilibrium and terminal solubilities of H in α-Zr in the range 425°–600°C at pressures of about 0.001–0.1 mm Hg. More recently Edwards, Levesque, and Cubicciotti (7) determined the solid-solution equilibria in the Zr-H system and presented a partial phase diagram of the system. H solubilities were determined at H pressures of 1–760 mm Hg in the range 600°–900°C. A phase diagram based on results of high temperature x-ray diffraction studies and solubilities established by Schwartz and Mallett (1) was published by Vaughan and Bridge (8).

Several investigators have given theoretical interpretations of the solubility of H in Zr. Martin and Rees (9) applied a statistical-mechanical theory of two-component interstitial solid solutions. They also accounted for the saturation (terminal) solubility of H in Zr-O solutions by observing that apparently oxygen atoms in solution at octahedral sites block neighboring tetrahedral sites normally available to H atoms. A similar explanation was suggested earlier (10). This would explain the decrease in H solubility with increase in oxygen content.

Considerable experimental data on the solid solution equilibria in the Zr-O-H system were reported by Edwards and Levesque (11). Their work was carried out in the range 600°–900°C at H pressures of 1–760 mm Hg.

Very little work has been reported on the diffusion of H in Zr. Schwartz and Mallett (1) determined diffusion coefficients at 400°, 500°, and 600°C. Gulbransen and Andrew (12), in investigating the mechanism of the reaction of pure H with Zr, determined diffusion coefficients for the diffusion of H and D through a hydride film. Their data cannot be compared with those of the present study since they were for a hydride phase rather than the metallic phase.

An important feature of all these investigations is that the Zr in each case contained 1 w/o or more of Hf. It is not known what effect the Hf may have had on the properties of the Zr-H system. Therefore, the present investigation was made with low-Hf (<0.02 w/o) Zr.

Experimental Work and Results

For the present study, the low-pressure solubility of H in Zr was determined in the range 700°–1000°C at pressures of 0.1–4 μ Hg. The effect of oxygen in solution on the H solubility at the low pressures was also investigated.

The rate of diffusion of H in Zr was studied in the range 300°–800°C.

Materials.—Zr used in this work was iodide metal, arc-melted, and cold rolled to $\frac{3}{8}$ in. and $\frac{3}{16}$ in. diameter rods. This material was analyzed by spectrographic, chemical, and vacuum-fusion techniques. Results are given in Table I.

Zr-O alloys were prepared from the above mentioned Zr stock by reacting known quantities of pure oxygen with the metal. The alloys were then double arc-melted and cold rolled to $\frac{3}{16}$ in. diameter rods. Alloys so prepared

TABLE I. *Analysis of arc-melted iodide Zr*

Element	Amount present, w/o
Fe	0.12
Cu	0.006
Al	0.005
Mg	0.005
Ca	0.003
Cr	0.003
Ni	0.002
Ti	0.002
Si	0.001
Hf	<0.02
Pb	<0.005
Mn	<0.001
N_2	0.003
O_2	0.032
H_2	0.0046

contained 0.14 and 0.43 w/o oxygen as determined by vacuum-fusion analysis.

Pure H for the study was obtained from thermal decomposition of uranium hydride. This hydride had been prepared by allowing dried commercial H to react with clean U turnings.

Low-pressure solubility of H *in* Zr—*Method.*—Studies of the low-pressure H solubility were made in an apparatus (13) consisting of three main sections: a pure H source, a heated specimen chamber, and a vacuum pumping system. H from the decomposition of uranium hydride was diffused into the apparatus through a Pd tube. The flow of H through the apparatus at the desired pressure level was controlled by proper manipulation of the temperatures of the uranium hydride and Pd tube. An ionization gauge was used for continual pressure indication. However, a McLeod gauge was used for periodic measuring of the absolute H pressure.

The H pressure in the apparatus could be regulated to any desired value in the range 0.1–4 μ Hg (range of this work) and maintained within $\pm$ 5% of that value for several hours.

The specimen chamber was heated with a wire-wound furnace. Temperatures were measured with a Pt-Pt + 10% Rh thermocouple in contact with the specimen. Temperatures of the specimens were controlled to $\pm$ 5°C.

Specimens, $\frac{1}{4}$ in. in diameter by $\frac{1}{2}$ in. long, were dry abraded with 240-grit SiC paper, washed in A. C. S. reagent grade acetone, and placed in the furnace tube of the apparatus.

All experiments were carried out for a period of 6 hr at constant temperature and pressure. The equilibrium solubility was obtained within this time, as shown by the fact that a few specimens heated for 12 hr did not show significantly different results. At the end of an experiment the furnace tube containing the specimen was quenched with cold water. The specimen was then analyzed for its H content by the vacuum-fusion method. Usually a duplicate specimen was prepared for metallographic examination to determine the structure of the metal under equilibrium solubility conditions.

Results and discussion.—Solubility limits were determined for H in massive Zr, and Zr-O alloys from 700° to 1000°C at 50°C intervals, and at pressures of 0.1-4 μ Hg. These solubility data are given in Table II. For the iodide Zr H solubility was determined in the α-phase at 700°–800°C and in the β-phase at 850°C–1000°C. In both phases H solubility decreased with increasing temperature for a given pressure. This was also the case for the Zr-O alloys. For the Zr + 0.14 w/o oxygen alloy, the solubility was determined in the α-phase at 700°–800°C, and in the β-phase at 900°–1000°C. At 850°C the alloy had an α-β structure. The Zr + 0.43 w/o oxygen was investigated in the α range 700°–850°C. Above 850°C the alloy had an α-β structure, and no reliable solubility measurements could be made. Even after this alloy had been heated for 12 hr in an effort to reach equilibrium, results were very erratic. Metallographic examination of these specimens indicated that a β-to-α transformation was occurring during equilibration. Apparently very long times in this temperature range would be necessary to reach equilibrium.

All solubility data for iodide Zr and Zr-O alloys follow Sieverts' Law, which states that the solubility of a diatomic gas in a metal is proportional to the square root of the gas pressure: $S = k \cdot p^{\frac{1}{2}}$. In this equation k is Sieverts' constant with units of $S/p^{\frac{1}{2}}$, S is H solubility in ppm H by weight, and p is pressure in microns of Hg. Fig. 1 and 2 show H solubility plotted against pressure according to Sieverts' Law, for α and β iodide Zr, respectively. All plots are drawn through the origin since there is no solubility at zero H pressure. Slopes of these lines are the Sieverts constants at the various temperatures. Similar plots (not shown) can be drawn for Zr-0.14 w/o oxygen and Zr-0.43 w/o oxygen alloys.

For an exothermic solution of H in metals, solubility can be related to pressure and absolute temperature by the general equation, $\log S/p^{\frac{1}{2}} = A/T + B$, where $S/p^{\frac{1}{2}}$ is Sieverts' constant, T is the absolute temperature, and A and B are constants. Plots of Sieverts' constant against reciprocal temperature for iodide Zr and the Zr-O alloys are given in Fig. 3. It is seen that at a given temperature and pressure, H solubility in α-Zr increases with oxygen content. This is evident because the Sieverts' constant, $S/p^{\frac{1}{2}}$ increases in a similar manner. Apparently, the oxygen in solution expands the α-Zr lattice to make more interstitial sites available for H. However, this is true only at low H pressures, since it has been shown (5, 14)

TABLE II. *Solubility of H in Zr and Zr-O alloys*

Material	Pressure, μ Hg	H solubility at temperature indicated, ppm						
		700°C	750°C	800°C	850°C	900°C	950°C	1000°C
Iodide Zr	0.10	—	—	—	—	5.0	—	—
(0.03 w/o	0.15	—	—	5.2	6.8	6.1	—	—
oxygen)	0.50	13	—	10	—	13	—	12
	1.0	—	—	13	—	18	—	—
	1.5	25	21	—	23	—	—	—
	2.0	—	—	19	—	26	—	24
	4.0	40	32	27	38	34	—	33
Zr + 0.14	0.50	16	12	10	—	11	8.9	6.7
w/o oxy-	1.5	26	21	17	21	18	16	12
gen	4.0	42	31	29	33	31	24	20
Zr + 0.43	0.50	18	13	9.3	8.0	—	—	—
w/o oxy-	1.5	30	22	18	14	—	—	—
gen	4.0	46	36	30	24	—	—	—

that terminal H solubility in the α-phase decreases with increasing oxygen content. Here the total number of interstitial sites available for H is decreased by the addition of oxygen.

Equations for the best straight lines through the points in Fig. 3 were determined by the method of least squares. Values of the constants A and B in the above equation are given in Table III. Heats of solution for H in Zr and Zr-O alloys are also given in Table III. It is seen that the heat of solution increases with increasing oxygen content. For each increase of 0.1 w/o in the oxygen content of α-Zr the heat of solution of H increases by about 500 cal/g-atom. This indicates that there is some interaction between the oxygen and H atoms within the Zr lattice in the concentration range of this work. At higher concentrations of both oxygen and H, Edwards and Levesque (11) found that the heat of solution did not change with oxygen concentration.

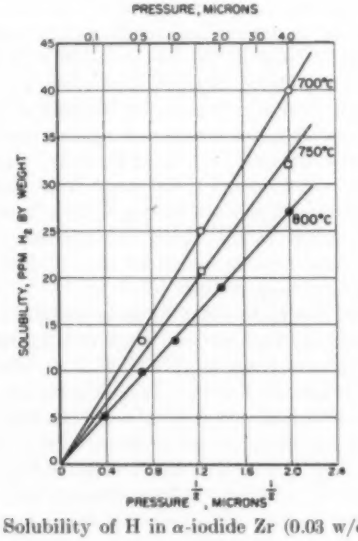

FIG. 1. Solubility of H in α-iodide Zr (0.03 w/o oxygen)

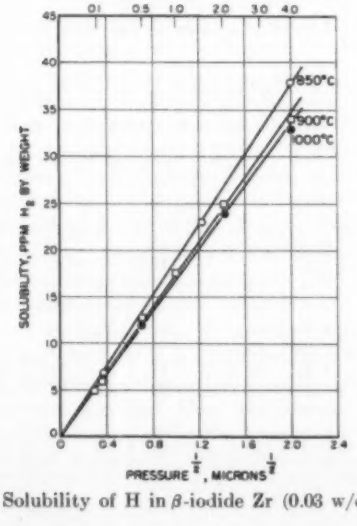

FIG. 2. Solubility of H in β-iodide Zr (0.03 w/o oxygen)

Diffusion of H *in* Zr—*Method.*—The technique used to determine diffusion of H in Zr has been described in the literature (14, 15). Essentially, the method consists of analyzing a H concentration gradient produced in a Zr cylinder by reaction for a predetermined length of time. For this work, Zr cylinders about $\frac{1}{4}$ in. in diameter and $1\frac{1}{2}$ in. long were degassed in a vacuum for 20 hr at 900°C. After this treatment, the residual H content in the metal was 2–3 ppm H by weight. A degassed cylinder was then dry abraded with 240-grit SiC paper. After physical measurements of the specimen were taken, a beaded junction of a Pt-Pt 10% Rh thermocouple was spot welded to one end of the Zr cylinder. The cylinder was then placed in the reaction tube of a modified Sieverts apparatus and heated with a resistance-wound furnace at 800°C for 1 hr in a vacuum of the order of 1×10^{-5} mm Hg. This heat treatment dissolved any superficial oxygen into the metal, leaving a clean active surface. The temperature was then lowered to the temperature of the run and maintained within $\pm$ 5°C of the desired value for the entire experiment. Pure H was then added to the reaction tube at about $\frac{1}{4}$ atm of pressure. At this pressure a thin hydride film could be maintained on the surface. At higher pressures the rate of surface reaction was so rapid that a very thick hydride film was formed.

A specimen was heated in H for a predetermined length of time to prepare a suitable H concentration gradient. At the end of the experiment the furnace was removed and the furnace tube containing the specimen was immediately quenched with a cold water bath.

Lengths equal to the radius of the cylindrical specimen were cut from the ends and discarded. The rest of the sample was machined radially into layers of equal weight. These layers were then analyzed for their H content by the vacuum-fusion method. The outer layers containing the hydride film and β-phase were thin enough to be ignored in calculations (14) of the rate of diffusion. Only the remaining inner layers, containing H that had diffused in the α-phase, were considered. Diffusion coefficients

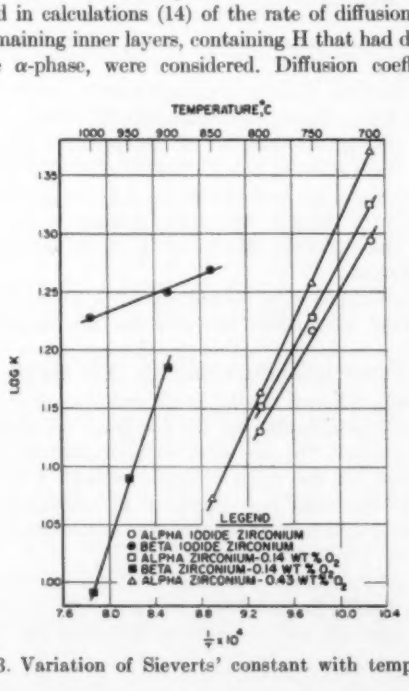

FIG. 3. Variation of Sieverts' constant with temperature

TABLE 3. *Summary of the constants in the equation* $\log S_{ppm}/(p_{micron})^{\frac{1}{2}} = A/T + B$

Material	α-Phase			β-Phase		
	A	*B*	H, cal/g-atom	*A*	*B*	H, cal/g-atom
Iodide Zr	1710	0.463	−7830 ± 400	390	0.921	−1780 ± 130
Zr − 0.14 w/o oxygen	1820	0.545	−8320 ± 270	2960	1.33	−13,540 ± 480
Zr − 0.43 w/o oxygen	2170	0.858	−9920 ± 90	—	—	—

TABLE IV. *Diffusion coefficients for H in α-Zr (gradient technique)*

Time, min	Temp, °C	C_0,* ppm	$D \times 10^6$ cm²/sec
75	305	86	1.7
50	350	140	2.0
35	410	270	3.7
13	446	340	5.2
10	486	530	6.9
10	567	470	9.7
6	610	430	13

* C_0, terminal solubility.

TABLE V. *Degassing coefficients of H in α-Zr*

Temp, °C	$D \times 10^6$ cm²/sec
635	2.9
690	7.4
717	9.8
745	10
780	21

were determined by the graphical method (14) using the average H concentrations of each layer, the average radii of the layers, and the time of diffusion.

An alternative method based on degassing rates (16) was used to determine rates of diffusion in iodide Zr. The technique and apparatus were the same as those described previously (13). The rate of H evolution from ¼ in. diameter Zr cylinders initially containing 46 ppm H by weight was measured. The diffusion (degassing) coefficient was calculated from the rates of evolution of H into a vacuum of 10^{-2}–10^{-6} mm Hg at various temperatures.

Results and discussion.—The diffusion of H in α-Zr was investigated in the range 305°–610°C by the gradient technique. The diffusion coefficients that were obtained are given in Table IV. Values of C_0 are also given. As defined previously (14), C_0 is the saturation concentration maintained at the surface of the α diffusion layer during preparation of the gradient. At higher temperatures, data were not obtained because of the rapidity of diffusion. The time needed to quench the specimen adequately was too long for preparation of a suitable diffusion gradient (which takes less than 5 min). At temperatures below 300°C, prepared gradients showed erratic behavior and could not be fitted to the diffusion theory.

Table V gives the degassing coefficients obtained in the range 635°–780°C. No data could be obtained at lower temperatures since very little or no H was evolved from a specimen. At higher temperatures, above 780°C, diffusion was too rapid to permit use of the degassing technique.

Variation of the diffusion coefficient with temperature

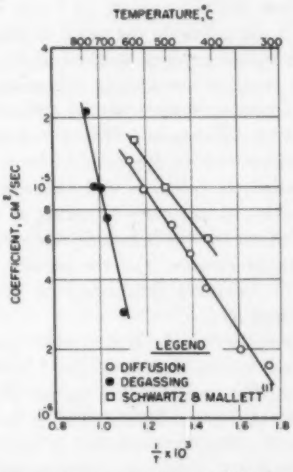

FIG. 4. Temperature variation of diffusion and degassing coefficients for H in Zr.

can be evaluated by the equation, $D = D_0 \exp(-Q/RT)$. Fig. 4 is a plot of logarithms of the diffusion coefficient against reciprocal temperature for the data obtained by the gradient technique. Results are compared with the coefficients reported by Schwartz and Mallett (1).

Degassing coefficients are also plotted in Fig. 4. It is seen that the gradient and degassing data give separate curves having quite different slopes. This indicates that the two sets of data represent different rate-controlling processes. Although the experimental temperature ranges do not overlap, the metal is single-phase α-Zr throughout. Therefore, if the controlling processes were diffusion in the metal (true diffusion mechanism), both sets of data should have the same slope and form a continuous curve for all temperatures.

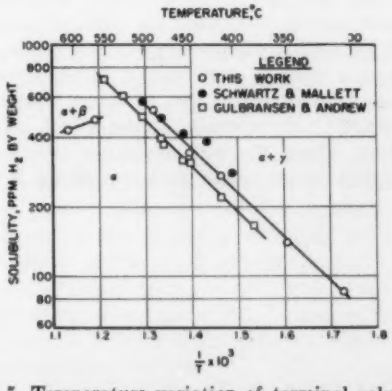

FIG. 5. Temperature variation of terminal solubility of H in α-Zr.

It is believed that the gradient method, which is based on direct analysis, gives the more nearly true diffusion coefficient. In the degassing technique, it is quite possible that surface effects are important in the determination of degassing rates. The rate of desorption of H from the metal surface may be the controlling process and not diffusion in the metal. Some such surface effect is evidenced by the fact that little or no H could be evolved from a Zr cylinder below 630°C at about 10^{-5} mm Hg, while it is known that H can diffuse in the metal at lower temperatures, as shown by the gradient method. It is evident that one should be wary of considering degassing as a pure diffusion phenomenon. Studies of the diffusion of H in Fe summarized by Johnson and Hill (17) showed in that case the controlling step in degassing to be a function of diameter. Degassing of cylinders with diameters less than ½ in. was dependent on processes occurring at the surface, while for larger diameters the degassing rate was dependent on a true diffusion process. For the present work with Zr, the effect of specimen dimensions on the degassing rate was not determined.

In Fig. 4, equations for the best straight lines through the various sets of points were determined by the method of least squares. The experimental energy of activation for diffusion in the range 305°–610°C is 7060 ± 260 cal/mole, and the diffusion coefficient in cm²/sec is $7.00 \times 10^{-4} \exp -7060/RT$. This is in fair agreement with the 5700 cal/mole calculated from the work of Schwartz and Mallett (1), whose studies were made with high-Hf Zr. The experimental energy of activation for the degassing of Zr in the range 635°–780°C is 22,000 ± 3,000 cal/mole, and the degassing coefficient in cm²/sec is $0.59 \exp -22{,}000/RT$.

Terminal solubility of H *in* α-Zr.—In previous studies (1, 14) it was pointed out that the terminal solubility (solubility limit) of H in α-Zr is the concentration in the α-phase at the α-3 interface. Therefore, the calculated values of C_0 obtained in the gradient study are the approximate terminal solubilities of H in α-Zr. These values are given in Table IV and plotted along with data of other investigators in Fig. 5. At the lower temperatures (300°–500°C) there appears to be good agreement between the present work and that of Schwartz and Mallett, who also obtained solubilities from diffusion studies. Less close agreement was obtained with the data of Gulbransen and Andrew (6), who used Sieverts plots and pressure-temperature plots to determine the terminal solubilities. Solubilities at the lower temperatures represent the boundary between α and α + γ phases in the Zr-H system (8).

It is also seen in Fig. 5 that at higher temperatures (571° and 610°C) the solubility decreases with increasing temperature. These terminal solubilities represent the boundary between the α- and the α + β-phases. However, these limited data do not permit prediction of the temperature of the isotherm where the α, β, and γ phases are in equilibrium. Vaughan and Bridge (8) show this temperature to be 560° ± 10°C.

The best equation expressing variation of terminal solubility with temperature in the range 305°–486°C is

$$\log C_0 \text{ (ppm } H_2 \text{ by weight)} = -1880/T + 5.18$$

The heat of solution for H in α-Zr obtained from this equation is 8600 ± 200 cal/g-atom. This is in very good agreement with the 8616 cal/g-atom obtained by Gulbransen and Andrew.

Acknowledgments

This work was performed under AEC Contract W-7405-eng-92. The authors gratefully acknowledge the assistance of Mr. B. G. Koehl in making the experimental diffusion gradients. Special thanks are given to Mr. W. R. Hansen for obtaining the experimental degassing data.

Manuscript received April 2, 1956.

Any discussion of this paper will appear in a Discussion Section to be published in the December 1957 JOURNAL.

REFERENCES

1. C. M. SCHWARTZ AND M. W. MALLETT, *Trans. Am. Soc. Metals*, **41**, 306 (1945).
2. W. L. MUDGE, JR. in "Zirconium and Zirconium Alloys", p. 146, American Society for Metals, Cleveland (1953).
3. A. D. SCHWOPE, *ibid.*, 292.
4. J. H. DEBOER AND J. D. FAST, *Rec. trav. chim.*, **55**, 350 (1936).
5. M. N. A. HALL, S. L. H. MARTIN, AND A. L. G. REES, *Trans. Faraday Soc.*, **41**, 306 (1945).
6. E. A. GULBRANSEN AND K. F. ANDREW, *Trans. Am. Inst. Mining Met. Engrs.*, **203**, 136 (1955).
7. R. K. EDWARDS, P. LEVESQUE, AND D. CUBICCIOTTI, *J. Am. Chem. Soc.*, **77**, 1307 (1955).
8. D. A. VAUGHAN AND J. R. BRIDGE, *Trans. Am. Inst. Mining Met. Engrs.*, **206**, 528 (1956).
9. S. L. H. MARTIN AND A. L. G. REES, *Trans. Faraday Soc.*, **50**, 343 (1954).
10. C. F. BEVINGTON, S. L. MARTIN, AND D. H. MATHEWS, *Proc. Intern. Congr. Pure and Appl. Chem. 11th Congr. London 1947*, **1**, 3 (1950).
11. R. K. EDWARDS AND P. LEVESQUE, *J. Am. Chem. Soc.*, **77**, 1312 (1955).
12. E. A. GULBRANSEN AND K. F. ANDREW, *This Journal*, **101**, 560 (1954).
13. C. B. GRIFFITH AND M. W. MALLETT in "Vacuum Metallurgy", p. 147, The Electrochemical Society, Inc., New York (1955).
14. M. W. MALLETT, E. M. BARRODY, H. R. NELSON, AND C. A. PAPP, *This Journal*, **100**, 103 (1953).
15. M. W. MALLETT, J. BELLE, AND B. B. CLELAND, *ibid.*, **101**, 1 (1954).
16. A. DEMAREZ, A. G. HOCK, AND F. A. MEUNIER, *Acta Metallurgica*, **2** (2), 214 (1954).
17. E. W. JOHNSON AND M. L. HILL, *ibid.*, **3**, 99 (1955).

Mechanisms of Aqueous Corrosion of Aluminum at 100°C

K. M. Carlsen[1]

Joint Establishment for Nuclear Energy Research, Lillestrøm, Norway

ABSTRACT

Various alloys of Al, as well as superpurity Al material, have been tested in aqueous solutions at 100°C. Samples have been polarized cathodically and anodically to study the effect of cathodic and anodic reactions, respectively, on the corrosion behavior. Results are interpreted as showing that the alkalinity produced at the cathodes facilitates film breakdown in these places. Consequently, alloys containing cathodic constituents were attacked where these constituents were situated, while polycrystalline superpurity material was attacked in the grain boundaries. The influence of bulk *p*H and inhibitors is discussed in some detail.

There is general agreement (1–3) that at higher temperatures the aqueous corrosion resistance of Al is smaller the greater the purity. Draley and Ruther (2) have drawn attention to the importance of providing cathodic sites, and in this way greatly clarified the difference in behavior between pure and impure material.

As for the influence of the composition of the aqueous phase, it is known that additions of H_2SO_4 and certain inhibitors produce beneficial effects, but it is not known for certain exactly how these additions influence corrosion behavior. However, it is clear that the idea of H_2– as the chief offender is not sufficient to explain all the observations satisfactorily.

Thus, there seems to be a need for a closer study of the corrosion mechanisms of various grades of materials in liquids of varying compositions, and it was with this in mind that the present investigation was started. Since the difference between pure and impure material is very pronounced at 100°C (4), it was hoped that results obtained at this temperature could be used to predict the behavior at higher temperatures.

There are obvious advantages in working at 100°C; no autoclaves are necessary, and corrosion reactions are so slow that they can be studied in detail by means of the microscope.

Experimental

The materials used were sheet of superpurity Al (99.99% purity, from British Aluminium, Ltd.) and Al alloys. Alloys were made from ingots of 99.99% purity Al (supplied by A/S Vigelands Brug), and high conductivity Cu, electrolytic Ni (99.98%), electrolytic Fe (British Drug House), and silicon powder (99.5% purity, from A/S Bjölvefossen), respectively. The alloys had the following compositions: 1.04% Ni, balance Al; 1.95% Cu, balance Al; 0.93% Fe, balance Al; 1.02% Si, balance Al, hereafter referred to as Al—1% Ni, Al—2% Cu, Al—1% Fe, Al—1% Si alloys, respectively.

Alloys were cast in graphite moulds and rolled to a thickness of approximately 1 mm. All test samples were given an anneal at 450°C for 1 hr and allowed to cool in the furnace, except in cases where cold-worked material was desired.

Some single crystals of superpurity Al were kindly supplied by R. W. K. Honeycombe, University of Sheffield.

All samples were carefully electropolished in a bath containing 100 ml perchloric acid (sp gr 1.54) and 900 ml ethyl alcohol.

In tests at 100°C, samples were suspended in Pyrex flasks fitted with reflux condensers. In some cases the samples were externally polarized making them anode and cathode, respectively, by means of a d-c potential, keeping the current density constant during the experiment.

After exposure, the samples were examined by means of a metallographic microscope.

Results

Superpurity Metal

On polycrystalline material immersed in distilled water at 100°C there develops during the first hours a pattern of spots, together with a delineation of grain boundaries. Fig. 1 and 2 show two samples during the first stages of development. After the pattern has formed, the matrix corrosion apparently slows down, while the attack on the grain boundaries continues (Fig. 3 and 4). After periods as long as 130 hr the grain boundary attack seems to fall off somewhat, while a blurring of the pattern suggests that the matrix has started corroding in a more uniform way.

These observations at 100°C are in agreement with those of other workers obtained at higher temperatures, as far as the grain boundary attack is concerned.

At temperatures as high as 230°C, single crystals of high-purity material are attacked very seriously, showing that grain boundary attack is not necessary for disintegration to occur.

Some samples were deformed to see if slip lines were preferentially attacked, but this was not found to be the case.

When polycrystalline material is cathodically polarized at a current density of approximately 0.1 ma/cm², grain boundaries are preferentially attacked as shown in Fig. 5. Besides a pattern of lines is found, nearly all of them joining each other at an angle of 90°. Because of this angular relationship, it is believed that they result from the relief of two-dimensional stresses.

[1] Present address: Pigments Dept., E. I. du Pont de Nemours & Co., Wilmington, Del.

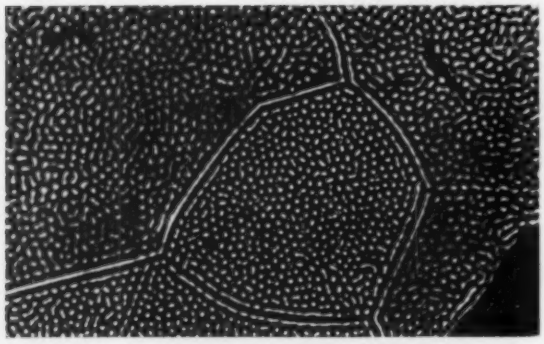

FIG. 1. Superpurity sample 3 hr at 100°C in distilled H_2O. 405×.

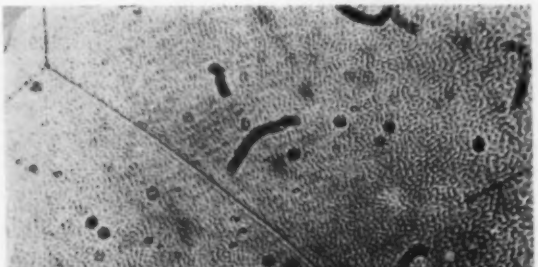

FIG. 2. Superpurity sample 10 min at 100°C in distilled H_2O. 765×.

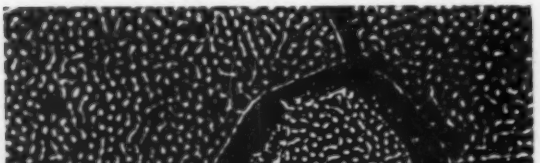

FIG. 3. Same sample as Fig. 1, but after 68½ hr at 100°C in distilled H_2O. 405×.

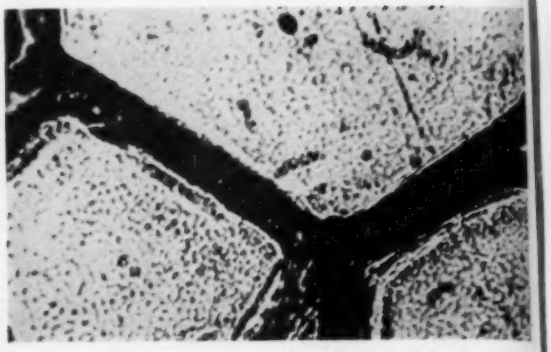

FIG. 4. Same sample as Fig. 2, but after 48½ hr at 100°C in distilled H_2O. 765×.

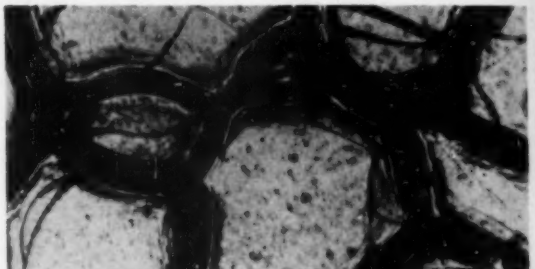

FIG. 5. Superpurity material, cathode for 48 hr at 100°C in distilled H_2O. 135×.

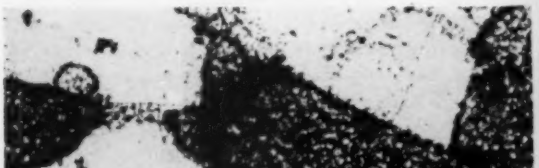

FIG. 6. Single-crystal superpurity material cathodically polarized in H_2O at 100°C. 135×.

When a single crystal was polarized cathodically at a current density of 0.16 ma/cm², much the same pattern of lines was found again. After 24 hr, a fairly thick layer of corrosion products had formed, but this layer was not adherent, and could be brushed off without difficulty. Fig. 6 shows the surface where part of the oxide layer has been removed, and part of it remains, showing up as dark bits. The layer is fragmented by lines very similar to the cracks found on ceramic objects. A notable feature was that the attack on the cathode was orientation dependent, being stronger on two of the crystal faces than on the remaining two faces (the single crystal was in shape of a square rod).

Polycrystals and single crystals show identical behavior when anodically polarized at 0.16 ma/cm²; in both cases pits, or rather heaps of oxide covering the pits, develop (Fig. 7). With time the number of pits increases somewhat; they also grow in size. Although the corrosion products obviously do not protect completely the underlying metal, as shown by the continued growth of the heaps, there is

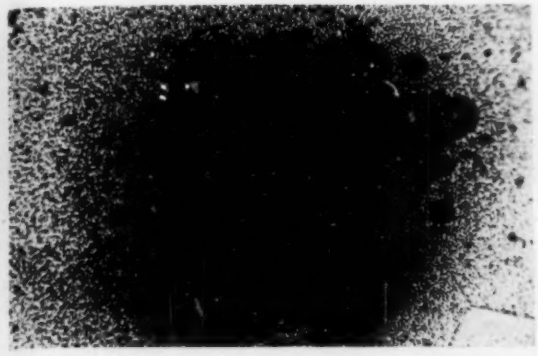

FIG. 7. Superpurity material, anode for 6 hr at 100°C in distilled H_2O. 285×.

some adherence to the metal, and they cannot be brushed off in the same way as are the cathodic corrosion products.

Alloy Materials

Rolled alloys with Ni and Fe additions show similar microstructures, viz., eutectics of $NiAl_3$ and Fe_2Al_7, respectively, with Al, embedded in a matrix of pure Al. The structure of an uncorroded Al-1% Ni sample is shown in Fig. 8. When such alloys are exposed to water at 100°C, the material in the eutectics is preferentially attacked both on cold worked and annealed specimens and the matrix is only very slightly attacked, as shown in Fig. 9. At 230°C, the eutectic regions are again attacked, but the matrix also starts to corrode in a more general manner; indeed, on some specimens the matrix seems to have suffered more attack than the eutectic regions. When Al-1% Ni samples were made cathodes at 0.1 ma/cm² they were severely attacked in the eutectic regions and anodic samples developed pittings.

The Al-Cu alloys show a microstructure different from that of Al-Ni and Al-Fe alloys. In the water-quenched condition no second phases can be seen; correspondingly, the attack on quenched specimen is fairly uniform to start with. At 100°C, the attack in the initial stages gives rise to beautiful interference colors when viewed in the microscope. After some time pits develop. These pits are not covered with corrosion products, nor does it seem that the

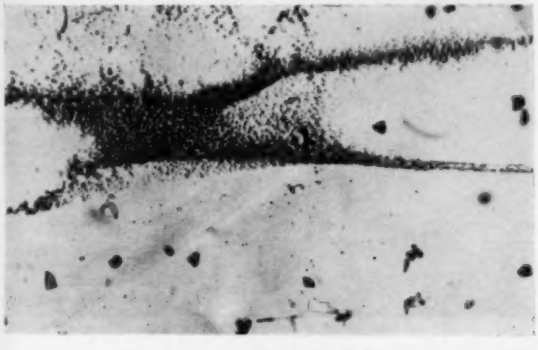

FIG. 8. Al-1% Ni-alloy, uncorroded. 285×

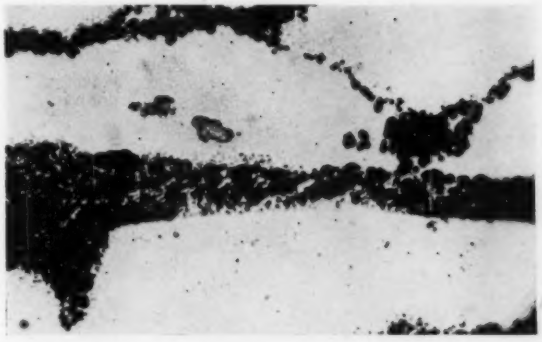

FIG. 9. Al-1% Ni-alloy, 21 hr in H_2O at 100°C. 285×

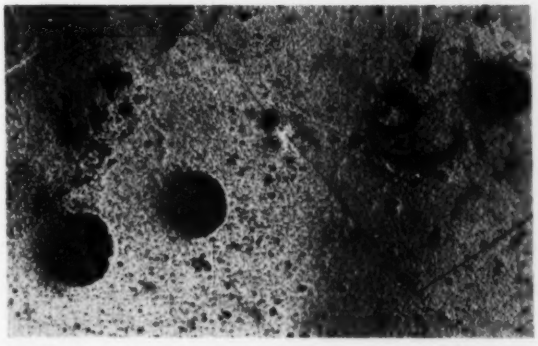

FIG. 10. Al-2% Cu-alloy (water-quenched) 45½ hr at 100°C in H_2O. 285×.

corrosion products have collected around the pits. Fig. 10 shows some big pits and numerous small ones. By using oblique light in the microscope one gets a very clear impression of the shape of the pits; unfortunately, it is difficult to get good photomicrographs with this type of illumination.

On specimens which had been furnace cooled (and consequently were overaged), pits developed very quickly. In addition an etching effect as shown in Fig. 11 was found,

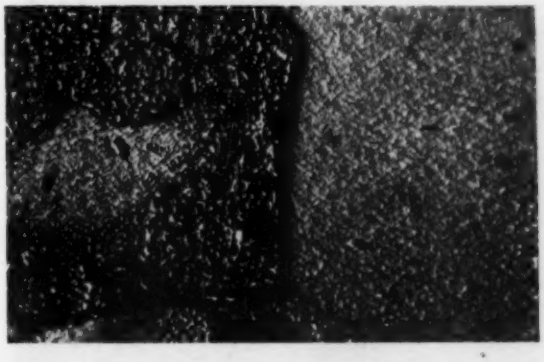

FIG. 11. Al-2% Cu-alloy (furnace-cooled) 21 hr at 100°C in H_2O. 765×.

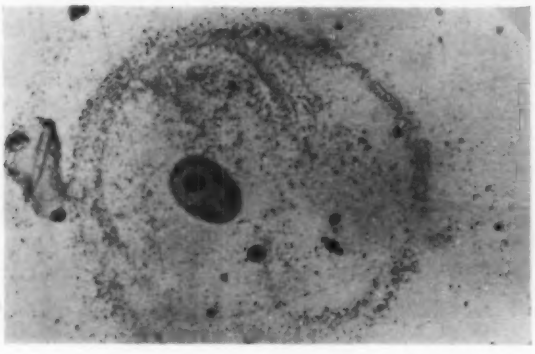

FIG. 12. Same sample as Fig. 10, 45½ hr at 100°C in H_2O. 285×.

where some regions were much more attacked than the neighboring matrix.

One might think that the development of pits was cathodically stimulated, because of precipitates acting as cathodes; this would serve to some extent as an explanation of the absence of corrosion products. Results on externally polarized specimens might seem to confirm this view. On the cathodic sample, the same type of pits are found as on unpolarized samples. Admittedly, such pits are also found on the anodically polarized sample, but here one finds in addition large pits covered with corrosion products, of the same shape as the pits found on anodic samples of pure material.

Fig. 12 shows a ring-like type of attack very frequently found on Al-Cu alloy samples (and occasionally on cast Al-Ni alloys). Sometimes the rings are not full, having the shape of a crescent.

At temperatures higher than 200°C, there is considerable aggregation of corrosion products on the surface, making it difficult to obtain a clear idea of the structural details of the attack.

When rolled Al-1% Si alloy samples are tested in overaged condition, the attack appears to be concentrated in the regions around the Si particles, although attack is also found elsewhere. The attack is probably of a type giving rise to very small pits, which at low magnifications gives the impression of a more or less general attack.

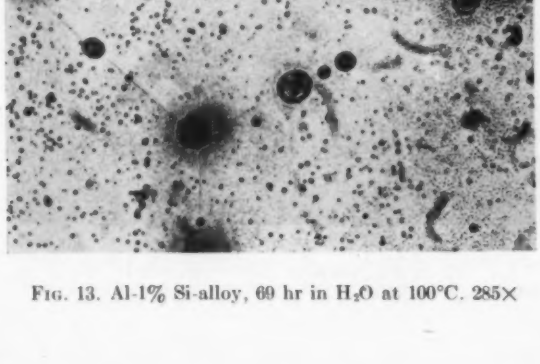

FIG. 13. Al-1% Si-alloy, 69 hr in H_2O at 100°C. 285×

In one case larger pits are observed, namely, after fairly long exposures of solution-treated and water-quenched specimens. Fig. 13 shows these pits, which are found on the grain boundaries and give an impression of grain boundary attack when viewed with the unaided eye. In some way these pits may be tied up with precipitation of Si in the grain boundaries. The structure of aged samples shows precipitate in the grain boundaries, with a denuded zone running along the boundaries.

When solution-treated and water-quenched specimens are cathodically polarized at a current density of approximately 0.16 ma/cm², the same type of intergranular attack is found as is observed on superpurity material. When furnace-cooled specimens are used the cathodic grain boundary attack is not so pronounced; instead, the matrix in the grains suffers corrosion.

Anodically polarized samples develop pits covered with corrosion products in the same manner as found for all the other materials.

Effect of Liquid Composition

As stated earlier, superpurity material suffers intergranular attack in distilled water at 100°C. When the *p*H is lowered to 4 by addition of H_2SO_4, this intergranular attack is suppressed to a great extent, while the matrix corrosion within the grains probably increases somewhat. Fig. 14 shows that the grains are attacked at different rates.

At *p*H 3, beautiful interference colors are produced in the grains, and grain boundary attack is slight.

At *p*H 2, there is considerable attack both in grain boundaries and in the grains. However, the grain boundary attack is of a type different from that met with in neutral water. Fig. 15 and 16 serve to emphasize the difference between the two types of grain boundary attack. It is believed that in the case of neutral water cathodic properties are responsible for the attack; anodic properties are responsible in the acid case.

Polarization experiments were carried out at various *p*H's and at a current density of 0.16 ma/cm². At *p*H 4, results on both cathodes and anodes are similar to results in distilled water, although the grain boundary attack on the cathode is less severe than in distilled water. At *p*H 3, the cathodic attack has not changed much, but on the

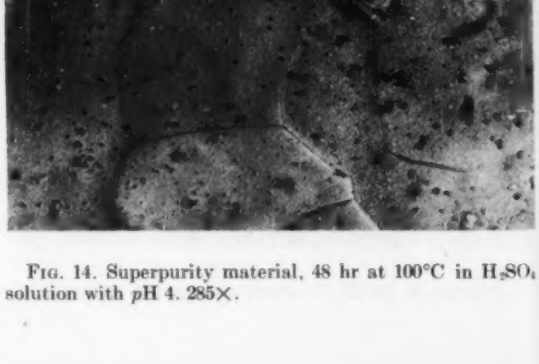

FIG. 14. Superpurity material, 48 hr at 100°C in H_2SO_4 solution with *p*H 4. 285×.

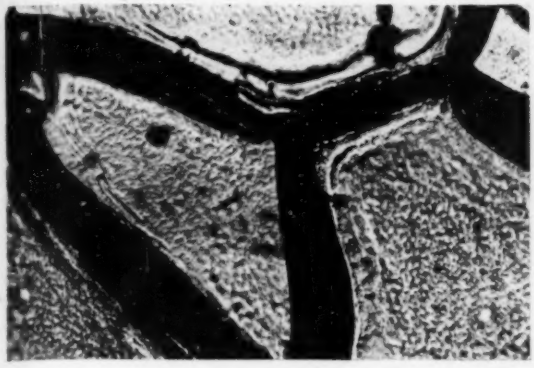

FIG. 15. Superpurity material 138 hr in H_2O at 100°C. 765×.

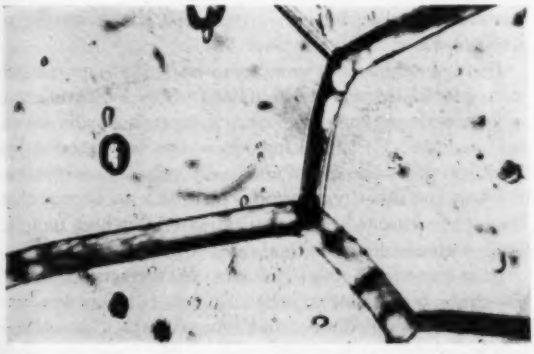

FIG. 16. Superpurity material 7 hr at 100°C in HCl solution with *p*H 2. 764×.

anode there are no longer pit-like breakdowns; instead interference colors can be seen in the microscope. At *p*H 2, there is general attack on both cathode and anode; no differences between the electrodes can be detected.

In NaOH solution (*p*H 10.7) the cathode is attacked apparently much more than the anode. When polarization experiments were carried out in 0.1% NaCl solution and in 1% Na_2SO_4 solution, respectively, grain boundary attack was observed on the cathodes, but to a smaller extent than in distilled water. On the anode in the sulfate-solution there was no breakdown of the type usually found on the anodes.

As reported elsewhere (3), it has been found that a 0.5% $K_2Cr_2O_7$ + 0.5% sodium silicate solution is a good inhibitor. Polarization experiments in this solution show quite strong general matrix attack on the cathode, but no attack whatsoever could be detected on the anode. Fig. 17 shows the cathode after 4 hr at 100°C; it is evident that the grains corrode at different rates. Microscopical examination at earlier stages show that attack starts in the form of numerous pits.

The same features are found in 1% $K_2Cr_2O_7$ solution, strongly indicating that the effects are due to the chromate.

Still another interesting effect was found in these solutions. As stated above, anodes from the solutions showed no attack, but when these anodes were exposed subsequently to boiling distilled water, strong general matrix attack similar to the cathodic attack was found, much stronger than and different from that found on samples which had not been treated anodically in advance.

FIG. 17. Superpurity material, cathode for 4 hr in 0.5% $K_2Cr_2O_7$-0.5% sodium silicate solution. 285×.

When 1% $K_2Cr_2O_7$ solution is made acidic (*p*H 2.4) by adding H_2SO_4, both anodes and cathodes suffered very little attack. However, when the chromate solution is made alkaline (*p*H 10.5) by adding NaOH, the cathode suffers strong grain boundary attack, while the anode suffers general attack.

Results from experiments in a solution of CrO_3 (*p*H 1.1) were very similar to those from the acid $K_2Cr_2O_7$ solution.

Experiments in 1% sodium silicate solution with *p*H 10.8 show that the anode is protected to some extent by the silicate addition. Some parts of the anode were virtually unattacked after 20 hr at 100°C at a current density of 0.1 ma/cm². It is not quite certain that an attack on the cathode is similarly reduced; it is probably correct to say that the general rate of attack on the cathode is reduced, while the grain boundary attack is still very pronounced.

Discussion

Role of Film Breakdown

Since it has been found that O_2 plays no significant role in high temperature corrosion, and since it has been reported from various sources (1, 2) that the corrosion product at high temperature is boohmite, the reaction can be written as

$$Al + 2H_2O \rightarrow AlO{\cdot}OH + \tfrac{3}{2} H_2$$

with the corresponding anodic and cathodic reactions

$$Al + 2H_2O \rightarrow AlO{\cdot}OH + 3H^+ + 3e \text{ and}$$

$$3H^+ + 3e \rightarrow \tfrac{3}{2}H_2$$

The experimental results quoted in the previous section nearly all have one thing in common; the attack is never uniformly and homogeneously distributed over the surface on a microscopical scale, nor, in most cases, on a macroscopical scale. Thus, in places where the attack is appreciable, corrosion has proceeded in some other way than by the continuous building up of a film. Let this attack be

called film breakdown, indicating that in some way or another the ordinary film growth has been interrupted.

In the previous section it was found that the film breakdown on cathodic samples differed from that on anodic ones. Let these phenomena be called cathodically stimulated breakdown and anodically stimulated breakdown, respectively.

Anodically stimulated breakdown.—The microscopical appearance is [illegible]ally as seen in Fig. 7. On superpurity material it seem[illegible]to have no relation to the grain boundaries, and experiments on single crystals indicate that crystal orientation does not have any effect on the occurrence of the breakdown. In the alloys containing Ni, Cu, or Fe, the breakdown seems to lie near the cathodic constituents, but this cannot be the only reason for breakdown, since the regions around the cathodic constituents are always attacked somewhat, without the attack developing into the large type of breakdown as exemplified by Fig. 7.

To some extent, the anodically stimulated breakdown can be looked on as caused by the inability of the solution to deliver ions for the building up of a protective oxide layer. In neutral solutions of tartaric and boric acid and in chromate solutions, such breakdowns are not observed, apparently because of the ability of these solutions to provide O^{--} ions for the formation of Al_2O_3 films, an explanation suggested by Huddle (5).

It is felt that pit formation cannot be explained satisfactorily without assuming that some autocatalytic process is involved. Edeleanu and Evans (10) and Huddle (5) point out that local acidity may be produced at the anode, and this acidity may, indeed, be the autocatalytic effect responsible for the pit formation.

Cathodically stimulated breakdown.—This type of attack occurs on samples which have been polarized cathodically in neutral solutions. On superpurity material it manifests itself as grain boundary attack, on Al alloys containing cathodic constituents as attack around these constituents, and as general attack on single crystals.

Having thus established that the attack is concentrated around the cathodes, one may look for an explanation of this behavior. One such explanation has been furnished by Draley and Ruther (2), who assume that the H produced is responsible for the stimulation of attack. A second explanation is that the increased OH^- concentration resulting from the removal of protons is the responsible factor, as suggested by a number of investigators, e.g., Groot (11).

It is believed that (*a*) the cathodic attack on single crystals, (*b*) the shape of attacked grain boundaries in polycrystalline pure material, (*c*) the fact that cathodic attack is reduced by lowering the *p*H, and (*d*) the attack around the cathodic constituents in Al alloys, all point away from H as the main factor in causing the cathodically stimulated attack observed in these experiments.

It is assumed, therefore, that the factor responsible for the attack is the increased concentration of OH^- in the immediate vicinity of the cathodes. The detrimental effect of OH^- ions on the corrosion of Al is well known, and experiments show that deviations from neutrality on the alkaline side are far more serious for the corrosion resistance than deviations on the acid side.

When protons are removed at the cathode, more water molecules dissociate to keep the ionic product constant, resulting in a more alkaline solution. At the same time, there will be an excess of negatively charged ions in the liquid next to the cathode, and the field set up by these ions will attract positively charged ions from the rest of the liquid. It is seen that a stationary state is reached, with a field in the liquid just strong enough to produce a current of positive ions toward the cathode, equivalent to the removal of protons at the cathode. Everything being equal, it is expected that the higher the purity of the water, and, correspondingly, the lower the conductivity, the stronger will be the field needed to force the necessary number of positive ions toward the cathode. Since the field is set up by OH^- ions, this means that the higher the purity of the water, the higher the local OH^- concentration to be expected. This may explain in part the aggressiveness of distilled water relative to pure Al.

Disintegration of superpurity material.—As seen from the micrographs, there is great similarity between corrosion of unpolarized specimens and attack on cathodically polarized samples. No such similarity exists between the behavior of unpolarized and anodically polarized specimens. For this and other reasons, it is justifiable to assume that the rapid corrosion of superpurity material in high temperature water is due to cathodically stimulated attack.

In polycrystalline material, the disintegration starts at the grain boundaries which, as pointed out earlier, are sites for the cathodic reaction. As the attack penetrates into the metal in a notch-like fashion, the tip of the notch will be the cathode, producing alkalinity where it is most dangerous. Corrosion products have greater volume than the metal from which they are formed, and tend to break up the metal, as evidenced by the deformation of the metal along the grain boundaries, seen on the photographs. It is not known whether the primary factor in the penetration of attack is the action of OH^- ions at the tip of the notch or the expansive action of the corrosion products. The fact that single crystals also disintegrate would seem to be in favor of the first hypothesis.

Lavigne (7) has pointed out that there is some resemblance between grain boundary attack on superpurity material in acid and in distilled water. In the author's opinion this resemblance is purely superficial. In acid, the grain boundaries are very evenly attacked, the metal dissolving away to yield a smooth, possibly U-shaped groove, the reason for attack probably lying in the smaller anodic polarization of the boundaries as compared to the matrix. In distilled water, on the other hand, the metal is broken up by the corrosion products, and the relevant factors in this case are thought to be the cathodic properties of the grain boundaries, as discussed above.

*Effect of Bulk p*H

As is well known, Al hydrates are soluble both in acid and alkaline solutions. The mechanisms of the solution of Al hydrate in acid cannot be said to be understood fully, and the concept of a solubility product of $Al(OH)_3$ will un-

doubtedly be found unsatisfactory as a description of the phenomena taking place. However, since little is known about the matter, the solubility product is used as a starting point for this discussion.

Assuming ideal conditions, the concentration of OH^- enters the product in 3rd power, thus showing that small decreases in OH^- concentration appreciably increase the concentration of Al^{+++}. Also, the solubility in acid is not due to the presence of H_3O^+ but to the absence of OH^-. Thus, if one could conceive of an acid with a low *p*H, but in which the *p*OH could be kept at 7, a protective layer of Al hydrate should be formed, which would prevent corrosion. Such an acid is impossible of course, but when an acid solution is heated to higher temperatures, the result is in fact somewhat similar to this unrealistic acid. The *p*H remains practically constant, if the acid is a strongly dissociating one, while the *p*OH decreases with increasing temperature. Consequently for Al, an acid should be less dangerous from a corrosion point of view the higher the temperature, provided the solubility product of $Al(OH)_3$ remained constant as a function of temperature.

For solutions on the alkaline side, there would be no corresponding effect, except perhaps for solutions very close to neutrality.

In distilled water, the *p*OH decreases markedly with temperature, and this may bring about serious corrosion, since it is known from low temperature work that deviations from *p*H 7 on the alkaline side is much more dangerous than deviations on the acid side. The reason for this behavior is not quite clear. Apparently it is connected with the greater rate of dissolution of the hydroxide in alkalies than in acids: in other words, it is more a question of dissolution kinetics than of equilibrium solubilities.

Thus, with increasing temperature of exposure the range in which the Al hydrate is able to protect the metal is displaced toward more acid solutions. It has been found by Draley and Ruther (8) that the *p*H of minimum corrosion is displaced toward lower values as the temperature is increased.

Apart from the effect of increasing OH^- concentration as a function of temperature, it is possible that a low *p*H is desirable also for another reason, viz., because of the alkalinity produced in the cathodic reaction. Indeed, there is evidence that even at temperatures as low as 100°C, a low *p*H arrests the damaging intergranular attack on superpurity metal met with in distilled water. Although the general rate of corrosion may be greater when the solution is made acidic, the total damage may nevertheless be smaller because of its more uniform nature. It appears, for instance, that superpurity metal suffers less dangerous attack in HCl with *p*H 2 at 100°C than in distilled water.

There is strong evidence that the anion of the acid plays an important role in corrosion, for instance if the anion can act as a carrier for O^{--} ions, as suggested by Huddle (5), but it is also to be expected that the anion influences corrosion by determining the nucleation conditions near the surface.

Effect of Inhibitors

The compounds which inhibit corrosion are to some extent those which can be used for building up anodically oxide films on Al. The action of such anions as SO_4^{--} or CrO_4^{--} may very well be tied up with their ability to donate O^{--} ions to the oxide lattice, as suggested by Huddle (5).

It is found that chromate additions do not protect annealed superpurity Al at 230°C, and it is also found that, when Al is made cathodic in chromate solutions at 100°C, the metal is attacked. These facts seem to suggest that when chromate is present where the cathodic reaction takes place on the Al surface, no protection, in fact the opposite action, is found. Possibly this is connected with the difference in potential needed to liberate H from Al and cathodic impurities, respectively; when no cathodic impurities are present, the potential may be negative enough to reduce hexavalent Cr to trivalent, producing alkalinity as a result of liberation of four O^{--} ions. (The green color found on superpurity specimens which had disintegrated in chromate solutions indeed points to the presence of trivalent Cr.) This would mean then that, in order to act in a protective way, there must be present sufficient amounts of cathodic impurities with a low H overpotential to give a compromise potential which is relatively positive.

When the chromate solution is made acid, there is no attack on samples made cathodic by external polarization, indicating that OH^{--} ions produced may indeed be the factor responsible for the breakdown. It is not clear whether Cr ions as such are incorporated in the protective layer. In any case, the experiments mentioned above where chromate treated samples were found to corrode faster than nontreated samples would indicate that the chromate plays a more active role than merely being an oxygen donator.

Silicate as an inhibitor presumably acts in a way different from chromate. Work is being carried out at present to clarify the matter, and the results hitherto obtained suggest that SiO_2 is incorporated in the surface layer (9).

Effect of Alloying Additions

In the light both of the observations described above on the effect of cathodic polarization on corrosion of superpurity Al, and of the reported success of Al-Fe, Al-Ni, and Al-Cu alloys, there seems to be no doubt that these alloying elements protect the metal by providing sites for the cathodic reaction.

Silicon can to some extent increase the corrosion resistance of superpurity metal toward water. Most probably it does not act as a cathodic impurity, but its effect on corrosion cannot be said to be understood.

Acknowledgment

The author wishes to acknowledge with thanks the valuable help given by J. L. H. Grinn and T. O. Wulff in carrying out the experiments. The author would also like to thank Mr. Grinn for fruitful discussions.

Manuscript received March 20, 1956. This paper was prepared for delivery before the Cleveland Meeting, September 30 to October 4, 1956.

Any discussion of this paper will appear in a Discussion Section to be published in the December 1957 JOURNAL.

REFERENCES

1. R. A. U. Huddle and N. J. M. Wilkins, M/R 1669, Atomic Energy Research Establishment, Harwell, Berkshire, England.
2. J. E. Draley and W. E. Ruther, Geneva Conference on the Peaceful Uses of Atomic Energy, P/535. Vol. 9, p. 391 (1955).
3. K. Carlsen, *ibid.*, P/880, Vol. 9, p. 397 (1955).
4. J. M. Bryan, *J. Soc. Chem. Ind.*, **69**, 169 (1950).
5. R. A. U. Huddle, Geneva Conference on the Peaceful Uses of Atomic Energy, P/411, Vol. **9**, p. 403 (1955).
6. K. Carlsen, Unpublished work.
7. M. J. Lavigne, *Met. Prog.*, **64** (3), 84 (1953).
8. J. E. Draley and W. E. Ruther, ANL-5001, Argonne National Laboratory, Lemont, Illinois.
9. J. Markali, Unpublished work.
10. C. Edeleanu and U. R. Evans, *Trans. Faraday Soc.*, **47**, 1121 (1951).
11. C. Groot, HW-33881, Hanford Atomic Products Operation, General Electric Co., Richland, Wash. (1955).

Rates of Oxidation of Germanium

J. T. Law and P. S. Meigs

Bell Telephone Laboratories, Murray Hill, New Jersey

ABSTRACT

Oxidation rates of the (110), (111), and (100) faces of a Ge crystal have been measured between 450° and 700°C and at various oxygen pressures. For all three faces, oxidation rates were inversely dependent on oxygen pressure at and above 550°C, and no differences in behavior between faces were observed. At 500°C only the (110) face oxidized appreciably. A theory has been developed to explain the effect of oxygen pressure on the oxidation rate and calculated values found to be in fair agreement with experiment.

Recent measurements of the electrical properties of a Ge surface (1) have shown that the thickness of the oxide film present has a marked effect on the magnitude of these quantities. Therefore, it would be of interest to be able to change the film thickness in a controlled way. One way of doing this is to preoxidize at some elevated temperature.

The only previous measurements on the high temperature oxidation of Ge were reported by Bernstein and Cubicciotti (2) who investigated an abraded surface between 575° and 700°C. As the roughness factor for this type of surface is uncertain it seemed worthwhile to repeat the work using definite crystal faces of known area.

Here oxidation rates from 450° to 700°C on the (100), (110), and (111) faces were measured as a function of oxygen pressure.

Experimental

The two principal means of following oxidation rates are (*a*) pressure change in a closed system, and (*b*) weight change of the sample as determined with a microbalance. Since any loss of Ge due to evaporation of GeO would make weight measurements very difficult to interpret, the former was used.

A modified form of Campbell and Thomas's apparatus (3) was used. It is essentially a constant volume differential pressure system with the two halves connected through an oil manometer. The silica bulbs containing the sample and the blank were placed in a furnace whose temperature was controlled by a potentiometer controller. As a check, the temperature was recorded on a millivoltmeter and found to be constant within ±2°C at all temperature settings. To prevent thermal fluctuations the two halves of the system were wrapped together with asbestos tape.

After location of the desired crystal face, slices 5.5 x 0.8 x 0.15 cm were cut and a small hole drilled near one end. These were then polished and etched in a mixture of equal volumes of HNO_3 and HF after which they were attached to a Pt wire winding device so that they could be lowered in vacuum into the furnace and degassed. The oxygen was prepared from $KMnO_4$ and purified by passage through a dry ice-acetone bath. After each run the sample was removed, lightly abraded with 600 mesh carborundum powder, and re-etched.

If the volumes of the various parts of the system are known, it is possible to calculate from the change in pressure how many oxygen molecules have been removed from the gas phase. Assuming a linear temperature gradient between the furnace and the system, no thermomolecular flow, and ignoring virial coefficients, equation (I) is obtained.

$$\Delta n = \frac{P_2}{R}\left(\frac{V_9 \Delta l}{T_1}\right) + \frac{\Delta P}{R}\left(\frac{V_1}{T_1} + \frac{V_3}{T_2} + \frac{V_7}{T_2 - T_1} \ln \frac{T_2}{T_1} - \frac{V_9 \Delta l}{2T_1}\right) \quad [1]$$

where P_2 is the final pressure in the system in mm Hg, ΔP is the change in pressure in mm Hg, Δl is the change in pressure in mm of oil, T_2 is furnace temperature, T_1 is the temperature of the remainder of the system, V_1 is the volume at temperature T_1, i.e., all the system outside the

furnace and temperature gradient, V_7 is the volume in the temperature gradient, V_5 is the volume in the furnace, V_9 is the volume/mm of the manometer tubing, and Δn is the number of oxygen molecules removed from the gas phase.

All the data were calculated by means of this equation. To obtain Δn in terms of molecules/cm² it is necessary to assume a roughness factor. Previous work (4) on the adsorption of gases on Ge gave a roughness factor of 1.3 ± 0.1 for a CP-4 etched surface which was found to be identical with ones prepared by the present technique; this value has been used in the present work. The size of the sample was measured immediately after each run.

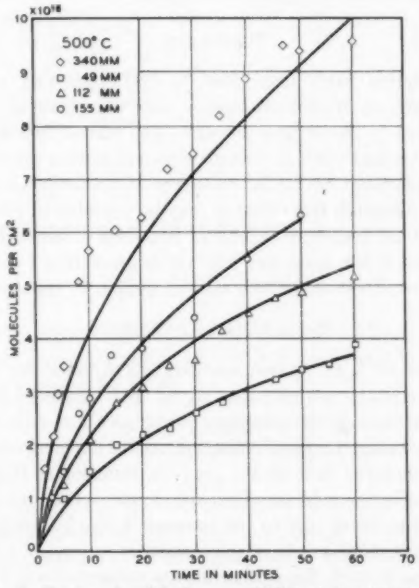

FIG. 1. Rates of oxidation at 500°C of the (110) face of Ge at various oxygen pressures. The points are experimental and the curves calculated from Eq. [24].

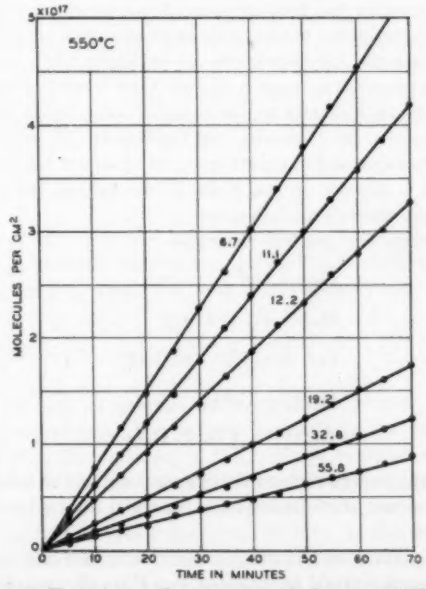

FIG. 2. Experimental rates of oxidation at 550°C of Ge at various oxygen pressures. Numbers indicate the oxygen pressure in mm.

RESULTS

No measurable uptake of oxygen was observed during 2 hr at 450°C for oxygen pressures between 5 and 350 mm. This does not imply that a clean Ge surface will not take up oxygen at 450°C. The surface under discussion, by its

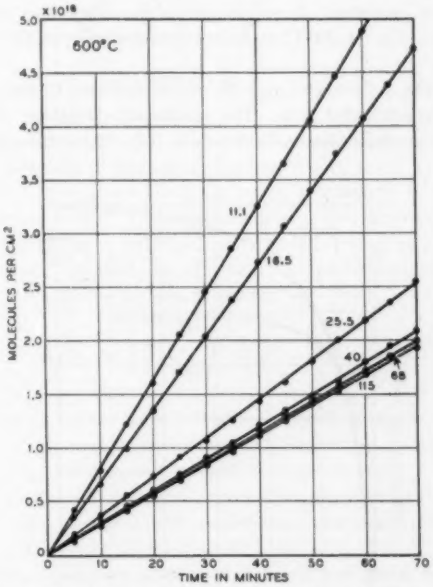

FIG. 3. Experimental rates of oxidation at 600°C. Numbers indicate the oxygen pressure in mm Hg.

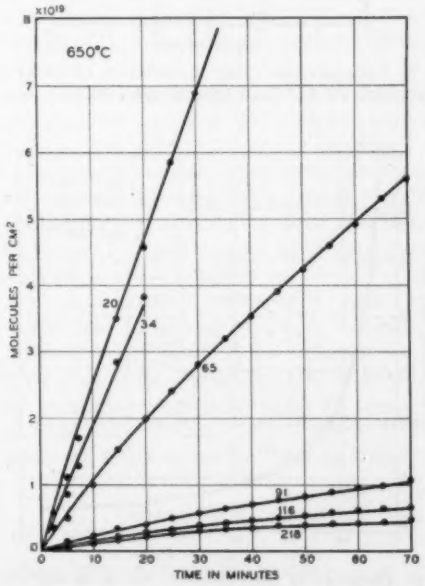

FIG. 4. Experimental rates of oxidation at 650°C plotted with oxygen pressure as parameter.

method of preparation, was almost certainly covered by one or more layers of oxygen before any measurements could be made.

Measured rates of oxidation of the (110) face at 500–700°C are shown in Fig. 1–5. The number of oxygen molecules removed from the gas phase is plotted as a function of time (in minutes) with the oxygen pressure as parameter. At and above 550°C the measured rates were found to be identical for the three faces studied. This is shown in Fig. 6 where the slopes of the rate curves at 550°C for the various faces are plotted as a function of oxygen pressure. A single curve describes the results adequately. At 500°C oxidation occurred only on the (110) plane.

In Fig. 2 through 5 smooth curves are used to represent the experimental data. The maximum deviation of the experimentally determined points from these curves was 1%. The reproducibility of duplicate runs at a given temperature and pressure was also within 1%.

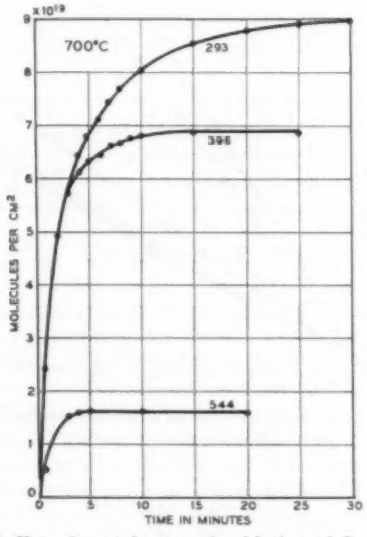

FIG. 5. Experimental rates of oxidation of Ge at 700°C. Numbers indicate the total oxygen pressure.

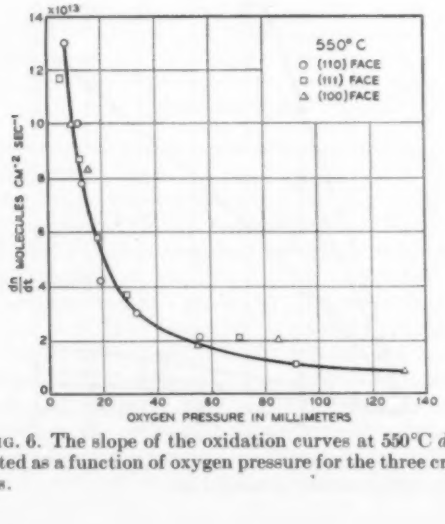

FIG. 6. The slope of the oxidation curves at 550°C dn/dt, plotted as a function of oxygen pressure for the three crystal faces.

The most interesting feature of the results is the strong inverse dependence of oxidation rate on oxygen pressure at 550°C and above. For most metals, oxidation rates at oxygen pressures above 1 mm are either independent of pressure or increase with increasing pressure. This effect was found only with Ge at 500°C as shown in Fig. 1. This was also the only temperature at which the oxidation rate was dependent on crystal orientation.

Discussion

Oxidation rates from 550° to 700°C showed no dependence on crystal orientation and were inversely proportional to the oxygen pressure. The main difference between Ge and other metals for which oxidation rates have been measured lies in the existence of a volatile Ge monoxide. Although this material may be unstable in the solid form at all temperatures, there is strong evidence for its existence in the gas phase. The vapor pressure of GeO over mixtures of Ge and GeO_2 corresponding to the reaction

$$Ge + GeO_2 \rightleftarrows 2\,GeO(g)$$

is available (5, 6). At temperatures above 550°C the vapor pressure is at least 10^{-3} mm Hg so that transport of this material through the gas phase could have a marked effect on the measured rates of oxidation. At the oxygen pressures used, transport through the gas is by diffusion so that one can explain the increase of oxidation rate as the pressure is lowered as being due to the increase in the interdiffusion coefficient. If this is true and a mixture of oxygen and an inert gas is used, the oxidation rate measured will be dependent on the total pressure and not on the partial pressure of oxygen. Mixtures of oxygen and nitrogen were used at 550°C and it was found that the rate is indeed determined by the total pressure. From these experiments one has confidence in proposing an evaporation mechanism to explain the $1/p$ dependence of oxidation rate.

An evaporation process of this type would obviously cause the Ge specimen to lose weight. Such a loss in weight was reported by Bernstein and Cubicciotti (2), and both these workers and the authors have observed the formation of a deposit on the walls of the tubing above the specimen after an oxidation run.

Consider the possible reactions

$$Ge_i \rightarrow Ge^\sigma \qquad \text{(I)}$$

$$Ge^\sigma + O_2 \rightarrow GeO_2^\sigma \qquad \text{(II)}$$

$$Ge^\sigma + GeO_2^\sigma \rightarrow 2GeO^\sigma \qquad \text{(III)}$$

$$GeO^\sigma \rightarrow GeO_{(g)} \qquad \text{(IV)}$$

$$GeO_{(g)} + \tfrac{1}{2}\,O_2 \rightarrow GeO_{2(\text{wall})} \qquad \text{(V)}$$

where the superscript σ refers to material at the solid-gas interface and the subscript i to material at the Ge-GeO_2 interface.

An equation for formation of GeO^σ from Ge^σ and oxygen at the surface could be included, but this only complicates matters without changing the form of the rate equation. Reaction (III) could also occur at the Ge-GeO_2 interface,

but any GeO produced there would have to reach the solid-gas interface before it could evaporate and be detected by the authors' measurements. Since the diffusion of a GeO species through the GeO_2 layer is unlikely, only (III) is considered as a source of GeO at the solid-gas interface.

Let c_1 be the concentration of Ge^σ in molecules cm^{-2}, c_2 be the concentration of GeO^σ in molecules cm^{-2}, and α be the number of molecular layers of GeO_2^σ. Then assuming that the rate of arrival of Ge at the surface is diffusion controlled,

$$\frac{dc_1}{dt} = \frac{K}{\alpha} - k_2 c_1 p^m - k_3 c_1 \qquad [2]$$

or at the steady state

$$\frac{K}{\alpha} = k_2 c_1 p^m + k_3 c_1 \qquad [3]$$

The rate of growth of the GeO_2 film is given by

$$\frac{d\alpha}{dt} = k_2 c_1 p^m - k_3 c_1 \qquad [4]$$

From Eqs. [3] and [4] c_1 can be determined and therefore so can the rate of formation of GeO_2^σ by reaction (II). The latter is equal to $k_2 c_1 p^m$ or

$$k_2 c_1 p^m = \left[\frac{K(k_2 p^m)^2}{2[(k_2 p^m)^2 - k_3^2]}\right]^{1/2} \frac{1}{t^{1/2}} \qquad [5]$$

Hence, Eq. [5] also describes the rate of oxygen removal by the formation of GeO_2^σ; but, oxygen is also removed by reaction (V) so that the total rate of removal is given by

$$-\frac{dn}{dt} = \frac{d[GeO_2^\sigma]}{dt} + 1/2\,\frac{dc_2}{dt} \qquad [6]$$

the second term accounts for oxygen removal via reaction (V). It is assumed that the rate of this reaction is governed by the rate of arrival of $GeO_{(g)}$ and since two molecules of GeO are required for the removal of one oxygen molecule the rate is given by $\frac{1}{2}\,dc_2/dt$. GeO^σ evaporates at a rate

$$-\frac{dc_2}{dt} = \frac{\gamma'}{p} \qquad [7]$$

where γ' includes the concentration gradient and pressure independent part of the interdiffusion coefficient or taking into account the limit for vacuum evaporation

$$-\frac{dc_2}{dt} = \frac{\gamma'}{\beta p + 1} \qquad [8]$$

Eqs. [7] and [8] assume the evaporation process is diffusion controlled. The inverse dependence on pressure arises from the variation of the diffusion constant D with pressure. It was also assumed that the equilibrium vapor pressure of GeO is always attained at the surface so that the evaporation rate is independent of c_2. If this assumption is not made, the final equation gives a rate that is independent of oxygen pressure, for as the pressure is increased, D decreases, but the concentration gradient increases and the product is nearly constant.

Adding the two terms for removal of oxygen from the gas phase

$$-\frac{dn}{dt} = \left[\frac{K(k_2 p^m)^2}{2[(k_2 p^m)^2 - k_3^2]}\right]^{1/2} \frac{1}{t^{1/2}} + \frac{\gamma''}{\beta p + 1} \qquad [9]$$

where $\gamma'' = \gamma'/2$ (because 2 molecules of GeO are oxidized by one molecule of oxygen).

Let

$$\left[\frac{K(k_2 p^m)^2}{2[(k_2 p^m)^2 - k_3^2]}\right]^{1/2} = B \qquad [10]$$

Then

$$\Delta n = 2B\,t^{1/2} + \frac{\gamma''}{\beta p + 1}\,t \qquad [11]$$

The assumption that the rate of evaporation of GeO^σ is independent of the concentration breaks down when c_2 becomes very small. It must go to zero when $c_2 = 0$. This is accounted for by including an extra term for the variation of the second term in [11] with c_2 when c_2 is very small. Let c_2' be the value of c_2 below which the equilibrium vapor pressure is no longer maintained. Then

$$\Delta n = 2B\,t^{1/2} + \frac{\gamma''}{\beta p + 1}\,(1 - e^{-c_2/c_2'})\,t \qquad [12]$$

When $c_2 \gg c_2'$ the term in the final brackets equals unity and the vapor pressure is constant; below this value of c_2 the term decreases to zero with c_2.

This equation has the correct form to explain the experimental results. If the second term predominates with $c_2 \gg c_2'$, a linear rate is obtained. If the first term is important, a parabolic or sum of parabolic and linear rates is obtained. With very thick GeO_2^σ films both terms should approach zero and a protective film should be formed. In Eq. [12] the first term describes the formation of an oxide film on the surface (parabolic), while the second refers to the oxidation of GeO which has evaporated to the walls of the apparatus.

It now remains to fit this equation to the experimental data and see if the values of the constants required are reasonable.

The values of the constants in the term for evaporation can be calculated. Following the treatment of Fuchs (7), suppose that the concentration of vapor at a distance Δ from the surface is c^* and that the equilibrium concentration at the surface is c_0 molecules cm^{-3}.

If the accommodation coefficient is λ, the rate of evaporation into a vacuum is $\Gamma\lambda\ c_0$ molecules cm^{-2} sec^{-1}, where $\Gamma = (kT/2\pi M)^{1/2}$, k is Boltzman's constant, and M the mass of the evaporating GeO molecule. Hence the rate at which molecules arrive at the plane, distant Δ from the surface is $\Gamma\lambda\ (c_0 - c^*)$. This may be equated to the rate at which molecules leave by diffusion or

$$\Gamma\lambda(c_0 - c^*) = -D\,\frac{\partial c^*}{\partial x} \qquad [13]$$

Assume a linear concentration gradient

$$c = Ux + W \qquad [14]$$

TABLE I. *Calculated quantities for the diffusion of* GeO *through oxygen*

Temp, °K	P_{mm}	Γ	$c_0\Gamma$	ΓL	D
773	4.0×10^{-4}	1.08×10^{4}	5.3×10^{16}	5.4×10^{3}	0.68
823	3.2×10^{-3}	1.12×10^{4}	4.1×10^{17}	5.6×10^{3}	0.76
873	2.0×10^{-2}	1.15×10^{4}	2.5×10^{18}	5.75×10^{3}	0.84
923	1.3×10^{-1}	1.18×10^{4}	1.6×10^{19}	5.9×10^{3}	0.92
973	6.3×10^{-1}	1.22×10^{4}	7.5×10^{19}	6.1×10^{3}	1.01

But at the wall, i.e., distant L from the surface, $c = 0$. Therefore

$$UL + W = 0 \qquad [15]$$

Then

$$\lambda(c_0 - c^*) = -\frac{DU}{\Gamma} \qquad [16]$$

Assume that the accommodation coefficient is unity and substitute for c^*

$$c_0 = U\left[(\Delta - L) - \frac{D}{\Gamma}\right] \qquad [17]$$

The rate of evaporation is equal to $-DU$ so on substituting for U

$$-\frac{dc_2}{dt} = \frac{-Dc_0}{\Delta - L - \frac{D}{\Gamma}} = \frac{Dc_0}{L - \Delta + \frac{D}{\Gamma}} \qquad [18]$$

Let

$$D = \frac{D_0 \times 760}{p}$$

Then

$$-\frac{dc_2}{dt} = \frac{c_0}{\frac{(L-\Delta)}{D_0 760}p + \frac{1}{\Gamma}} = \frac{c_0\Gamma}{\frac{\Gamma L p}{D_0 760} + 1} \qquad [19]$$

assuming that Δ, the mean free path of the molecule, is small compared to the distance to the wall at all the pressures investigated. As $p \geq 5$ mm Hg this is a good approximation. Hence comparing coefficients of [8] and [19]

$$\gamma' = c_0\Gamma \qquad [20]$$

and

$$\beta = \frac{\Gamma L}{D_0 760} \qquad [21]$$

All the quantities in Eq. [19] can be calculated or estimated so that the rates of evaporation of GeO^g may be obtained and therefore the rates of uptake of oxygen due to its subsequent oxidation.

No data are available in the literature for the diffusion constant of GeO in oxygen. However, it is approximately true that $D = K/M^{1/3}$, where M is the mass of the diffusing species. Using data for the diffusion of H_2, CO_2, and O_2 in oxygen K was found to be unity, and D for GeO equal to 0.106 at 273°K and 760 mm. On the basis of a simple theory D should vary as $T^{3/2}$, but Lonius (8) has found that the exponent is nearer 1.75. Using $D = D_0\ (T/273)^{1.75}(760/p)$ the values of D at 760 mm and various temperatures have been calculated and listed in Table I. The average velocity (Γ) of GeO molecules leaving the surface was obtained from $\Gamma = (kT/2\pi M)^{1/2}$ and the product $c_0\Gamma$ from

$$c_0\Gamma = 3.95 \times 10^{20} P_{mm}\left(\frac{M}{T}\right)^{1/2} \text{ molecules cm}^{-2}\,\text{sec}^{-1} \qquad [22]$$

where P_{mm} is the vapor pressure of GeO.

The value of the vapor pressure of GeO over a mixture of GeO_2 and Ge is not well established but the data of Jolly and Latimer (6) have been used in the present calculations. Inaccuracies in the vapor pressure data make the calculated values of the oxidation rate equally uncertain, but give values correct at least within an order of magnitude. In the derivation of Eq. [19], the accommodation coefficient λ was assumed to be unity. If it is included in the final equation

$$-\frac{dc_2}{dt} = \frac{\lambda c_0\Gamma}{\frac{\lambda\Gamma L p}{D_0 760} + 1} \qquad [23]$$

TABLE II. *Calculated and experimental values of dn/dt in molecules cm^{-2} sec^{-1}*

Oxygen pressure	dn/dt (Calculated)	dn/dt (Experimental)
t = 550°C		
6.7	2.6×10^{15}	1.3×10^{14}
11.1	1.7×10^{15}	1.0×10^{14}
12.2	1.6×10^{15}	7.8×10^{13}
19.2	1.0×10^{15}	4.2×10^{13}
32.8	6.0×10^{14}	3.0×10^{13}
55.8	3.6×10^{14}	2.1×10^{13}
t = 600°C		
11.1	1.2×10^{16}	1.3×10^{15}
16.6	8.4×10^{15}	1.1×10^{15}
40.0	5.5×10^{15}	6.1×10^{14}
68.0	2.0×10^{15}	4.9×10^{14}
115.0	1.2×10^{15}	4.7×10^{14}

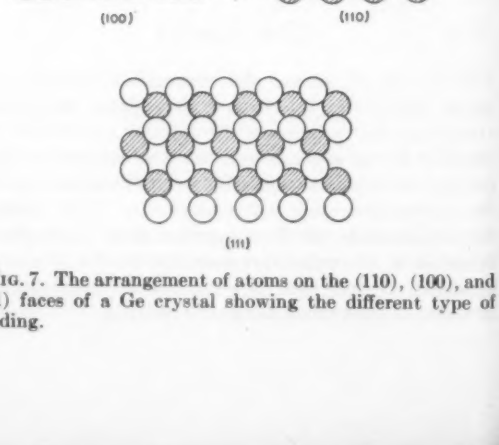

FIG. 7. The arrangement of atoms on the (110), (100), and (111) faces of a Ge crystal showing the different type of bonding.

In general, λ will be less than unity and probably between 1 and 10^{-3}.

From the values listed in Table I it is possible to calculate dc_2/dt from 773° to 973°K and at any pressure. From these results the second term in Eq. [6] can be evaluated and hence the linear parts of the rate curves predicted. Unfortunately it is impossible to carry out an independent calculation of the first term which includes several rate constants.

Oxidation rates at 550° and 600°C are shown in Fig. 2 and 3 as linear curves. However, at very short time intervals ≤ 3 min they were practically parabolic. Because of the difficulty of obtaining accurate data at the beginning of the run only the linear portions were plotted by moving the zero of time to +3 min. It is believed that this initial region describes the growth of an oxide film. This film grows until its growth rate is just equal to the rate of evaporation of GeO. It then remains at a constant thickness and the oxidation curve becomes linear with respect to time.

This theory predicts that the linear part of the rate curves describes the diffusion of GeO through the oxygen atmosphere. In Table II the experimental and calculated (from Eq. [6] and [23]) values of dn/dt in molecules cm^{-2} sec^{-1} at 550° and 600°C are given as a function of oxygen pressure. Calculated values are all higher than experimental ones, although the agreement is satisfactory. The difference could be due to either inaccurate vapor pressure data for GeO or to the use of unity for the accommodation coefficient (λ). In general λ is less than one and therefore reduces the calculated value of dn/dt.

At temperatures above 600°C no comparison of theory and experiment is possible since the oxidation curves are no longer linear. That evaporation of GeO is still important is shown by the inverse dependence of rate on oxygen pressure, but this process is reduced and finally (at 700°C) prevented by the growth of a protective film of GeO_2. Once a stable GeO_2 film has been formed at 700°C no further oxidation is observed even if the oxygen pressure is lowered. The difference between the uptakes at the various pressures is due to the amount of GeO that can evaporate before a complete GeO_2 film is formed. This is certainly greater at the low pressures.

The data at 500°C shown in Fig. 1 differ from all the others in that the oxidation rate increases with increasing oxygen pressure. The term due to diffusion of GeO away from the surface is found to be quite small, being approximately 5×10^{12} molecules cm^{-2} sec^{-1} at a pressure of 50 mm. The linear term in Eq. [11] is therefore unimportant and there is left

$$\Delta n = 2Bt^{1/2} \qquad [24]$$

where B is a function of oxygen pressure. In other words, the oxidation rate under these conditions is controlled by the thickness of the oxide film and a parabolic law results. It is not possible to calculate a value for B, which contains a number of rate constants. However Eq. [24] may be written as $\Delta n = c\, p^m\, t^{1/2}$ and values of c and m may be calculated from two runs and used to compare the rest of the data. The solid lines in Fig. 1 were all calculated from $\Delta n = 9.10^{15} p^{1/2} t^{1/2}$; agreement between them and experiment is good at all pressures.

Effect of Crystal Orientation on Oxidation Rate

The lack of dependence of rate on crystal orientation at 550°C is to be expected if the oxidation process is indeed diffusion controlled. The slopes of the rate curves at 550°C for the three faces are shown in Fig. 6 as a function of oxygen pressure. A single curve describes all the results.

At 500°C no removal of oxygen from the gas phase by the (100) and (111) faces could be detected over a period of 2 hr at oxygen pressures between 50 and 700 mm. This was in contrast to the (110) face where appreciable oxidation occurred, as shown in Fig. 1. At this temperature the results show that diffusion through the gas phase is unimportant, so the rate-determining step must be either the removal of a Ge ion from the lattice or its transport across the oxide film. For any difference between crystal faces to be important the former of these must be operative. In Fig. 7 the arrangement of Ge atoms on the (100), (111), and (110) faces is shown. On the (100) face each surface atom is bonded to two atoms in the layer below, while on the (111) face each surface atom is bound to three in the next lowest layer. These numbers remain constant even when the surface layer is partially depleted. On the (110) face, however, each surface atom is bound to two neighboring surface atoms but to only one atom in the underlying layer. Thus, if one atom is removed from the surface, the bonding of the two neighboring atoms is weakened and one can get progressive removal along the chain. Therefore, from the crystal structure it does not seem unreasonable that the (110) plane is more reactive than either the (100) or the (111). Further measurements at temperatures below 500°C are needed for confirmation.

Conclusions

At and above 550°C the oxidation process is controlled by the diffusion of GeO away from the surface and no effect of crystalline orientation is found.

Between room temperature and 550°C little data are available but these results suggest that in this region the (110) plane oxidizes more readily than either the (100) or the (111) and that the rate of oxidation is controlled by either the removal of a Ge ion from the lattice and/or its transport across the oxide film.

Manuscript received April 24, 1956. This paper was prepared for delivery before the San Francisco Meeting, April 29 to May 3, 1956.

Any discussion of this paper will appear in a Discussion Section to be published in the December 1957 Journal.

REFERENCES

1. W. H. Brattain and J. Bardeen, *Bell System Tech. J.*, **32**, 1 (1953).
2. R. B. Bernstein and D. Cubicciotti, *J. Am. Chem. Soc.*, **73**, 4112 (1951).
3. W. E. Campbell and U. B. Thomas, *Trans. Electrochem. Soc.*, **91**, 623 (1947).
4. J. T. Law, *J. Phys. Chem.*, **59**, 543 (1955).
5. W. Bues and H. V. Wartenberg, *Z. anorg. u. allgem. Chem.*, **266**, 281 (1951).
6. W. L. Jolly and W. M. Latimer, *J. Am. Chem. Soc.*, **74**, 5757 (1952).
7. N. Fuchs, *Phys. Z. Sowetunion*, **6**, 224 (1934).
8. A. Lonius, *Ann. Physik*, **29**, 664 (1909).

Electrolytic Reduction of Cyanamide

KEIJIRO ODO AND KIICHIRO SUGINO

Laboratory of Organic Electrochemistry, Department of Chemical Engineering, Tokyo Institute of Technology, Tokyo, Japan

ABSTRACT

The electrolytic reduction of cyanamide was investigated in order to confirm each product and thus to clarify the reduction mechanism.

Ten per cent aqueous cyanamide solution was reduced electrolytically in 8% $(NH_4)_2SO_4$ catholyte at *p*H range 3–7 at a spongy Sn cathode. Final products were NH_3 and methylamine as previously reported. In addition, a considerable amount of formamidine was isolated in the form of picrate. Formic acid was also obtained as a product of the reduction. No proof was obtained for the existence of hydrocyanic acid in the catholyte during electrolysis. On these bases, the intermediate compound of the cyanamide reduction to NH_3 and methylamine is not hydrocyanic acid, but formamidine, contrary to the results of earlier workers. The main side reaction is hydrolysis of formamidine to NH_3 and formic acid.

Drechsel (1) first observed that cyanamide could be reduced to give methylamine and NH_3 by prolonged treatment with Zn and HCl. He supposed that cyanamide was first reduced to NH_3 and hydrocyanic acid, the latter compound being further reduced to methylamine.

$$NH_2CN + 2H \rightarrow NH_3 + HCN \qquad (I)$$

$$HCN + 4H \rightarrow CH_3NH_2 \qquad (II)$$

Kameyama (2) later carried out this reduction by an electrolytic method. He used a 1.3–6.7% aqueous solution of cyanamide prepared by extracting commercial calcium cyanamide as catholyte, and Cd, Zn, Pb, Hg, etc., as cathode. By combining the measurement of H absorption at the cathode and simple identification of the product, he concluded, as did Drechsel, that cyanamide was reduced to give methylamine and NH_3. He also supposed the mechanism to be the same as Eqs. (I) and (II).

Nothing further has been reported, and it appears that a complete separation and identification of cyanamide reduction products had not been made before the present work. Therefore, an investigation was made in order to confirm each reduction product and thus to clarify the reduction mechanism.

In this paper, the detection of formamidine as an intermediate product and the proposed mechanism based on this discovery are reported. Experiments were carried out mainly at a spongy Sn cathode and in a catholyte containing $(NH_4)_2SO_4$ at *p*H 3–7. Work on the quantitative study of the effect of cathode materials and other electrolytic conditions on the yield of each product is in progress.

EXPERIMENTAL, RESULTS, AND DISCUSSION

Apparatus.—Apparatus used was similar to that described earlier (3). Area of the cathode was 80 cm^2. The catholyte was thoroughly agitated by a magnetic stirrer to maintain the *p*H of the catholyte as constant as possible.

Material used.—Crystalline cyanamide was freshly prepared from commercial calcium cyanamide by a previously reported procedure (4), and its purity was determined by the usual method (as silver cyanamide) before use.

Formation of methylamine and ammonia.—Several runs were made using various cathodic materials such as Pb, Hg, Sn, Zn, Cu, etc. The reduction of cyanamide was found to occur with all cathodes, but spongy Sn gave the most favorable results (Table I).

Cyanamide converted was calculated by subtracting the amount of remaining cyanamide in the catholyte from that in the starting catholyte. Remaining cyanamide was determined by the usual method (as silver cyanamide).

Methylamine and ammonia were isolated by the following procedure.

Ammonia.—After reduction, the catholyte (102 cc) was neutralized with H_2SO_4, and 20 cc was pipetted into the beaker; 100 cc methanol was added to it and the mixture was allowed to stand for several hours. Precipitated $(NH_4)_2SO_4$ was filtered, washed with 20 cc methanol, and weighed. Solubility correction was applied (0.47 g/20 cc). Then, NH_3 formed by the reduction was calculated by subtracting the amount of NH_3 in the starting catholyte.

Methylamine.—Each 40–60 cc of catholyte was pipetted into the beaker, and five times that amount of methanol was added to it. The precipitated $(NH_4)_2SO_4$ was filtered off and washed with 40 cc methanol. The filtrate was combined with washing solution and concentrated under diminished pressure. The residue was diluted to 150 cc with water, poured into a Kjeldahl flask, and heated with 60 g 50% NaOH solution. Methylamine was distilled into HCl, and the resulting solution was evaporated to dryness. The residue was extracted with 40 cc then 10 cc hot butanol to separate NH_4Cl; the extract was again evaporated to dryness to give crude methylamine hydrochloride, which was weighed. The analytical sample was recrystallized from butanol.

It was confirmed that the reduction of cyanamide gave NH_3 and methylamine as final products in fair yield under suitable conditions. But the amount of methylamine was relatively small as compared with the amount of NH_3 expected from:

$$NH_2CN + 6H \rightarrow NH_3 + CH_3NH_2 \qquad (III)$$

It may be that part of the NH_3 was formed not by direct reduction, but by decomposition of some intermediate

product. So, further experiments were carried out to seek the intermediate product of the reduction of cyanamide.

Isolation of formamidine, the intermediate product.—By careful observations, it was found that formamidine existed in the reduction product. Isolation of this compound was difficult and incomplete quantitatively; it could be caught as picrate by the following procedure.

Ten grams cyanamide (purity 97.5%, 9.75 g as pure cyanamide) was reduced at a spongy Sn cathode with 40 amp-hr of current. Other conditions were the same as in Table I; 5.17 g of cyanamide was converted.

After the reduction, 25 cc of the catholyte (total 110 cc) was pipetted into the beaker. To it, a suitable amount of picric acid was added either as solid, aqueous solution, or methanolic solution. Formamidine picrate (solubility about 0.2 g/100 cc) could be precipitated together with ammonium picrate.[1] The quantitative separation of formamidine picrate from this mixture was very difficult,[2] but after adding a hot methanolic solution of picric acid (1.5 g/5 cc) very cautiously, 1.57 g crude formamidine picrate was obtained (mp 232°–234°C). Recrystallization from 30 cc hot water gave 0.91 g of pure compound. Yield 12.0%, mp 242°–244°C. Calc'd for $C_7H_7N_5O_7$: N, 25.64%; found: N, 25.95%.

A mixed melting point with the product[3] prepared from thiourea showed no depression.

Identity was further confirmed by converting the picrate into the hydrochloride. Pure formamidine picrate (2.15 g, mp 242°–244°C) obtained by the reduction was converted to hydrochloride (0.51 g, mp 66°–70°C). Calc'd for CH_5N_2Cl: N, 34.78%; found: N, 35.05%.

Isolation of formic acid.—Since formamidine was found to be the intermediate product, hydrolysis of this compound to ammonia and formic acid may be expected as follows:

$$NH_2 \cdot CH = NH \xrightarrow{H_2O} NH_3 + HCONH_2 \xrightarrow{H_2O} 2NH_3 + HCOOH \qquad (IV)$$

The existence or formation of this compound in the reduction product was verified by the following procedure.

Ten grams cyanamide (purity 96%, 9.60 g as pure cyanamide) was reduced at a spongy Sn cathode with 35.8 amp-hr of current. Other conditions were the same as in Table I, and 4.37 g cyanamide was converted. After the reduction, 30 cc of the catholyte (total, 105 cc) was pipetted into the beaker; 30 cc 20% H_2SO_4 was added to it, and the mixture was distilled in a Kjeldahl flask to give 50 cc of distillate. Formic acid content in the distillate was determined by titration with 0.1*N* NaOH solution. Yield: 0.35 g (total, 1.21 g), sodium formate obtained from the distillate had mp 250°–255°C (decomposition), and the mixed melting point with the known sample showed no depression.

TABLE I. *Reduction of cyanamide at* Sn

Catholyte:* 10 g cyanamide in 100 cc 8% $(NH_4)_2SO_4$. *p*H range adjusted at 3–7 by adding small amount of H_2SO_4 during the electrolysis.
Current: 34.4 amp-hr (5 Faradays).
Current density: 5 amp/dm²
Temp: Kept at 15°C by cooling catholyte with ice water.
Results: Cyanamide used: 10.00 g (purity 97.6%, 9.76 g as pure cyanamide)
Cyanamide converted: 3.96 g
$(NH_4)_2SO_4$ obtained: 3.12 g
Methylamine hydrochloride obtained: 1.87 g, mp 196°–200°C (recrystallized); Calc'd for CH_6NCl: N, 20.74%; found: N, 21.40%.

* Acidic catholyte is also applicable to this reduction. For example: 10 g cyanamide in 100 cc 5% H_2SO_4. Concentration of H_2SO_4 is controlled so as to be 5–2% during electrolysis.

FIG. 1. Formamidine picrate

Existence of formaldehyde.—The existence of small amounts of formaldehyde in the distillate of the run described above was proved. The distillate had a very indistinct odor of formaldehyde and gave a very weak silver mirror reaction. Moreover, it gave a little precipitate when treated with dimedon.

Existence of hydrocyanic acid.—Careful observation was also made in order to determine the existence of hydrocyanic acid in catholyte during the electrolysis. This test was made by prussian blue formation. Two or three cubic centimeters of the catholyte was pipetted into the test tube and made alkaline with a drop of NaOH. To it, a piece of crystalline ferrous sulfate was added, and the solution was boiled for 30 min. The resulting solution was acidified with HCl, and a solution of $FeCl_3$ was added. Color change to blue could not be observed throughout the experiments.

Side reactions other than reduction.—Cyanamide is expected to dimerize to dicyandiamide at *p*H 8–12. But during the reduction, under the conditions described above, an appreciable amount of dicyandiamide was not

[1] When the amount of formamidine in the catholyte was small, the speed of crystallization of the picrate was relatively slow, so that it might have been better to let the mixture stand for a few days. Formamidine picrate could be recognized easily by the characteristic form.

[2] Indeed, in another run, separation of formamidine picrate from the mixture was even more difficult, and it could be accomplished only by the careful technique of picking out characteristic picrate crystals from the mixture.

[3] Prepared from thiourea by the procedure of D. J. Brown (5), mp 246°C.

detected. Also, any conversion of cyanamide to urea by hydration in the presence of acid is unlikely to occur during the reduction.

Conclusion

It is interesting to note that a fairly large amount of formamidine was obtained in the reduction product of cyanamide. Formation of this compound was completely missed by earlier workers. Since hydrocyanic acid was absent, the reduction of cyanamide is best represented by the following succession of reactions:

$$NH_2CN \xrightarrow{2H} NH_2 \cdot CH = NH \xrightarrow{2H} [NH_2 \cdot CH_2NH_2] \xrightarrow{2H} NH_3 + CH_3NH_2 \quad (V)$$

Main side reaction is the hydrolysis of formamidine to give NH_3 and formic acid.

$$NH_2 \cdot CH = NH \xrightarrow{H_2O} [NH_3 + HCONH_2] \xrightarrow{H_2O} 2NH_3 + HCOOH \quad (VI)$$

The mechanism proposed by Drechsel (1) and adopted by Kameyama (2) for the electrolytic reduction is disproved by this experiment.

Acknowledgment

This investigation was promoted by a grant for fundamental scientific research from the Ministry of Education of Japan and also a grant from Nippon (Japan) Carbide Industries Inc., for which the authors wish to express their deep appreciation.

They are also indebted to Mr. E. Ichikawa and H. Kawada for their generous assistance in carrying out the experiment.

Manuscript received November 2, 1955. This paper was prepared for delivery before the Pittsburgh Meeting, October 9 to 12, 1955.

Any discussion of this paper will appear in a Discussion Section which will be published in the December 1957 Journal.

References

1. E. Drechsel, *J. prakt. Chem.*, **11**, 319 (1875).
2. N. Kameyama, *J. Fac. Eng. Tokyo Imp. Univ.*, **13**, 271 (1924).
3. M. Yamashita and K. Sugino, *This Journal*, **104**, 100 (1957).
4. K. Sugino, Y. Takenouchi, Y. Aiya, and H. Usui, Japanese Pat. 179,981 (Aug. 19, 1949).
5. D. J. Brown, *J. Appl. Chem. (London)*, **2**, 202 (1952).

The Voltage of Sodium Chlorate Cells

Vivion de Valera

Department of Chemistry, University College, Dublin, Ireland

ABSTRACT

The cell voltage of technical chlorate cells with carbon anodes and rod iron cathodes is correlated with reported overvoltage values. At working current densities the cell voltage is expressible as the sum of a constant, the overvoltages, and an ohmic term. Results are found to be consistent with the theory that the anode potential is conditioned by hydroxyl discharge. Back emf measurements are discussed.

To calculate the energy efficiency of a chlorate cell a value for the theoretical cell voltage must be assumed but, owing to the complexity of the reactions involved, the value to be taken is not obvious. Knibbs (1) quotes 1.43 v as being the theoretical voltage required according to Luther for producing chlorate from chloride, but he further points out that the voltage corresponding to the thermal absorbtion in the change:

$$NaCl\ (aq.) + 3H_2O\ (liq.) = NaClO_3\ (Aq.) + 3H_2\ (Gas) - 224\ (Cal.)$$

is 1.62 v. In subsequent literature this value has been adopted (2). On the other hand, Koehler (3) states that the decomposition potential of NaCl solutions may be taken as 2.3 v and uses this factor for calculating the efficiency of chlorine-caustic cells. Generally, it is not easy to interpret voltage measurements recorded in the literature and a systematic correlation of cell voltages with current densities is needed. This prompted the present investigation.

Although it is difficult to get reproducible values, current voltage curves for chloride electrolysis are always more or less definite in form. Apart from the peculiarities at low current densities, especially at the commencement of electrolysis, they have the usual approximately logarithmic shape (4). In the case of simpler electrolytes, such curves are usually resolvable as the superposition of a linear ohmic increase of potential with current on a logarithmic overpotential. This suggests that chlorate cell voltages might also be separable approximately into the sum of the electrode overvoltages, the electrolyte resistance, and a constant, provided other variables are suitably controlled and that values for the overvoltages are known.

An analysis of data relating to the operation of chlorate cells both on the semitechnical and technical scales confirmed that the curves obtained by plotting current against voltage were of the type expected. The results of Pfleiderer (5) and others (4) then indicated correlation with H and oxygen overvoltages obtained by the direct method. As the values of Knobel, *et al.* (6) (assembled in the International

Critical Tables) seemed the most appropriate, these were used.

Analysis of Routine Factory Data

During the operation of an experimental installation, results heretofore unpublished of routine observations over a period of nearly two years became available. These were extracted from the log sheets and analyzed. The data related to concrete cells fitted with electrode assemblies of the rod cathode type similar to those described by McLaren and co-workers (7). The anodes consisted of 2 in. diameter graphite rods with an effective length of 20 in. Each anode was surrounded by 20 steel rods, $\frac{3}{16}$ in. diameter, forming its cathode. Cells were operated on a batch basis and current, voltage, and other readings were taken hourly throughout a run. Cell temperatures ranged from 23° to 31°C. One lb of $K_2Cr_2O_7$ was added to the electrolyte at the beginning of each run and the *p*H was maintained between the limits 6.2–6.9 by addition of HCl. A large number of readings were available corresponding to ten runs. Results shown in Table I relate to two runs with cells of approximately 470-l capacity fitted with 30 electrode units per cell. Cell conditions were practically the same during both these runs, and the figures given here are representative of the results for other runs. In one of the runs in question 8 cells were operated in series. Observations were made each hour on one master cell and one other observed cell. Throughout the run, cell conditions and performance were almost the same for the 8 cells. In the second run, 32 similar cells were operated in series. The figures taken were hourly observations made on two master cells. Cell conditions and performance for the two master cells were closely parallel, but some of the remaining 30 cells showed wider variations than those noticed in the 8-cell run. As far as current-voltage relations were concerned these variations seemed to be explainable in terms of varying cell resistances. These runs were selected because they afforded the largest number of comparable readings at various current values. Great accuracy cannot be claimed for these measurements.

Figures given in Table I refer to early portions of these runs after the cells had settled down but before the chloride concentration had fallen below 200 g/l. Cell resistance can be taken as approximately constant in this interval although it rises toward the end of a run. In the present case, cell resistance, R, was estimated at 4×10^{-4} ohms. The voltages E_{obs} are mean values obtained by plotting observed voltages against the corresponding current. Overvoltages V_a and V_c were taken from the graphs obtained by plotting the values given in the International Critical Tables[1] for the oxygen overvoltages on graphite and the H overvoltages on Fe, against current density. The seventh column of the table gives the sum of the anode and cathode overvoltages together with the ohmic term RI, corresponding to the current values in the first column, while the last column gives the difference of the observed voltages, E_{obs}, and this sum. The difference so obtained is practically constant over a wide current range, the average value being 1.09 v. In fact, the result for the runs in question may be written in the form:

$$E_{obs} = 1.09 + (V_a + V_c) + RI \qquad (I)$$

[1] International Critical Tables, vol. VI, pp. 339, 340.

TABLE I. *Current-voltage: average from plant log sheets*

I (amp)	C.D. anode (amp/cm²)	V_a (v)	C.D. cathode (amp/cm²)	V_c (v)	RI (R = 0.0004) (v)	$V_a + V_c + RI$	E_{obs} (v)	Difference (v)
30	0.0012	0.55	0.0006	0.36	0.01	0.92	1.92	1.00
300	0.012	0.91	0.006	0.53	0.12	1.56	2.60	1.04
400	0.016	0.94	0.008	0.55	0.16	1.65	2.71	1.06
500	0.020	0.96	0.010	0.56	0.20	1.72	2.82	1.10
600	0.024	0.98	0.012	0.57	0.24	1.79	2.92	1.13
700	0.028	0.99	0.014	0.58	0.28	1.85	2.98	1.13
850	0.034	1.00	0.017	0.59	0.34	1.93	3.06	1.13
900	0.036	1.01	0.018	0.60	0.36	1.97	3.08	1.11
1000	0.040	1.01	0.020	0.61	0.40	2.02	3.14	1.12
1100	0.044	1.02	0.022	0.62	0.44	2.08	3.18	1.10
1200	0.048	1.02	0.024	0.62	0.48	2.12	3.22	1.10
1300	0.052	1.03	0.026	0.63	0.52	2.18	3.29	1.11

Note: I is cell current; V_a is oxygen overvoltage on anode; V_c is hydrogen overvoltage on cathode; R is cell resistance; and E_{obs} is observed cell voltage.

Correlation with Reported Values

The value 1.09 v is very close to the value found experimentally for the "reversible" oxygen electrode with reference to a reversible H electrode in the same aqueous solution. Taken in conjunction with the fact that the overvoltages concerned are those of H and oxygen, this coincidence seemed to be of some significance. It was therefore of interest to inquire how far the above result could be fitted to the cell data published by other workers.

It is unfortunate that the information given in the literature usually omits to specify the cell resistance, R, so that the extent to which the above equation can be tested on the figures given is very limited. However, Pitman and co-workers (8) describe the operation of two cells for which they give the necessary data (Cells Nos. 2 and 4). Taking the voltages and current densities experimentally determined for these cells in conjunction with the overvoltages V_a and V_c obtained in the same way as before, the following result was obtained:

Cell No.	C.D. anode (amp/cm²)	C.D. cathode (amp/cm²)	V_a (v)	V_c (v)	RI (v)	E_{calc} (v)	E_{obs} (v)
2	0.019	0.011	0.96	0.56	0.22	2.83	2.81
4	0.022	0.012	0.97	0.57	0.22	2.85	2.91

McLaren and associates (7) measured the components of the over-all cell voltage of small chlorate cells with rod cathodes. They determined anode and cathode potentials with a saturated calomel reference cell. They state that the voltage measured depended on many cell conditions but give "representative values." Table II gives their values in relation to the overvoltages V_a and V_c.

Notice that the difference between the measured anode potential and the corresponding oxygen overvoltage is almost constant, the average value of this difference being about 0.26 v. The figures indicate a similar constancy for the cathode relations, but values of V_c taken are those corresponding to the anode current densities given. In the

TABLE II. *Electrode potentials and overvoltages*

Anode C.D. (amp/cm²)	Anode potential (v)	V_a (v)	Diff. $E_a - V_a$ (v)	Cathode potential (v)	V_c (v)	Diff. $E_c - V_c$ (v)
0.01	1.17	0.90	0.27	1.27	0.56	0.71
0.02	1.22	0.96	0.26	1.42	0.61	0.81
0.04	1.28	1.01	0.27	1.46	0.67	0.79
0.06	1.30	1.04	0.26	1.49	0.73	0.76
0.09	1.33	1.07	0.26	1.52	0.79	0.73
0.12	1.34	1.10	0.24	1.55	0.85	0.70
0.16	1.37	1.12	0.25	1.58	0.91	0.67

TABLE III. *Voltages calculated from results of McLaren, et al.* (7)

NaCl (g/l)	I (amp)	C.D. anode (amp/cm²)	V_a (v)	C.D. cathode (amp/cm²)	V_c (v)	R (ohms)	RI (v)	E_{calc} (v)	E_{obs} (v)
250	200	0.04	1.01	0.03	0.64	0.0006	0.12	2.86	2.80
100	200	0.04	1.01	0.03	0.64	0.0011	0.22	2.96	2.95
50	200	0.04	1.01	0.03	0.64	0.0012	0.24	2.98	3.00
250	400	0.09	1.07	0.06	0.73	0.0006	0.24	3.13	3.25
100	400	0.09	1.07	0.06	0.73	0.0011	0.44	3.33	3.40
50	400	0.09	1.07	0.06	0.73	0.0012	0.48	3.37	3.55
250	600	0.12	1.10	0.09	0.79	0.0006	0.36	3.34	3.35
100	600	0.12	1.10	0.09	0.79	0.0011	0.66	3.64	3.66
75	600	0.12	1.10	0.09	0.79	0.0012	0.72	3.70	3.70
250	800	0.16	1.12	0.12	0.85	0.0006	0.48	3.54	3.6
100	800	0.16	1.12	0.12	0.85	0.0011	0.88	3.94	3.9
75	800	0.16	1.12	0.12	0.85	0.0012	0.96	4.02	4.0
250	185	0.08	1.06	0.06	0.73	0.0020	0.37	—	3.25
250	110	0.16	1.12	0.09	0.79	—	—	—	3.9

paper referred to, the authors omit cathode current densities and hence the anode values are taken in default. It is almost certain that the correct cathode current densities were less than the corresponding anode values and a correction in this direction would tend to make the sum of the two differences more nearly approach the value 1.09 v.

In the same paper the authors tabulate data relating to the operation of cells at various current loads and salt concentrations (7). They do not give the values of their cell resistances but, if the cell voltages are calculated by means of the equation under test on the assumption that the values of R were: 6×10^{-4} ohms at a chloride concentration of 250 g/l, 11×10^{-4} ohms at 100 g/l, and 12×10^{-4} ohms at 50–75 g/l, the resulting voltages accord with the observed values. Table III shows that agreement is good except in the case of the 400-amp run. The authors, however, point out that the data for this run were obtained after the anodes had worn from 2 in. diameter to 1¾ in. diameter. Data for the 185-amp run were also obtained with worn anodes. Thus, an increased cell resistance is to be expected in the case of both of these runs. Table III, then, affords a circumstantial check on Eq. (I).

Direct Experimental Test

The matter was then submitted to a direct test with the 32-cell installation already mentioned. The cells were charged with fresh brine from the one mixing and 1 lb dichromate was added to each cell. The initial *p*H of the electrolyte was 9.4 and the initial cell temperature was 9°–10°C for all cells. Care was taken to insure that starting conditions were the same for all cells. The current was switched in at a low value, and, after some preliminary measurements, it was raised to the vicinity of 1000 amp. Cell temperatures were allowed to rise to 25°C and thereafter maintained at this value. A standard glass electrode *p*H meter was used to control the *p*H of the cell liquors and HCl was added to each cell in regulated quantities to reduce the *p*H of the electrolyte slowly and uniformly for all cells. The cells were then run for 20 hr under these conditions before the observations discussed below were taken.

It is necessary to make a slight digression at this point to refer briefly to the resistances of chlorate cells. These do not remain constant but increase with time, manifesting themselves as a rise in cell voltage. This increase is due to two distinct causes: (*a*) the specific resistance of the electrolyte increases with rising chlorate concentration from about 4 to 6 ohms/cm³ at chloride concentrations above 100 g/l (1); (*b*) resistances of electrodes and electrode connections tend to increase with time because of corrosion, rusting, or anode wear (7). It is also conceivable that local emf's may develop at connections if these are faulty and exposed to damp spray from the cells. The first factor made it necessary to take all readings within a relatively narrow chlorate and chloride concentration range. The second factor is noticeable in cells fitted with graphite anodes and iron rod cathodes after about four successive batch runs. The age and history of an assembly of this type must be taken into consideration when estimating its resistance. In the present case, the age and history of the electrode assemblies in the 32 cells was practically the same and the performance and characteristics of the individual cells were sufficiently uniform to warrant the consideration of average values taken over all the cells (±0.15 v at 1000 amp, maximum deviation from average).

It was decided to take current and voltage readings before the chloride concentration had fallen below 250 g/l but after a reasonable time had been allowed for the cells to settle down. On the basis of cell dimensions and the specific resistance of the electrolyte, taken as 4.7 ohms/cm³, it was estimated that the corresponding resistance of the electrolyte would be 1.5×10^{-4} ohms/cell. The resistance of the graphite anodes was estimated at 0.5×10^{-4} ohms/cell. Voltage drops over the anode and cathode connections and the voltage drops in the leads had been measured in detail with current passing, by means of an accurate millivoltmeter toward the end of a previous run very shortly before the present run commenced. On the basis of these measurements and check measurements made during the present run, the resistance of the anode and cathode connections combined was taken as 2×10^{-4} ohms/cell. The total resistance was thus estimated at 4×10^{-4} ohms/cell. This should approximate to the actual value for new cells; data available indicated that this was so. However, examination of the increase in voltage at specified current values during successive previous runs indicated that the internal cell resistance had increased with age to the average extent of $1.0–1.5 \times 10^{-4}$ ohms/cell. Accordingly, it was expected that the average resistance during the present run should be about $5.0–5.5 \times 10^{-4}$ ohms/cell for the period selected.

Current flowing through the cells was measured by an

ammeter of standard type. The total voltage drop over the 32 cells was measured by means of a voltmeter of suitable range and from the readings so taken, together with the known corrections for the potential drops in the leads, average cell voltages corresponding to observed current values were determined. In addition, one cell was selected for individual observation, the voltage for this cell being measured by means of a separate instrument of suitable range. Before the voltage readings were taken for any selected amperage the cells were run at this value for some time. Presumably because of polarization effects, when the cell current is altered the cell voltage does not adjust itself to the new equilibrium value at once. With the installation in question it took approximately 30 min for the cell voltage to settle down for current changes of 100–200 amp at current values above 200 amp. Below 200 amp a longer time was required. In the present experiment, two series of observations were made. In each series, observations were commenced at high current values. The current was then reduced by stages, one hour at least being allowed to elapse between the current change and voltage readings for the new value. Values so obtained were then checked by restoring the current to its original high value, again by stages with suitable intervals. Invariably under these conditions, readings corresponding to a particular amperage were effectively the same whether the approach was from a higher or a lower value. The first series of observations were made while the *p*H of the cell liquors was slightly on the alkaline side, the initial and final average *p*H values for this series being 7.4 and 7.1, respectively. The second series were taken on the acid side, the corresponding average *p*H values being 6.9 to 6.8, respectively. At the beginning of the first series the chlorate concentration was 39 g/l and the chloride concentration was 260 g/l. At the end of the second series the chlorate concentration was 67 g/l and the chloride concentration was 251 g/l. Cell temperatures were maintained at the desired value by a suitable control of the cooling water to each cell until all measurements were completed.

Results of this experiment for the observed cell are given in Table IV. The figures for one series only are given since those for the other series were almost identical. Average values for the 32 cells are given in Tables V and VI.

Tables V and VI show that the average cell voltages observed in this experiment agree well with the values calculated from Eq. (I) when the cell resistance R is taken as 5.5×10^{-4} ohms. The cell voltage for the observed cell, however, was consistently lower than the corresponding average value for all the cells. Assuming that the differences in voltage between individual cells is attributable to differences in cell resistance, results indicate that the resistance of the observed cell was about 4.8×10^{-4} ohms. E_{calc} in Table IV is derived on this basis.

TABLE IV. *Current-voltage: values for 1 cell*

Temp, 25°C *p*H 6.8–6.9

I (amp)	E_{calc} (v)	E_{obs} (v)	I (amp)	E_{calc} (v)	E_{obs} (v)
50	2.07	2.12	795	3.06	3.03
150	2.40	2.44	900	3.13	3.12
200	2.50	2.52	925	3.14	3.13
260	2.61	2.58	1000	3.19	3.20
300	2.66	2.65	1100	3.26	3.26
325	2.70	2.66	1150	3.28	3.30
665	2.97	2.94	1250	3.35	3.35

TABLE V. *Current-voltage: averages for 32 cells*

Temp, 25°C *p*H 7.4–7.1

I (amp)	Anode C.D. (amp/cm²)	V_a (v)	Cathode C.D. (amp/cm²)	V_c (v)	RI (ohms)	E_{calc} (v)	E_{obs} (v)
50	0.002	0.56	0.001	0.40	0.03	2.08	2.26
100	0.004	0.67	0.002	0.45	0.06	2.27	2.35
200	0.008	0.82	0.004	0.49	0.11	2.51	2.49
300	0.012	0.91	0.006	0.52	0.17	2.69	2.63
500	0.020	0.96	0.010	0.56	0.27	2.88	2.87
650	0.026	0.98	0.013	0.58	0.36	3.01	3.00
810	0.032	1.00	0.016	0.59	0.45	3.13	3.11
955	0.038	1.01	0.019	0.60	0.53	3.23	3.25
1000	0.040	1.01	0.020	0.61	0.55	3.26	3.27
1100	0.044	1.02	0.022	0.62	0.61	3.34	3.34
1250	0.050	1.03	0.025	0.63	0.69	3.44	3.44

TABLE VI. *Current-voltage: averages for 32 cells*

Temp, 25°C *p*H 6.9–6.8

I (amp)	Anode C.D. (amp/cm²)	V_a (v)	Cathode C.D. (amp/cm²)	V_c (v)	RI (ohms)	E_{calc} (v)	E_{obs} (v)
50	0.002	0.56	0.001	0.40	0.03	2.08	2.13
150	0.006	0.76	0.003	0.48	0.08	2.41	2.46
200	0.008	0.82	0.004	0.49	0.11	2.51	2.52
260	0.010	0.90	0.005	0.50	0.14	2.63	2.65
300	0.012	0.91	0.006	0.52	0.17	2.69	2.67
325	0.013	0.93	0.006	0.52	0.18	2.72	2.70
665	0.027	0.98	0.013	0.58	0.37	3.02	3.02
795	0.032	1.00	0.016	0.59	0.44	3.12	3.10
900	0.036	1.01	0.018	0.60	0.50	3.20	3.20
925	0.037	1.01	0.018	0.60	0.51	3.21	3.22
1000	0.040	1.01	0.020	0.61	0.55	3.26	3.27
1100	0.044	1.02	0.022	0.62	0.61	3.34	3.36
1150	0.046	1.02	0.023	0.62	0.63	3.36	3.41
1250	0.050	1.03	0.025	0.63	0.69	3.44	3.46

Back EMF Measurements

In earlier runs with the cells mentioned above it was noticed that the back emf of these cells when freshly filled, and before electrolysis was started, was in the neighborhood of 1.6 v. At the commencement of the experimental run already described, before any current was passed, it was found to be 1.60 v for the observed cell and the average cell back emf for the 32 cells was found to be 1.59 v. Corresponding initial cell temperatures were 10° and 9.5°C, respectively. The current was then switched in at a very low amperage and gradually increased to 40 amp. Simultaneously, voltage readings were taken and it was found that cell voltage increased nearly linearly with current over this range. The circuit was then broken and the back emf was again measured. This was now found to be 1.75 for the observed cell and 1.85 (avg) for the remainder. It showed no tendency to fall below this value on being left standing for 30 min. The current was again switched in after this interval and again increased by stages. It was now found that the voltage increased regularly with the current, the shape of the current-voltage curve being generally similar to those obtained by plotting data given in Tables IV, V, and VI.

There was no evidence of a definite decomposition voltage at any stage.

After the cells had settled down, some measurements were made to determine the back emf of the cells at various current values. The method adopted was simply to open the main switches of the cell circuit at the current values selected and observe changes in cell voltage. These measurements could not be very precise under the conditions of the experiment, but they definitely indicated a back emf corresponding to each current value which was reproducible. On cutting out the cells it was observed that the voltage dropped suddenly to a certain value and then decreased very slowly thereafter. It was found that the back emf decreased slightly as the corresponding current was decreased. The decrease appeared to be fairly regular. In the vicinity of 1000 amp the recorded back emf was 2.37 v; in the vicinity of 500 amp it was 2.32; in the vicinity of 200 amp it was 2.30 v. On reducing the current to zero slowly and then isolating the cells it was found to be approximately 2.10 v but this value seemed to depend on the rate at which the current was reduced before isolating the cells. On leaving the cells standing on open circuit the emf fell to 1.85 v in 1 hr. These measurements were made at 25°C.

It was noticed in the course of the foregoing experiments that the needle of the voltmeter frequently paused momentarily at a somewhat higher value than that at which it steadied and which was taken as the back emf. For instance, at 670 amp when the cells were quickly isolated, the voltage dropped rapidly, paused at about 2.4 v, and then quickly dropped to the value 2.34 v. Although successive readings were not very concordant, there is an indication that this happens at all parts of the current range investigated. It might have been, however, an inductive effect.

Discussion and Conclusion

Variation in cell voltage at 25°C with electrode current densities appears to be accounted for adequately by Eq. (I) for anode current densities above 0.005 amp/cm². At lower anode current densities, calculated values deviate from those observed. Indeed, the closeness of the agreement between observed and calculated voltages above this value is rather surprising since one would expect greater irregularities in measurements involving electrode overvoltages which were not made under very carefully controlled laboratory conditions. Fluctuations of at least 0.05 v would be expected and variations in the condition of the electrode surfaces should be reflected in variations in overvoltage values.

A laboratory investigation confirmed the results reported above (9). The experimental cells used were fitted with graphite anodes and iron cathodes. A linear equation in the form of (I) was found in all cases to apply above 0.015 amp/cm², the value for the constant at 25°C being always close to 1.1 v., and the reproducibility of the measurements was sufficient to justify the conclusion.

The most obvious interpretation is that above a certain anode current density the reaction system adjusts itself to constitute a cell having a reversible potential of 1.09 v. This in turn suggests that the anode of a chlorate cell is essentially an oxygen electrode rather than a chlorine electrode. On the other hand, at very low current densities, the anode probably behaves as a chlorine electrode and this conclusion would appear to accord with the results of Foerster, Müller, Luther, and others (4). It may be said in passing that the behavior of the cell voltage at low current densities noticed in the present experiments was generally what would be expected from the results of these workers.

It would be interesting to repeat calculations using chlorine overvoltages instead of the oxygen values. However, comparable values for chlorine overvoltages on graphite at 25°C are not available for current densities below 0.04 amp/cm², that is, for a great part of the range considered above. Nevertheless, if the values given by Knobel and co-workers (6) are plotted against current density as was done in the case of the oxygen overvoltages, the chlorine overvoltage curve so obtained is parallel to the corresponding oxygen curve in the range 0.04–0.20 amp/cm². In fact for this range, $V_o \simeq V_{Cl} + 0.84$ v. Assuming that this parallelism continued down to low values for the anode current densities, experimental results would be equally well expressed by the equation:

$$E_{obs} = 1.93 + (V_{Cl} + V_c) + RI \qquad \text{(II)}$$

Considering the cell back emf, at about 800 amp, this was approximately the same as that noted by Knibbs and Palfreeman (1) for a cell which had a Pt anode. However, they found that the back emf was independent of current density over a fairly wide range, whereas the present experiments indicated a decrease with current density. It is to be noted that they attempted to correlate their results with Newbery's overvoltage values, but were unable to account for the cell voltage on this basis. Why this was so is now clear. Newbery's overvoltages were obtained by the original commutator method which only measures a part of the total electrode polarization when the current is flowing. In addition, the back emf does not measure the quantity represented above as $1.09 + V_a + V_c$, the discrepancy between this quantity, (2.71 v at 1000 amp in the foregoing experiments), and the back emf corresponding (2.37 v) apparently arising in the same way as the similar discrepancies noticed between overvoltages measured by the direct and commutator method. Hence, the precise significance to be attached to back emf measurements in the present case is not clear but it may possibly be worth noticing that the values obtained by Newbery (10) for a laboratory cell with carbon electrodes and H_2SO_4 bear a close resemblance to the values noted above.

Over-all, the results appear to be in harmony with the idea that both hydroxyl and chlorine ions are discharged at the anode. This conclusion would seem consistent likewise with the results of Pfleiderer (5) and earlier workers. It is also supported by the work of Glasstone and Hickling (11) and accords with the theory of the process recently given (12). Hydroxyl discharge and the associated oxygen overpotential perhaps may be the principal factors determining the anode potential at appreciable current densi-

ties. In any case, the results furnish a basis for assessing the energy efficiency of a chlorate cell at specific current densities.

ACKNOWLEDGMENT

The author must thank Professor T. S. Wheeler for his interest and the many facilities he made available during the course of the work.

Manuscript received April 27, 1956.
Any discussion of this paper will appear in a Discussion Section to be published in the December 1957 issue of the JOURNAL.

REFERENCES

1. N. V. S. KNIBBS AND H. PALFREEMAN, *Trans. Faraday Soc.*, **16**, 402 (1920).
2. P. H. GROGGINS, A. L. PITMAN, AND F. H. DAVIS, *Chem. & Met. Eng.*, 468 (1940); Rogers "Industrial Chemistry," 1942, I, 458.
3. H. J. CREIGHTON AND W. A. KOEHLER, "Electrochemistry," Vol. II, p. 280 (1935).
4. F. FOERSTER, "Elektrochemie Wässeriger Lösungen," Chap. 14, Leipzig, 1923; R. LUTHER AND F. J. BRISLEE, *Z. Phys. Chem.*, **45**, 216 (1903); and ref. (5) below.
5. G. PFLEIDERER, *Z. Phys. Chem.*, **68**, 49 (1909).
6. M. KNOBEL, P. CAPLAN, AND M. EISEMAN, *Trans. Am. Electrochem. Soc.*, **43**, 55 (1923).
7. J. MCLAREN, J. TURER, F. H. DAVIS, A. L. PITMAN, AND P. H. GROGGINS, *ibid.*, **79**, 93 (1941).
8. A. L. PITMAN, J. MCLAREN, F. H. DAVIS, AND P. H. GROGGINS, *Chem. & Met. Eng.*, **45**, 692 (1938).
9. V. DE VALERA, Dissertation, National University of Ireland (1955).
10. E. NEWBERY, *Trans. Faraday Soc.*, **15**, 126 (1919).
11. S. GLASSTONE AND A. HICKLING, *J. Chem. Soc.*, **1932**, 2345, 2800; **1933**, 829; **1934**, 10.
12. V. DE VALERA, *Trans. Faraday Soc.*, **62**, 250 (1956); *ibid.*, **49**, 1338 (1953).

Influence of Impurities in the Electrolyte in Chlorine-Caustic Electrolysis by the Mercury Cell Process

VI. Investigation of the Influence of Graphite Particles on Amalgam Decomposition and Cathodic Current Efficiency

GÖSTA ANGEL, ROLF BRÄNNLAND, AND STIG DAHLERUS

Division of Applied Electrochemistry, Royal Institute of Technology, Stockholm, Sweden

ABSTRACT

The influence of graphite particles on the Hg cell process for the production of chlorine and caustic soda has been investigated using the technique described in a series of earlier papers, *viz.*, partly by shaking sodium amalgam with buffered solutions of NaCl and measuring the decomposition rate, and partly by studying the cathodic current efficiency of a Hg cell for laboratory use.

The experiments show that the effect of moderate quantities of graphite (< 3 g/l) is small in pure brine but that, in the presence of Mg or Al, the loss of current efficiency is appreciable. The simultaneous presence of graphite and either Fe, Ca, or small quantities of V (< 0.1 mg/l) does not affect the electrolysis process. Silicates and stannates inhibit the action of the graphite particles.

Besides the metallic impurities earlier investigated (1–5), graphite is usually present in technical brines, viz., in the form of a suspension. Opinions are very much divided about the influence of the graphite; considering the action of graphite in the amalgam decomposer, a strong decrease of the cathodic current efficiency may be expected in the presence of graphite particles in the brine. On the other hand, it has been shown practically that it is possible to run a Hg cell with an extremely graphite-rich brine without any noticeable influence on the current efficiency.

In order to elucidate the effect of the graphite, a series of experiments with graphite-contaminated brines was performed. The investigation was carried out partly as amalgam decomposition experiments and partly as electrolysis experiments in a laboratory cell. Varying particle size and concentration of the graphite as well as the simultaneous presence of Mg, Al, Fe, and V were investigated. In all cases, the graphite powder was obtained by crushing and screening fresh anode pieces of various origins.

AMALGAM DECOMPOSITION EXPERIMENTS

Complete agreement could not be expected between amalgam decomposition and electrolysis experiments since the reaction conditions are quite different in the two cases. In the latter, a well-defined cathode film is formed over a quiet Hg surface (6) and the graphite particles are affected mainly by convection forces caused by the gases

formed at the cathode. In the former, the contact surface between brine and Hg is continuously regenerated and simultaneously a relatively high concentration of buffering substances contributes to a breakdown of the alkaline film at the Hg surface. Furthermore, the graphite particles come into very close contact with the Hg phase when, due to shaking, thin layers of the brine are forced toward the walls of the reaction vessel by the Hg. Deviations in results of the two types of experiments, however, make it possible to draw important conclusions concerning the mechanism of the reactions investigated.

Amalgam decomposition experiments were carried out in exactly the same manner as those described earlier (1–3) except that a certain quantity of graphite powder, after careful washing and classification with respect to particle size, was added to the buffered brine. The decomposition rate of the amalgam was studied by measuring the volume of H formed per minute.

Influence of particle size.—The following particle sizes were investigated: G_0 < 0.30 mm; G_1 0.30 – 0.43 mm; G_2 0.55 – 1.00 mm.

The experiments showed that the large particles were crushed in a few minutes to smaller dimensions. Some representative results are shown in Fig. 1. These curves indicate that larger particles would have only a small effect but, due to crushing, form a finer and more active powder. For unknown reasons, the finest grains on the other hand seem to be gradually de-activated.

Influence of graphite concentration.—A series of experiments was performed with the smallest particle size (<0.3 mm) in which the graphite concentration was varied. These experiments demonstrate, Fig. 2, that the reaction rate increases with increasing graphite concentration only to a certain extent. However, for higher graphite concentrations, the reaction rate falls off gradually, possibly due to an agglomeration of the graphite particles to larger aggregates.

Influence of graphite in the presence of metal ions.—In the presence of 250 mg/l of the finest graphite fraction, the effect of a number of cations, viz., Fe, Mg, and Al, was studied. Their concentrations in the brine were 25 mg/l in the case of Fe and Mg and 5 mg/l in the case of Al. In all experiments no increased H evolution beyond that of the pure graphite effect could be observed.

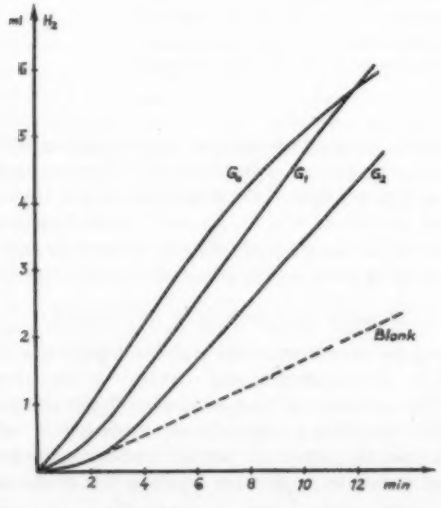

FIG. 1. Amalgam decomposition rate vs. particle size (500 mg/l graphite).

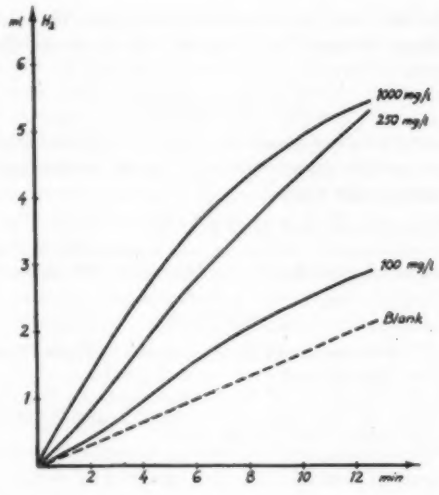

FIG. 2. Amalgam decomposition rate vs. graphite concentration (particles <0.30 mm).

ELECTROLYSIS EXPERIMENTS

Experiments were performed in the apparatus previously described (4, 5). In order to facilitate the reaction in the amalgam decomposer, an electric preheater for the water was supplied. A temperature of 40°–60°C in the secondary cell was thereby obtained and the electrolyzer could be run without difficulty with a cathodic current efficiency of 99.6–99.9%. The brine feeding rate was 0.40–0.45 l/h, the current density 25 amp/dm², and the Hg circulation rate about 10.4 ml/min, corresponding to a Na concentration of 0.1% in the amalgam. Current efficiency was determined either by analysis of the departing Hg or by determination of the H content in the chlorine gas.

Since it was impossible to maintain a uniform graphite content in the feeding brine, graphite was added directly to the electrolysis cell. When other impurities were investigated, the cell was fed with brine containing the actual metal salt, while the graphite was added directly to the cell.

Influence of particle size.—For electrolysis experiments with pure brine, a weighed quantity of graphite (0.1 g) dispersed in saturated brine, was added to the cell.

No influence on the electrolysis process could be observed with particle sizes > 0.3 mm. Graphite particles did not seem to come into contact with the cathode, were gradually broken up into smaller pieces, and were conveyed out of the cell together with the departing brine.

With particle sizes < 0.3 mm, a slight H evolution was observed (0.5–1.5%) immediately after the graphite addition, but the electrolysis then proceeded undisturbed and the graphite was gradually removed with the brine. H evolution was mainly concentrated at the Hg seal and, to a very slight extent, at the boundary between Hg and

glass wall. Graphite entered the cell as a thick suspension and part of it was immediately conveyed by the Hg to the seal where, owing to the vigorous streaming of the Hg, it came into contact with the amalgam, the decay of which was thereby promoted. After the graphite had become more uniformly dispersed in the cell, H evolution ceased.

Influence of graphite concentration.—Graphite was added in quantities up to 0.4 g, corresponding to about 3 g/l in the cell. No measurable increase in the activity in this concentration range and also no differences between graphite samples of various origins could be observed. Thus, graphite particles in otherwise pure brines do not interfere with the electrolysis process.

If very large graphite particles fall on to the cathode, they may come into direct contact with the Hg and, owing to the low overvoltage of H on graphite, H gas is formed at the graphite surface. Since such pieces generally have a small area compared with the whole of the cathode, the resultant H evolution seems to be of no practical importance.

Influence of graphite and Mg *when present simultaneously.*—On electrolyzing Mg-containing brine, it was found that the addition of graphite may have a disastrous influence on the current efficiency. It has already been reported (5) that, with high Mg concentrations, the cathode is covered with a layer approximately 1 mm thick, probably consisting of a mixture of hydroxide and amalgam.

If graphite is present in the brine, it will stick in the hydroxide film and thereby come into firm electrical contact with the Hg. Owing to the low H overvoltage on graphite and the large surface of the graphite particles, a very considerable decrease in the cathodic current efficiency is caused. Fig. 3 shows a typical current efficiency curve from an experiment with 5 mg/l Mg and 0.1 g graphite. Only the first part of the curve (corresponding to 10-min electrolysis) could be reproduced exactly since the hydroxide film caused a very irregular streaming of the Hg and, hence, considerable error in the analyses.

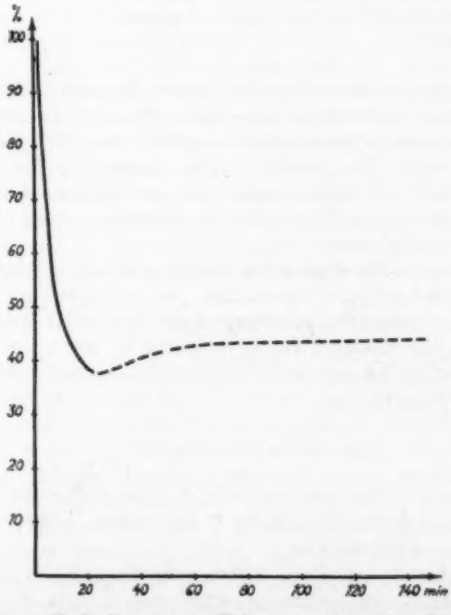

FIG. 3. Cathodic current efficiency vs. time (5 mg/l Mg + 100 mg/l graphite, particles <0.30 mm).

The reaction seemed to be practically independent of the quantity of graphite added; experiments were performed with graphite additions down to 0.01 g with a current efficiency of about 40%. Brines containing 1.0 and 2.5 mg/l Mg were also investigated, but in these cases no decrease in the current efficiency could be observed.

Thus the experiments show that Mg in concentrations above 5 mg/l and in the presence of graphite particles affect the cathodic current efficiency disastrously. However, owing to the special streaming conditions of Hg, the electrolysis cell used for these experiments is considerably more sensitive to impurities of this kind than are technical Hg cells.

Influence of Al *and graphite when present simultaneously.*—In experiments with Al as a brine contaminant (5), it was found that this also forms a thin cover on the Hg. If graphite particles were present simultaneously, they stuck in the layer and, with 5 mg/l Al, a reaction analogous to that of Mg-containing brine was obtained, cf. Fig. 3. Current efficiency thus decreased to about 40%. Experiments with 1.0 and 2.5 mg/l Al caused no decrease in current efficiency.

Influence of graphite and either V, Fe, or Ca *when present simultaneously.*—Addition of graphite to a solution containing either V (100 γ/l), Fe (10 mg/l), or Ca (25 mg/l) had no influence on current efficiency.

De-activation of Graphite by Addition of Sodium Silicate or Stannate

In a special series of experiments it was shown that it is possible to de-activate the interfering graphite particles by addition of sodium silicate or sodium stannate (10–50 mg/l Si or Sn). Both of these substances were very efficient inhibitors of graphite and the blank values for H evolution, i.e., values obtained with pure brine, were obtained in amalgam decomposition experiments with 250 mg/l graphite. This de-activation of the graphite particles may depend possibly on a covering of the electrochemically active centers on the particles with inhibitor molecules which are deposited on the graphite when the *p*H is lowered. This is also indicated by the fact that the sedimentation rate of the graphite particles is considerably increased on addition of both these inhibitors.

However, it should be observed that the colloidal silicic and stannic acids may be transported to the cathode in the electrolysis cell, thus hindering the diffusion of the Na ions and causing H evolution. Consequently, it would appear necessary to allow the inhibitors to flocculate and then to separate the precipitate from the brine before it is added to the cell.

Summary

The experiments have shown that graphite particles have a negligible influence on the cathodic current efficiency in Hg cells when the brine is pure. In the presence of Mg and Al in concentrations sufficient to form a hydroxide layer on the cathode, graphite particles cause an additional H evolution which decreases the current

efficiency to about 40%. Silicates and stannates inhibit the action of graphite particles.

These results explain why, in the chlorine-caustic field, one is generally anxious to avoid graphite in the brine whereas, on the other hand, examples are known of technical brines with high graphite contents which were regularly used without disturbances. Evidently these brines must have been very pure with respect to interfering metal salts.

ACKNOWLEDGMENTS

This investigation was promoted by a grant from Elektrokemiska AB, Bohus; Mo och Domsjö AB, Örnsköldsvik; Svenska Cellulosa AB, Sundsvall; and Uddeholms AB, Skoghall, for which the authors wish to express their deep appreciation.

Manuscript received July 16, 1956.

Any discussion of this paper will appear in a Discussion Section to be published in the December 1957 JOURNAL.

REFERENCES

1. G. ANGEL AND T. LUNDÉN, *This Journal*, **99**, 435 (1952).
2. G. ANGEL AND R. BRÄNNLAND, *ibid.*, **99**, 442 (1952).
3. G. ANGEL, T. LUNDÉN, AND R. BRÄNNLAND, *ibid.*, **100**, 39 (1953).
4. G. ANGEL, T. LUNDÉN, R. BRÄNNLAND, AND S. DAHLERUS, *ibid.*, **102**, 124 (1955).
5. G. ANGEL, T. LUNDÉN, R. BRÄNNLAND, AND S. DAHLERUS, *ibid.*, **102**, 246 (1955).
6. L. BARR, *ibid.*, **101**, 497 (1954).

Streaming Potential in Spherical-Grain Sands

WILLIAM SCHRIEVER AND CARL E. BLEIL

Department of Physics, University of Oklahoma, Norman, Oklahoma

ABSTRACT

Streaming potentials in very uniform spherical-grain sands were measured with doubly distilled atmosphere-saturated water and with NaCl, NaI, Na_2SO_4, $MgSO_4$, and $MgCl_2$ solutions. A vacuum tube electrometer was used to measure the potential differences.

The streaming potential, V, was directly proportional to the pressure difference, P, in every case, and V/P was independent of changes in configuration of the sand matrix as well as changes in its porosity and its length. A variation of V/P with grain diameter was only partially accounted for by surface conductance alone. Also neither Wood's equation nor Ghosh, Rakshit, and Chattoraj's equation fit the data well.

The data fit the empirical equation:

$$V/P = (V/P)_\infty(1 + k/d + k^2/d^2)\exp(-k/d)$$

where $(V/P)_\infty$ is the value approached in sands having large grains. For water $k = 535 \times 10^2\ \mu$ and $(V/P) = 51.2$ mv/cm-of-water. k is characteristic of spherical-grain sands since it was the same for all solutions, and $(V/P)_\infty$ is a function of solution composition at constant temperature. The ζ potential of a water-glass interface has a positive temperature coefficient whose approximate value is 0.039/°C, and the streaming potential has a positive temperature coefficient of 0.0535/°C.

It has long been known that the streaming potential for a liquid flowing through circular capillary tubes, all of one kind of glass, is proportional to the pressure difference and is independent of the length and radius of the tube. One might infer from this that the streaming potential per unit of pressure difference for a column of sand should be independent of the length of the column and of the diameter of the sand grains if the flow is laminar. In fact, the Helmholtz-Smoluchowski (1) theory predicts that the streaming potential is independent of the size and shape of the pore through which the liquid flows. A development given by Kruyt (2) leads to the same result. However, Bull and Gortner (3) reported a dependence of streaming potential on grain size for sand columns composed of sieved crushed quartz grains; for the smaller sizes the streaming potential decreased with the grain size. Their attempts (4) to explain these results by using the measured conductance of the liquid-filled matrix, instead of the conductance of the bulk liquid, were not completely successful.

Later Bull and Moyer (5) attempted to account for Bull and Gortner's results by taking into account the influence of the surface conductance, the electrical backpressure due to the electro-osmotic effect, and the change in viscosity of water with the capillary size. Their conclusion was: "The peculiar results obtained by Bull and Gortner with quartz particles . . . are still unexplained and are apparently inexplicable on the basis of any of the above calculations".

Rutgers (6) studied the variation of the ζ potential with the radius of the capillary. By taking into account surface conduction he arrived at the "true zeta potential" from the measured values computed by the use of the Helmholtz-Smoluchowski equation. His expression for the true ζ potential is:

$$\zeta = \zeta_0(1 + 2\lambda_s/r\lambda) \qquad (1)$$

where ζ_0 is the measured value, λ_s is the surface conductivity, λ is the conductivity of the solution, and r is the radius of the capillary.

Wood (7) arrived at a Helmholtz-Smoluchowski type equation in which the conductivity term λ_t is the effective conductivity of the tube of solution; thus surface conduct-

ance is taken into account. By making certain assumptions he arrived at an expression for the streaming potential in a column of sand, namely:

$$\eta V\lambda_t/P = M - A/d \qquad \text{(II)}$$

where η is the coefficient of viscosity, V is the streaming potential for a pressure difference P, d is the diameter of the sand grains, and M and A are empirical constants. He found that a proper choice of M and A made this equation a good fit to Bull and Gortner's data for quartz sands.

It is interesting to note that Rutger's equation can lead to an equation similar to Wood's if Wood's assumption, that the effective diameter of the pore space between the sand grains is directly proportional to the diameter of the grains, is made. When this is done one can write:

$$P/\eta V\lambda = N + B/d \qquad \text{(III)}$$

where λ is the conductivity of the solution, and N and B are adjustable constants.

Ghosh, Rakshit, and Chattoraj (8) arrived at a relation for the ζ potential, determined in a sand, that is exactly of the same form as Eq. (I). Therefore, their equation leads directly to Eq. (III). They tested their equation with the data of Bull and Gortner and found it satisfactory.

It may be observed that if A/d in Eq. (II) is very small compared to M, the reciprocal of $(M - A/d)$ is approximately equal to $(M + A/d)$, and that therefore Eq. (II) can be put in the exact form of Eq. (III). Both of these equations are empirical equations even though the capillary tube theory was used as a background in setting them up. They differ in that Eq. (II) takes surface conductance into account in λ_t and any other effect of grain diameter in the terms M and A/d, whereas Eq. (III) takes account of both of these effects in the two terms N and B/d.

In order to make certain practical applications of streaming potential it is important to know how the streaming potential in a sand column depends on the size of the sand grains. In the study of this problem it was deemed advisable to use the most nearly ideal sands that could be provided, namely, sands each composed of spherical glass grains of very uniform size.

The purpose of this research was to establish the effect of grain-size on streaming potential in spherical-grain sands and to determine the effect of temperature and solution composition on such streaming potentials.

Experimental

Apparatus

Flow-tubes.—Two flow-tubes were used. The first was constructed of a rod of Lucite by boring an accurate hole 2 cm in diameter throughout its entire length. Two accurately machined Lucite pistons were arranged so that the distance between them was adjustable over a range of 11 cm. Holes were drilled in each piston to allow liquid to pass freely through it, and a 150-mesh (58 mesh/cm) Pt screen, forming the face of the piston, served both as a potential probe and to prevent the sand from passing through the holes. A port-hole provided with a plug and covered by a cap was made in the side of the tube; this permitted additions of sand to be made without completely disassembling the apparatus.

This flow-tube was mounted in a metal box which was partially submerged in a thermostatically controlled water bath. It was found necessary to use a stirrer driven with an induction motor since arcing at the brushes was observed to disturb seriously the potential measuring electrometer.

The pressure on the solution was supplied by compressed air acting on top of a glass piston in a large vertical glass tube which served as a reservoir. The liquid was heated to the desired temperature by an electric preheater. The line from the reservoir to the flow-tube was Pyrex glass. Very short lengths of Saran tubing were used for connectors. The pressure difference across the sand column was measured with a suitable mercury and water manometer. The volume rate of flow of the solution was determined with a calibrated flow-meter which consisted of an inclined open-end manometer for indicating the pressure difference across a short length of small-bore tubing.

The entire system was electrically shielded with sheet metal, and shielded leads connected the electrodes in the flow-tube to the shielded electrometer. All metal shielding was grounded to a water pipe.

Preliminary experiments with this plastic flow-tube revealed a variation of streaming potential per unit of pressure difference, V/P, with the diameter of the sand grains. Although different batches of the distilled water used for these experiments were as nearly identical as could be produced by a careful double distillation, one could not be certain that at least a part of the observed change of V/P with grain diameter was not due to slight variations in the distilled water. Therefore, a second flow-tube was constructed in such a manner that exactly the same liquid flowed through each of the different sands.

This second flow-tube was made of a 1.5 cm. diameter Pyrex glass tube. Five 1 cm-long No. 28 B&S gauge Pt wire probes were sealed through the wall of the tube at 3.5 cm intervals. Directly above each electrode an open manometer tube was sealed to the flow-tube. Two additional Pt electrodes were sealed through the glass near each end of the flow-tube; these were used to send an electric current through the sand columns during the resistance measurements. Each of the four 3.5-cm intervals was filled with a sand having a different grain diameter. The ends of this flow-tube were equipped with ground joints so that the flow of the solution could be reversed easily through the contiguous sand columns. The solution was supplied at the desired constant pressure from a Mariotte's bottle which was mounted on a vertically continuously adjustable platform. A plug of glass wool prevented the sand from entering the lower end of each manometer. The volume rate of flow was calculated from the mass of the solution caught in an observed time interval. This entire system was mounted in a wire screen cage and shielded leads were used to connect the probes to the electrometer.

Spherical grain sands.—The sands were composed of spheres of soft glass.[1] They were sorted very carefully by

[1] Obtained from the Cataphote Corp., Toledo, Ohio.

retaining only those spheres which stuck in the meshes of the appropriate Tyler sieves. Four sizes were prepared: 50, 80, 90, and 100-mesh (0.300, 0.175, 0.153, 0.147 mm). After sorting, beads of each size were washed in water containing a detergent, rinsed several times, and dried. The beads next were washed in concentrated nitric acid for 24 hr, and then at least 12 times in doubly distilled water until the *p*H of the water was the same before and after rinsing. Finally the beads were dried in an electric oven at 400°C.

Liquids.—The water was distilled first in a tin-lined still and then in an all-Pyrex glass system. It was allowed to stand in contact with the atmosphere with periodic stirring for 2–4 days, after which it was found that the Beckman *p*H meter indicated a constant *p*H in the range 5.48–5.65.

NaCl solutions in concentrations of 10^{-6}, 10^{-5}, 10^{-4}, and 10^{-3} mole/kg of water, and solutions of concentrations 10^{-5}, 10^{-4}, and 10^{-3} mole/kg of each of the salts $MgCl_2$, $MgSO_4$, Na_2SO_4, and NaI, were prepared with the distilled water described above, and with AR grade salts.

Electrometer.—A vacuum-tube electrometer having a Victoreen 5803 electrometer tube, was used to make all potential difference measurements. The circuit included a multiple contact key which, when depressed connected a highly insulated 0.001 mf condenser to the two probes whose potential difference was desired; when the key was released it connected the charged condenser to the grid and filament of the tube. The resulting change in plate current was indicated by the steady deflection of a critically damped galvanometer containing the magnet and coil of a L&N type 2420 instrument, but having a 50 cm scale distance. The electrometer contained its own calibrating circuit. It was found that the scale deflection was directly proportional to the potential difference of the condenser for steady deflections both to the right and to the left of zero. The two sensitivities used were 3.63 mv/mm and 10.06 mv/mm.

The rate at which charge was delivered by the streaming through a sand column was found to be so small that it required nearly 5 sec to charge the 0.001 mf condenser to a potential difference of the order of 0.1 v. Therefore the key was depressed for 5 sec for each potential measurement; this gave duplicable results.

It was found necessary to have all elements of the grid-probe circuit, including switches and the multiple-contact key, provided with polystyrene insulation. The shielded leads to the probes had polyethylene insulation.

Microammeter.—A two-megohm potential divider connected across a 45-v dry-cell battery was used to send a current through a sand column for resistance measurements. This current was measured with a Rubicon galvanometer shunted with a critical-damping resistor of 12,000 ohms. This current meter had a sensitivity of 2.28×10^{-8} amp/mm.

Experimental Procedure

The procedure for obtaining data showing streaming potential as a function of pressure difference was essentially the same for both flow-tubes. The sand was placed in the flow-tube in the presence of water to insure the removal of all the air. The tube was jarred gently with a rubber mallet, and mechanical pressure was applied to pack it securely in place. In the case of the plastic tube, pressure was applied by tightening the plastic screw above one of the pistons.

The sand column was then flushed out by running the desired liquid through it for an hour. Next, the liquid-filled column was allowed to stand for 24 hr after which it was thoroughly flushed out again. In addition, just before streaming potential measurements were made the liquid was allowed to flow through the system for about an hour, the flow was stopped, and the potential difference of the probes was measured; hereafter, this is designated the self-potential of that pair of probes.

The flow was started again and, after the system reached dynamic equilibrium as indicated by the manometer, the potential difference of the probes was measured again. Such potential differences were then measured for various pressure differences. After the series of measurements at different pressures was completed the self-potential was measured again. This self-potential was subtracted from the potential difference observed during the streaming of the liquid; this difference was the observed "streaming potential". These observed streaming potentials turned out to be zero for zero pressure difference, to within the reproducibility of the measurements. For each pressure difference the volume rate of flow was measured.

At the end of each set of measurements at various pressures the electrical resistance of the liquid-filled sand column was measured. This was achieved by measuring the fall of potential across the sand column for a measured direct current through the column. In the plastic flow-tube the current was introduced at the screens; it was always less than 3×10^{-7} amp. In the Pyrex flow-tube the current was introduced at the two end-electrodes and the potential differences of the different pairs of probes were measured; again the currents were kept below 3×10^{-7} amp.

Results

Streaming potential as a function of pressure difference.—A typical set of curves depicting streaming potential, V, as a function of pressure difference, P, for four sizes of spherical-grain sands, is shown in Fig. 1. These curves were obtained with the Pyrex flow-tube.

Similar sets of curves were obtained for the doubly distilled atmosphere-saturated water and for each of the solutions listed earlier. In every case V was found to be directly proportional to P. Usually the pressure differences ranged from 1 to 10 cm-of-water for the 100-mesh beads and from 1 to 3 cm-of-water for the 50-mesh beads. For the water V/P varied regularly from 42.5 mv/cm-of-water for the 50-mesh beads to 13.4 mv/cm-of-water for the 100-mesh beads. The value of V/P decreased with increasing concentration of solution.

Streaming potentials in several sand columns were measured up to pressure differences of 1 atm. Here again V was found to be directly proportional to P.

The resistances of the water-filled sand columns in the Pyrex tube varied from 3.2×10^5 ohms for the 50-mesh to 1.7×10^5 ohms for the 100-mesh beads. Resistances of

the salt-solution-filled sand columns were less than those for water, and they decreased with increasing concentration for each salt.

In every case the volume rate of flow through a sand column was proportional to the pressure difference. Rates of flow varied from 0.01 cm³/sec at the lowest pressure used up to 0.12 cm³/sec for the highest pressure differences. For any one set of curves the temperature was held constant in the neighborhood of 27°C.

The data described above were used for making calculations concerning the variation of V/P with grain size.

Effect of configuration and porosity of the sand matrix on V/P.—The 90-mesh glass beads in the plastic flow-tube were used in these experiments. A fixed mass of the beads was packed to a fixed length of column several different times; between packings the beads were thoroughly shaken up. With water as the liquid it was found that the values of V/P obtained for the different packings agreed well within the reproducibility of the measurements. These data showed that V/P did not vary with the configuration of the matrix.

A column of the beads approximately 17 cm long was packed successively to porosities of 0.432, 0.411, and 0.392. It was found that V/P was constant within the reproducibility of the measurements for these three packings. As would be expected the volume rate of flow decreased regularly as the porosity decreased. These results show that V/P does not vary measurably with experimentally obtainable porosities.

Effect of length of sand column on V/P.—Three different columns of the 90-mesh beads, having lengths of 4.05, 13.23, and 17.02 cm, were packed successively to the same porosity in the plastic flow-tube. It was found that V/P was the same for all three columns to within the reproducibility of the measurements. These results demonstrated that V/P is independent of the length of column of a spherical grain sand.

Effect of grain diameter on V/P.—As was explained earlier the Pyrex tube with its four contiguous sand columns was designed especially for this study. Although exactly the same liquid passed through each column there was the possibility that modification of the liquid occurred during its passage through the successive sands. Two separate checks showed that such a change did not take place. First the *p*H's of the incoming and outgoing liquid were measured, the latter being made after the liquid had been standing in the sands for 48 hr and then as a function of time thereafter. It was found after about an hour of flow that the two *p*H's were the same. The second check was accomplished by reversing the flow through the entire system and observing V/P for each direction. It was observed that V/P for each of the four sand columns was the same for both directions of flow. If appreciable modification of the liquid had occurred during its passage through the four contiguous columns, this result would not have been observed. Thus it is clear that the change of V/P with grain diameter, as shown by Fig. 1, was not due to change in the constitution of the liquid.

Exactly the same four sand columns were used in obtaining all the data for all the solutions. It should be added that, before using the sands for the solutions of a new salt, the sands were washed with the doubly distilled water until the V/P for each sand had returned to the original value obtained with water.

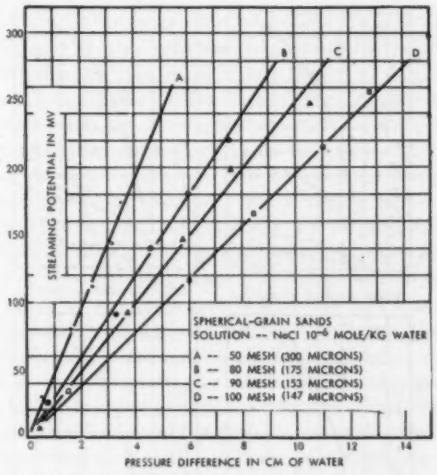
STREAMING POTENTIAL IN MV
PRESSURE DIFFERENCE IN CM OF WATER
SPHERICAL-GRAIN SANDS
SOLUTION -- NaCl 10⁻⁶ MOLE/KG WATER
A -- 50 MESH (300 MICRONS)
B -- 80 MESH (175 MICRONS)
C -- 90 MESH (153 MICRONS)
D -- 100 MESH (147 MICRONS)

FIG. 1. Streaming potential as a function of pressure difference for four sizes of spherical-grain sands.

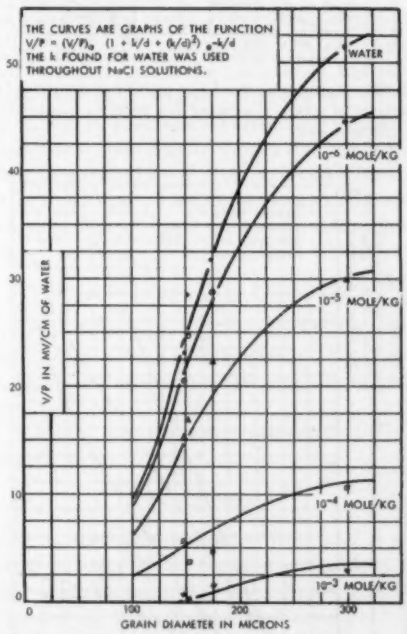

FIG. 2. Streaming potential per unit of pressure difference as a function of grain diameter for water and NaCl solutions.

Variation of V/P with grain diameter for water and for the four concentrations of NaCl are shown in Fig. 2. Similar curves for NaI, Na_2SO_4, $MgSO_4$, and $MgCl_2$ are shown in Fig. 3. Each of the 15 different liquids exhibited a V/P that decreased with decrease in diameter of the spherical sand grains, and that for any one salt the magnitude of the decrease became less as the concentration of the salt became greater.

Resistance of a liquid-filled sand column.—It has been suggested that the variation of the streaming potential

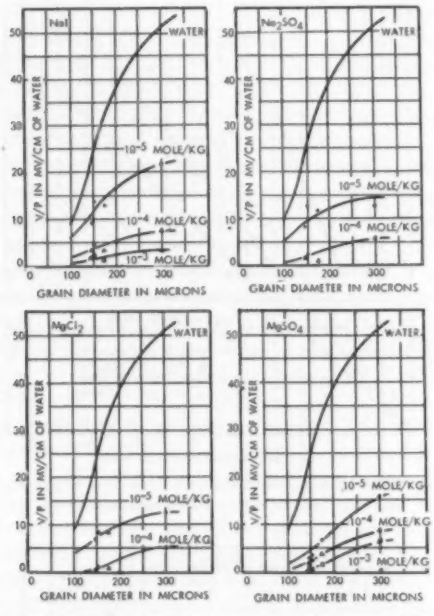

FIG. 3. Streaming potential per unit of pressure difference as a function of grain diameter for various concentrations of four different salts.

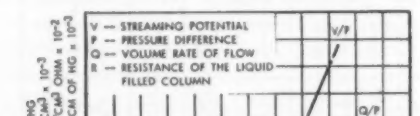

FIG. 4. Effect of temperature on streaming potential

with diameter of sand grain might be explained by the change in the fraction of the conductance of the liquid-filled sand column that is due to the conductance of the liquid-glass interface. For this reason the resistance of each liquid-filled sand column was measured by sending a measured current of less than 3×10^{-7} amp from a battery through the four contiguous columns in the Pyrex flow-tube, and then observing the potential drop between each pair or probes with the electrometer. The self-potential was subtracted from each of the observed potential differences. It was difficult to obtain satisfactory results. Fortunately, with four columns in series the resistance of two or more columns in series could be checked against the sum of the resistances of the separate columns. These resistance determinations were made with the liquid at rest in the sand but after the liquid had flowed through the sand for at least an hour.

If the observed curves of the streaming potential as a function of grain diameter are to be explained solely by the increase in the surface conductance of the liquid-glass interfacial layer, then V/PR (R is resistance of column) should be independent of the diameter of the sand grain. Dividing the values of V/P in Fig. 2 by the appropriate resistances did bring the curves much closer together, but each curve still showed that V/PR decreased regularly with decrease in grain diameter, and to an extent that was much greater than the variability of the measurements. With water V/PR for the 300 μ sand was twice as large as it was for the 147 μ sand.

Thus it must be concluded that the change in V/P with grain diameter for a uniform spherical-grain sand cannot be accounted for by surface conductance alone.

Effect of temperature on V/P.—The volume rate of flow per unit pressure difference, Q/P, and the streaming potential per unit pressure difference, V/P, were measured as functions of the temperature, θ, with the plastic flow-tube apparatus. Doubly distilled water was the liquid and 90-mesh glass beads formed the sand. These results are shown by two of the curves in Fig. 4. The data show that V/P was a linear function of the temperature between 25° and 45°C.

The fact that $\eta Q/P$ for any one sand was observed to be constant in accord with Darcy's law, (η is the coefficient of viscosity of water) showed that the flow was laminar. If the temperature coefficient of V/P were due almost entirely to viscosity changes, then $\eta V/P$ should be a constant for all values of θ. Since $\eta Q/P$ is a constant, $(\eta V/P)(\eta Q/P)^{-} = V/Q$ should be constant for all temperatures. The graph of V/Q as a function of θ is shown in Fig. 4. Since the value of V/Q increases about 25% in the temperature range 25°–45°C, the temperature coefficient of V/P cannot be due to changes in viscosity alone.

The fact that V/QR changes even more rapidly with temperature than does V/Q (*see* curves Fig. 4) demonstrates that the change in conductance of the sand column with temperature is also an important factor in determining the temperature coefficient of V/P. Other factors are treated later.

Effect of concentration of solution on V/P.—Data obtained with the NaCl solutions are presented in another form in Fig. 5 which shows V/P as a function of log $1/c$, where c is the concentration of the solution, for each of the four sizes of spherical-grain sands. Similar sets of curves were obtained for each of the other salts used. These curves are roughly of the form already reported by others (2, 9). They show that the effect of concentration on V/P diminishes with the diameter of the sand grain and that V/P is small for NaCl solutions even as dilute as 10^{-3} mole/kg.

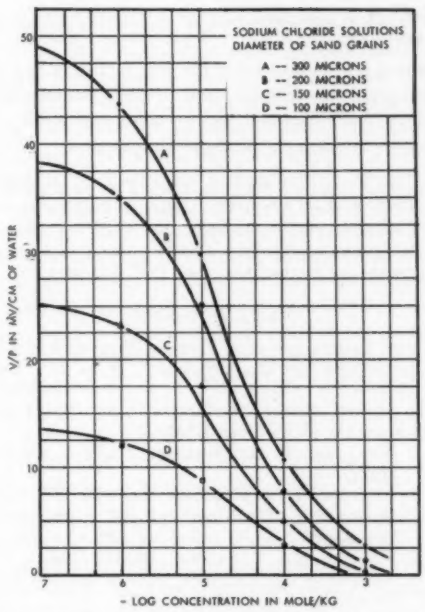
SODIUM CHLORIDE SOLUTIONS
DIAMETER OF SAND GRAINS
A — 300 MICRONS
B — 200 MICRONS
C — 150 MICRONS
D — 100 MICRONS
V/P IN MV/CM OF WATER
- LOG CONCENTRATION IN MOLE/KG

FIG. 5. Effect of concentration of the solution on streaming potential per unit of pressure difference for four sizes of spherical-grain sands.

DISCUSSION OF RESULTS AND EMPIRICAL EQUATIONS

Effect of grain diameter on V/P.—Marked variations of V/P with diameter of the spherical sand grains were obtained for all concentrations of all the solutions (Fig. 2 and 3). Since V/PR decreases with grain diameter, surface conductance alone does not account for all the variation of V/P with grain diameter.

Data shown along the curves of Fig. 2 were used to test both Eq. (II) and (III). Data for a fifth sand ($d = 127\ \mu$) were available; they were included.

For any one solution η, M, and A of Eq. (II) are constants. Therefore $\lambda_t V/P$ should be a linear function of $1/d$ if this equation represents the data. The plot was not a straight line. In fact the negative slope of the curve decreased as the value of $1/d$ increased, which suggests that $\lambda_t V/P$ was approaching a limiting value for very small sand grains.

In Eq. (III) η, λ, N, and B are constants for any one solution. Thus, a plot of P/V as a function of $1/d$ should be a straight line if this equation represents the data. Again the plot was not a straight line. In fact the positive slope of the curve decreased as $1/d$ decreased, which suggests that P/V was approaching a limiting value for very large grains.

The following empirical equation was devised.

$$V/P = (V/P)_a(1 + k/d + k^2/d^2) \exp(-k/d) \quad \text{(IV)}$$

where $(V/P)_a$ is the value of V/P for grains of large size, and k is a constant. In the constant $(V/P)_a$ is included the factor $\zeta\epsilon/\eta$ where ϵ is the dielectric constant of the solution.

Data given for water in Fig. 2 were used to determine the constants $(V/P)_a$ and k in the equation; the method of least squares as described by Scarborough (10) was employed, and the datum for the largest size grain was given extra weight. With d expressed in microns the value of k was found to be $5.35 \times 10^2\ \mu$ and that of $(V/P)_a$ to be 51.2 mv/cm-of-water. In Fig. 2 the curve for water represents this empirical curve; observed data are shown also.

The other four curves of Fig. 2 are also plots of this empirical equation for the four concentrations of NaCl. For all these curves the value of k was that determined from the data for water, namely $5.35 \times 10^2\ \mu$. Each value of $(V/P)_a$ was determined by the method of least squares from the observed data; again the datum for the largest grain diameter was given extra weight. The fact that these empirical curves fit the data fairly well indicates that the constant k is the same for all concentrations of all the solutions and therefore is a characteristic of spherical-grain sands, and that $(V/P)_a$ is a function of the kind and concentration of the electrolyte. It is reasonable that V/P should be zero for $d = 0$, but V/P might become zero for d slightly greater than zero. It also appears reasonable that V/P should approach a limiting value (or perhaps a maximum) as d increases.

These experimental results demonstrate beyond reasonable doubt that V/P varies greatly with the diameter of the grain for uniform spherical-grain sands. Bull and Gortner (4) observed much smaller variations of V/P with size of grain. However, their sands were made of sharp crushed quartz and they undoubtedly were sorted much less carefully than were the spherical glass grains used here.

Effect of temperature.—In Fig. 4 the curve showing V/P as a function of temperature may be represented by an equation of the form:

$$V/P = (V/P)_{25}[1 + \beta(\theta - 25)] \quad \text{(V)}$$

where $(V/P)_{25}$ is the value of V/P at 25°C, θ is the temperature in degrees, and β is a constant. The value of β was found by the method of least squares to be 5.35×10^{-2}/°C.

The equation for streaming potential derived from fairly simple theory (11) is:

$$V = \epsilon\zeta P/4\pi\eta\lambda \quad \text{(VI)}$$

where ϵ is the dielectric constant of the liquid, η is the coefficient of viscosity of the liquid, λ is the electrical conductivity of the liquid, and ζ is the ζ potential. This has been reported (6, 12) to hold well for capillary tubes of circular section, especially if the effective conductivity is calculated from the measured resistance of the liquid-filled tube and the dimensions of the tube. Thus it appears reasonable to suppose that the streaming potential in a spherical-grain sand may be expressed as:

$$V/P = K\epsilon\zeta f(d)/\eta\lambda \quad \text{(VII)}$$

where $f(d)$ is some function of the diameter of the sand grain, and K is a constant.

It has already been shown in connection with Fig. 4 that the effect of temperature on η and λ together does not account for all the effect of temperature on V/P, namely, V/QR varies with temperature. This variation (Fig. 4) may be expressed by an equation of the form:

$$V/QR = (V/QR)_0(1 + a\theta + b\theta^2) \quad \text{(VIII)}$$

where $(V/QR)_0$ is the value of V/QR at 0°C, θ is the temperature in degrees, and a and b are constants.

By Darcy's law for laminar flow $Q = SAP/\eta L$, where S is the permeability of the sand matrix, L is its length, and A is its sectional area. Also the effective conductivity, $\lambda = L/RA$. From these relations Eq. (VII) can be written:

$$V/QR = K\zeta\epsilon f(d)/S \qquad \text{(IX)}$$

The term $Kf(d)/S$ is essentially constant for all temperatures. The dielectric constant of water varies with the temperature (13) according to the equation:

$$\epsilon = \epsilon_0(1 - \gamma\theta) \qquad \text{(X)}$$

where $\epsilon_0 = 88$ and $\gamma = 4.55 \times 10^{-3}$/°C. Since the ζ potential [Eq. (IX)] for a spherical-grain sand may be expressed as:

$$\zeta = SV/KQR\epsilon f(d) \qquad \text{(XI)}$$

its variation with temperature may be written, in view of Eqs. (VIII) and (X):

$$\zeta = \frac{S}{Kf(d)}\left(\frac{V}{QR}\right)_0 \frac{1}{\epsilon_0}\left(\frac{1 + a\theta + b\theta^2}{1 - \gamma\theta}\right) \qquad \text{(XII)}$$

The approximate magnitude of the temperature coefficient of the ζ potential may be calculated. Eq. (XII) may be written in the form:

$$\zeta = \zeta_0[1 + (a + \gamma)\theta + (a\gamma + \gamma^2 + b)\theta^2] \qquad \text{(XIII)}$$

From the slope of the greater portion of the V/QR curve of Fig. 4 the approximate value of the temperature coefficient of V/QR was found to be $a = 3.4 \times 10^{-2}$/°C. Since $\gamma = 4.55 \times 10^{-3}$/°C the temperature coefficient of ζ for the water glass interface was approximately $(a + \gamma) = 3.9 \times 10^{-2}$/°C.

Thus it appears that each of the four factors η, λ, ζ, and ϵ has a temperature coefficient and that the temperature coefficient of V/P is caused by the combined effect of the temperature coefficients of these four factors.

Manuscript received May 16, 1955. This paper was submitted by C. E. Bleil to the University of Oklahoma in partial fulfillment of the requirements for the Ph.D. degree.

Any discussion of this paper will appear in a Discussion Section to appear in the December 1957 JOURNAL.

REFERENCES

1. M. VON SMOLUCHOWSKI, "Graetz Handbuch der Elektrizitat und des Magnetismus," II, p. 379, Leipzig (1921).
2. H. R. KRUYT, Editor, "Colloid Science," Vol. I, p. 202, Elsevier Co., New York (1952).
3. H. B. BULL AND R. A. GORTNER, *J. Phys. Chem.*, **36**, 111 (1932).
4. H. B. BULL AND R. A. GORTNER, *ibid.*, **39**, 577 (1935).
5. H. B. BULL AND L. S. MOYER, *ibid.*, **40**, 9 (1936).
6. A. J. RUTGERS, *Trans. Faraday Soc.*, **36**, 67 (1940).
7. L. A. WOOD, *J. Am. Chem. Soc.*, **68**, 432 (1946).
8. B. N. GHOSH, S. C. RAKSHIT, AND D. K. CHATTORAJ, *J. Indian Chem. Soc.*, **30**, 601 (1953).
9. J. A. V. BUTLER, Editor, "Electrical Phenomena at Interfaces," p. 75, Methuen & Co., London (1951).
10. J. B. SCARBOROUGH, "Numerical Mathematical Analysis," p. 375, Johns Hopkins Press, Baltimore (1930).
11. D. A. MACINNES, "The Principles of Electrochemistry," p. 439, Reinhold Publishing Co., New York (1939).
12. D. A. MACINNES, *loc. cit.*, p. 440.
13. N. E. DORSEY, "Properties of Ordinary Water Substance," p. 363, Reinhold Publishing Co., New York (1940).

The Galvani Electrode Potential

PAUL RÜETSCHI

Research Department, The Electric Storage Battery Company, Philadelphia, Pennsylvania

ABSTRACT

The surface potential of Hg can be evaluated by comparing the real potential α_i (negative work function) of different impurity ions, dissolved in Hg. The real potential of an ion is the sum of a chemical term, corresponding to the interaction energy with the Hg in the bulk of the phase (depending on the ionic radius), and a constant electrical term corresponding to the surface potential of Hg (independent of the ionic radius).

An electrostatic model is developed to calculate the chemical term of the real potential. This chemical component becomes negligible for very large ionic radii, and the surface potential χ_{Hg} of Hg can be determined by extrapolation. A value of $0 < \chi_{Hg} < +0.5$ v is obtained. The fact that χ_{Hg} is positive indicates that the surface dipoles of Hg are oriented with their negative poles against the vacuum.

Using the free energies of hydration given by Latimer, a value of $0.44 < \Delta\phi < 0.94$ v is calculated for the Galvani electrode potential of a N-calomel electrode This result compares with the value of 0.5 v quoted by Latimer, Pitzer, and Slansky. The latter authors neglected the surface potential of Hg.

The object of the present paper is to compute approximately the surface potential of Hg and the Galvani potential of the N-calomel electrode. It has recently been pointed out (1) that this can be achieved by use of a thermodynamic cycle involving a dilute amalgam and a non-thermodynamic calculation of the interaction energies of impurity ions with the Hg in the dilute amalgam. In the following discussion a more accurate and detailed calculation is presented.

Guggenheim (2) considered the theory of electric poten-

tial differences between dissimilar media, based on the work of Gibbs (3). He claimed that such potential differences have no physical meaning and cannot even be defined, whereas Gibbs stated only that such potential differences are not accessible to measurements and are thermodynamically not defined. In more recent work, however, it was realized by theoretical electrochemists (4) including Guggenheim (5) that such differences of potential could be calculated in principle. However, Guggenheim's older point of view has been taken by Grahame (6) in a recent review on the electrical double layer and it has been stated that a definition of an absolute potential difference is unnecessary, since it is possible to describe all the actual experimental observations in terms of potential differences of the types already known. This is true for purely thermodynamic considerations. In studies on the kinetics of electrode reactions, however, and in all the cases where the electric fields at the interfaces are investigated, electric potential differences between the phases are important. The reality and importance of such potential differences can hardly be denied in view of the fact that in all the overvoltage studies the changes of these potentials are observed and it is hard to see why a quantity whose changes can indeed be measured experimentally should not have a definite physical meaning.

In fact, it is possible to calculate theoretically such electric potential differences on the basis of an exact knowledge of the interaction energies between the particles in the bulk of the phases or on the basis of a precise picture of the free surfaces and especially the surface dipoles (surface double layer) of the phases against vacuum. The definition of the Galvani-potential given by Lange (7–9) has made it possible to discuss the subject of electrical potential differences between dissimilar media without ambiguity. The terms "absolute," "single," or "true" electrode potentials should not be used in future discussions. It must be stressed, however, that the Galvani potential discussed below corresponds precisely to the meaning of such "absolute," "single," or "true" electrode potentials which were considered to have no physical meaning by Guggenheim (2) and Grahame (6).

In this discussion the Galvani, Volta, and surface potentials as introduced by Lange (7–9) are used.

The electrochemical potential $\bar{\mu}_i$ of a particle i in the bulk of a material phase can be written as the sum of three terms:

$$\bar{\mu}_i = Z_i e_0 \psi + Z_i e_0 \chi + \mu_i \qquad \text{(I)}$$

$Z_i e_0$ is the charge of the particle i; ψ is the Volta potential (outer potential); and $Z_i e_0 \psi$ the electric energy involved in bringing a unit positive charge from a point at charge-free infinity to a point just outside the phase, where the influence of the image force is negligible, i.e., at 10^{-4} cm from the surface of the phase. χ is the surface potential and $Z_i e_0 \chi$ the electric energy required to transfer a unit positive charge from a point just outside of the phase, across the surface dipole layer, into the phase. μ_i is the chemical potential or the energy corresponding to the interaction of the particle i with the other particles of the phase in which it has been transferred. The name "chemical potential" is misleading because all forces between atoms and ions are fundamentally electric in nature. μ_i can include terms of simple electrostatic interactions, polarization interactions, dispersion interactions, etc., according to the nature of the material.

The sum of the Volta potential ψ and the surface potential χ is defined as the Galvani potential ϕ

$$\phi = \psi + \chi \qquad \text{(II)}$$

When a phase has no net charge, its Volta potential is zero. In this case it is convenient to define another potential, viz., the real potential α_i,

$$\alpha_i = \mu_i + Z_i e_0 \chi \qquad \text{(III)}$$

which is the negative work function of the ion i. The difference between the Volta potentials of two phases may be determined experimentally (8, 9, 11), but the Galvani potential difference cannot be measured by any means.

Chemical and Surface Potentials of Aqueous Solutions

The real potential α_i is a quantity which is determinable experimentally. The chemical potential μ_i and the surface potential χ are not measurable and can be calculated only on a theoretical basis, somewhat like the activity coefficients in the Debye-Hückel theory.

According to Eq. (III) a calculation of the real potential α_i of an ion in a condensed phase consists of two parts: (*a*) the calculation of the chemical potential μ_i, and (*b*) the calculation of the surface potential χ. The apriori evaluation of the surface potentials is usually more difficult than the evaluation of the chemical potential. Therefore, most workers have calculated only μ_i and have estimated the surface potential by comparison with the measured real potential α_i [Eq. (III)].

By this semiempirical method the surface potential χ_s of diluted aqueous solutions has been determined (4, 12, 13). The index s designates a liquid phase (solution). χ_s is, of course, the surface potential of this liquid phase against vacuum. χ is essentially independent of the electrolyte (8), if no electrocapillary active substances are present, and if the solutions are not too concentrated. The surface potential results primarily from the orientation of water multipoles, mainly dipoles, in the surface. The validity of the results for χ_s depends on the reliability of the calculated values for the chemical potentials μ_i. Using the values for the free energy of hydration given by Latimer (14, 15), the surface potential of diluted aqueous solutions becomes (4, 12, 13, 16):

$$\chi_s = -0.33 \text{ v} \qquad \text{(IV)}$$

Latimer, Pitzer, and Slansky obtained the free energy of hydration for single ions by separating the experimental energy of hydration for salts according to the Born equation (17). In order to fit this equation, 0.85Å was added to the crystal ionic radii of the positive ions, and 0.10Å to the crystal ionic radii of the negative ions.

Many objections could be made against the values for the free energies of hydration quoted by Latimer and coworkers:

1. The model of Born, who regarded the ion as a rigid sphere of radius r_i and charge $Z_i e_0$ in a continuous dielectric medium, is an oversimplification.

TABLE I. *Free energy of hydration*

Metal	Kcal/mole
Li^+	−114
Na^+	−91
K^+	−74
Rb^+	−68
Cs^+	−61
Be^{++}	−565
Mg^{++}	−434
Ca^{++}	−363
Sr^{++}	−334
Ba^{++}	−304
Zn^{++}	−466
Cd^{++}	−413
Al^{+++}	−1090
In^{+++}	−965
Tl^{+++}	−962

2. The ion-dipole interaction in the primary hydration sheath is neglected.

3. The repulsion between the ion and the water molecules is not taken into account.

The theoretical values for the single ion free energies of hydration by Eley and Evans (18) are, according to Conway (19), based on a more correct model; however, a discrepancy of 20–30 kcal/mole exists between added values given by Eley and Evans for cations and anions, and experimental values given by Latimer for the salts.

At the present time the assignment of values to the individual ions is still highly questionable. Values quoted by Latimer are used tentatively in this study.

This assignment seems to be consistent with the absolute entropies of the single ions (15).

Table I gives the free energy of hydration for some ions according to Latimer (14, 15).

It must be pointed out that the use of enlarged radii ("effective Born radii") in the theory by Latimer does not correspond strictly to the idea of dielectric saturation in the vicinity of the ion. The two models have been incorrectly identified in the past. Fig. 1a illustrates the model used by Born (enlarged radii) and Fig. 1b the model with dielectric saturation in the vicinity of the ion. The electric energy of the system 1a is given by:

$$E = \frac{(Z_i e_0)^2}{8\pi\epsilon_0} \cdot \frac{1}{\epsilon r_e} \qquad (V)$$

but the electric energy of the system in Fig. 1b is given by:

$$E = \frac{(Z_i e_0)^2}{8\pi\epsilon_0} \cdot \left\{\frac{1}{r_i} - \frac{1}{r_e} + \frac{1}{\epsilon r_e}\right\} \qquad (VI)$$

where e_0 is the unit charge ($1.6\ 10^{-19}$ coulomb) Zi the valence of the ion i, ϵ_0 the dielectric constant for vacuum ($8.854\ 10^{-12}$ amp sec volt^{-1}. m^{-1}), ϵ the relative dielectric constant (vacuum = 1), r_i the crystal ionic radius (in meters) and r_e the cavity radius (in meters). E is the electric energy in wattseconds (Joule).

If the ion in the initial state (at charge free infinity) has the enlarged radius r_e in case 1a, but the correct crystal ionic radius r_i in case 1b, then the free energy of hydration (for one particle) is the same for both instances, viz.:

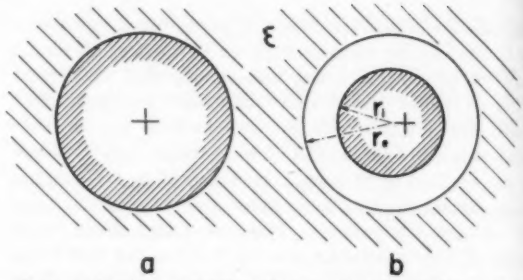

FIG. 1. Models of hydrated ions (a) enlarged radii, (b) dielectric saturation.

$$\mu_{i_s} = -\frac{(Z_i e_0)^2}{8\pi\epsilon_0} \cdot \frac{1}{r_e}\left\{1 - \frac{1}{\epsilon}\right\} \qquad (VII)$$

which is the Born equation.

If model of Fig. 1a is correct, the addition to the radii should be independent of the solvent and the free ions in a gas would have larger radii than in the crystals. Enlarged radii for ions in a dissolved state have been proposed by Eucken (20, 21), but are unlikely in view of modern work on the electronic structure of atoms and ions.

Both models are based on the use of a uniform dielectric constant in atomic dimensions, and are subject to the objections mentioned above.

Surface Potentials of Metals

Theoretical calculation of surface potentials of metals has been attempted several times (22–24). Table II illustrates some results.[1]

Values in Table II have been obtained from the difference between the real potential α_e (negative work function) and the chemical potential μ_e of an electron in the metal. Calculations for μ_e, based on the simple electron gas theory, are valid only for the alkali metals. The surface potentials listed for Cu, Mg, Ca, Be are highly questionable.

Recently it has been shown that there is still another way to evaluate the surface potentials of the metals (1). Summarizing shortly, this method makes use of a thermodynamic cycle involving an alloy system whereby only a trace of a foreign metal M′ is alloyed with a pure metal phase M. The following cycle is then applied: One mole of the added metal M′ is removed from the alloy. The removed metal M′ is thereafter vaporized, ionized in the gas phase, the ions and electrons are added separately to the alloy, and finally recombined in the bulk of the alloy to the initial state. From this cycle the real potential α_i of the impurity ions can be obtained.

$$-\alpha_i = -A + S + J - \theta - J^* \qquad (VIII)$$

where A = free energy of alloying (free energy of mixing); S = free energy of sublimation of the metal M′; J =

[1] Parsons (10) gives a complete table of calculated surface potentials. Although the absolute values of the surface potentials are cited correctly by this author, the signs in his table are in error. The surface potentials of the metals must be given positive signs.

TABLE II. *Surface potentials of metals*

Metal	Surface potential χ_M in volts	
	Herring (22)	Seitz (26)
Li	0.7	0.1
Na	0.3	0.1
K	0.2	0.4
Cu	0.8	
Ca	1.3	
Mg	2.5	
Be	5.1	

ionization energy for the first electron of M′; θ = electronic work function of the alloy (identical with the electronic work function of the metal M); and J^* = ionization energy of M′ in the alloy for the first electron (energy to lift an electron of the impurity center from its energy level to the conduction band of the alloy).

The term J^* is in many cases small and can be neglected. Sometimes J^* can be determined separately (i.e., ionization energy of impurity centers in semiconductors). In the following treatment it is assumed that the impurity atoms are completely ionized and J^* is therefore zero. It should be noted that the terms in Eq. (VIII) correspond to free energies, and α_i depends, therefore, on the concentration.

The real potential α_i of impurity ions can be calculated with Eq. (VIII) from experimental data. According to Eq. (III) the real potential α_i is the sum of the surface potential term $Z_i e_0 \chi$ and the chemical potential μ_i, the surface potential χ now being constant for different impurity ions and identical with the surface potential of the "solvent" metal M.

Difference in the real potentials from one impurity ion to another must correspond to difference in the chemical potentials. The differences may be obtained from experimental data, and can be correlated to the radii and to the electronic configuration of the ions.

Equations for the interaction energies between the impurity ions and the excess metal can be derived on a quantum-mechanical basis (25, 26). These calculations are difficult, especially for metals other than those of the alkali group, and show that the main interaction terms are inversely proportional to the ionic radii or to the square of the ionic radii. In the following, a simple electrostatic model is used to estimate the interaction energy of ions dissolved in Hg.

The dissolved ions are treated as small charged spheres with the crystal radii r_i. They will be surrounded by a cloud of electrons in the Hg.

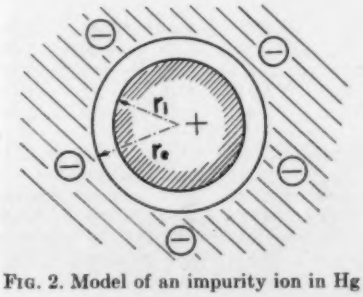

FIG. 2. Model of an impurity ion in Hg

With this model the dissolved ion can be described as a very small spherical condenser, as it is shown in Fig. 2. The capacity of this spherical condenser is given by:

$$c = 4\pi\epsilon_0 \cdot \epsilon \cdot \frac{r_i r_e}{r_e - r_i} \qquad \text{(IX)}$$

where r_i is the crystal radius of the ion, r_e the cavity radius and ϵ the relative dielectric constant in the gap.

The electric energy of this system equals

$$E_1 = \frac{(Z_i e_0)^2}{2c} = \frac{(Z_i e_0)^2}{8\pi\epsilon_0 \epsilon} \cdot \frac{\delta}{r_i^2 + r_i \delta} \qquad \text{(X)}$$

whereby:

$$\delta = r_e - r_i$$

Since the electric energy of the free ion in vacuum is given by

$$E_2 = \frac{(Z_i e_0)^2}{8\pi\epsilon_0} \cdot \frac{1}{r_i} \qquad \text{(XI)}$$

the energy of amalgamation equals

$$\mu_{iM} = \Delta E = -\frac{(Zie_0)^2}{8\pi\epsilon_0} \cdot \frac{1}{r_i} \left\{ 1 - \frac{\delta}{(r_i + \delta)\epsilon} \right\} \qquad \text{(XII)}$$

The free energy of amalgamation, μ_{iM}, varies inversely with the ionic radii r_i. According to Eq. (III) the real potential then becomes:

$$\alpha_i = -\frac{(Z_i e_0)^2}{8\pi\epsilon_0 r_i} \cdot \left\{ 1 - \frac{\delta}{(r_i + \delta)\epsilon} \right\} + Zie_0 \chi \qquad \text{(XIII)}$$

The term in the brackets becomes approximately 1 if one inserts reasonable values for δ and ϵ. (δ is probably in the order of $\frac{1}{10} r_i$ and ϵ in the order of 10.) With these approximations one obtains:

$$\alpha_i = -\frac{C}{r_i} + Z_i e_0 \chi \qquad \text{(XIV)}$$

where c is a constant. A plot of the experimental values of the real potentials α_i against $1/r_i$ should therefore be a straight line. The intersection of this straight line with the ordinate at $1/r_i = 0$ corresponds to the surface potential χ.

It should be pointed out that an identical type of relation between the chemical potential μ_i and the ionic radii r_i could be derived on a quantum-mechanical basis (25, 26) which shows that the simple condenser model gives a reasonable result. In the less rigorous treatment given recently (1) it was assumed that the leading term of the chemical potentials of the impurity ions is inversely proportional to the square of the ionic radii. A relation of this type can be derived on a theoretical basis using the free electron theory and the theorem of Clausius, according to which the total energy of an electron equals the negative kinetic energy of the electron. The interaction energy between the impurity ions and the Hg is then essentially determined by the Fermi-energy of the electrons (25). It should be noted that under this assumption the ionic radii should not be identified with the crystal ionic radii (given by Pauling) and that it is reasonable to assume them to be larger than the crystal ionic radii. This fact was, indeed, confirmed in the cited paper (1).

TABLE III. *Data on real potentials of impurity ions in Hg**

Metal	A	S	J	θ_{Hg}	α_i	r_i[Å]
Li^+	−0.942	1.266	5.363	4.530	−3.041	0.68
Na^+	−0.854	0.810	5.120	4.530	−2.254	0.95
K^+	−1.040	0.634	4.318	4.530	−1.462	1.33
Rb^+	−1.052	0.579	4.159	4.530	−1.260	1.48
Cs^+	−1.070	0.531	3.870	4.530	−0.941	1.69

* Pauling's values for the ion radii r_i have been used with the exception of Li. For the latter metal the value quoted by Pauling (0.60Å) is probably too small [*see* Strehlow (4), Latimer (15)]. The free energies of amalgamation A of the alkali metals have been taken from a recent polarographic study (27). The free energies of sublimation S are taken from "Selected Values of Thermodynamic Properties," National Bureau of Standards, Washington, D. C., Series 1, Tables 91-1 to 95-1 (1950). The ionization energies and the electronic work function θ_{Hg} of Hg correspond to the values given in "Handbook of Chemistry and Physics," 33rd ed., pp. 2125–2126 and p. 2129, Chemical Rubber Publishing Co., Cleveland (1951/1952).

Table III shows the data used to calculate the real potentials α_i of alkali ions dissolved in mercury (energy terms in ev).

The free energies of amalgamation A of the alkali metals are, of course, dependent on the concentration of the amalgams. The influence of the concentration is, however, rather small since a factor of 10 in the concentration changes the value of A only in the order of 100 mv, which is less than the error limits for α_i. The values of A listed in Table III correspond to polarographic concentrations (in the order of 10^{-3} mole/liter). The values for S given in Table III are free energies of sublimation. It should be noted that in the earlier treatment (1) the heats of sublimation were used (in lack of proper references) which caused the real potential to become too large by an amount of 0.3 ev, and the upper limit for the surface potential χ_{Hg} to become too small by the same amount. If the correct values for the free energies of sublimation S are inserted in the earlier treatment, the value of the surface potential becomes identical with the value computed below. This fact is particularly interesting and shows that the described "trace method" seems to be not very sensitive to the model used as long as this model is a reasonable approximation. It must also be mentioned that in the earlier paper (1) α_i designated the work function of the ions. Here it is used for the real potential of the ions (which is the negative work function) according to the nomenclature given by Lange (7–9).

Fig. 3 shows a plot of the real potentials α_i against $1/r_i$. The slope of the straight line does not correspond exactly to the value predicted by Eq. (XIII), but is somewhat smaller. An exact agreement cannot be expected.

The condenser model has merely been used to derive the $1/r_i$ relation, which takes in account the Coulambic interaction. The value of χ can therefore be obtained by extrapolation without a theoretical evaluation of the other factors in the $1/r_i$ term, if these other factors can be assumed to be constant for a series of similar ions. This point shows the main advantage of the "trace method". The chemical potentials (or the slope on the plot $\mu_i \longrightarrow 1/r_i$) need no longer be calculated apriori in detail. It is sufficient to know the type of relation between μ_i and r_i. This relation can, indeed, be studied experimentally.

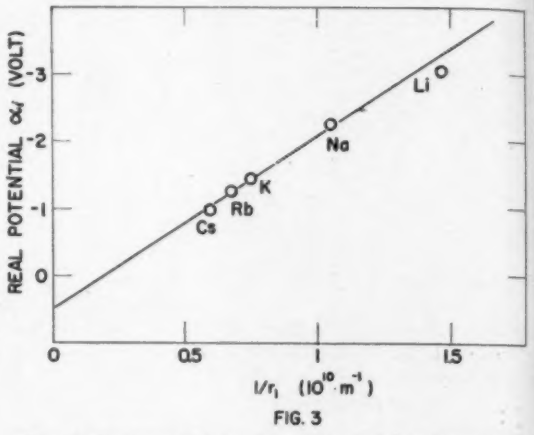

FIG. 3

FIG. 3. Real potentials of impurity ions in Hg plotted against reciprocal ionic radii.

From the plot of α_i against $1/r_i$ it is concluded that the surface potential of Hg amounts to

$$0 < \chi_{Hg} < 0.5 \text{ v} \qquad \text{(XV)}$$

The value of 0.5 v gives the upper limit rather than an average for χ_{Hg}, because of the fact that the repulsion terms of μ_i have been neglected.

The positive value of the surface potential indicates that the surface dipoles are oriented with their negative pole toward the gas phase. This is reasonable since one would expect the electrons to overlap into the vacuum beyond the positive cores.

The free energies of amalgamation can now be obtained with Eq. (III):

$$\mu_{iM} = \alpha_i - Z_i e_0 \chi_M$$

From Eq. (I) and (II) one deduces that the difference in Galvani potentials $\phi_I - \phi_{II}$ between two phases I and II in equilibrium ($\bar{\mu}_{i_I} = \bar{\mu}_{i_{II}}$) is given by $\phi_I - \phi_{II} = \phi_{Hg} - \phi_s = \dfrac{\mu_{i_s} - \mu_{i_{Hg}}}{Z_i e_0}$.

Using the free energies of amalgamation of the ions obtained in this study and the free energies of hydration of

TABLE IV. *Data on Galvani potentials of amalgam electrodes and the N-calomel electrode*

Electrode	μ_{i_S}	$\mu_{i_{Hg}}$	$\Delta\phi_{amalgam}$	E	$\Delta\phi_{N\text{-calomel}}$
Li (Hg)/Li^+...	−4.95	−3.54	−1.41	−2.38	0.97
Na (Hg)/Na^+.	−3.95	−2.75	−1.20	−2.14	0.94
K (Hg)/K^+....	−3.21	−1.96	−1.25	−2.17	0.92
Rb (Hg)/Rb^+.	−2.95	−1.76	−1.19	−2.15	0.96
Cs (Hg)/Cs^+..	−2.65	−1.44	−1.21	−2.14	0.93

μ_{i_S} = free energy of hydration according to Latimer of the ion i. $\mu_{i_{Hg}}$ = free energy of amalgamation according to this work of the ion i. $\Delta\phi_{amalgam}$ = Galvani electrode potential of the amalgam electrode. E = electrode potential of the amalgam electrode measured against a N-calomel electrode. $\Delta\phi_{N\text{-calomel}}$ = Galvani electrode potential of the N-calomel electrode.

the ions given by Latimer, the Galvani potential difference $\phi_{Hg} - \phi_s = \Delta\phi_{amalgam}$ of the diluted amalgam electrodes may be obtained. In Table IV Galvani potential differences are listed together with the experimental electrode potentials of the amalgam electrodes against a N-calomel electrode (27). The difference between these two potentials should be constant and should be equal to the Galvani potential of a N-calomel electrode. Table IV shows that this is indeed the case. The latter fact of course does not provide any measure for the degrees of correctness and accuracy of the presented method, although it does present further evidence that relation (XIV) is adequate.

Experimental values for the free energies of hydration listed in Table IV correspond to equal concentrations of the ions in the gas phase and in the liquid phase; ion (gas) = ion (aq) = 0.041M, that is with no change in volume (14, 15). Values listed for E correspond to somewhat smaller concentrations, but the error introduced by this fact can again be neglected in view of the approximate nature of all the calculations at the present stage of refinement of the described "trace method".

Therefore, it can be concluded that the Galvani potential of a N-calomel electrode $\Delta\phi_{N\text{-calomel}} = \phi_{Hg} - \phi_{sN\text{-calomel}}$ has a value of $\Delta\phi_{N\text{-calomel}} \simeq 0.94$ v, which is again the upper limit for the Galvani potential.

If the surface potential of mercury were zero, a value of 0.44 v, would be obtained. Therefore,

$$0.44 < \Delta\phi_{N\text{-calomel}} < 0.94 \text{ v} \qquad \text{(XVI)}$$

Latimer, Pitzer, and Slansky (14), neglecting the surface potential of Hg, have calculated a value of $\Delta\phi_{N\text{-calomel}} = 0.495$ v. As has been noted (4, 16, 28–31) the surface potential of Hg must be added to the calculated value of 0.495 v in order to obtain the correct Galvani potential of the N-calomel electrode:

$$\Delta\phi_{N\text{-calomel}} = +0.495 \text{ v} + \chi_{Hg}$$

[*see* Eq. 5, reference (16).]

The value of the surface potential of Hg is of particular interest in the theory of zero charge electrodes (16). It should also be noted that the outlined theory can be applied to an apriori calculation of polarographic half-wave potentials of metal ions.

Finally, it must be stressed that the present treatment is only a first approximation, although the principle of the "trace method" is quite fundamental and will be applied in the future for more rigorous evaluations of the Galvani potentials on the basis of more accurate experimental data for work functions and real potentials and on the basis of more accurate quantum mechanical calculations for the interaction energies in condensed phases.

Manuscript received January 16, 1956. This paper was prepared for delivery before the San Francisco Meeting, April 29 to May 3, 1956.

Any discussion of this paper will appear in a Discussion Section to be published in the December 1957 JOURNAL.

REFERENCES

1. P. RÜETSCHI, *Z. Elektrochem.*, **60**, 29 (1956).
2. E. A. GUGGENHEIM, *J. Phys. Chem.*, **33**, 842 (1929); **34**, 1758 (1930).
3. W. GIBBS, "Collected Works," Vol. I, p. 429, Longmans and Green, New York (1928).
4. H. STREHLOW, *Z. Elektrochem.*, **56**, 119 (1952).
5. R. FOWLER AND E. A. GUGGENHEIM, "Statistical Thermodynamics," p. 488, Cambridge Univ. Press (1952).
6. D. C. GRAHAME, *Chem. Rev.*, **41**, 441 (1947).
7. E. LANGE, "Handbuch der Experimentalphysik," Vol. 12, Pt. 2, p. 267 ff, Akademische Verlagsgesellschaft, Leipzig (1933).
8. O. KLEIN AND E. LANGE, *Z. Elektrochem.*, **43**, 570 (1937).
9. E. LANGE, *ibid.*, **55**, 76 (1951); **56**, 94 (1952).
10. An excellent discussion by R. PARSONS in J. O'M. BOCKRIS, "Modern Aspects of Electrochemistry," Academic Press, Inc., New York (1954).
11. K. MÖHRING, *Z. Elektrochem.*, **59**, 102 (1955).
12. E. VERWEY, *Rec. Trav. Chim.*, **61**, 564 (1942).
13. R. HUSH, *Aust. J. Sci. Res.*, **AI**, 482 (1948).
14. W. M. LATIMER, K. S. PITZER, AND C. M. SLANSKY, *J. Chem. Phys.*, **7**, 108 (1939).
15. W. M. LATIMER, *J. Chem. Phys.*, **23**, 90 (1955).
16. P. RÜETSCHI AND P. DELAHAY, *ibid.*, **23**, 697 (1955).
17. M. BORN, *Z. Physik.*, **1**, 45 (1920).
18. D. D. ELEY AND M. G. EVANS, *Trans. Faraday Soc.*, **34**, 1093 (1938).
19. B. E. CONWAY AND J. O'M. BOCKRIS, "Modern Aspects of Electrochemistry," p. 47, Academic Press Inc., New York (1954).
20. A. EUCKEN, "Lehrbuch der Chemischen Physik," II, 2, p. 992, Geest and Portig, Leipzig (1949).
21. G. PASSOTH, *Z. Phys. Chem.*, **203**, 275 (1954).
22. C. HERRING, "Metal Interfaces," American Society of Metals, Cleveland (1952).
23. C. HERRING AND M. NICHOLS, *Rev. Mod. Phys.*, **21**, 185 (1949).
24. A. HUANG AND E. WYLLIE, *Proc. Phys. Soc.*, **62A**, 180 (1949).
25. H. FRÖHLICH, "Elektronentheorie der Metalle," pp. 256–285, Springer, Berlin (1936).
26. F. SEITZ, "The Modern Theory of Solids," McGraw-Hill Book Co., New York (1940).
27. A. VLCEK, *Coll. Czech. Chem. Commun.*, **20**, 400 (1955).
28. P. VAN RYSSELBERGHE, *J. Chem. Phys.*, **21**, 1550 (1953).
29. A. FRUMKIN, *ibid.*, **7**, 552 (1939).
30. W. C. BURGERS, *Chem. Weekblad*, **39**, No. 16-17, 1, (1942).
31. R. PIONTELLI, Int. Committee Electrochem. Therm. Kin. Proc. 2nd Meeting, pp. 344–369, Milan (1951).

Hydrogen Evolution Reaction on Copper, Gold, Molybdenum, Palladium, Rhodium, and Iron

Mechanism and Measurement Technique under High Purity Conditions

N. PENTLAND

Technical College, Brighton, England

J. O'M. BOCKRIS

University of Pennsylvania, Philadelphia, Pennsylvania

E. SHELDON

Technical College, Acton, London, England

ABSTRACT

Various aspects of technique in measurements of electrode kinetics under conditions where competing reactions due to the presence of trace impurities in the solution are important are examined.

The kinetics of the hydrogen evolution reaction in acid and alkaline solutions on several transition metals has been examined with special reference to the low current density region. Inferences concerning the rate-determining step in the reactive $2H^+ + 2e_0^- \rightarrow H_2$ are thus drawn. In general, there is a tendency for the metals examined in acid solution to have a rate-controlling electrochemical desorption reaction and for those in alkaline solution to have a rate-determining discharge step.

During the past five years, a number of experimental and theoretical techniques have been devised whereby the attack on the mechanism of electrode reactions need no longer be prosecuted by qualitative inference but by the evaluation of diagnostic criteria which allow unambiguous decisions between mechanisms to be made (1). Two different modifications of these approaches have been made, the first depending on d-c measurement of the rate of the reaction as a function of the overpotential, and the second depending on the evaluation of the impedance of the reaction as a function of frequency (2). Roughly, these two approaches have maximum applicability for slow electrode reactions (exchange current density $<10^{-3}$ amp cm^{-2}) and fast reaction (exchange current density $>10^{-3}$ amp cm^{-2}), respectively. The hydrogen evolution reaction has relatively low rate constants on all metals. Detailed studies of the mechanism of this reaction on several metals have been published (1). In this paper, the determination of the most important relevant parameters used for the evaluation of diagnostic criteria for the hydrogen evolution reaction have been applied to Cu, Au, Mo, Pd, Rh, and Fe cathodes. The necessary details of the technique of measuring currents at electrodes under ultra-high-purity conditions for electrode reactions which are easily vitiated by the presence of trace impurities are also here published for the first time.

EXPERIMENTAL METHODS

Electrolytic Cell

The cell used (Fig. 1) was fundamentally that of Bockris and Pentland (3) with the following modifications: (*a*) provision of a water-cooled, water-sealed tap (Fig. 2); (*b*) provision of a trident shaped graphite anode, for use with pre-electrolysis at high current density (Fig. 3). The cathode compartment of the cell was of As-free glass ("Hysil"). Gases entering the cell escaped through water-sealed non-return valves; all joints, caps, and valves were sealed with equilibrium water to avoid use of tap grease. The cell was attached to a paxolin base and positioned inside a polythene tray to ensure electrical insulation.

The H reference electrode was constructed by pinch sealing Pt to glass, spot welding being avoided in order to reduce contamination by foreign metals. After platinization (without use of lead acetate), the electrode was washed in equilibrium water, then in conductivity water, and its potential checked against that of a calomel electrode. The electrode was stored in conductivity water for 30 hr before use and checked frequently. When not in use it was kept in equilibrium water. The same electrode maintained potential to 0.2 mv for more than 14 months.

The cathode compartment contained the electrode-bulb breaker F, which entered the cell obliquely through a ground glass sleeve which allowed the plunger to be withdrawn from the catholyte without exposing the latter to the air. The cathode cap (Fig. 4) carried five parallel ground glass sleeves, thus enabling the electrodes to be rotated and moved vertically without subjecting the solution to contact with the air. Each syringe tube carried a cup at its upper end for sealing with solvent against atmospheric contamination.

For alkaline work, concentrated pure NaOH solution entered through H and for acid preparation HCl gas was admitted via J. Conductance water distilled in H_2 was led

through H and pure H_2 through the capillary K. Concentration of the electrolyte was determined by measurement of conductance between fixed Pt electrodes L, the cell constant of which had been previously established. The arrangement of L high in the anode compartment limited the time of contact of a solution to the short period of adjustment of solution concentration. After the solution had attained concentration and was shared with the cathode compartment, its level was below that of L.

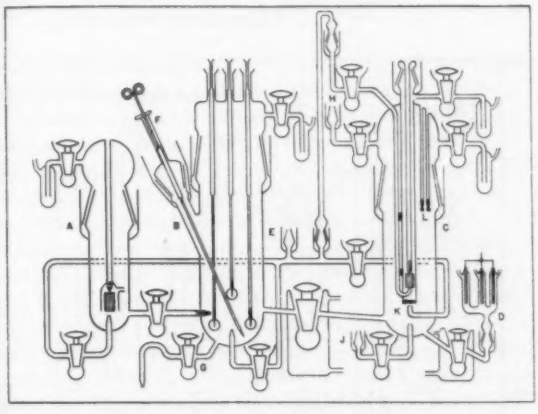

FIG. 1. Cell for measurement of hydrogen evolution under pure conditions at low current densities. A = reference hydrogen electrode; B = cathode compartment; C = anode compartment and solution preparation vessel; D = supplementary anode; D = trident shaped anode; E = H_2 inlet; F = plunger for breaking electrode bulbs; G = tap for removal of washing; H = inlet to anode compartment; J = inlet for HCl gas; K = inlet for H_2 gas; L = conductivity points for establishing concentration.

The anode cap (Fig. 1 and 5) consisted of an additional central tube sealed at the lower end by a sintered glass disc, porosity 3, inside which was a Pt foil, over which H_2 (discarded via a water-sealed bubbler at the top of the cap) swept to carry off anodically produced gases. During long pre-electrolysis, the solution level sometimes fell below the Pt, so that a supplementary anode was also employed and in work at the highest c.d.'s the trident shaped anode (Fig. 3) was utilized. The latter consisted of rods, 6.5 mm diameter graphite, 10 cm long, sealed into Hysil tubes (Fig. 6). A hole 1 mm diameter and 2 cm long was drilled in the top of the graphite and a side hole for escape of liberated Cl_2 was attached below the seal.

Cathode preparations.—Each metal used was of spectroscopic purity. Each cathode material, except Mo, was attached to a short length of 28 S.W.G. Pt wire so that a good metal-glass seal could be obtained (Table I). Mechanical attachment was performed by flattening one end of the electrode, using cleaned stainless steel pliers, and a $\frac{1}{64}$-in. hole was drilled. Pt was secured in the hole by pinching. This procedure was employed for Cu. For Au and Pd cathodes, fusion to Pt in an oxygen flame was used. Rh and Fe were spot welded to Pt. The metal under investigation was cut with cleaned Cr plated cutters and handled only with Pt tipped tweezers or filter paper.

Mo electrodes contained traces of surface oxide and carbide, introduced in drawing-down, which were difficult to remove except as follows: 30 cm lengths of wire were clamped in a bell jar of a high vacuum coating unit. Pressure was reduced to 10^{-5} mm Hg and 28 amp was passed through the wire for 10 min, the temperature being about 2200°C. The wire was cooled and air admitted to raise the pressure to 10^{-2} mm Hg. Mo was heated to red heat for

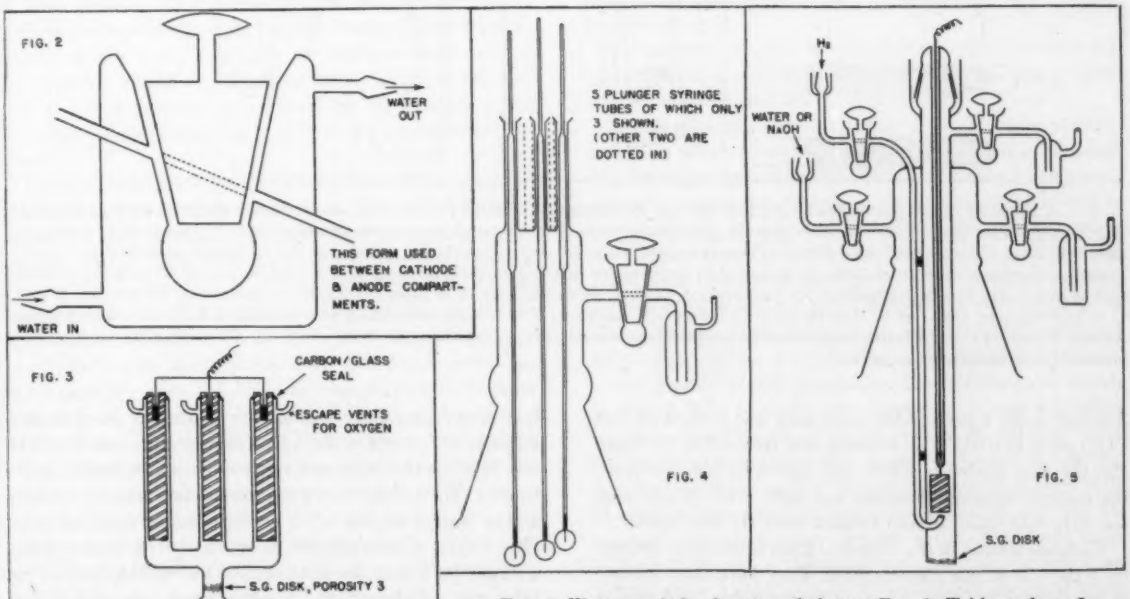

FIG. 2. Water cooled solvent sealed tap. FIG. 3. Trident shaped anode. FIG. 4. Cathode cap. FIG. 5. Anode cap.

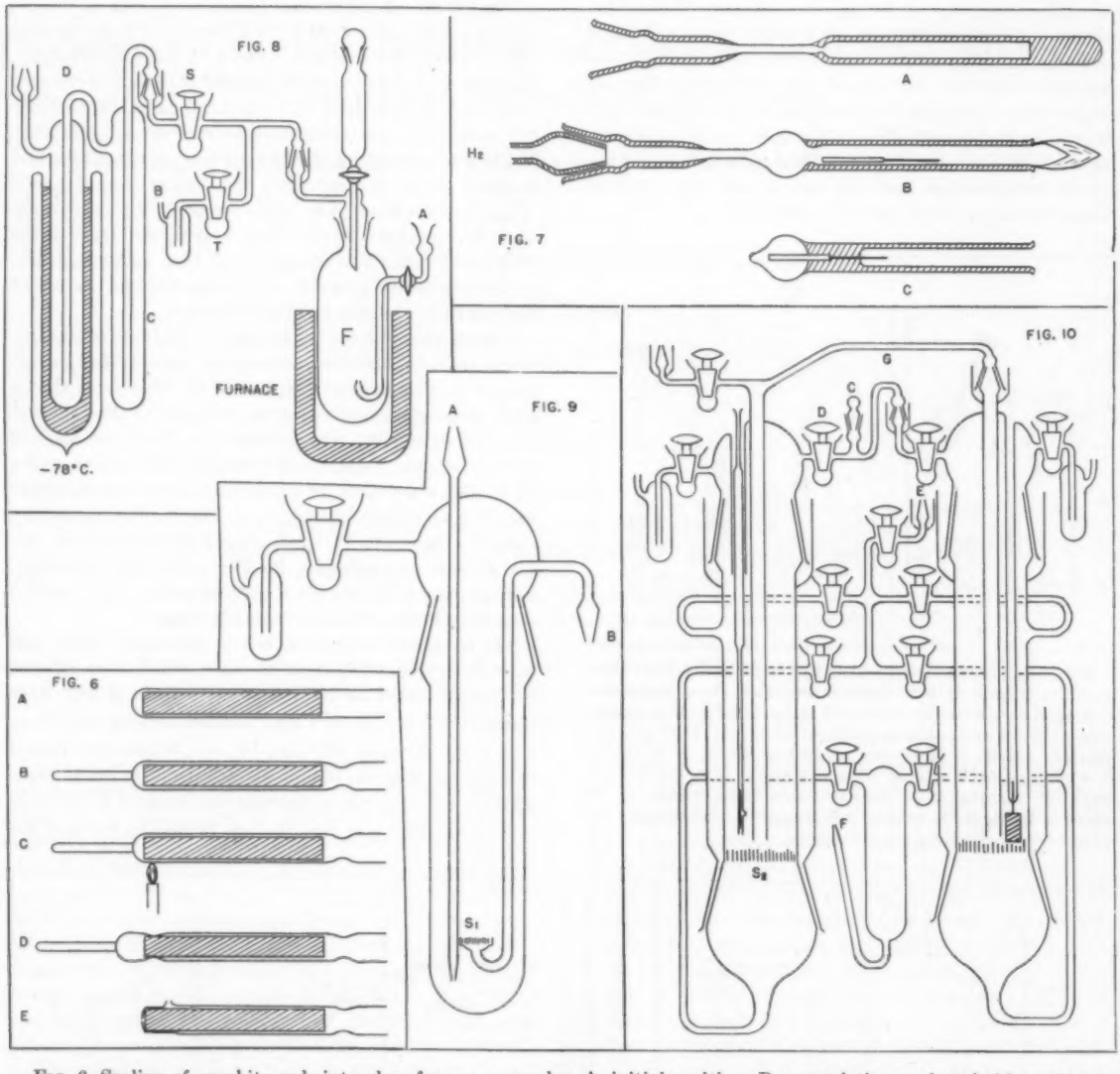

FIG. 6. Sealing of graphite rods into glass for use as anodes: A, initial position; B, constriction made to hold graphite in place, and holder fused on end; C, heating; D, glass pulled rapidly over graphite surface and annealed; E, top portion drawn off and vent blown at top near seal. FIG. 7. Preparation of cathode, sealed into bulb containing H_2. A, socket attached to tube of arsenic-free glass; B, wire of cathode material in position for heating with H_2 passing over it and burnt out at end; C, cathode sealed into bulb. FIG. 8. Apparatus for preparation of pure HCl solutions. A = inlet for H_2; B = sealed trap for escape of gas; C = preliminary trap; D = trap in solid CO_2 freezing mixture; F = vessel containing recrystallized KCl onto which drops Analar H_2SO_4. FIG. 9. Preliminary alkaline preparation vessel (for annotation, *see* text). FIG. 10. Main alkaline purification vessel (for annotation, *see* text).

2–5 min, until a perceptible oxide film was formed (C and CO_2 now removed). The pressure was reduced to 10^{-6} mm Hg, the wire heated to 2200°, and the oxide film removed, the surface becoming lustrous and light gray. When cool, the wire was removed and treated with H_2 (see below).

Electrode sealing in H_2.—As-free glass tubes were cleaned for 5 days in strong chromic acid. They were then washed in tap water, followed by equilibrium water, and stored therein. One such tube was withdrawn using Pt-tipped, cleaned tweezers, dried, and attached at one end to a piece of Hysil tubing by which it could be manipulated. [The rest of the procedure was similar to that of Bockris and Conway (4) except in the following way.] A cleaned socket was fused to the other end and a constriction made 2.5 cm from it. The tubing before the constriction was drawn into a thin walled section (c) 5 cm long and 2 mm diameter (Fig. 7A). A minute intense oxy-gas flame was used to blow a fragile bulb near the constriction, the subsidiary holding tube was withdrawn, and simultaneously the end of the electrode tube was blown open, its form being as in Fig. 7B. (In all glass blowing operations, the pressure is transmitted from the mouth through cotton wool pads and silica gel to

TABLE I. *Dimensions and preparation of metal electrodes*

Metal	Diameter (cm)	Approximate length (cm)	Method of attachment to Pt
Cu	0.0914	1.0	Mechanical
Au	0.0914	1.0	Mechanical and fusion
Mo	0.100	4.5	—
Pd	0.100	1.0	Fusion
Rh	0.150 and 0.050	0.7 1.3	Spot welding
Fe	0.0914	1.0	Spot welding

remove contaminants from the breath.) The electrode tube was then plugged to a cone from which issued H_2, led from a distribution head by means of cleaned glass tubing, containing only water-sealed joints, and passed through an empty trap, a trap at liquid air temperatures and a T piece, its entire limb leading to the atmosphere via a tap and bubbler, sealed with equilibrium water. H_2 was led to the cone by a very short length of polyethylene tubing, necessary to give flexibility.[1] The electrode was inserted into the tube and the H_2 issuing from the end was ignited, whereupon the composite electrode was heated to red heat before being tapped forward into the bulb. A seal was made over the metal-Pt junction and continued for 1.5 cm along the Pt, the surplus H_2 being allowed to escape via the T piece bubbler. After allowing the glass-metal seal to cool, the bulb was closed and simultaneously drawn away from the thin walled section by momentary application of an intense flame beyond the bulb. The electrode appeared as in Fig. 7C. This was then attached to a plunger of the ground glass tubes of the cathode cap, and washed with equilibrium water. Mo electrodes would not seal to Hysil and Chance GSC glass was used.

This method has the following advantages compared with its predecessor (4): (*a*) volatile impurities cannot condense on the bulb walls; (*b*) an improved seal over a considerable length of Pt can be achieved; (*c*) cooling of this seal before sealing bulb caused the H_2 pressure inside the bulb to remain uniform (otherwise implosion is frequent).

Vacuum heating and sealing of electrodes.—This was used mainly for Mo cathodes which, in method (*a*), had to be exposed to air between heating in high vacuo and introducing into H_2-filled bulbs. A 12 cm length of As-free Chance GSC glass tubing, 4 mm ID and 5 mm OD was cleaned as for the Hysil glass above. Two thickened constrictions were made, one at the end of the tube, and a fragile bulb was blown at this end. A 5 cm spectroscopically pure Mo wire, 0.1 cm diameter, previously vacuum heated in an Edwards unit, was introduced and arranged so that 1 cm projected into the bulb without touching the sides. The other end of the Mo was attached lightly to the glass by heating the second constriction sufficiently just to melt the glass and allow the wire to sink into it. The electrode tube was then fused horizontally to a Pyrex glass pump head, Chance GSC glass forming an intermediate seal, and was evacuated to 10^{-5} mm (until no discharge could be observed), the electrode holder being isolated from the pump by a liquid air trap. The electrode tube was thereupon surrounded by the coil of a radio frequency electronic heater and 2000°C induced in the Mo by 85 amp in about 2 sec. The temperature was maintained for 1 min. A seal over the Mo wire was made by heating the constriction near the bulb with an oxy-gas flame. The Mo-glass seal was 2–3 cm long; about 1 cm of light gray, lustrous Mo projected into the bulb. The electrode tube was withdrawn from the GSC/GSD glass joint at the end remote from the bulb and sealed to preserve a high vacuum inside the tube. This was then immersed in 1:1 HNO_3-H_2SO_4 mixture for 1 hr and washed with distilled, equilibrium, and conductivity water. The closed end away from the bulb was opened, and the tube mounted in the cell. Tubes were handled only by tweezers or filter paper.

[1] Caution must be taken in choice of the polyethylene tubing. Certain varieties show slight change of color after passage of H_2 for many hours and hence must be avoided.

Materials

Purification of hydrogen.—The "oxygen free" H_2 in cylinders contained 0.001% O_2, 0.001% CO, and 0.05% hydrocarbons. It passed through a few inches of polyethylene tubing to a two-way T trap through which the whole of the purification train could be evacuated, through a trap (5) and pressure indicator, SiO_2 gel, hopcalite (removes CO in absence of moisture), and soda lime. H_2 was then passed through palladised asbestos (5%) at 550° and further tubes of SiO_2 gel to remove water produced in the Pd tube. Four glass traps followed, the central two containing activated charcoal and the extreme ones empty. The first three traps were immersed in liquid N_2, the level of which was always maintained above that of the charcoal. The fourth trap served to retain water spray which sometimes arises during evacuation of the H_2 purification train. Traps were flamed out and charcoal reactivated after each run and then evacuated and flushed with H_2 for 1 hr before any was allowed to enter the cell.

H_2 was also purified by passage through a heated Pd tube but the maximum convenient yield was only 7 l/hr and the method was not extensively used.

Purification of water.—Distilled water from an electric still from which all rubber connections had been removed was redistilled from alkaline $KMnO_4$ and fractionally condensed in a block tin condenser. About 60% of the distillate was used. Its specific conductance was 1×10^{-6} mhos cm^{-1}. This water was transferred by pure H_2 pressure to a Hysil flask, refluxed in pure H_2 for 15 hr, and distilled into the cell when it had a conductance of 1×10^{-7} mhos cm^{-1}. The water purification apparatus was periodically cleaned with nitric-sulfuric acid, distilled and equilibrium water.

Preparation of acid solutions.—The apparatus is shown in Fig. 8. KCl of analytical reagent grade was placed in reaction vessel F and air swept out by H_2 entering at A and escaping by a valve. The vessel was heated at 500° for 3–4 hr. Capillary active impurities were thus removed. H_2 was still passed until the salt was cooled, and the H-passage allowed to occur through S into the anode compartment through a vigorously cleaned glass bridge. Trap D was then cooled to −78°C and H_2SO_4 dropped upon the KCl. Trap C caught acid spray (which otherwise blocks D). D condenses H_2S, etc.

After use the apparatus was always washed with nitric-

sulfuric mixtures for 24 hr, and rinsed many times with distilled and equilibrium water, being finally dried in an oven at 150°C.

Preparation of pure alkaline solutions.—The method used closely resembled that of Bockris and Potter (6), but its description has not been published previously. Pickering (7) showed that large amounts of solid separates from concentrated NaOH solution in ranges −22° to −2° and 20°–52°. The former range was chosen because of lessened attack on the glass.

The purification cell is shown in Fig. 9 and 10. A concentrated solution of A.R. NaOH pellets in conductance water was prepared in the vessel of Fig. 9, and transferred to the main vessel. (Both preliminary and main vessel were washed several times with conductance water before use.) 70 g of NaOH were introduced i..to the preliminary vessel, and first H_2, and then conductance water, were introduced from the conductance still while the lower part of the vessel was cooled in ice. The vessel was then disconnected from the still, sealed from air, and dissolution in H_2 proceeded. After sweeping out all air from bridges and connecting tubes, the solution in the preliminary vessel was transferred to the left hand limb of the main vessel (Fig. 10) by connecting joint B to joint C of the main vessel by applying pressure at A. Solid impurities were trapped by the sintered glass disc S1, porosity 1; after transfer of solution, tap D of the main vessel was closed, and H_2 bubbled through the solution via E and the sintered glass disc S2, porosity 3. Into the glass jacket surrounding the left limb (Fig. 10) was now introduced a CO_2 alcohol mixture. Solid CO_2 is added very gradually, until crystallization just commences. Supernatant liquor is drawn off through S2 from the crystals which were left dry, by applying a vacuum line at F. The crystals were liquified. The concentrated solution was transferred to the right-hand limb via tube G and again recrystallized, the left-hand limb meanwhile being washed with conductance water. After three or four recrystallizations in alternate limbs, the remaining highly concentrated solution was diluted by distilling in conductance water. The solution was shared between the two limbs, and electrolysis commenced by lowering the cathode (on a syringe plunger) into the solution. The current was $5–7 \times 10^{-2}$ amp. Wire, not foil, was used to increase current density and thus impurity removal. Pre-electrolysis was continued for a minimum of 30 hr and indefinitely during storage of the NaOH solution, H_2 always being passed through the solution. Termination of pre-electrolysis was carried out by raising the Pt cathode by means of its ground glass syringe (it is important to allow cessation of current to be brought about by the electrode removal).

When required, a few milliliters of concentrated purified solution were transferred by H_2 pressure to the anode compartment of the cell of Fig. 1 and diluted to required concentration. Solutions prepared in this way were subject to further pre-electrolysis in the cell.

Suitable glass.—The rate of the hydrogen evolution reaction is noticeably altered by 10^{-10} moles l^{-1} of As_2O_3 which diffuses out of glass containing it (8). Pyrex glass contained 0.6% AS_2O_3 until recently; at present it contains 0.01–0.02%. It is important not to let solution come into contact with As-containing glass; in particular, electrode preparation tubes must be As-free. Hysil, containing no AS_2O_3, was the glass generally used. A number of other As-free glasses, particularly that of Chance GSC, were also used.

Nitric-sulfuric mixtures are to be preferred for cleaning; rinsing with tap water lasted several hours, followed by washing with equilibrium and conductance water. (The advisability of rinsing with tap water depends on its local quality; if sufficiently bad, it is better to omit entirely and use only distilled water.)

Electrical Apparatus

This was as previously described. A powerpack giving 1,500 v was used for pre-electrolysis in dilute solutions. All leads were coaxial screened types, the screens being earthed. A Doran electrometer tube potentiometer was used to measure potentials to 0.5 mv and drew off balance currents of less than 10^{-11} amp. On Rh, potentials were measured to 0.01 mv by means of a Pye d-c potentiometer. Numerous continuous recording devices for current and potential were also used for preliminary and rough work.

Preparation of Experiment

Each piece of apparatus was left overnight in HNO_3-H_2SO_4, exposed joints being closed by ground glass caps. Washing with various stages of water of increasing purity followed, taps and joints were sealed with equilibrium water, and the air swept out by pure H_2, passing through rigorously cleaned glass tubing. The cell was then washed further with conductance water and the five electrodes in the ground glass syringe units introduced with the cathode cap, air expelled from the cell which is again washed with conductance water, this now washing also the bulbs of the electrodes and the breaker. Washing with further portions of hydrogen-saturated conductance water was carried out until the conductance water from the washings had a specific conductance of less than 5×10^{-7} mhos cm^{-1}. Fresh conductance water was distilled into the anode compartment and then, for acid solutions, HCl led in. Allowance must be made for diminution in strength of the solution during pre-electrolysis.

After sharing the solution thus prepared with the cathode compartment, each electrode bulb was lowered into the catholyte and tested to insure insulation. The bulb of one electrode was then broken and pre-electrolysis commenced under appropriate conditions (see below), H_2 bubbling in the catholyte, and with the breaker and all insulated electrode bulbs immersed in solution, so that impurities upon their outsides might be removed during pre-electrolysis This was ceased by raising the auxiliary cathode clear of the solution while still polarizing.

Polarization on a first test electrode was prepared for by making electrical connections to this electrode and setting controls such that on subsequent breaking of the protective glass bulb the current density would be a few μamp cm^{-2}. The electrode was lowered into the solution, the bulb broken, and polarization commenced. The current density was reduced to zero and it was confirmed that the electrode potential attained the value of a reversible hydrogen electrode. (This attainment is itself evidence of high

purification.) Hydrogen bubbling was now stopped to decrease diffusion of remaining impurities up to the electrode surface. The current density was now gradually increased from zero, about 30 current densities being established while the overpotential increased from 0 to 30 mv. (On Mo and Fe electrodes, some time variation was still observable even after pre-electrolysis; the 30 values at low current densities were therefore taken very rapidly.) For overpotential of greater than 30 mv, values were recorded at current density intervals of about 0.2 decade. The Tafel line was then remeasured in descending and ascending order of current densities.

The used electrode was raised above the solution during polarization, electrical connection made to another, this one lowered into solution, the bulb broken, and so on.

Photomicrographs

Photomicrographs of the electrode surfaces were taken through an optical microscope, having a 16 mm objective, with a six times or ten times eye piece. The electrode was illuminated by a Pointolite arc lamp. Front, side, and oblique illumination was used to highlight the surface characteristics. The net magnification upon enlargement was about 150.

Pre-electrolysis Conditions

Those used for each cathode after preliminary investigations of the variations of parameters with degree of pre-electrolysis are shown in Table II.

Miscellaneous

The most important factor in the technique of obtaining results unvitiated by side reactions is certainly pre-electrolysis. However, pre-electrolytic purification is certainly a method for removing trace impurities, i.e., those with concentrations of, say, less than 10^{-6} moles l^{-1}. If the preliminary purification of reagents, etc., is not thorough, pre-electrolysis is ineffective in any practical time. Some 20% of experiments still fail, even with the use of pre-electrolysis, presumably because of undetected contamination before the commencement of pre-electrolysis.

Glass blowing operations on the cell usually necessitate a particularly long period of cleaning. There is some evidence that this difficulty is removed by using pure N_2 pressure.

Grease traces are difficult to eliminate, even with procedures described here. They depend greatly on the original water supply. They can always be observed on the glass walls of the cell by the adherence of drops. Experiments in the presence of such adsorbed water drops are generally vitiated.[2]

The extreme sensitivity to trace impurities exhibited by the hydrogen evolution reaction at low current densities is not likely to be an isolated instance in electrode kinetics. A similar sensitivity to impurities (successfully removed by pre-electrolysis) has also been established for the oxygen evolution reaction, for a number of redox reactions and for certain technological deposition reactions. It is unlikely that electrode kinetic measurements carried out without attention to the extreme purities needed refer to clean electrode surfaces.[3]

[2] Traces of fats in conductance water can be eliminated by distillation through a column containing glass chips at 400°–500°C (9).

TABLE II. *Preëlectrolysis conditions*

Metal	Solution	Current density (μamp cm^{-2})	Duration (hr)	Quantity (coulombs)
Cu	0.001*N* HCl	550	36	24
	0.01*N* HCl	330	17	8
	0.1*N* HCl	900–75,000	43–37	60–3,000
	0.01*N* NaOH	360	14	6
	0.1*N* NaOH	450	13	7
Au	0.001*N* HCl	600	13	12
	0.01*N* HCl	5,000	16	100
	0.1*N* HCl	27,000	42	1,400
	0.001*N* NaOH	2,400	63	124
	0.01*N* NaOH	12,000	22	550
	0.1*N* NaOH	180,000	43	7,000
Mo	0.001*N* HCl	600	36	24
	0.01*N* HCl	8,500	58	530
	0.1*N* HCl	75,000	37	3,000
	0.001*N* NaOH	3,000	37	89
	0.01*N* NaOH	30,000	42	1,800
	0.1*N* NaOH	240,000	71	14,000
Pd	0.01*N* HCl	35,000	36	1,000
	0.1*N* HCl	240,000	13	1,600
	0.001*N* NaOH	1,200	24	63
	0.01*N* NaOH	21,000	40	800
	0.1*N* NaOH	120,000	38	4,500
Rh	0.1*N* HCl	50,000	34	1,700
	0.01*N* NaOH	6,000	20	250
Fe	0.001*N* HCl	1,400	16	14
	0.01*N* HCl	18,000	36	500
	0.01*N* NaOH	15,000	35	260
	0.1*N* NaOH	25,000	35	3,600

Experimental Results

Variation of overpotential with time at constant current density.—It has been shown that the variation of overpotential with time is largely an impurity-dependent phenomenon and is removed or very greatly reduced by pre-electrolytic purification (8). This result was confirmed in the present work on all cathode materials except Mo, in acid and alkaline solutions, and Fe, in alkaline solutions. If the bulb surrounding these electrodes were broken under the solution without application of external potential, these electrodes would indicate the reversible hydrogen electrode potential as expected, but upon passage of a constant current density, an upward drift of overpotential occurred for some 10 min before constancy was attained. If the $\eta - i_c$ relation at low c.d.'s were plotted using the η values attained at the end of this variation, anomalous values of η were obtained. If the values were those taken very soon (3 sec) after the setting up of a certain c.d., rational values of η were obtained.

Gross contamination effects.—In certain cases the seal on Mo electrodes cracked and the solution became contaminated. Such contamination was not removed by pre-electrolysis. All Tafel lines measured in the solution (on electrodes the bulbs of which were broken after the contamination) showed deviations at low c.d.'s from theoretical behaviors expected for one reaction.

[3] The analogy with the situation in the kinetics of reactions at the solid-gas interface is clear.

TABLE III. *Statistically computed values of exchange current density and transfer coefficient as a function of metal and concentration*

Metal	Solution	$\bar{n}$	$-\bar{a}$ (v)	$\bar{b}$ (v)	$\overline{-\log i_o}$	conf $\bar{b}$	$\frac{\text{conf}}{\overline{\log i_o}}$	Range of $-\log i_o$
Cu	0.001*N* HCl	7	0.822	0.109	7.56	0.007	0.58	5.75–4.05
	0.01*N* HCl	5	0.844	0.116	7.25	0.010	0.29	5.23–3.98
	0.1*N* HCl	6	0.778	0.114	6.84	0.008	0.05	4.51–3.47
	0.01*N* NaOH	11	0.714	0.117	6.09	0.006	0.12	5.19–3.75
Au	0.001*N* HCl	17	0.524	0.072	7.32	0.005	0.20	6.33–4.62
	0.01*N* HCl	15	0.558	0.084	6.63	0.010	0.24	5.26–3.93
	0.1*N* HCl (1st)	19	0.468	0.071	4.59	0.006	0.23	5.63–4.02
	0.1*N* HCl (2nd)	13	0.548	0.097	5.64	0.010	0.23	3.67–2.41
	0.001*N* NaOH	13	0.548	0.097	5.64	0.010	0.23	3.67–2.41
	0.01*N* NaOH	17	0.832	0.118	7.05	0.006	0.15	5.90–4.54
	0.1*N* NaOH	12	0.836	0.119	7.04	0.007	0.24	5.92–3.68
Mo	0.001*N* HCl	5	0.577	0.081	7.12	0.016	0.41	5.56–4.19
	0.01*N* HCl	15	0.543	0.076	7.19	0.003	0.27	5.23–3.72
	0.1*N* HCl (1st)	21	0.586	0.080	7.30	0.004	0.21	5.52–3.48
	0.1*N* HCl (2nd)	23	0.671	0.104	6.45	0.004	0.21	3.34–1.80
	0.001*N* NaOH	4	0.667	0.092	7.27	0.010	0.46	5.87–4.42
	0.01*N* NaOH	11	0.664	0.103	6.42	0.010	0.52	4.89–3.59
	0.1*N* NaOH (1st)	15	0.641	0.087	7.35	0.003	0.21	4.74–3.72
	0.1*N* NaOH (2nd)	10	0.739	0.116	6.37	0.008	0.34	3.58–2.10
Pd	0.01*N* HCl	19	0.447	0.107	4.18	0.006	0.45	3.87–3.13
	0.1*N* HCl	15	0.321	0.099	3.25	0.003	0.11	2.89–1.41
	0.001*N* NaOH	5	0.589	0.100	5.88	0.015	0.61	5.04–3.92
	0.01*N* NaOH	23	0.610	0.110	5.56	0.004	0.48	5.35–3.98
	0.1*N* NaOH	4	0.637	0.125	5.01	0.002	0.33	4.14–3.08
Rh	0.01*N* HCl	30	0.209	0.055	3.80	0.003	0.09	3.38–3.08
	0.01*N* NaOH	25	0.579	0.119	4.85	0.003	0.21	4.18–3.51
Fe	0.001*N* HCl	6	0.787	0.127	6.19	0.008	0.23	4.02–3.76
	0.01*N* HCl	5	0.741	0.118	6.29	0.015	0.32	4.06–3.19
	0.01*N* NaOH	6	0.776	0.117	6.62	0.007	0.47	4.52–3.82
	0.1*N* NaOH	29	0.726	0.120	6.06	0.002	0.08	4.09–2.16

In acid solutions when high pre-electrolysis currents were employed, the original graphite anode, having a small area, tended to disintegrate. Subsequent transport of carbon to the catholyte turned the solution yellow brown. The Tafel line became strikingly anomalous, the b value rising to 0.8 v.

The micrographs[4] were taken under numerous states of oxidation and contamination, as well as for the pure surface before and after a run. Contamination and oxidation caused by a few seconds' contact with the atmosphere were clearly visible. No alteration of the appearance of the electrode before and after a run was visible.

Statistically computed Tafel parameters.—Tafel parameters from the "first up," "second up," and subsequent lines coincided well. Reproducibility between "up" and "down" lines was excellent; at low c.d.'s it declined and the $i_c - \eta$ line was sometimes slightly displaced although $\left(\frac{\partial \eta}{\partial i_c}\right)_{\eta=0}$ from up and down runs retained excellent concordant values. In instances of significant discrepancy between up and down lines, up lines were preferred, the electrode not having attained highly negative potentials, which encourage impurity depositions.

Tafel lines observed could be divided into three classes: (*a*) those showing the form in the $\eta - i_c$ relation expected if the hydrogen evolution reaction is not interferred with by competitive reactions with trace impurities; (*b*) slightly imperfect lines, i.e., form and slope indicate lack of impurity effects except at the lowest current densities where slight deviations occurred; (*c*) lines showing a large scatter of points, and distinct deformities from the theoretically expected relation, particularly at low current densities.

[4] Some 25 photomicrographs are available (10).

TABLE IV. *Statistically computed values of exchange current density and transfer coefficient summarized for each metal*

Metal	Solution	$\bar{n}_T$	$\bar{b}$	$\overline{-\log i_o}$	$\bar{a}$	conf $\bar{b}$	$\frac{\text{conf}}{\overline{\log i_o}}$
Cu	HCl	18	0.113	7.23	0.814	0.033	0.31
	NaOH	11	0.117	6.09	0.714	0.006	0.12
Au	HCl-1st	37	0.073	6.83	0.496	0.003	0.16
	-2nd	13	0.097	5.64	0.548	0.010	0.23
	NaOH	52	0.120	7.00	0.844	0.003	0.03
Mo	HCl-1st	41	0.079	7.24	0.569	0.003	0.14
	-2nd	23	0.104	6.45	0.671	0.004	0.21
	NaOH-1st	30	0.094	7.00	0.656	0.005	0.26
	-2nd	10	0.116	6.37	0.739	0.008	0.34
Pd	HCl	34	0.103	3.77	0.389	0.004	0.30
	NaOH	42	0.110	5.54	0.811	0.004	0.35
Rh	HCl	30	0.055	3.80	0.209	0.003	0.09
	NaOH	25	0.119	4.85	0.579	0.003	0.21
Fe	HCl	11	0.123	6.24	0.766	0.007	0.15
	NaOH	35	0.119	6.16	0.735	0.002	0.12

Only class (*a*) results have been considered in the statistical evaluation for Fe, Cu, Rh, Au, and Pd. For Mo, the remaining time variation made it necessary to accept some results of class (*b*).

The statistical terms used in the next section have their usual significance. Values of exchange current densities

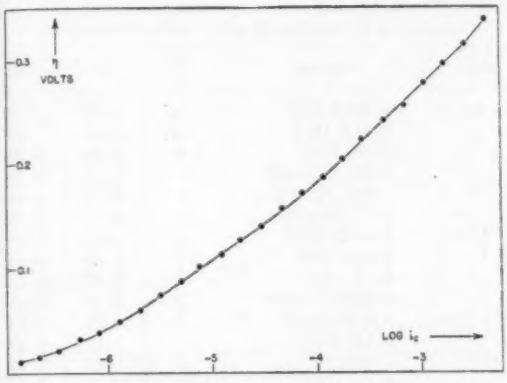

FIG. 11. Typical Tafel line on Au in 0.1*N* HCl solutions

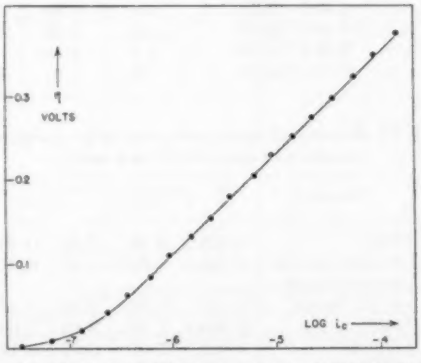

FIG. 12. Typical Tafel line on Au in 0.01*N* NaOH solutions.

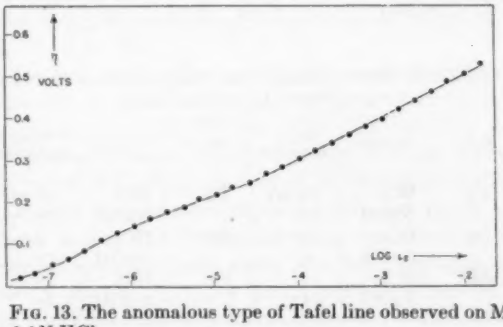

FIG. 13. The anomalous type of Tafel line observed on Mo in 0.1*N* HCl.

were calculated by the extrapolation of the linear sections of Tafel lines to zero overpotential. Stoichiometric numbers were calculated from

$$\nu = -2i_0 \frac{F}{RT}\left(\frac{\partial \eta}{\partial i_c}\right)_{\eta \to 0}$$

The term $\bar{n}$ represents the number of Tafel lines used in the statistical analysis; $\bar{a}$ represents the mean value of a in the Tafel equation, and $\bar{b}$ the same for b in this equation. The term i_c represents the net cathodic current at an electrode and "Range of η − log i_c" means the range of values

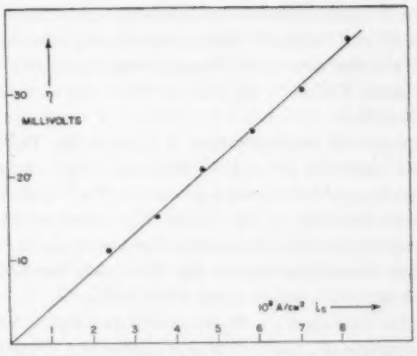

FIG. 14. The current density-overpotential relation at current densities in the neighborhood of the reversible potential on Mo in 0.1*N* HCl.

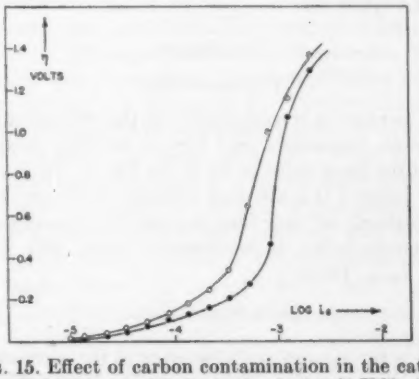

FIG. 15. Effect of carbon contamination in the catholyte on the Tafel lines at Pd electrodes in 0.01*N* HCl. (—● —— = first up;—⊙— = first down).

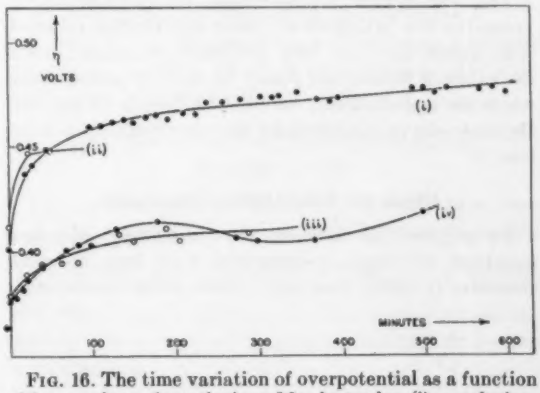

FIG. 16. The time variation of overpotential as a function of degree of pre-electrolysis on Mo electrodes: (i) = polarization at 7.10^{-4} amp/cm^{-2} after pre-electrolysis of 50 hr at 1.10^{-3} amp/cm^{-2}; (ii) = polarization at 1.10^{-3} amp/cm^{-2} after p.e. of 36 hr at 1.10^{-3} amp/cm^{-2}; (iii) = polarization at 9.10^{-4} amp/cm^{-2} after p.e. of 20 hr at 1.10^{-3} amp/cm^{-2}; (iv) = polarization at 6.10^{-4} amp/cm^{-2} after 36 hr p.e. at 1.10^{-3} amp/cm^{-2}.

of log i_c during which the η − log i_c relation was observed and linear. The term conf. means "95% confidence limits."

Concentration effects on the parameters are not significant. If values are grouped together for each metal, irre-

spective of concentration, and meaned, one obtains Table IV ("first" and "second" refer to the appropriate reactions of the Tafel line when twin linearity was observed).

Analogous Tables to III and IV follow for the stoichiometric number.

The graphical representation of most of the Tafel lines indicates expected theoretical behavior. Fig. 11 and 12 represent typical behaviors, e.g., on Au. Fig. 13 shows the anomalous behavior of Mo, while Fig. 14 shows that although the Tafel line is anomalous, the corresponding $\eta - i_c$ graph has theoretical shape. Fig. 15 shows the behavior of Au electrodes contaminated with carbon.

The time variation on Mo electrodes in alkaline solution (cf. "Variation of Overpotential with Time . . .") is represented in Fig. 16 as a function of pre-electrolysis. The result is qualitatively similar to observations of the effect of pre-electrolysis on the time variation at Ni cathodes in acid solution (8).

Discussion

Reproducibility

The measure of reproducibility of the determination of the kinetic parameters used here is the 95% confidence limit of the mean value of log i_0. In Fig. 17, BC is "conf. log i_0," where CD is the most probable Tafel line (and its extrapolation). AC may then be suggested as a measure of the reproducibility in overpotential units, and AC = $\bar{b}$ conf. $\overline{\log i_0}$. Hence:

$$\overline{\Delta\eta} = \bar{b} \text{ conf. } \overline{\log i_0}$$

and $\overline{\Delta\eta}$ is the meaned probable error of the overpotential measurements for 95% confidence limits. Table VII shows these values for the present work.

The over-all mean reproducibility for overpotential expressed on this basis is 19 mv. More reproducible values on solid metals have not been published previously, except the values of Bockris and Potter (6) on Ni in acid solutions where the reproducibility on the same basis is 15 mv. (On Hg electrodes in acid solutions, the reproducibility is about 5 mv.)

Ohmic and Concentration Components

For a cylindrical electrode, the approximate correction equations for ohmic overpotential have been discussed elsewhere (1); they yield only values of the correct order

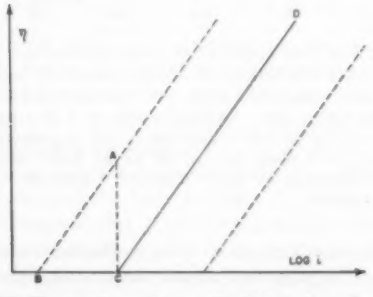

Fig. 17. Expression of reproducibility in overpotential measurements.

TABLE V. *Statistically computed values of the stoichiometric number as a function of metal and concentration*

Metal	Solution	$\bar{n}$	$\bar{v}$	conf $\bar{v}$
Au	0.001*N* HCl	8	1.02	0.16
	0.01*N* HCl	5	1.07	0.35
	0.1*N* HCl	9	0.99	0.20
	0.001*N* NaOH	7	1.93	0.30
	0.01*N* NaOH	9	2.10	0.14
	0.1*N* NaOH	11	0.88	0.16
Mo	0.001*N* HCl	4	1.09	0.11
	0.01*N* HCl	7	0.95	0.18
	0.1*N* HCl	6	0.97	0.21
	0.001*N* NaOH	3	0.76	0.24
	0.01*N* NaOH	7	0.86	0.18
	0.1*N* NaOH	7	1.13	0.22
Pd	0.01*N* HCl	13	1.88	0.19
	0.1*N* HCl	10	2.12	0.20
	0.001*N* NaOH	5	1.97	0.55
	0.01*N* NaOH	10	2.01	0.17
Rh	0.01*N* HCl	30	0.96	0.06
	0.01*N* NaOH	13	1.86	0.10
Fe	0.01*N* NaOH	2	1.36	—
	0.1*N* NaOH	16	1.01	0.10

TABLE VI. *Statistically computed values of the stoichiometric number summarized for each metal*

Metal	Solution	$\bar{b}$	$\overline{-\log i_0}$	$\bar{v}$	conf $\bar{v}$	$\bar{n}$
Au	HCl	0.076	6.85	1.02	0.10	22
	0.001*N* NaOH	0.118	7.05	2.03	0.14	16
	0.01*N* NaOH					
	0.1*N* NaOH	0.123	6.96	0.88	0.16	11
Mo	HCl	0.078	7.20	0.99	0.09	17
	NaOH	0.094	7.01	0.95	0.14	17
Pd	HCl	0.104	3.72	1.98	0.14	23
	NaOH	0.112	5.45	1.99	0.17	15
Rh	HCl	0.055	3.80	0.96	0.06	30
	NaOH	0.119	4.85	1.85	0.10	13
Fe	NaOH	0.118	6.34	1.05	0.11	18

TABLE VII. *Mean probable error (95% confidence limits) in overpotential for various metals*

Metal	Solution	Reproducibility	Metal	Solution	Reproducibility
Cu	HCl	35 mv	Pd	HCl	31 mv
	NaOH	14		NaOH	38
Au	HCl	12	Rh	HCl	5
	NaOH	4		NaOH	25
Mo	HCl	11	Fe	HCl	18
	NaOH	24		NaOH	14

because of various factors not taken into account, e.g., bubbles near the electrode surface.

The equation for η_0 can be applied to the present results in instances where the Tafel line indicated positive deviations from linearity at high overpotential, e.g., for Rh (Fig. 18). If the deviations are plotted against current density, a linear relation should exist if they are due to ohmic errors. No linear relation was found. Application of an ohmic correction formula to the Rh results, with values of 0.1 cm or greater for the distance between the Luggin capillary tip and the electrode (the intended value in the experiments was always apparently less than this), gave

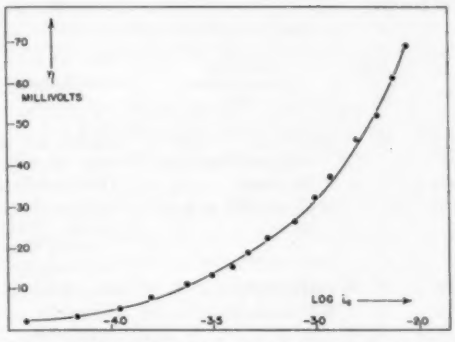

FIG. 18. Positive deviations at high current densities for Rh electrodes in 0.01*N* acid solutions.

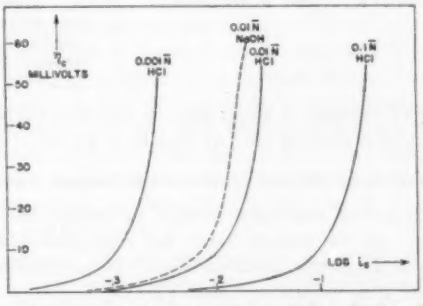

FIG. 19. Concentration overpotential (calculated for a diffusion layer thickness of 0.005 cm and $t_+ = 0.82$) in acid solutions of various strengths and in 0.01*N* NaOH solutions.

poorly defined "corrected" Tafel lines with no linear portions. Therefore, no ohmic errors affect the Rh results.

Similar results were found for Pd, which also indicated slight positive deviations at current densities of 10^{-1} amp cm^{-2} in 0.1*N* HCl.

The limits of the concentration overpotential can be calculated from well-known equations (1) in which the only adjustable term is the thickness of the diffusion layer. For the present conditions, in which stirring is almost entirely by means of hydrogen evolved at the electrodes, the appropriate value is approximately 0.005 cm. Values are shown in Fig. 19. The concentration component in the overpotential can therefore be considered negligible for 0.001*N* solution of HCl or NaOH below 10^{-3} amp cm^{-2}; for 0.01*N* solution below 10^{-2} amp cm^{-2}, and for 0.1*N* solution below 10^{-1} amp cm^{-2}. The statistical computation of Tafel lines were carried out only for current densities lower than these limits.

Variations with Time

An essential improvement in measurements brought about by the technique of pre-electrolytic purification is a considerable reduction in the total amount of time variation and an elimination of the irregular time variation (*see* Fig. 16) which formerly made comparison of overpotential measurements carried out by two different authors of little significance. The absence of time variation on Cu, Au, Pd, and Rh reported here makes the regular variation on Mo and Fe in alkaline solutions of particular interest. Possible interpretations would be: (*a*) presence of impurities after pre-electrolysis. If this were the cause of time variation, or of the imperfect Tafel lines on Mo, the drift should be augmented by increasing the rate of transport of impurities to the electrode, i.e., by stirring. This effect was absent. Further, the impurity will only compete with the hydrogen evolution reaction if its concentration is sufficient to give it a sufficiently high limiting current density.[5] Calculation shows that, to cause the deviation observed in the Tafel lines on Mo (Fig. 13), the impurity concentration would have to be 10^{-6} moles l^{-1}, which is improbably high after the pre-electrolysis detailed in Table II [cf. calculations of the rate of "clean up" of a solution during pre-electrolysis (1)]. (*b*) Oxide film dissolution. Reduction of an oxide film would cause a decrease of overpotential with time at constant current density (11). In the present work, an increase was observed at low current densities. (*c*) Hydrogen diffusion into the interior. No time variations were observed on Pd, where diffusion would be greater than on Mo. Change of the Mo wire thickness did not alter the observed time variation, as would be expected if diffusion were rate determining. (*d*) Change of "activity." Progressive deactivation of the electrode surface may be invoked to explain the increase of overpotential with time at a given current density, but only with great caution, because many systems where this explanation has been applied have been proved later to exhibit no time variation in the absence of impurities. Deactivation would lead to a steady increase of overpotential with time and probably to a linear relation between η and log time;[6] neither of these behaviors were observed on Mo or Fe. Therefore, none of these explanations appears applicable to the time variations observed on Mo electrodes

Results of the present work confirm previous work that there is no variation of the stoichiometric number with time, even on Mo electrodes.

Rate-Determining First Order Combination of Hydrogen Atoms

The rate-determining combination reaction between two hydrogen atoms both adsorbed on a metal surface gives rise to a Tafel line for which $b = 2.303\,\frac{RT}{2F} = 0.029$ at 25°C. The model in which one H atom is adsorbed and the other is not has not yet been formulated [but cf. Bockris (12)]. Consider

$$H_3O^+ + e_0^- \underset{V_{-1}}{\overset{V_1}{\rightleftharpoons}} MH \qquad (I)$$

Let it be supposed that a negligible rate of combination occurs between the H on the surface and that the formation of H_2 is by reaction between one adsorbed H and one nonadsorbed H atom, as is the mechanism of formation

[5] For details of this calculation, see (8).

[6] Cf. Bockris and Huq (9), where such a view has been worked out in some detail.

of H_2 at a catalytic surface in the gas phase, i.e.,

$$MH \underset{V_{-2}}{\overset{V_2}{\rightleftharpoons}} H_{(g)} + M \qquad (II)$$

$$MH + H_{(g)} \underset{V_{-3}}{\overset{V_3}{\rightleftharpoons}} H_2 \qquad (III)$$

Then,

$$v_1 = k_1 e^{-\Delta\phi F/2RT}(1 - k^1 c_H)c_{H\cdot} \qquad (IV)$$

where $\Delta\phi$ is the Galvani p.d. between metal and solution; c_H is the concentration of H on the surface, $(1 - k^1 c_H)$ is the fraction of the surface free, and $c_{H\cdot}$ is the hydroxonium ion concentration in the Helmholtz double layer.

$$v_{-1} = k_{-1} c_H e^{\Delta\phi F/2RT} \qquad (V)$$

$$v_2 = k_2 c_H \qquad (VI)$$

$$v_{-2} = k_{-2} c_{H,g}(1 - k^1 c_H) \qquad (VII)$$

$$v_3 = k_3 c_{H,g} c_H \qquad (VIII)$$

from which the Christiansen coefficients (13) follow as

$$w_1 = k_1 c_{H\cdot} \qquad (IX)$$

$$w_{-1} = k_1 k^1 e^{-\Delta\phi F/2RT} c_{H\cdot} - k_{-1} e^{\Delta\phi F/2RT} \qquad (X)$$

$$w_2 = k_2 + k_{-2} k^1 c_{H,g} \qquad (XI)$$

$$w_{-2} = k_{-2} \qquad (XII)$$

$$w_3 = k_3 c_H \qquad (XIII)$$

where c_H is the concentration of adsorbed H and $c_{H,g}$ is the nonadsorbed H atom concentration.

It follows that the current density for this path is

$$i_c = 2F\left[\frac{k_1 c_{H\cdot} e^{-\Delta\phi F/2RT}(k_2 + k_{-2}k^1 c_{H,g})k_3 c_H}{k_1 e^{-\Delta\phi F/2RT} c_{H\cdot}(k_2 + k_{-2}k^1 c_{H,g}) + k_1 e^{-\Delta\phi F/2RT} k^1 c_{H\cdot} + (k_1 k^1 e^{-\Delta\phi/2RT} - k_{-1})k_{-2}}\right]$$

whence, with $k_3 \to 0$ and at high negative potentials, i.e., reaction (III) is rate determining,

$$i_c = 2F\left[\frac{(k_2 + k_{-2}k^1 c_{H,g})k_3 c_H}{(k_2 + k_{-2}k^1 c_{H,g}) + k_{-2}k^1}\right] \qquad (XIV)$$

Therefore, if $k_{-2}k^1 \ll (k_2 + k_{-2}k^1 c_{H,g})$, then,

$$i_c = 2Fk_3 c_H = 2Fk_3 \frac{k_1}{k_{-1}} c_{H\cdot} e^{-\Delta\phi/RT} \qquad (XV)$$

or:

$$\frac{\partial\eta}{\partial \log i_c} = 2{\cdot}303\,\frac{RT}{F} \qquad (XVI)$$

Eq. (XVI) is the result formally obtained if one calculates the reaction on the basis of a first order hydrogen atom combination, and the Tafel line to be expected for such a condition has been mentioned by Knorr (14), although without formulation. However, it does not seem a likely mechanism because (XV) results from the assumption that the coverage of the surface with adsorbed H is small, so that $c_H = c_{H\cdot} Ke^{-\Delta\phi F/RT}$. If this is so, the value of $c_{H,g}$ is small and hence it is less probable that the condition quoted for the simplification (XIV) – (XV) will occur. As the surface becomes saturated, and the condition for (XV) becomes no longer true, c_H becomes independent of $\Delta\phi$ and a limiting current density is set up.

TABLE VIII. *Diagnostic criteria and rate in the hydrogen evolution reaction* (1)

Tafel slope	Stoichiometric no.	Consistent rate-determining step	Remarks
0.116	2	$H_3O^+ + e_0^- \to MH$ (Followed by combination)	Implies low coverage of electrode with adsorbed H
0.116	1	$H_3O^+ + MH + e_0 \to H_2$	Implies that coverage with adsorbed H is near to complete
0.058	1	$(MH)_1(MH)_2$	Slow diffusion
0.058	1	$MH + H_g\ H_2$	Physically improbable
0.038	1	$H_3O^+ + MH + e_0^- \to H_2$	Implies low coverage of electrode with adsorbed H
0.029	1	$MH + MH \to H_2$	Could show limiting current at sufficiently high current density.

Deduction of Detailed Mechanism at Various Cathodes

Summary of connection between parameters and mechanisms.[7] At the present time, the connections between observed diagnostic parameters and the mechanism they indicate is as shown in Table VIII.

Copper (3).—The absence of a stoichiometric number value for Cu in acid solution (not determinable owing to its dissolution) leaves the distinction between a rate-determining proton discharge and electrochemical desorption to be made on secondary grounds, i.e., the invariance of the capacity with frequency. This indicates a small coverage of the metal surface with H in the steady state and hence favors a rate-determining proton discharge mechanism in acid solution.

For alkaline solutions, the values of $\nu = 2$ and $b = 0.116$ indicate a rate-determining proton discharge, probably from a water molecule.

Gold.—In acid solutions, the relevant values are $b = 0.076$ at low current densities and $b = 0.097$ at higher current densities, while $\nu = 1$. Had the lower slope been near to 0.058, then, with $\nu = 1$ it would have seemed probable that under these conditions a rate-determining diffusion mechanism was taking place. A value of $b = 0.076$ does not refer, however, to any characteristic parameter of a given rate-determining step, and the fact that the Tafel line remains linear for some two decades of current density precludes the possibility of the contribution of two mechanisms to the reaction. The slope is in fact one between 0.116 and 0.058 which was recently shown (15) to follow for an electrode in the vicinity of the electrocapillary maximum if the slope fundamentally associated with the mechanism was 0.116, as is confirmed by the fact that the slope becomes 0.097 at potentials sufficiently far from the electrocapillary maximum. On grounds of the Tafel slope, the mechanism could be the discharge of protons or the slow electrochemical desorp-

[7] These mechanisms are not complete, cf., e.g., the development of a new mechanism involving H_2 (10).

tion, and these are distinguished by the value of unity for the stoichiometric number. Therefore, these results indicate a rate-determining electrochemical desorption on Au in acid solutions.

The results for Au in alkaline solutions are $b = 0.116$ but $\nu = 2$ for solutions of concentration < 0.1 and 1 at $0.1N$. For the results in the solutions at lower concentrations, Table VIII indicates that the rate-determining mechanism must be proton discharge. [The parameters would also be consistent with the combination of H_2O and Na atoms as the rate-determining reaction but it can be shown that the rate of deposition of Na on Au in alkaline solution is negligibly small (10).]

In $0.1N$ NaOH, with $b = 0.123$, and $\nu = 1$, the two possibilities are rate-determining proton discharge from water molecules, followed by a fast electrochemical desorption step, or, proton discharge from water, followed by a slow electrochemical desorption. No evidence is available, e.g., on coverage of the surface with adsorbed H in the steady state, to indicate which of these two mechanisms is preferable. It may be supposed, however, that as the slow discharge step has been established as slow in the more dilute solutions (where the value of $\nu = 2$, combined with $b = 0.116$, indicated slow proton discharge, followed by rapid atomic combination), it will remain relatively sluggish in $0.1N$ NaOH.

Molybdenum.—In acid solutions, the values of $b = 0.078$ and $\nu = 1$ at low current densities, together with a higher value of b (0.104) at more negative potentials, suggest the same type of explanation as for Au in acid solution (cf. "Gold"). The mechanism is therefore a rate-determining electrochemical desorption mechanism.

In alkaline solutions, the values are $b = 0.094$ and $\nu = 1$ at low current densities with a value of $b = 0.116$ at higher current densities. Two possibilities would be consistent with these parameters. Assuming that the Tafel slope unaffected by the $\frac{\partial \phi_2}{\partial \Delta \phi}$ term (where ϕ_2 is the potential of the Gouy-Helmholtz layer), which becomes important near the electrocapillary maximum (15), is 0.116, then the rate-determining step may be proton discharge from a water molecule, followed by the electrochemical desorption step, or a rate-determining electrochemical reaction. The latter seems probable by analogy to the unambiguous result in acid solutions.

Palladium.—The values of $b = 0.103$ and $\nu = 2$ and the mechanism is therefore a rate-determining discharge of a proton from a hydroxonium ion, followed by rapid combination of H atoms.

These conclusions for Pd differ from those of Frumkin and Aladjalowa (16) and also of Bockris and Azzam (17), both of these workers recording a Tafel slope of 0.03 in acid solution. These earlier results were obtained under sufficiently rigorous conditions of solution preparation, but the method of preparing the electrode involved heating in air, while here the electrodes were prepared by the method of sealing in hydrogen. There was absence of time variation in the present results, whereas the former workers found considerable variations with time (in their purified solutions) indicating the effect of H diffusion into the electrode was important. Owing to the mode of electrode preparation used here, H diffusion would doubtless have already occurred into the Pd before electrolysis. This would mean that the d levels of the Pd lattice would be already filled with the electrons of diffused H at the commencement of the electrolysis so that the disappearance of electrons from the atoms from the discharge step into the d holes would be improbable. The discharged H would therefore behave like free H atoms on a holeless metal and hence combine rapidly, making the discharge step rate-determining.

It may be observed that on Pt, where the Tafel slope in pure solution is 0.03 and the stoichiometric number is 1 [cf. Pd as measured by Bockris and Azzam (17)], it is possible to induce a slope about 0.12 (cf. Pd as measured by Pentland, Bockris, and Sheldon), by poisoning the solution. However, it is improbable that the present results on Pd are due to poisoning because of the very high degree of pre-electrolytic purification which was carried out [considerably higher, for example, than that used by Frumkin and Aladjalowa (16)]. The difference in observed slopes provides an example of mechansim change caused by change of the electronic character of the electrode by the presence of H.

In alkaline solutions, $b = 0.112$ and $\nu = 2$ indicates that the mechanism is the rate-determining discharge of protons from water, followed by the fast atomic combination. (As with Au, it can be shown that the discharge step of Na onto Pd is very slow compared with that of H_2O, so that the possibility of a rate-determining reaction between H_2O and Na, also consistent with the observed parameters, is to be rejected.)

Rhodium.—In an acid solution the parameters of $b = 0.056$ and $\nu = 1$ would be consistent with a rate-determining slow diffusion reaction, or with the first order atomic combination. No direct distinction between these mechanisms is possible. The parameters could be consistent with a rate-determining electrochemical desorption mechanism if the section of slope 0.056 were in the vicinity of the electrocapillary maximum potential. However, there is no twin linearity with the upper slope of about 0.1 as would be expected if this were the mechanism, the behavior being similar to that observed for a Pt electrode prepared in air (15).

In alkaline solution, $b = 0.119$ and $\nu = 2$, indicating that the rate-determining step is the discharge of protons from water molecules, followed by the rapid atomic combination. Na^+ discharge is too slow to be of consequence, as with Au and Mo.

Iron.—No stoichiometric number for acid solutions is available, owing to the dissolution which occurs near to the reversible potential. The slope of 0.122 would be consistent with a rate-determining electrochemical or slow discharge reaction.

In alkaline solution, the value of $b = 0.118$ and $\nu = 1$ are consistent with either a rate-determining proton discharge reaction from water molecules or a proton discharge from water, followed by a rate-determining electrochemical desorption reaction.

There is only qualitative evidence to distinguish the two steps here. Fischer and Heiling (18) have shown that on Fe, overpotential is easily "transferred" from the

"polarization side" to the "diffusion side" of an electrode. It follows that there is a large concentration of H on the polarization side in the steady state and this is in favor of a rate-determining electrochemical mechanism, which demands a well covered surface, compared with a rate-determining slow proton discharge reaction, which requires low coverage of the electrode with H atoms in the steady state.

Acknowledgments

The authors wish to acknowledge the facilities afforded by the Governing Body of Acton Technical College, where the experimental work was carried out; one of them (E.S.) wishes to acknowledge a grant given him by the Middlesex Education Committee.

Manuscript received April 25, 1956.
Any discussion of this paper will appear in a Discussion Section to be published in the December 1957 JOURNAL.

REFERENCES

1. J. O'M. Bockris, "Modern Aspects of Electrochemistry," Chap. IV, Academic Press, New York (1954).
2. D. C. Grahame, *Ann. Rev. Phys. Chem.*, **6**, 337 (1955).
3. J. O'M. Bockris and N. Pentland, *Trans. Faraday Soc.*, **48**, 833 (1952).
4. J. O'M. Bockris and B. E. Conway, *J. Sci. Inst.*, **25**, 283 (1948).
5. A. M. Azzam, J. O'M. Bockris, B. E. Conway, and H. Rosenberg, *Trans. Faraday Soc.*, **46**, 918 (1950).
6. J. O'M Bockris and E. C. Potter, *J. Chem. Phys.*, **20**, 614 (1952).
7. S. U. Pickering, *J. Chem. Soc.*, **63**, 890 (1893).
8. J. O'M. Bockris and B. E. Conway, *Trans. Faraday Soc.*, **45**, 989 (1949).
9. J. O'M. Bockris and A. K. M. S. Huq, *Proc. Roy. Soc.*, **237A**, 277 (1956).
10. E. Sheldon, Thesis, London (1955).
11. R. Parsons, Thesis, London (1948).
12. J. O'M. Bockris, *J. Chem. Phys.*, **24**, 817 (1956).
13. A. Christiansen, *Z. physik. Chem.*, **33B**, 145 (1936).
14. C. A. Knorr, *Z. Elektrochem.*, **57**, 599 (1953).
15. J. O'M. Bockris, I. A. Ammar, and A. K. M. S. Huq, *J. Phys. Chem.*, In press.
16. A. Frumkin and A. Aladjalowa, *Acta Physicochim.*, **19**, 1 (1944).
17. J. O'M. Bockris and A. M. Azzam, *Trans. Faraday Soc.*, **48**, 145 (1952).
18. H. Fischer and A. Heiling, *Z. Elektrochem.*, **54**, 184 (1950).

Kinetics of Silver–Silver Ion Exchange

Cecil V. King and Ann-Mari Simonsen

Department of Chemistry, New York University, New York, New York

ABSTRACT

Silver is known to exchange rapidly with its own ions on initial immersion in solution, with much slower exchange continuing through a sluggish layer of adsorbed salt. In the present work Ag coupons were immersed repeatedly in radioactive $AgNO_3$ of four concentrations, with hot water washing to remove adsorbed salt between immersions. Followed in this way, the exchange was found to be kinetically of first order, with one immersion as the time unit. The "rate constant" is nearly independent of concentration, and the calculated maximum exchange corresponds to the Ag in 35-50 atomic layers, based on measured area. Four-day measurement of the slow exchange which follows initial immersion indicated an equilibrium exchange current of about 4×10^{-9} amp/cm^2 in 0.5*N* $AgNO_3$.

Radioactive tracers make it possible to measure the amount of adsorption of metal salts on metal specimens of small surface area, and to study the nature, extent, and kinetics of metal ion exchange. Such studies give useful information concerning the nature of the metal and especially of its surface layers, and assist in explaining its behavior as an electrode. To study adsorption it is necessary to use radioactive anions, which cannot exchange with the metal. In the study of exchange, the amount of adsorption can be neglected usually since it is comparatively small; however, adsorption does have profound influence on the kinetics of exchange, at least in the case of Ag.

The Ag-Ag ion exchange has been studied from several viewpoints (1–4). It is apparent that three stages need to be considered: (*a*) rapid initial exchange, quickly blocked by a slow adsorption-desorption process; (*b*) slow exchange through the adsorbed layer and extending through several atomic layers of the metal; and (*c*) final equilibration throughout the metal, negligibly slow at room temperature.

King and Levy (3) studied the effect of repeated brief immersion of Ag coupons in $AgNO_3$ solutions with Ag^{110} as tracer, with long washing between immersions to remove adsorbed salt. The present experiments are an extension of that work, with a study of the effect of washing in hot and cold water, of the role of solution concentration on the kinetics and amount of exchange, and of other matters of interest.

Experimental

Inch-square coupons of commercial rolled silver sheet were cleaned and treated as described before (3). They

TABLE I. *Amount of exchange on 30-sec immersions in active $AgNO_3$ of the concentrations given, followed by 5-min washing*

No. of immersions	Equivalents/cm², × 10^{10}				
	0.025*N*	0.1*N**	0.1*N*	0.25*N*	0.5*N*
2	80	91	67	148	123
4	109	115	114	214	167
6	150	109	163	242	225
8	164	114	185	273	287
10	223	120	235	310	335
12	236	128	262	320	367
14	275	131	274	346	407
16	290	154	321	360	435
18	317	161	354	378	470
20	330	165	374	410	491
22	361	169	412	437	531
24	375	179	437	452	552
26	409	190	447	465	562
28	430	210	467	486	584
30	—	217	479	—	596
32	470	226	504	—	611
34	479	244	513	—	670
36	—	262	532	—	688
38	520	270	552	—	704
40	—	274	561	—	720
42	529	288	570	—	748
44	525	316	580	—	773
46	—	340	598	—	780
48	537	347	602	—	781
50	539	—	605	—	782

* Washed in stirred water at room temperature; all others in boiling water.

were kept in 0.1*N* inactive $AgNO_3$ until needed (at least one week). The conversion of counts per minute to equivalents exchanged was made as before. Immersions were at room temperature, 25°–30°C, in 100 ml of solution, and numerical values are the averages from two coupons, which seldom differed more than 10% except in the first series as noted below. The solutions contained enough radioactivity to insure at least 100 cpm above background, after one immersion.

Removal of activity by washing.—Coupons were immersed in 0.1*N* active $AgNO_3$, blotted dry with tissue, and counted; then washed for 1-min periods, or longer, by suspending in 400 ml of distilled water at room temperature, with a motor stirrer. After a 30-sec immersion, the activity remaining after three 1-min washes was not reduced by further washing up to 60 min. However, if the coupons remained in the active solution 24 hr, washing up to a total of 40 min was necessary to reduce activity to a minimum.

Boiling water removed more activity than cold water. In one experiment cold water reduced activity to 465 cpm, further washing in hot water decreased it to 425 cpm. The drop in activity is not great, but since it is due to removal of firmly adsorbed salt it is important in the exchange kinetics as shown below.

Exchange on repeated immersion.—Coupons were given 30-sec immersions, followed by 5-min washes in cold or hot water, with results as shown in Table I. Since in the first runs (0.1*N* $AgNO_3$) it became obvious that hot water washing was much more effective in promoting further exchange, it was used in further experiments. In the first experiments the coupons were counted after every washing; later, to save time, after every second washing. Only every second immersion is reported in Table I.

The series done in 0.1*N* $AgNO_3$ with cold washing shows irregularities near the start and near the end, and the two coupons eventually differed in count by 30%. The experiments were done over a 3-week period, and the coupons acquired a slight visible tarnish. They were now cleaned by a 5-min immersion in 0.1M KCN solution, which was deaerated (30 min in advance) with N (passed over hot Cu and through $CrCl_2$ solution). The activity remaining corresponded to the fourth previous immersion. On the first new immersion it jumped to the 15th previous value, and thereafter for 22 immersions, carried out within three days, exchange proceeded at a "rate" 25% greater than in the original series. It is concluded that the Ag area was probably increased by the cyanide treatment.

Kinetics of the exchange.—With hot water washing the exchange per immersion decreases steadily, and this suggests an upper limit far short of equilibrium distribution of the activity. Plots of the reciprocal of the amount exchanged ($1/x$) vs. the reciprocal of the number of immersions ($1/n$) are nearly linear if the first several points are disregarded. They all extrapolate at $1/n = 0$ to points corresponding to end-values near 1000×10^{-10} equiv/cm² of exchange. With two coupons (25 cm²) in 100 ml of 0.025*N* solution, 0.1% of the active Ag ion would finally enter the metal; equilibrium through all the Ag would require that 90% of the activity be found in the metal.

Data were compared with the first-order rate equation in the form

$$kn = \ln a - \ln (a - x) \qquad \text{(I)}$$

With a, the maximum exchange, taken as 1000×10^{-10} equiv/cm², plots of log $(a - x)$ vs. n are nearly straight lines. From the slopes the constant k can be determined.

Since the above extrapolation is somewhat uncertain, k was evaluated by the Guggenheim method (5), which does not require prior knowledge of a in a first-order process. The equation used in the present case is

$$kn = \text{constant} - \ln (X_2 - X_1) \qquad \text{(II)}$$

where X_2 and X_1 represent exchange values a constant number of immersions apart. By plotting log $(x_{28} - x_2)$, log $(x_{28} - x_4)$, etc., vs. n (either subscript), straight lines are obtained, and k is found from the slopes. From the equation

$$n_{\frac{1}{2}} = 0.693/k \qquad \text{(III)}$$

the number of immersions for half-complete exchange is determined, and $X_{\frac{1}{2}}$ read from the data of Table I. The value of a was actually obtained by starting from the second immersion and adding its value to $2\,X_{\frac{1}{2}}$ later.

TABLE II. *"Rate constants" for* Ag-Ag *ion exchange*

C_{AgNO_3}	k	a, eq/cm² × 10^{10}
0.025	0.029	740
0.10*	(0.007)	—
0.10	0.034	760
0.25	0.032	760
0.50	0.028	1010

* Washed in cold water.

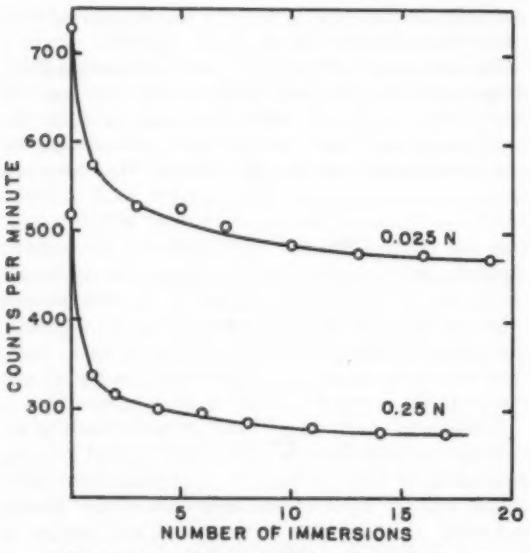

FIG. 1. Loss of activity in inactive solution

Values of a and k determined in this way are given in Table II. More exchange measurements in 0.25N $AgNO_3$ would have been helpful. The method could not be applied to the series with cold washing and k as given is an approximation from the first method described above.

Reversibility of exchange.—After the experiments of Table I with 0.025N and 0.25N $AgNO_3$, immersions were continued in inactive solutions of the same concentrations, with hot water washing as before. Fig. 1 indicates that continued treatment would not be effective in removing all activity. This is similar to the results found by other experimenters (1, 2, 4), who did not, however, wash with hot water between immersions.

Exchange current.—To obtain information about the exchange current, i_0, after adsorption equilibrium has been reached, it is necessary to immerse coupons for longer periods of time, and subtract the immediate exchange from the total. The following experiments were carried out: (*A*) two coupons were given four 30-sec immersions in 0.5N $AgNO_3$, with 5-min hot water washing, all within 2 hr; (*B*) two coupons were immersed for 30 sec each day for 4 days; (*C*) two coupons were immersed and removed each day for a 1-hr wash in hot water and counting. The amount of exchange is given in Table III.

Exposure to laboratory air or simply the 24-hr time lapse may be responsible for the greater exchange in (*B*) than in (*A*), and the same factor may account for some of the irregularities in Table I. In any case, if the values of column (*A*) are subtracted from those of (*C*), the indicated exchange current density is about 4×10^{-9} amp/cm². Actually, the rate of slow activity pickup should be extrapolated to zero time to calculate i_0 properly. Similar values are estimated from previous work (2, 3, 7).

TABLE III. *Exchange under various conditions, equiv/cm² × 10¹⁰*

Immersion	*A*	*B*	*C*
1	56	63	69
2	80	100	165
3	97	133	212
4	120	150	236

DISCUSSION

The ordinarily close agreement of exchange with two coupons treated identically, and the general agreement of "rate constants" and maximum exchange values (Table II), indicate that the experimental method used here was satisfactory. The lack of detailed reproducibility shows that small, perhaps uncontrollable variations in technique may lead to large variations in the results obtained. The true surface area is easily changed by slight corrosion or etching. Unknown amounts of sulfide were picked up from the laboratory air. Adsorbed oxygen may be present but it is doubtful if any oxide is formed at room temperature; it has been reported that no oxide is formed on polishing Ag in air (6).

Gerischer and Tischer (2) found that the rate of activity pickup is essentially the same on single crystals as on polycrystalline silver, and that deaeration of the solutions has little effect.

Tingley, Henderson, and Coffin (4) showed that the method of preparing Ag specimens makes a large difference in the rate and extent of exchange. Annealed, etched samples exchanged to a maximum of about 10 atomic layers in 10 hr, while unannealed, polished samples exchanged about 100 layers in 40 hr of constant immersion. This compares with the authors' values on commercial rolled sheet of 35–50 layers, only 25% of which was reached in 4 days of immersion (Table III). Tingley, *et al.*, also found that the apparent depth of exchange increased with solution concentration, which agrees with the results of Table II.

It is clear that the initial exchange is quickly blocked by adsorption of the Ag salt, not hampered by slow diffusion within the metal or by deposition of impurities from the solution, since the type of washing is more important than other factors. Both initial adsorption and initial exchange rates are no doubt proportional to solution concentration; this accounts for an activity pickup per immersion which is not highly dependent on concentration.

Baerg and Winkler (1) introduced a technique which could be used to remove adsorbed salt more quickly and certainly than washing alone. After brief immersion and rinsing the Ag specimen, they discharged adsorbed Ag ions cathodically. On reimmersion the activity pickup was similar to that shown in Table I. Baerg and Winkler thought this due entirely to chemisorption, and repeated the procedure only 5 times. If continued, results similar to those reported here should be obtained, the discharged ions adding a small amount to the activity. No surface compounds such as sulfide would accumulate.

Gerischer postulated that a concentration gradient of radioactive ions is set up at the Ag surface, in dilute solutions. Data of Table I support this view, since there was more apparent initial exchange from the more concentrated solutions. For complete exchange in only one atomic layer (20×10^{-10} equiv/cm²), the equivalent of all the Ag ions in a layer of 0.1N solution 2×10^{-5} cm thick must enter the metal. The concentration of active ions is about 10^{-11} equiv/cm³, and they could be replaced by

diffusion across a definite layer of the above thickness at a rate of about 5×10^{-12} equiv/cm²/sec. Each immersion must result in some surface deficiency of active ions, so that the measured exchange is always less than the true exchange. The effect is minimized in more concentrated solutions or when the exchange is slow.

Stirring has little or no effect on the amount of activity pickup per immersion (3). This is understandable even though diffusion is involved, since even extremely vigorous stirring has little effect on liquid less than 10^{-4} cm from the surface.

The irreversible part of the exchange is not due appreciably to interior diffusion. Extrapolation of self-diffusion coefficients in Ag from temperatures at which they can be measured to 25° or even 100°C gives negligible values (7), and interior diffusion would be incompatible with definite end-values of exchange. The present experiments with hot water washing show that it is not merely a question of low rate because of adsorbed salt. Gerischer and Tischer report that the amount of immobilized Ag depends on the time and temperature of storage. Tingley, Henderson, and Coffin found similar results; certain samples of active Ag which were stored for 220 days did not lose activity at all to an inactive solution, although they acquired more activity in an active solution.

Gerischer and Tischer showed that a fresh Ag surface, prepared by cathodic reduction of a layer of AgCl, becomes smoother in contact with $AgNO_3$ solution. Different faces of Cu single crystals show a difference in potential for a long time (8), and less stable faces rearrange to expose more stable planes (9). Long pre-equilibration in inactive solution should minimize local cell action, but autoradiographs have shown that Ag acquires more activity at scratches and edges than elsewhere, even after 5 months of pre-equilibration (7).

Local cell electrolysis no doubt buries some of the acquired activity, but can take place only when the metal is immersed. Additional trapping of activity may be explained in the following way: (*a*) It is assumed that most of the exchange takes place at comparatively few active centers, which are too close and uniformly spaced to be detected by autoradiographs. These centers may be due to a high surface concentration of lattice vacancies, to surface dislocations, or to imperfections or irregularities in the distorted layer of polished or cold-worked surfaces. (*b*) Rapid diffusion can occur around and under these centers, perhaps to a few thousand Å in depth, depending on the surface preparation. (*c*) In the course of time most or all of these active centers are obliterated, while new ones are formed, by vacancy migration, surface diffusion, etc. It is known that surface and grain boundary diffusion are much faster in Ag than lattice diffusion (10), but it is not known to what depth the faster diffusion takes place.

Exchange current.—This term is defined as the rate of exchange at the equilibrium potential, but values are usually estimated from measurements in which the electrode is not at equilibrium with the solution, as from the relation of double layer capacity to overvoltage, or from the constants of the Tafel equation (11). Gerischer and Tischer calculated i_0 from the initial Ag-Ag+ exchange rates; in one series of experiments they attempted to dissolve Ag anodically at a rate just sufficient to prevent activity pickup. Under these conditions i_0 is about 10^{-3} amp/cm².

Vielstich and Gerischer used a potentiostatic method to measure i_0 for Ag in cyanide and ammonia solutions (12). The current at constant potential, extrapolated to zero time, was plotted vs. overvoltage in both cathodic and anodic directions. From the slope at equilibrium potential ($\eta = 0$) i_0 was estimated, the values being near 10^{-2} amp/cm² in both types of solution. Measurements were also made without complexing agents but not published, since the authors felt that metal lattice formation was partially rate-controlling, and thus a complicating factor (13). The exchange current was estimated as about 2×10^{-3} amp/cm².

Exchange current as measured at an active electrode is greatly influenced by inhibitors and even by minute traces of firmly adsorbed impurities. In the present case adsorption of the Ag salt evidently reduces i_0 to a low value, and anything from 10^{-5} to 10^{-9} amp/cm² might be obtained, depending on how much the experimental method disturbs the adsorbed layer. The exchange current at adsorption equilibrium is evidently large enough to allow potential measurements without undue difficulty, or perhaps the adsorbed layer has always been disturbed in making such measurements. As explained by Akimov (14), if i_0 is less than 10^{-10} amp/cm² the potential becomes unstable; even very small forced currents polarize the electrode so much that equilibrium is not restored in a reasonable time, and usually other reactions will take over. The effects of impurities and competing reactions have been summarized and discussed by Bockris (15).

Manuscript received January 23, 1956. This paper was prepared for delivery before the San Francisco Meeting, April 29 to May 3, 1956, and is taken from a Master's Thesis submitted by Ann-Mari Simonsen to the Graduate School Faculty of New York University.

Any discussion of this paper will appear in a Discussion Section to be published in the December 1957 JOURNAL.

REFERENCES

1. A. BAERG AND C. A. WINKLER, *Can. J. Chem.*, **31**, 319, 521 (1953).
2. H. GERISCHER AND W. VIELSTICH, *Z. Elektrochem.*, **56**, 380 (1952); H. GERISCHER AND R. P. TISCHER, *ibid.*, **58**, 819 (1954).
3. C. V. KING AND B. LEVY, *J. Phys. Chem.*, **59**, 910 (1955).
4. I. I. TINGLEY, I. H. S. HENDERSON, AND C. C. COFFIN, *Can. J. Chem.*, **34**, 14 (1956).
5. E. A. GUGGENHEIM, *Phil. Mag.*, (7) **2**, 538 (1926).
6. S. DOBINSKI, *ibid.*, **23**, 397 (1937).
7. C. V. KING, *Ann. N. Y. Acad. Sci.*, **58**, 910 (1954).
8. H. LEIDHEISER AND A. T. GWATHMEY, *Trans. Electrochem. Soc.*, **91**, 97 (1947).
9. W. E. TRAGERT AND W. D. ROBERTSON, *This Journal*, **102**, 86 (1955).
10. W. C. WINEGARD AND B. CHALMERS, *Can. J. Phys.*, **30**, 422 (1952).
11. G. KORTÜM AND J. O'M. BOCKRIS, "Textbook of Electrochemistry", p. 441, Elsevier Publishing Co., Houston (1951).
12. W. VIELSTICH AND H. GERISCHER, *Z. Physik. Chem.*, **4**, 10 (1955).
13. W. VIELSTICH, Private communication.
14. G. W. AKIMOV, *Corrosion*, **11**, 477t, 515t (1955); a translation prepared by R. B. Mears and J. D. Gat.
15. J. O'M. BOCKRIS, "Modern Aspects of Electrochemistry", Chap. IV, Academic Press, Inc., New York (1954).

FUTURE MEETINGS OF
The Electrochemical Society

Washington, D. C., May 12, 13, 14, 15, and 16, 1957

Headquarters at the Statler Hotel

Sessions will be scheduled on
Electric Insulation, Electronics (including Luminescence, Semiconductors, Thermionic Cathodes, Instrumentation, and Screen Application), Electrothermics and Metallurgy, Industrial Electrolytics, and Theoretical Electrochemistry (including a special symposium on electrolytes)

* * *

Buffalo, October 6, 7, 8, 9, and 10, 1957

Headquarters at the Statler Hotel

Sessions will be scheduled on
Batteries, Corrosion, Electrodeposition (symposium on "Metal Powders"), Electrodeposition—Corrosion (Joint Symposium on "Corrosion of Electrodeposited Metals"), Electronics (Semiconductors), Electro-Organics, and Electrothermics and Metallurgy

* * *

New York, April 27, 28, 29, 30, and May 1, 1958

Headquarters at the Statler Hotel

* * *

Ottawa, September 28, 29, 30, October 1, and 2, 1958

Headquarters at the Chateau Laurier

* * *

Papers are now being solicited for the meeting to be held in Buffalo, N. Y. Triplicate copies of each abstract (*not exceeding 75 words in length*) are due at the Secretary's Office, 216 West 102nd St., New York 25, N. Y., *not later than June 1, 1957* in order to be included in the program. *Please indicate on abstract for which Division's symposium the paper is to be scheduled.* Complete manuscripts should be sent in triplicate to the Managing Editor of the JOURNAL at the same address.

Washington Program

THE ELECTROCHEMICAL SOCIETY

One Hundred and Eleventh Meeting

~~o~~

Sunday through Thursday

May 12, 13, 14, 15, and 16, 1957

CONDENSED TECHNICAL PROGRAM

Corrosion — Electrothermics and Metallurgy (Abstracts 103–108)
(Both sessions in South American Room)

Tuesday, May 14—9:00 A.M.–12:00 M.

Tuesday, May 14—2:00 P.M.–5:00 P.M.

Electric Insulation (Abstracts 1–21)

Monday, May 13—9:30 A.M.–11:30 A.M. (Congressional Room)

Monday, May 13—2:00 P.M.–5:00 P.M. (Congressional Room)

Tuesday, May 14—9:00 A.M.–11:30 A.M. (Pan American Room)

Tuesday, May 14—2:00 P.M.–4:30 P.M. (Pan American Room)

Wednesday, May 15—9:00 A.M.–12:00 M. (Pan American Room)

Wednesday evening, May 15—8:00 P.M.–10:15 P.M. (Pan American Room)

Electronics — Luminescence (Abstracts 22–54)

Tuesday, May 14—9:00 A.M.–11:50 A.M. (Congressional Room)

Tuesday, May 14—2:00 P.M.–5:00 P.M. (Congressional Room)

Wednesday, May 15—9:00 A.M.–12:00 M. (Congressional Room)

Wednesday, May 15—2:00 P.M.–4:00 P.M. (Federal Room)

Thursday, May 16—9:00 A.M.–12:00 M. (Congressional Room)

Thursday, May 16—2:00 P.M.–5:00 P.M. (Congressional Room)

Electronics — Semiconductors (Abstracts 55–73)

Tuesday, May 14—9:00 A.M.–11:45 A.M. (Presidential Ballroom)

Tuesday, May 14—2:30 P.M.–5:00 P.M. (Presidential Ballroom)

Wednesday, May 15—9:00 A.M.–12:00 M. (Presidential Ballroom)

Wednesday, May 15—2:00 P.M.–4:00 P.M. (Congressional Room)

Electronics — Thermionic Cathodes (Abstracts 74–85)
(All sessions in Ohio Room)

Wednesday evening, May 15—7:30 P.M.–10:15 P.M.

Thursday, May 16—9:00 A.M.–12:00 M.

Thursday, May 16—2:00 P.M.–5:00 P.M.

Electronics — Instrumentation (Abstracts 86–92)
(Both sessions in Pan American Room)

Thursday, May 16—9:00 A.M.–11:15 A.M.

Thursday, May 16—2:00 P.M.–3:30 P.M.

Electronics — Screen Application (Abstracts 93–97)

Thursday, May 16—2:00 P.M.–4:30 P.M. (Foyer No. 3)

Electrothermics and Metallurgy (Abstracts 98–102)

Monday, May 13—2:00 P.M.–4:30 P.M. (South American Room)

Electrothermics and Metallurgy—Corrosion (Abstracts 103–108)

Tuesday, May 14—9:00 A.M.–12:00 M. (South American Room)

Tuesday, May 14—2:00 P.M.–5:00 P.M. (South American Room)

Electrothermics and Metallurgy (Abstracts 109–129)

Wednesday, May 15—9:00 A.M.–11:30 A.M. (South American Room)

Wednesday evening, May 15—7:30 P.M.–9:55 P.M. (South American Room)

Thursday, May 16—9:00 A.M.–11:30 A.M. (South American Room)

Thursday, May 16—2:00 P.M.–4:30 P.M. (South American Room)

Industrial Electrolytic (Abstracts 130–137)
(Both sessions in Pan American Room)

Monday, May 13—9:30 A.M.–11:30 A.M.

Monday, May 13—2:00 P.M.–4:00 P.M.

Theoretical Electrochemistry—Joint Symposium with the National Science Foundation (Abstracts 138–190)
(All sessions in Federal Room)

Monday, May 13—9:30 A.M.–12:00 M.

Monday, May 13—2:00 P.M.–5:00 P.M.

Tuesday, May 14—9:00 A.M.–12:10 P.M.

Tuesday, May 14—2:00 P.M.–5:00 P.M.

Wednesday, May 15—9:00 A.M.–11:30 A.M.

Wednesday evening, May 15—7:30 P.M.–10:40 P.M.

Thursday, May 16—9:00 A.M.–11:45 A.M. General session.

Thursday, May 16—1:45 P.M.–4:45 P.M. General session.

GENERAL INFORMATION

Conventional Headquarters will be at the Hotel Statler, 16th St. at K&L Sts., N.W., Washington, D. C.

Rates per day for rooms (with bath) will be: single room $10.00, 11.00, 12.00, 13.00; double-bed room $15.00, 16.00; twin-bed room $15.00, 16.00, 17.00, 18.00, 20.00; suites for one or two $35.00 to $75.00.

Requests for room reservations at the Headquarters Hotel should be mailed to the Front Office Manager, Hotel Statler, 16th St. at K&L Sts., N.W., Washington 13, D. C.

Other hotels within two blocks of the Headquarters Hotel and their minimum rates are:

Ambassador, 14th & K Sts., N.W.—single $6.00, double $8.00, twin $10.00, parlor suite $14.00.

Hamilton, 14th & K Sts., N.W.—single $6.00, double $9.00, twin $10.50, parlor suite $25.00.

Lee House, 15th & L Sts., N.W.—single $7.75, double $11.25, twin $11.25, parlor suite $21.00.

Requests for room reservations should include mention of The Electrochemical Society.

The Office of the Secretary will be in the Michigan Room on the Mezzanine Floor.

All technical sessions will be held on the Mezzanine Floor.

Ladies' Headquarters will be in the New York Room on the Mezzanine Floor. For details, see program under Ladies' Program.

REGISTRATION

The registration desk will be in the upper lobby on the Mezzanine Floor. Following is the registration schedule:

Sunday, May 12—3:00 P.M. to 9:00 P.M.

Monday, May 13—8:00 A.M. to 5:00 P.M.

Tuesday, May 14—8:30 A.M. to 5:00 P.M.

Wednesday, May 15—8:30 A.M. to 5:00 P.M.

Thursday, May 16—8:30 A.M. to 12:00 M.

Registration fees are:

Members	$7.00
Ladies	$3.00
Nonmembers	$13.00
Students	$2.00

INFORMATION ABOUT WASHINGTON

As the Nation's Capital, Washington has many attractions which those attending the 111th Meeting of the Society will want to see. Three blocks from the Headquarters Hotel is the White House, flanked by the old Treasury and State Department buildings. Within walking distance of the White House is the Washington Monument, situated on the Mall, which is faced by the Lincoln Memorial on one end and the Capitol on the other. Congress will undoubtedly be in session and visitors may watch the proceedings of the Senate or the House of Representatives from the galleries. Famous historical shrines in the area include Mt. Vernon, Custis-Lee Mansion, Arlington Cemetery, and the Tomb of the Unknown Soldier.

While there are many monuments, parks, historical sights, and Govern-

ment buildings, visitors may also want to visit the Smithsonian Institute, Folger Shakespearean Library, the National Zoological Park, the National Gallery of Art, and the embassies and legations of the nations of the world.

Electrochemists will be interested in the Government research laboratories and the scientific installations in the area. Naval Research Lab., Naval Ordnance Lab., National Bureau of Standards, Naval Observatory, Geological Survey, Bureau of Mines, Dept. of Agriculture, and the National Institutes of Health have extensive research facilities in the area. In addition, there are the universities: Georgetown University, George Washington University, American University, Catholic University, and the University of Maryland and the Johns Hopkins University Applied Physics Lab., and, of course, the Headquarters of the American Chemical Society is just a short distance from the Hotel Statler.

Those working on Government research contracts may want to see where the money comes from. Congress, the Dept. of the Treasury, and its Bureau of Engraving and Printing play their part (not to mention taxpayers), but the Air Research and Development Command, the Atomic Energy Commission, the National Advisory Committee for Aeronautics, the Office of Naval Research, and the National Science Foundation make many of the contracts from their offices in Washington.

While attending the 1957 Spring Meeting of the Society, you will want to take advantage of the opportunity to go sight-seeing in the Nation's Capital, or to visit your colleagues in Washington in their laboratories, or to call on your contract sponsor.

SYMPOSIA

The Electric Insulation Division has scheduled symposia on: New Material Developments; Thermal Evaluation and Classification of Materials; Insulation Life; Prefabricated Circuitry; and a Panel Discussion on High Temperature Capacitors.

The Corrosion Division and Electrothermics and Metallurgy Division have scheduled a joint symposium on the Role of Metal and Oxide Structure in Oxidation and Corrosion.

The Electrothermics and Metallurgy Division has scheduled a symposium on Chemical Metallurgy, and another Symposium on Columbium (Niobium).

The Industrial Electrolytic Division has scheduled one symposium on Fused Salt Electrolysis, and another on Chlor-Alkali Processes.

The Theoretical Electrochemistry Division and the National Science Foundation have scheduled a joint symposium of six sessions on the Structure of Electrolytic Solutions (Electrolytes); this symposium was made possible by the generous financial support of the National Science Foundation, Washington, D. C. The Division has also scheduled two general sessions.

GENERAL FUNCTIONS

Symposia Chairmen Breakfasts

On **Monday, Tuesday, and Wednesday,** May 13, 14, and 15, at 7:45 A.M., special breakfasts for all symposia chairmen will be held in the Ohio Room. On **Thursday,** May 16, the breakfast will be held in the California Room.

Monday Evening Mixer

On Monday, May 13, all those registered at the meeting are invited to attend the get-acquainted Mixer in the Presidential Ballroom from 8:00 to 11:00 P.M. Beer, soft drinks, potato chips, and pretzels will be served on a complimentary basis. A bar will be available for the purchase of mixed drinks.

Tuesday Luncheon and Annual Business Meeting

The Electrochemical Society Luncheon and Annual Business Meeting will be held Tuesday, May 14, at 12:15 P.M. in the Presidential Ballroom.

Tuesday Evening Reception and Banquet

A reception for President and Mrs. Hans Thurnauer will be held at 6:30 P.M. in the Federal Room. Cocktails will be served from 6:30 to 7:30 P.M., followed by dinner at 7:30 P.M. in the Congressional Room. President Thurnauer will deliver the Presidential Address.

Wednesday Electronics Division Cocktail Mixer

The Electronics Division will hold a Cocktail Mixer from 5:00 to 6:30 P.M. on Wednesday, May 15, in the South American Room.

LABORATORY TRIPS

Three laboratory trips have been arranged for this meeting. Participation in these visits must be arranged for at the time of registration. Transportation tickets should be purchased at this time.

Monday, May 13, 1:45 P.M.—Citizens of the United States attending the meeting will be conducted on a tour of the U. S. Naval Research Lab. in Washington. The radioactive cobalt facilities, the van de Graff installation, and the nuclear reactor will comprise part of the tour. Also, the Electric Insulation Section where work on the thermal evaluation of dielectrics is being carried on will be shown. Finally, a visit to the Electrochemical Branch will be made to witness the work on batteries and gas detection. Transportation will be by chartered bus from the 16th St. entrance of the Hotel Statler ($1.00). The estimated time of return to the hotel is 5:00 P.M.

Tuesday, May 14, 12:15 P.M.—Citizens of the United States attending the meeting will be conducted on a tour of the U. S. Naval Ordnance Lab., White Oak in Silver Spring, Md. The guided tour will include visits to the Ordnance Environmental Lab., where experimental ordnance items are subjected to a variety of simulated conditions, such as shock, vibration, temperature and climate, and deep sea pressure; the Plastics and Battery Labs., and the Supersonic Wind Tunnels and Ballistic Ranges, where scale models are used in wide-range studies of the aerodynamic and physical problems encountered in extremely high speed flight. The visiting group will have lunch in the NOL cafeteria at the visitor's expense. Transportation will be by chartered bus from the 16th St. entrance of the Hotel Statler ($1.00). The estimated time of return to the hotel is 5:00 P.M.

Wednesday, May 15, 1:45 P.M.—A tour of the National Bureau of Standards has been arranged (attendance will be limited to 200). The tour will begin with a short address by Dr. Wallace R. Brode, Associate Director for Chemistry. Immediately following the address the guests will visit various active research projects at the Bureau. Transportation will be by chartered bus from the 16th St. entrance of the Hotel Statler ($1.00). The estimated time of return to the hotel is 4:45 P.M.

LADIES' PROGRAM

Ladies' Headquarters will be in the New York Room throughout the meeting. A member of the Ladies' Committee will be in the Ladies' Headquarters on Sunday from 3:30 to 9:00 P.M. to welcome and assist the ladies in every way.

The temperature in Washington during May is usually in the 70°-80° range. The height of the azalea and rhododendron season is at this time of the year.

Monday morning, May 13—A get-together period with coffee will be held in the Ladies' Headquarters, starting at 9:30 A.M. (complimentary).

Monday afternoon, May 13—A luncheon and fashion show will be held at the Mayflower Hotel, starting at 1:00 P.M. The ladies will leave from the 16th St. entrance of the Hotel Statler at 12:30 P.M. and will return about 2:30 P.M. The remainder of the afternoon will be open for shopping or individual sight-seeing.

Monday evening, May 13—The ladies are invited to accompany their husbands to the Mixer at 8:00 P.M. (complimentary).

Tuesday morning and afternoon, May 14—Coffee will be served in the Ladies' Headquarters at 9:30 A.M. (complimentary). At 10:30 A.M. the ladies will meet at the 16th St. entrance of the hotel to board a bus for a tour of the Capitol and Supreme Court Buildings. Luncheon will be served at the well-known Hogate's Sea Food Restaurant. The bus will return to the hotel about 3:30 P.M.

Tuesday evening, May 14—The ladies are invited to attend the Reception and Banquet at 6:30 P.M.

Wednesday morning and afternoon, May 15—Coffee will be served in the Ladies' Headquarters at 9:30 A.M. (complimentary). At 10:15 A.M. the ladies will meet at the 16th St. entrance of the hotel to board the bus for a trip to historic Arlington Cemetery, Alexandria, and Mt. Vernon. Luncheon will be served en route and the bus will return to the hotel about 3:30 P.M.

Thursday morning, May 16—Coffee will be served at 9:30 A.M. in the Ladies' Headquarters (complimentary). This morning and afternoon have been left open for informal tours. There is ample transportation by taxi, bus, or street car, and many points of interest are within walking distance of the Hotel Statler.

LUNCHEONS AND BUSINESS MEETINGS OF DIVISIONS

Electric Insulation Division Luncheon and Business Meeting, Monday, May 13, at 12:00 M. in the Congressional Room.

Electronics Division Luncheon and Business Meeting, Wednesday, May 15, at 12:30 P.M. in the South American Room.

Electrothermics and Metallurgy Division Luncheon and Business Meeting, Wednesday, May 15, at 12:30 M. in the Pan American Room.

Industrial Electrolytic Division Luncheon and Business Meeting, Mon-

day, May 13, at 12:00 M. in the South American Room.

Theoretical Electrochemistry Division Luncheon, Wednesday, May 15, at 12:00 M. in the Federal Room honoring foreign speakers whose presence have been made possible by the joint sponsorship of the National Science Foundation; Business Meeting, Thursday, May 16, at 11:45 A.M. in the Federal Room.

BOARD AND COMMITTEE MEETINGS

Sunday, May 12, 2:00 P.M.—Meeting of the Board of Directors in the Pan American Room.

Monday, May 13, 4:30 P.M.—Meeting of the Council of Local Sections in the California Room.

Tuesday, May 14, 4:30 P.M.—Meeting of the Membership Committee in the California Room.

Wednesday, May 15, 4:00 P.M.—Meeting of the Editorial Staff of the Journal in the California Room.

Thursday, May 16, 12:00 M.—Meeting of General Chairmen of Future Meetings in the Michigan Room.

COST OF VARIOUS FUNCTIONS

(other than registration)

Symposia Chairmen Breakfasts	$2.50
Division Luncheons	$3.75
Society Luncheon	$3.75
Monday Evening Mixer	Complimentary
Tuesday Reception and Banquet	$7.50
Trip to U. S. Naval Research Lab. (transportation)	$1.00
Trip to U. S. Naval Ordnance Lab. (transportation)	$1.00
Trip to National Bureau of Standards (transportation)	$1.00
Electronics Division Cocktail Mixer	$2.50
Ladies' Functions	
Monday—Fashion-Luncheon	$4.00
Tuesday—Capital Tour and Luncheon	$4.50
Wednesday—Tour and Luncheon	$5.00
(Book of three tickets.. $9.00)	

(The above prices include gratuities and taxes)

JOURNALS

Copies of the February, March, April, and May issues of the JOURNAL of The Electrochemical Society will be available at the registration desk. The price of a single copy of the JOURNAL is $1.25 to members and $1.75 to nonmembers.

EXTENDED ABSTRACTS

The Electronics Division and Theoretical Electrochemistry Division are making available extended abstract booklets containing 1000-word abstracts of the papers presented at the Divisions' Washington symposia.

The Electronics Division booklet should be available by about April 15 from Martin F. Quaely, Research Dept., Lamp Div., Westinghouse Electric Corp., Bloomfield, N. J., at the price of $2.00 each.

The Theoretical Electrochemistry Division booklet can be obtained, probably before the meeting, from Dr. Ralph Roberts, 3308 Camalier Drive, Washington 15, D. C., at the price of $3.00 each.

Copies of both booklets will be on sale at the registration desk at the Washington Meeting.

DISCUSSION

There will be no recordings made of oral discussions. Those contributing to the discussion of a paper and desiring their remarks published will be supplied by the symposium chairman with a printed form on which any discussion may be written. These forms should be given to the Secretary-Treasurer of the Division or to the Managing Editor of the JOURNAL after the session, or can be forwarded to the Managing Editor of the JOURNAL, 216 West 102nd St., New York 25, N. Y. The discussion will then be referred to the authors for reply. Publication of the discussion and the comments of the authors depends on publication of the article in the JOURNAL.

Written discussion should be submitted within two months following publication of any article in the JOURNAL.

A Discussion Section is published semiannually in the JOURNAL.

EMPLOYMENT POSTERS

Companies which desire to recruit employees at the Washington Meeting will have posters to this effect on a bulletin board near the registration desk.

Technical Program

Monday, May 13, 1957

9:00 A.M.—Formal Opening of the 111th Meeting with Introduction by General Chairman Fielding Ogburn and Response by President Hans Thurnauer (Federal Room).

NOTES

Address of author(s) is included with the abstract. In the Index to Authors, the abstract number is used instead of the page number.

Only two technical sessions, Electronics—Luminescence and Electronics—Semiconductors, are scheduled for the afternoon of Wednesday, May 15. Sessions that would normally be held at this time will be held Wednesday evening.

CORROSION—ELECTROTHERMICS AND METALLURGY

Joint Symposium

Tuesday, May 14, 1957

Role of Metal and Oxide Structure in Oxidation and Corrosion

(SOUTH AMERICAN ROOM)

9:00 A.M. and 2:00 P.M.—*See* Electrothermics and Metallurgy—Corrosion Program on p. 58C.

ELECTRIC INSULATION

Monday, May 13, 1957

New Material Developments with D. A. Lupfer presiding

(CONGRESSIONAL ROOM)

9:30 A.M.—**"Electric Moments of Certain Partially Fluorinated Esters"** by J. B. Romans and T. D. Callinan (Abstract No. 1)

10:00 A.M.—**"A New Dielectric Liquid for Impregnating Fixed Paper Capacitors"** by T. D. Callinan and J. B. Romans (Abstract No. 2)

10:30 A.M.—**"Progress Report on the Development of Metal Fiber Paper"** by H. F. Arledter (Abstract No. 3)

11:00 A.M.—**"Electric Strength of Perchloryifluoride (ClO_3F) Gas"** by J. J. Chapman and L. J. Frisco (Abstract No. 4)

12:00 M.—Electric Insulation Division Luncheon and Business Meeting in the Congressional Room. Guest speaker, K. N. Mathes, General Electric Co., Schenectady, N. Y.

Electric Insulation (cont'd)

Monday, May 13, 1957

Panel Discussion with D. A. Lupfer presiding

(CONGRESSIONAL ROOM)

2:00 P.M.—Panel Discussion of High Temperature Capacitors: K. H.

MEETING ROOM SCHEDULES

Meeting	Monday		Tuesday		Wednesday			Thursday	
	A.M.	P.M.	A.M.	P.M.	A.M.	P.M.	Eve.	A.M.	P.M.
Corrosion—Electrothermics and Metallurgy			SA	SA					
Electric Insulation	C	C	PA	PA	PA		PA		
Electronics:									
Luminescence			C	C	C	F		C	C
Semiconductors			P	P	P	C			
Thermionic Cathodes							O	O	O
Instrumentation								PA	PA
Screen Application									N
Electrothermics and Metallurgy		SA	SA	SA	SA		SA	SA	SA
Industrial Electrolytic	PA	PA							
Theoretical Electrochemistry	F	F	F	F	F		F	F	F

SA = South American Room.
C = Congressional Room.
PA = Pan American Room.
F = Federal Room.
P = Presidential Ballroom.
O = Ohio Room.
N = Foyer No. 3.

Brandt, Convair, Pomona, Calif.; R. G. Breckenridge, National Carbon Co., Parma, Ohio; J. G. Breetlove, American Lava Corp., Chattanooga, Tenn.; J. M. Booe, P. R. Mallory & Co., Indianapolis, Ind.; C. E. Doyle, Wright Air Development Center, Wright-Patterson Air Force Base, Ohio; J. F. Fabricius, Sprague Electric Co., North Adams, Mass.; R. S. Hower, Allen-Bradley Co., Milwaukee, Wis.; S. E. Rose, Avco Mfg. Co., Lawrence, Mass.; N. H. Terhune, Signal Corps Engineering Labs., Fort Monmouth, N. J.; H. T. Wensel, American Machine and Foundry, Alexandria, Va.

Electric Insulation (cont'd)

Tuesday, May 14, 1957

Thermal Evaluation and Classification of Materials with E. L. Brancato presiding

(PAN AMERICAN ROOM)

9:00 A.M.—"International Activities in the Evaluation of Electrical Insulation" by L. J. Berberich (Abstract No. 5)

9:30 A.M.—"Chemical Rate Phenomena in the Deterioration of Electrical Insulation" by T. W. Dakin (Abstract No. 6)

10:00 A.M.—"Principles for Classification of Insulating Materials" by K. N. Mathes (Abstract No. 7)

10:30 A.M.—"Thermal Evaluation of Electrical Insulating Materials" by J. F. Dexter (Abstract No. 8)

11:00 A.M.—"Thermal Stability of Laminated Thermosetting Plastics" by W. B. Kouwenhoven and G. G. Knickerbocker (Abstract No. 9)

12:15 P.M.—Society Luncheon and Business Meeting in the Presidential Ballroom.

Electric Insulation (cont'd)

Tuesday, May 14, 1957

Insulation Life with E. L. Brancato presiding

(PAN AMERICAN ROOM)

2:00 P.M.—"Statistical Methods Useful in Predicting Insulation Life" by W. E. Horton (Abstract No. 10)

2:30 P.M.—"Application of Extreme Value Statistics on Breakdown Phenomena" by J. H. Davidson (Abstract No. 11)

3:00 P.M.—"Derivation of Electronic Part-Failure Statistics from Material Properties" by J. A. Connor and D. I. Troxel (Abstract No. 12)

3:30 P.M.—"Corona and Its Effect on Insulation—A Résumé" by T. W. Liao (Abstract No. 13)

4:00 P.M.—"Effects of High-Energy Gamma Radiation on Dielectric Solids" by P. H. Klein (Abstract No. 14)

Electric Insulation (cont'd)

Wednesday, May 15, 1957

Prefabricated Circuitry with C. E. Coy presiding

(PAN AMERICAN ROOM)

9:00 A.M.—"Some Aspects of Missile Package Design" by J. P. Morone (Abstract No. 15)

9:45 A.M.—"Production of Prefabricated Circuitry" by M. F. Patrick (Abstract No. 16)

10:30 A.M.—"Component Parts for Printed Wiring Assemblies" by H. C. Frankel and Wilbur Gross (Abstract No. 17)

11:15 A.M.—"Application of Prefabricated Circuitry to Airborne Electronics Equipment" by G. B. Way and N. R. Dunbar (Abstract No. 18)

Electric Insulation

Wednesday, May 15, 1957

Prefabricated Circuitry (cont'd) **with C. E. Coy presiding**

(PAN AMERICAN ROOM)

8:00 P.M.—"Use of Shape as a Design Tool" by R. K. Jenny (Abstract No. 19)

8:45 P.M.—"Quality Improvement in the Manufacture of Printed Wiring" by E. J. Lorenz (Abstract No. 20)

9:30 P.M.—"An Approach for Meeting Future Needs of Electronic Components" by A. A. Lawson (Abstract No. 21)

ELECTRONICS—LUMINESCENCE

Tuesday, May 14, 1957
with J. F. Waymouth presiding

(CONGRESSIONAL ROOM)

9:00 A.M.—Keynote Address—"Electroluminescent and Field Effects in Phosphors" by H. F. Ivey (Abstract No. 22)

9:50 A.M.—"Effect of Electron Traps on the Brightness Waveform of Electroluminescent ZnS:Cu" by F. F. Morehead, Jr. (Abstract No. 23)

10:20 A.M.—"Field Enhancement of X-Ray Excited Luminescence in ZnS·CdS:Mn(Au)" by Georges Destriau (Abstract No. 24)

10:50 A.M.—"Characteristics of Electroluminescence at Audio Frequencies" by R. M. Rulon and F. Koury (Abstract No. 25)

11:20 A.M. — "Electrocathodoluminescence" by P. M. Jaffe (Abstract No. 26)

12:15 P.M.—Society Luncheon and Business Meeting in the Presidential Ballroom.

Electronics—Luminescence (cont'd)

Tuesday, May 14, 1957
with R. J. Ginther presiding

(CONGRESSIONAL ROOM)

2:00 P.M. — "AC Conductivity Measurements on CdS Crystals under Various Types of Illumination" by S. Jaffe, H. Kallmann, B. Kramer, and G. M. Spruch (Abstract No. 27)

2:30 P.M.—"Action of Temperature on the X-Ray Electroenhancement Effect" by J. Mattler (Abstract No. 28)

3:00 P.M.—"Thin Film Phosphors" by L. R. Koller (Abstract No. 29)

3:30 P.M.—"Diffusion of Excitation in CdS Crystals" by H. Kallmann, B. Kramer, and A. Orenstein (Abstract No. 30)

4:00 P.M.—"Variations of the Fermi Level in ZnS Phosphors Contaminated with Iron Family Impurities" by N. Arpiarian (Abstract No. 31)

4:30 P.M. — "Investigations in $CuGaS_2$-ZnS and $AgGaS_2$-ZnS Systems" by E. F. Apple (Abstract No. 32)

Electronics — Luminescence (cont'd)

Wednesday, May 15, 1957
with H. C. Froelich presiding

(CONGRESSIONAL ROOM)

9:00 A.M.—"Energy Storage and Decay in Various Phosphors" by H. Kallmann and E. Sucov (Abstract No. 33)

9:30 A.M.—"Luminescence of 'Self-Coactivated' ZnS-Cu" by M. H. Aven and R. M. Potter (Abstract No. 34)

10:00 A.M.—"Process of Light Stimulation in ZnS Phosphors" by H. Kallmann, W. Schneider, and M. Sidran (Abstract No. 35)

10:30 A.M.—"Energy Transfer and Sensitization in Single-Crystal Phosphors" by R. Leach (Abstract No. 36)

11:00 A.M. — "Some Aspects of Quenching of Fluorescence in Organic Liquids" by M. Furst and H. Kallmann (Abstract No. 37)

11:30 A.M.—"Infrared Photography with the Help of Various Inorganic Phosphors" by H. Kallmann and J. Rennert (Abstract No. 38)

12:30 P.M.—Electronics Division Luncheon and Business Meeting in the South American Room.

Electronics—Luminescence (cont'd)

Wednesday, May 15, 1957
with L. Thorington presiding

(FEDERAL ROOM)

2:00 P.M. — "Time Constants of Alpha- and Electron-Produced Light Flashes" by G. Brucker and H. Kallmann (Abstract No. 39)

2:30 P.M.—"Resolution of Thermoluminescence Curves" by C. H. Haake (Abstract No. 40)

3:00 P.M.—"Potential Energy Curves for Phosphors" by K. H. Butler (Abstract No. 41)

3:30 P.M.—"A Review of the Measurement of the Quantum Efficiency of Inorganic Phosphors" by J. Tregellas-Williams (Abstract No. 42)

5:00 P.M. to 6:30 P.M.—Electronics Division Cocktail Mixer in the South American Room.

Electronics—Luminescence (cont'd)

Thursday, May 16, 1957
with A. H. McKeag presiding

(CONGRESSIONAL ROOM)

9:00 A.M.—"Temperature Characteristics of Phosphors for Use in High Pressure Mercury Vapor Lamps" by A. H. McKeag (Abstract No. 43)

9:30 A.M.—"Temperature Dependence of Fluorescence" by R. W. Mooney (Abstract No. 44)

10:00 A.M.—"Gray Discoloration in Calcium Halophosphates" by W. L. Wanmaker and M. G. A. Tak (Abstract No. 45)

10:30 A.M. — "Cerium-Activated Halophosphate Phosphors" by S. T. Henderson and P. W. Ranby (Abstract No. 46)

11:00 A.M.—"Luminescence of Tin-Activated Strontium Orthophosphate" by H. Koelmans and A. P. M. Cox (Abstract No. 47)

11:30 A.M.—"Zinc Modified Orthophosphate Phosphors" by M. J. B. Thomas and K. H. Butler (Abstract No. 48)

Electronics—Luminescence (cont'd)

Thursday, May 16, 1957
with J. H. Schulman presiding

(CONGRESSIONAL ROOM)

2:00 P.M.—"Transition Probability Ratios in KCl:Tl and KCl:In" by F. E. Williams, P. D. Johnson, and B. Segall (Abstract No. 49)

2:30 P.M.—"Shape of the F-Band in KCl" by J. J. Markham and J. D. Konitzer (Abstract No. 50)

3:00 P.M.—"Interaction of Color Centers in the Alkali Halides" by W. D. Compton and John Lambe (Abstract No. 51)

3:30 P.M.—"Luminescence of Color Centers" by John Lambe and W. D. Compton (Abstract No. 52)

4:00 P.M.—"Experiments on Color Center Production in KI:Tl" by H. N. Hersh (Abstract No. 53)

4:30 P.M.—"Color Centers in Cadmium Fluoride" by M. Rubenstein and E. Banks (Abstract No. 54)

ELECTRONICS—SEMICONDUCTORS

Tuesday, May 14, 1957
with H. L. Goering presiding

(PRESIDENTIAL BALLROOM)

9:00 A.M.—Introductory Remarks by H. M. Pollack

9:10 A.M.—Keynote Address—"Compound Semiconductors" by D. A. Jenny (Abstract No. 55)

9:55 A.M.—"New Semiconductors" by J. H. Wernick and K. E. Benson (Abstract No. 56)

10:15 A.M.—"Carrier Transport Phenomena in Germanium Bicrystals" by H. F. Mataré and B. Reed (Abstract No. 57)

10:35 A.M.—"Photosensitivity of Ge Grain Boundaries" by O. Weinreich and H. F. Mataré (Abstract No. 58)

10:55 A.M.—"Growth and Definition of Bicrystals" by R. Wegener and H. F. Mataré (Abstract No. 59)

11:15 A.M.—"Dissociation Pressure and Cohesive Energy of Indium-Phosphide" by K. Weiser (Abstract No. 59A)

12:15 P.M.—Society Luncheon and Business Meeting in the Presidential Ballroom.

Electronics—Semiconductors (cont'd)

Tuesday, May 14, 1957
with W. Webster presiding

(PRESIDENTIAL BALLROOM)

2:30 P.M.—"Impurity Diffusion in Germanium and Silicon" by M. Tanenbaum (Invited Paper) (Abstract No. 60)

3:15 P.M.—"Effects of Heat Treatment on Silicon Diffusion-Created Devices" by C. Levi and I. Weiman (Abstract No. 61)

3:30 P.M.—"Oxygen as an Impurity in Transistor Grade Silicon" by W. Kaiser and P. H. Keck (Abstract No. 62)

4:00 P.M.—"Ternary Distribution Coefficients in Silicon" by David Navon (Abstract No. 63)

4:20 P.M.—"Evaporation and Alloying of Metals to Silicon" by J. M. Goldey, M. Tanenbaum, and N. Holonyak, Jr. (Abstract No. 64)

4:40 P.M.—"Recent News" Papers. Titles and short abstracts will be available at the Registration Desk.

Electronics—Semiconductors (cont'd)

Wednesday, May 15, 1957
with W. Dills presiding

(PRESIDENTIAL BALLROOM)

9:00 A.M.—"Transistor-Grade Silicon, I. Preparation of Ultrapure Silicon Tetraiodide" by Bernard Rubin, G. H. Moates, and J. R. Weiner (Abstract No. 65)

9:20 A.M.—"Transistor-Grade Silicon, II. Zone Purification of Silicon Tetraiodide" by G. H. Moates and Bernard Rubin (Abstract No. 66)

9:40 A.M.—Paper withdrawn. (Abstract No. 67)

10:10 A.M.—"Contribution to the Floating Zone Technique for Refining Silicon" by E. Buehler (Abstract No. 68)

10:35 A.M.—"Heat Treatment of Silicon Using Zone Heating Techniques" by H. C. Theuerer, J. M. Whelan, H. E. Bridgers, and E. Buehler (Abstract No. 69)

11:00 A.M.—"Recent News" Papers. Titles and short abstracts will be available at the Registration Desk.

12:30 P.M.—Electronics Division Luncheon and Business Meeting in the South American Room.

Electronics — Semiconductors (cont'd)

Wednesday, May 15, 1957
with B. J. Rothlein presiding

(CONGRESSIONAL ROOM)

2:00 P.M.—"Optical Measurement of Film Growth on Silicon and Germanium Surfaces in Room Air" by R. J. Archer (Abstract No. 70)

2:25 P.M.—"Bonding Material for Making Contact to Etched *P*-Type Silicon" by D. R. Mason and J. C. Sarace (Abstract No. 71)

2:45 P.M.—"Description of Electrochemical Jet Etching of Silicon" by Albert Mark (Abstract No. 72)

3:15 P.M.—"Mechanism of Electrolytic Rectification" by P. F. Schmidt (Abstract No. 73)

3:35 P.M.—"Recent News" Papers. Titles and short abstracts will be available at the Registration Desk.

5:00 P. M. to 6:30 P.M.—Electronics Division Cocktail Mixer in the South American Room.

ELECTRONICS—THERMIONIC CATHODES

Wednesday, May 15, 1957
with R. C. Hughes presiding

(OHIO ROOM)

7:30 P.M.—Introductory Remarks by R. H. Plumlee

7:35 P.M.—Keynote Address—"Recent Work on Surface Properties of Oxide Semiconductors" by J. J. Lander (Abstract No. 74)

8:15 P.M.—"Thermionic Emission Characteristics of Thoriated Rhenium" by W. E. Nexsen, Jr., and G. B. Gaines (Abstract No. 75)

8:45 P.M. — "Thermionics and Evaporation Properties of Some Lanthanide Oxides" by D. L. Schaefer (Abstract No. 76)

9:15 P.M.—"Emission from Barium on Tantalum Carbide" by J. E. White (Abstract No. 77)

9:45 P.M.—"Preparation and Properties of the Magnesium Oxide Cold Cathode" by Dietrich Dobischek (Abstract No. 78)

Electronics—Thermionic Cathodes (cont'd)

Thursday, May 16, 1957
with S. Wagener presiding

(OHIO ROOM)

9:00 A.M.—"Reactions of Oxide Cathodes with Gases at Low Pressures" by R. J. Ruka and E. A. Gulbransen (Abstract No. 79)

9:30 A.M.—"The Electron Microscopy of Alkaline Earth Carbonates" by C. F. Tufts (Abstract No. 80)

10:00 A.M.—"Relationship between Thermal Decomposition in Vacuum and Macrostructure of Alkaline Earth Carbonates" by B. Wolk and J. G. Buck (Abstract No. 81)

10:30 A.M.—"Study of Interface Impedance Characteristics of Seven Commercial Cathode Nickel Alloys" by C. D. Richard, Jr., and A. M. Bounds (Abstract No. 82)

11:00 A.M.—"Considerations of Oxide Cathode Interface Impedance" by A. P. Haase, R. E. Holmes, and F. J. Schmidt (Abstract No. 83)

11:30 A.M.—"A Study of the Molded Nickel Cathode" by C. P. Hadley, W. G. Rudy, and A. J. Stoeckert (Abstract No. 84)

Electronics—Thermionic Cathodes (cont'd)

Thursday, May 16, 1957
with J. E. White presiding

(OHIO ROOM)

2:00 P.M.—"New Developments in the L-Cathode" by C. A. M. van den Broek and A. Venema (Abstract No. 85)

2:30 P.M.—Unscheduled Reports on Recent Developments.

3:00 P.M.—Round-Table Discussion. The purpose of this round table is to promote an entirely unrestricted exchange of ideas between the audience and a panel of active workers in the field. Controversial subjects will be welcomed for discussion. Members of the audience may be called on for comments on the discussion.

ELECTRONICS—INSTRUMENTATION

Thursday, May 16, 1957
with A. E. Martin presiding

(PAN AMERICAN ROOM)

9:00 A.M.—"Equipment for the Autographic Determination of the

Electrical Resistance of Metals at High Temperatures" by G. A. Moore (Abstract No. 86)

9:40 A.M.—"Methods of Measuring High Resistances" by E. F. Turner, Jr. (Abstract No. 87)

10:10 A.M.—"Calibration of Kinescope Test Sets for Color Balance and Light Output" by G. P. Kirkpatrick and A. E. Hardy (Abstract No. 88)

10:40 A.M.—"Interferometric Calibration of Kinescope Aluminum Film Thickness Meters" by G. P. Kirkpatrick and T. A. Saulnier (Abstract No. 89)

Electronics—Instrumentation (cont'd)

Thursday, May 16, 1957
with A. E. Martin presiding

(PAN AMERICAN ROOM)

2:00 P.M.—"An Apparatus for Vacuum and Atmospheric Differential Thermal Analysis" by J. G. Rabatin and C. S. Card (Abstract No. 90)

2:30 P.M.—"Application of Lead Sulfide Detector to the Study of Luminescence in the Near Infrared Region" by J. M. Goldstein, W. M. McNabb, and J. F. Hazel (Abstract No. 91)

3:00 P.M.—"Effect of Current Drains on Cadmium Standard Cells" by G. D. Vincent (Abstract No. 92)

ELECTRONICS—SCREEN APPLICATIONS

Thursday, May 16, 1957
with M. Sadowsky presiding

(FOYER NO. 3)

2:00 P.M.—"Wet and Dry Strengths of Cathode Ray Screens" by R. W. Spencer, N. W. McCready, and Wm. Stericker (Abstract No. 93)

2:30 P.M.—"Sedimentation Volumes of a Phosphor Powder in Potassium Silicate and Potassium Silicate-Barium Acetate Settling Media" by J. F. Hazel and Louis Fiorito (Abstract No. 94)

3:00 P.M.—"Surface Phenomena Associated with the Application of Organic Films to Phosphor Screens" by R. W. Dudding (Abstract No. 95)

3:30 P.M.—"Photodeposition of Luminescent Screens" by M. Sadowsky and D. Payne, Jr. (Abstract No. 96)

4:00 P.M.—"Phosphor Slurry Process for Color-Kinescope Screening" by D. J. Donahue and T. A. Saulnier (Abstract No. 97)

ELECTROTHERMICS AND METALLURGY

Monday, May 13, 1957

Chemical Metallurgy
with John Blocher presiding

(SOUTH AMERICAN ROOM)

2:00 P.M.—"High Temperature Oxidation of High Purity Nickel between 750° and 1050°C" by E. A. Gulbransen and K. F. Andrew (Abstract No. 98)

2:30 P.M.—"Ten-Gram Levitation Melted Ingots" by G. Comenetz and J. W. Salatka (Abstract No. 99)

3:00 P.M.—"Growth of Whiskers by Reduction of Halogenides" by H. Wiedersich (Abstract No. 100)

3:30 P.M.—"Zone Melting of Uranium" by C. I. Whitman, V. Compton, and R. B. Holden (Abstract No. 101)

4:00 P.M.—"Molybdenum Plating inside of Large Bore Tubes" by P. L. Raymond (Abstract No. 102)

ELECTROTHERMICS AND METALLURGY—CORROSION

Joint Symposium

Tuesday, May 14, 1957

Role of Metal and Oxide Structure in Oxidation and Corrosion
with W. E. Tragert presiding

(SOUTH AMERICAN ROOM)

9:00 A.M.—"Influence of Crystal Face on Some Electrochemical Properties of Single Crystals of Copper" by A. T. Gwathmey (Abstract No. 103)

10:00 A.M.—"Structural and Chemical Factors Associated with the Fracture of Metals" by W. D. Robertson (Abstract No. 104)

11:00 A.M.—"Influence of Structural Factors on the Corrosion of Stainless Steel" by N. A. Nielsen and M. A. Streicher (Abstract No. 105)

12:15 P.M.—Society Luncheon and Business Meeting in the Presidential Ballroom.

Electrothermics and Metallurgy—Corrosion (cont'd)

Joint Symposium (cont'd)

Tuesday, May 14, 1957

Role of Metal and Oxide Structure in Oxidation and Corrosion
with D. A. Vermilyea presiding

(SOUTH AMERICAN ROOM)

2:00 P.M.—"Role of Metal and Oxide Structures in High Temperature Oxidation Processes" by C. E. Birchenall (Abstract No. 106)

3:00 P.M.—"Effect of Dislocations in Oxide Films on Oxidation" by N. Cabrera (Abstract No. 107)

4:00 P.M.—"Interaction of Oxide and Metal Crystal Structures" by J. T. Waber (Abstract No. 108)

Electrothermics and Metallurgy (cont'd)

Wednesday, May 15, 1957

Symposium on Columbium (Niobium)
with Bruce Gonser presiding

(SOUTH AMERICAN ROOM)

9:00 A.M.—Introductory Remarks by Bruce Gonser.

9:05 A.M.—"The Element Columbium and Its Compounds" by J. R. Darnell and L. F. Yntema (Abstract No. 109)

9:35 A.M.—"Supplies of Columbium" by K. B. Higbie (Abstract No. 110)

10:00 A.M.—"Some Sources and Production Statistics for Columbium" by H. P. Croft (Abstract No. 111)

10:30 A.M.—"Economic Aspects and Supply Situation for Columbium" by R. L. Carmichael (Abstract No. 112)

11:00 A.M.—"A Review of the Extractive Metallurgy of Niobium" by M. E. Sibert, A. J. Kolk, and M. A. Steinberg (Abstract No. 113)

12:30 M.—Electrothermics and Metallurgy Division Luncheon and Business Meeting in the Pan American Room.

Electrothermics and Metallurgy (cont'd)

Wednesday, May 15, 1957

Symposium on Columbium (Niobium) (cont'd)
with E. M. Sherwood presiding

(SOUTH AMERICAN ROOM)

7:30 P.M.—"Informal Comments on the ONR Program of Basic Research on Columbium" by N. E. Promisel (Abstract No. 114)

7:45 P.M.—"Separation of Ta and Nb" by J. L. Tews and S. L. May (Abstract No. 115)

8:15 P.M.—"Preparation and Properties of High Purity Tantalum and Columbium" by R. C. Bourke, J. M. Blocher, Jr., and I. E. Campbell (Abstract No. 116)

8:45 P.M.—"Preparation of High Purity, Ductile Niobium by Fusion Electrolysis" by A. J. Kolk, M. E. Sibert, and M. A. Steinberg (Abstract No. 117)

9:15 P.M.—"Analysis of Certain Metallic Impurities in Niobium" by J. F. Reed and A. H. Wolfe (Abstract No. 118)

9:35 P.M.—"Analysis of Oxygen and Nitrogen in Niobium" by W. Harris (Abstract No. 119)

Electrothermics and Metallurgy (cont'd)

Thursday, May 16, 1957

Symposium on Columbium (Niobium) (cont'd)
with A. U. Seybolt presiding

(SOUTH AMERICAN ROOM)

9:00 A.M.—"Hydrogen and Niobium—Reaction and Diffusion Kinetics" by M. W. Mallett and W. M. Albrecht (Abstract No. 120)

9:30 A.M.—"Tensile Properties of Niobium on the Basis of Purity and Prior Stress History" by F. J. Anders, Jr., and W. I. Pollock (Abstract No. 121)

10:00 A.M.—"Ductile - to - Brittle Transition in Niobium" by E. T. Wessel and D. D. Lawthers (Abstract No. 122)

10:30 A.M.—"Effect of Rare Earth Additions on the Ductility of Arc Melted Group V-A Metals" by J. W. Semmel, Jr. (Abstract No. 123)

11:00 A.M.—"Electroplating on Columbium" by J. G. Beach (Abstract No. 124)

Electrothermics and Metallurgy (cont'd)

Thursday, May 16, 1957

Symposium on Columbium (Niobium) (cont'd)
with E. M. Mahla presiding

(SOUTH AMERICAN ROOM)

2:00 P.M.—"Oxidation of Niobium between 375° and 700°C" by E. A. Gulbransen and K. F. Andrew (Abstract No. 125)

2:30 P.M.—"Development of Oxidation-Resistant Niobium Alloys" by H. T. Kling (Abstract No. 126)

3:00 P.M.—"Effect of Alloy Additions on the Oxidation Resistance of Niobium" by F. J. Clauss and C. A. Barrett (Abstract No. 127)

3:30 P.M.—"Oxidation of Niobium-Chromium Alloys at Elevated Temperatures" by C. A. Barrett and F. J. Clauss (Abstract No. 128)

4:00 P.M.—"Vacuum Reactions of Niobium during Sintering" by W. D. Klopp, C. T. Sims, and R. I. Jaffee (Abstract No. 129)

INDUSTRIAL ELECTROLYTIC

Monday, May 13, 1957

Fused Salt Electrolysis with M. Janes presiding

(PAN AMERICAN ROOM)

9:30 A.M.—"Electromagnetic Forces in a Large Aluminum Furnace" by O. Chr. Böckman and J. Wleügel (Abstract No. 130)

10:00 A.M.—"Electrical Conductivity of Molten Fluorides, I. Apparatus and Method" by E. W. Yim and Morris Feinleib (Abstract No. 131)

10:30 A.M.—"Electrical Conductivity of Molten Fluorides, II. Conductance of Alkali Fluorides, Cryolites, and Cryolite-Base Melts" by E. W. Yim and Morris Feinleib (Abstract No. 132)

11:00 A.M.—"Uranium Metal Preparation by Electrolytic Reduction of Its Oxides" by L. W. Niedrach and B. E. Dearing (Abstract No. 133)

12:00 M.—Industrial Electrolytic Division Luncheon and Business Meeting in the South American Room. J. C. Cole will give the Chlor-Alkali Committee Report. (Abstract No. 134)

Industrial Electrolytic (cont'd)

Monday, May 13, 1957

Chlor-Alkali Processes with J. C. Cole presiding

(PAN AMERICAN ROOM)

2:00 P.M.—"Influence of Impurities in the Electrolyte in Chlorine-Caustic Electrolysis by the Mercury Cell Process, VI. Investigation of the Influence of Graphite Particles on Amalgam Decomposition and Cathodic Current Efficiency" by Gösta Angel, Rolf Brännland, and Stig Dahlerus (Abstract No. 135)

2:30 P.M.—"The Castner-Kellner Shunt Circuit for Mercury Chlor-Alkali Cells" by M. Janes (Abstract No. 136)

3:00 P.M.—"Electrolytic Production of Sodium Perchlorate Using Lead Dioxide Anodes" by J. C. Schumacher, D. R. Stern, and P. R. Graham (Abstract No. 137)

THEORETICAL ELECTROCHEMISTRY

Monday, May 13, 1957

Joint Symposium

Structure of Electrolytic Solutions (Electrolytes)

Sponsored by the National Science Foundation and the ECS with W. J. Hamer presiding

(FEDERAL ROOM)

9:30 A.M.—Introductory Remarks by W. J. Hamer

9:35 A.M.—"Interpretation of Activity and Osmotic Coefficients" by George Scatchard (Abstract No. 138)

10:05 A.M.—"Electrolytic Solution Problem in Statistical Mechanics" by J. E. Mayer (Abstract No. 139)

10:35 A.M.—"Successes and Limitations of the Theory of Debye and Hückel" by E. A. Guggenheim (Abstract No. 140)

11:05 A.M.—"Statistical Mechanical Theory of Plasmas and Liquid Metals" by J. G. Kirkwood (Abstract No. 141)

11:35 A.M.—"Properties of Concentrated Solutions of Acids and Alkalies" by R. P. Bell (Abstract No. 142)

Theoretical Electrochemistry (cont'd)

Monday, May 13, 1957

Joint Symposium

Structure of Electrolytic Solutions (Electrolytes) (cont'd)

Sponsored by the National Science Foundation and the ECS with E. Yeager presiding

(FEDERAL ROOM)

1:45 P.M.—"Present State of the Electrolyte Problem" by C. A. Kraus (Abstract No. 142A)

2:00 P.M.—"Properties of Rare Earth Salts in Electrolytic Solutions" by F. H. Spedding and Gordon Atkinson (Abstract No. 143)

2:30 P.M.—"Nuclear Magnetic Resonance Studies of Aqueous Solutions" by H. S. Gutowsky (Abstract No. 144)

3:00 P.M.—"Raman Spectral Studies of Ionic Equilibria in Solutions of Strong Electrolytes" by T. F. Young (Abstract No. 145)

3:30 P.M.—"Melting Mechanisms of Ionic Crystals" by A. R. Ubbelohde (Abstract No. 146)

4:00 P.M.—"Influence of Complex Ions on Structure and Reactivity of Fused Salts" by E. R. Van Artsdalen (Abstract No. 147)

4:30 P.M.—"A Point of View on Ion Clouds; A Suggested Explanation of an Activity Anomaly in Dilute Aqueous LiCl Solutions" by H. S. Frank and P. T. Thompson (Abstract No. 148)

Theoretical Electrochemistry (cont'd)

Tuesday, May 14, 1957

Joint Symposium

Structure of Electrolytic Solutions (Electrolytes) (cont'd)

Sponsored by the National Science Foundation and the ECS with Ralph Roberts presiding

(FEDERAL ROOM)

9:00 A.M.—"Incomplete Dissociation in Aqueous Salt Solutions" by C. W. Davies (Abstract No. 149)

9:30 A.M.—"Hydration and Association in Aqueous Electrolyte Solutions" by E. Glueckauf (Abstract No. 150)

10:00 A.M.—"Hydrogen Bond Structures, Hydration of Protons, and Proton Transfer in Aqueous Solutions" by M. Eigen (Abstract No. 151)

10:30 A.M.—"Quantitative Measurements of Ionic Vibration Potentials" by E. Yeager, J. Booker, and F. Hovorka (Abstract No. 152)

10:55 A.M.—"A Physical Theory of Ion Solvation" by M. Balkanski (Abstract No. 153)

11:20 A.M.—"Aquo-ions and Ion Pairs" by J. F. Duncan and D. L. Kepert (Abstract No. 154)

11:50 A.M.—"Ionization of the Bisulfate Ion; Notes on the Electromotive Force Method of Determining Ionization Constants" by W. J. Hamer (Abstract No. 155)

12:15 P.M.—Society Luncheon and Business Meeting in the Presidential Ballroom.

Theoretical Electrochemistry (cont'd)

Tuesday, May 14, 1957

Joint Symposium

Structure of Electrolytic Solutions (Electrolytes) (cont'd)

Sponsored by the National Science Foundation and the ECS with Ernest Yeager presiding

(FEDERAL ROOM)

2:00 P.M.—"Heats of Dilution of Very Dilute Solutions of Weak and Strong Electrolytes" by E. Lange (Abstract No. 156)

2:30 P.M.—"Anion Exchange Studies of Metal Complexes" by K. A. Kraus (Abstract No. 157)

3:00 P.M.—"Electrophoresis and Conductivity in Solutions Containing Polyelectrolytes" by J. J. Hermans (Abstract No. 158)

3:30 P.M.—"Normal and Abnormal Ionic Mobilities in Anhydrous Hydrofluoric Acid and Hydrogen Peroxide-Water Systems" by Martin Kilpatrick (Abstract No. 159)

4:00 P.M.—"Mobilities of Ions and Uncharged Molecules in Solutions in Relation to Viscosity" by R. H. Stokes (Abstract No. 160)

4:30 P.M.—"Conductance Equations of Robinson-Stokes and Wishaw-Stokes Applied to the Regions of Dilute and of Concentrated Solutions, Respectively" by A. N. Campbell (Abstract No. 161)

Theoretical Electrochemistry (cont'd)

Wednesday, May 15, 1957

Joint Symposium

Structure of Electrolytic Solutions (Electrolytes) (cont'd)

Sponsored by the National Science Foundation and the ECS with Ralph Roberts presiding

(FEDERAL ROOM)

9:00 A.M.—"A Redetermination of the Value of the Faraday with the Iodine Coulometer" by D. A. MacInnes and A. R. Pray (Abstract No. 162)

9:30 A.M.—"Diffusion and Activity Coefficients of Electrolytes in Dilute Aqueous Solutions" by H. S. Harned (Abstract No. 163)

10:00 A.M.—"Thermal Diffusion and Related Effects in Solutions of Electrolytes" by J. N. Agar (Abstract No. 164)

10:30 A.M.—"Temperature Dependence of the Thermal Diffusion of Aqueous KCl" by L. G. Longsworth (Abstract No. 165)

11:00 A.M.—"Data for the Concentration Dependence of the Four Diffusion Coefficients of the System NaCl-KCl-H_2O at 25°" by I. J. O'Donnell and L. J. Gosting (Abstract No. 166)

12:00 M.—Theoretical Division Luncheon honoring foreign speakers of the symposium whose presence have been made possible by the joint sponsorship of the National Science Foundation, in the Federal Room. Professor Peter Debye, Cornell University, speaker.

Theoretical Electrochemistry (cont'd)

Wednesday, May 15, 1957

Joint Symposium

Structure of Electrolytic Solutions (Electrolytes) (cont'd)

Sponsored by the National Science Foundation and the ECS with W. J. Hamer presiding

(FEDERAL ROOM)

7:30 P.M.—"Thermodynamic Functions of Single Ionic Species in Solutions" by Pierre Van Rysselberghe (Abstract No. 167)

8:00 P.M.—"Some Thermodynamic Properties of Solutions of Salts of Bivalent Metals" by J. M. Austin, R. A. Matheson, and H. N. Parton (Abstract No. 168)

8:30 P.M.—"Ionization Constants of Weak Acids from Spectrophotometric Measurements" by R. A. Robinson (Abstract No. 169)

9:00 P.M.—"Conductance and *p*H Measurements in Methanol-Water Mixtures" by Theodore Shedlovsky (Abstract No. 170)

9:25 P.M.—"Ionization Equilibria in Ammonia-Water Solutions from 5° to 55° as Obtained from High Field Conductance Measurements" by Emil Arnold, Harlow Freitag, and Andrew Patterson, Jr. (Abstract No. 171)

9:50 P.M.—"An Isopiestic Unit for High Temperature Studies" by B. A. Soldano, R. J. Fox, and R. W. Stoughton (Abstract No. 172)

10:15 P.M.—"Thermodynamics of Hydrogen Chloride in Ethyl Alcohol from EMF Measurements" by G. J. Janz and Harry Taniguchi (Abstract No. 173)

Theoretical Electrochemistry (cont'd)

Thursday, May 16, 1957

General Session with E. Yeager presiding

(FEDERAL ROOM)

9:00 A.M.—"Kinetics of Bromoacetate-Thiosulfate Ionic Reaction" by Gerald Corsaro and H. L. Stephens (Abstract No. 174)

9:20 A.M.—"Zinc Standard Potential in Water-Organic Mixtures" by Gerald Corsaro and H. L. Stephens (Abstract No. 175)

9:40 A.M.—"Uncommon Valency Ions and the Difference Effect" by M. E. Straumanis (Abstract No. 176)

10:00 A.M.—"Streaming Potentials in Spherical-Grain Sands" by C. E. Bleil and Wm. Schriever (Abstract No. 177)

10:20 A.M.—"EDL Capacities at Solid Metal-Solution Interfaces" by J. J. McMullen and Norman Hackerman (Abstract No. 178)

10:40 A.M.—"Impedance at Polarized Platinum Electrodes in Various Electrolytes" by J. N. Sarmousakis and M. J. Prager (Abstract No. 179)

11:00 A.M.—"Catalytic Activity and Electronic Structure" by Sigmund Schuldiner and J. P. Hoare (Abstract No. 180)

11:20 A.M.—"Mechanism of Hydrogen Producing Reactions on Palladium, IV. Electrochemical Kinetics on the α-Palladium-Hydrogen System in Acid Solutions" by J. P. Hoare and Sigmund Schuldiner (Abstract No. 181)

11:45 A.M.—Theoretical Electrochemistry Division Business Meeting.

Theoretical Electrochemistry (cont'd)

Thursday, May 16, 1957

General Session (cont'd) **with Paul Delahay presiding**

(FEDERAL ROOM)

1:45 P.M.—"A Tentative Theory of Inhibitions of Aqueous Kolbe Electrolyses" by G. W. Thiessen (Abstract No. 182)

2:05 P.M.—"Electrochemical Polarization, II. Ferrous-Ferric Electrode Kinetics on Stainless Steel" by Milton Stern (Abstract No. 183)

2:25 P.M.—"Relation between Pitting Corrosion and the Ferrous-Ferric Oxidation-Reduction Kinetics on Passive Surfaces" by Milton Stern (Abstract No. 184)

2:45 P.M.—"The Potential of an Electrode of a Voltaic Cell. A New Definition with Justification for the Use of Two Sign Conventions" by J. B. Ramsey (Abstract No. 185)

3:05 P.M.—"The Silver and Thallium Oxide Coulometer" by W. T. Foley (Abstract No. 186)

3:25 P.M.—"Voltammetric Studies at Constant Current in Fused Chlorides" by J. M. Wood, Jr. (Abstract No. 187)

3:45 P.M.—"Rates of Oxidation of Titanium in Fused Salt Baths" by M. E. Straumanis and Ch. Chiou (Abstract No. 188)

4:05 P.M.—"Cathode Potentials during the Electrodeposition of Molybdenum Alloys from Aqueous Solutions" by D. W. Ernst and M. L. Holt (Abstract No. 189)

4:25 P.M.—"Electrodeposition of Iron-Molybdenum Alloys" by Albertine Krohn, L. O. Case, and N. W. Hovey (Abstract No. 190)

ABSTRACTS

Note

In the Index to Authors, the Abstract Number is listed instead of the number of the page on which the Abstract or listing in the Technical Program appears.

ELECTRIC INSULATION

Abstract No. 1

Electric Moments of Certain Partially Fluorinated Esters

J. B. Romans and T. D. Callinan (present address: IBM, Poughkeepsie, N. Y.) U. S. Naval Research Lab., Washington 25, D. C.

Electric moments of six partially fluorinated esters have been determined. Materials studied were liquids at room temperature, known to be chemically inert and thermally stable. All six esters were found to be highly polar compounds exhibiting marked tendencies to associate molecularly; they possessed dipole moments of the order of 2.8–3.8 × 10^{-18} esu-cm. From experimentally determined permanent electric moments, the most probable molecular configurations were calculated for each of the esters. The predominating structure includes one cis-type configuration. It is evident that the molecules exist, for the most part, in a nonpolar form.

Abstract No. 2

A New Dielectric Liquid for Impregnating Fixed Paper Capacitors

T. D. Callinan (present address: IBM, Poughkeepsie, N. Y.) and J. B. Romans, U. S. Naval Research Lab., Washington 25, D. C.

Fixed capacitors, using kraft paper as the solid dielectric and bis (1H, 1H, 7H-dodecafluoroheptyl) 3-methylglutarate (PFE-774) as the impregnant have been found to possess capacitance to volume ratios higher than similar capacitors impregnated with pentachlorodiphenyl. Furthermore, change in capacitance with temperature is less than 4% within the range −55° to 85°C. Such capacitors have passed military specification MIL-C-25A for accelerated aging by withstanding 85°C and 130% rated voltage for 250 hr. Because the impregnant is unusually flame resistant, thermally stable, of low viscosity, and does not irritate the skin or cause rubber and plastics to swell and become tacky, this partially fluorinated ester is considered to be worthy of commercial development as a capacitor impregnant. It is believed results of this investigation open possibilities for production of new smaller capacitors particularly adapted to low temperature operation.

Abstract No. 3

Progress Report on the Development of Metal Fiber Paper

H. F. Arledter, Hurlbut Paper Co., South Lee, Mass.

The possibility of manufacturing metal fiber paper in a continuous web on a pilot plant Foudrinier paper machine of 9-in. width has been demonstrated. Paper made of blends of metal fibers with cellulose and inorganic or organic synthetic fibers, as well as 100% metal fiber paper, seems to be feasible. This paper outlines the mechanical properties of metal fiber paper and laminates and their possible uses. Further progress in the manufacture of metal fiber paper will depend on the availability of metal fibers in sufficient amounts and quality to make more extensive trials.

Abstract No. 4

Electric Strength of Perchloryl-fluoride (ClO_3F) Gas

J. J. Chapman and L. J. Frisco, Dielectrics Lab., The Johns Hopkins University, Baltimore 2, Md.

A new gas (ClO_3F) has been examined in uniform and heterogeneous fields. In the former case, 2-cm diameter spheres were used and, in the latter case, point-to-point breakdowns were observed. Observations were extended to mixtures of perchlorylfluoride with SF_6 and N. The contrasting behavior among the pure gases offered by the study of visual corona proved to be of particular interest in nonuniform fields. Perchlorylfluoride may be classified as a high dielectric strength gas since its performance exceeds that of SF_6 under certain circumstances.

Abstract No. 5

International Activities in the Evaluation of Electrical Insulation

L. J. Berberich, Westinghouse Electric Corp., East Pittsburgh, Pa.

The present AIEE and international temperature standards, except for several minor revisions, date back to 1912. At that time, insulating materials could conveniently be grouped into two categories, viz., "organic" and "inorganic" or combinations of these. With the advent of many new synthetic materials having thermal stabilities extending over a wide range, it was recognized recently that present standards do not fill the needs of a dynamic electrical industry. Thus, with the U. S. leading the way, a gradual change is taking place in the philosophy of insulation classification by definition to classification by test and performance. The paper reviews, in a broad way, how this is being accomplished on an international basis.

Abstract No. 6

Chemical Rate Phenomena in the Deterioration of Electrical Insulation

T. W. Dakin, Westinghouse Research Lab., East Pittsburgh, Pa.

The basis is presented for a more accurate interpretation of results of physical-type tests to measure the thermal aging of insulation together with a more accurate method of applying results of such tests to predicting insulation deterioration in practice. Since observed physical changes during thermal aging are the result of internal chemical changes in organic material, it is shown that the theory of chemical reaction rates can be applied to analyze experimental data of aging.

Abstract No. 7

Principles for Classification of Insulating Materials

K. N. Mathes, General Electric Co., Schenectady, N. Y.

Classification of insulating materials may be desirable in three important areas: thermal capability, mechanical suitability, and voltage utility. Up to the present, most attention has been paid to the area of the development of functional tests for determining the thermal capability of insulating materials. But mechanical characteristics of insulating materials may be fully as important as thermal properties, and the ability to withstand voltage is implied in the definition of insulation itself. In setting up functional tests, it is important to represent service conditions fairly. In the development of test samples, a "ladder" of tests must be considered. Selection of adequate test conditions and the choice of proper and significant end points is important, as are the use of statistics and avoidance of its overuse in the interpretation of data. The cost of tests and scope to be covered by material suppliers, fabricator, manufacturer, and user must be considered and balanced carefully. Proper use of functional tests in classifying insulating materials has tremendous implication in the simplification of design and the efficient use of materials.

Abstract No. 8

Thermal Evaluation of Electrical Insulating Materials

J. F. Dexter, Dow Corning Corp., Midland, Mich.

Revisions being made in AIEE Standards will specify that the temperature classification of insulating materials should be based on thermal aging data obtained by functional testing. This radical departure from the traditional method of classification based on chemical composition is necessary because of the rapid development of new synthetic materials. The thermal stability of many of these new materials cannot be established by the simple expedient of classifying them as organic and inorganic.

This new philosophy requires the development of realistic test methods for determining the relative thermal stability of insulating materials. This paper reviews problems associated with the development of test procedures and the progress that is being made.

Abstract No. 9

Thermal Stability of Laminated Thermosetting Plastics

W. B. Kouwenhoven and G. G. Knickerbocker, The Johns Hopkins University, Baltimore, Md.

This paper presents data on mechanical and electrical properties of thermosetting plastics, including paper base, linen base, asbestos and glass base materials at elevated temperatures for periods varying from 1 to 1000 hr. In addition, the paper describes the development of a method of determining the dielectric strength at elevated temperatures in a liquid medium.

Abstract No. 10

Statistical Methods Useful in Predicting Insulation Life

W. E. Horton, Westinghouse Electric Corp., East Pittsburgh, Pa.

Evaluation of insulation materials and/or systems either as samples or in motors under extreme environmental conditions is necessary if experimental data on the insulation life are to be realized in a reasonable length of time. In general, the regression technique is used to estimate the relationship between insulation life and operating condition. The purpose of this paper is to illustrate how this technique and other statistical methods can be used effectively in predicting insulation life.

Abstract No. 11

Application of Extreme Value Statistics on Breakdown Phenomena

J. H. Davidson, General Electric Co., Schenectady, N. Y.

Many engineers have expressed difficulty in analyzing life test data. For many reasons, the conditional failure density concept is to be preferred over all other methods of analyzing life characteristics. Conditional failure density is the probability that an item (or a particular "chain link") will fail at a particular time, provided it has survived up to that time. Conditional failure density has proved most useful in the study of metal fatigue and its value is now being explored in the testing of dielectric materials.

This new concept represents a "breakthrough" in the study of failure phenomena. Very often, insight is given into the failure behavior of a particular product, such as early failures. Conditional failure density might even be used as a property characteristic of a particular material.

Abstract No. 12

Derivation of Electronic Part-Failure Statistics from Material Properties

J. A. Connor and D. I. Troxel, Radio Corp of America, Camden, N. J.

There is a mounting need for suitable "mortality" statistics for component parts to be used in military electronic equipment. Materials investigation studies are potential "gold mines" of correlation data. The selection, analysis, and interpretation of this data must be based on certain compromise factors dictated by the ultimate statistical utility of the end result. That such efforts can be effective is shown by providing a number of specific examples.

Abstract No. 13

Corona and Its Effect on Insulation —A Résumé

T. W. Liao, General Electric Co., Pittsfield, Mass.

This paper attempts to review the subject of corona and its effect on insulation based on some of the pertinent published articles in this field. The content consists of the following sections: what is corona? how does corona occur? corona inception, effect on insulation with regard to insulation life, insulation surface damage; corona in capacitors, cables, transformers, and other electrical equipment. The references cited in each of the articles give leads to many findings which broaden what is discussed briefly in this paper.

Abstract No. 14

Effects of High-Energy Gamma Radiation on Dielectric Solids

P. H. Klein, General Electric Co., Syracuse, N. Y.

The kinds and magnitudes of radiations present in the various locations

near nuclear reactors are discussed as well as the mechanisms of interaction of radiation with matter, viz., group fragmentation, molecular scission, and polymerization. Techniques and locations for obtaining high dose rates are presented. Results of 60-cycle short-time voltage breakdown tests on polyethylene, cellulose acetate, and polyvinyl chloride films along with Formex-varnished wire are given as a function of integrated dosage up to 10^8 roentgens. Extensive electrical tests on a mica-glass-silicone-resin insulation simulating that used in the Submarine Intermediate Reactor's electromagnetic pump are described. Measurements of mechanical property changes of irradiated resins by means of a newly developed penetrometer are presented.

Abstract No. 15

Some Aspects of Missile Package Design

J. P. Morone, P. R. Mallory & Co., Inc., Indianapolis, Ind.

The Signal Corps Engineering Labs., Fort Monmouth, N. J., sponsored a program, recently completed, leading to the establishment of "Principles and Techniques of Integration and Packaging of Printed Circuit Assemblies for Missile Applications" (Contract No. DA-36-039-sc-64451). A number of problems confronting the missile package designer were investigated. Among these were problems related to package integration; mechanical, thermal, and climatic adequacy; miniaturization; and maintenance. The approaches investigated and conclusions reached constitute the basis for this paper.

Abstract No. 16

Production of Prefabricated Circuitry

M. F. Patrick, Westinghouse Electric Corp., Baltimore, Md.

A fundamental approach to the creation of prefabricated circuitry is discussed, covering drafting procedures for implementing a design from schematic to production stage. Also included is a review of some of the various parameters to be recognized by the designer, such as electrical characteristics, mechanical and environmental requirements, and fabrication techniques.

Abstract No. 17

Component Parts for Printed Wiring Assemblies

H. C. Frankel and Wilbur Gross, Signal Corps Engineering Labs., Fort Monmouth, N. J.

The design of component parts used with prefabricated circuits in military and commercial equipment should be guided by those requirements considered necessary to promote satisfactory service with regard to functional suitability, reliability, compatibility with machine handling, etc., during production, transportation, storage and/or operation. Following a summation of these requirements, types available at present of printed and separately fabricated (conventional) components, including resistive, reactive, electrochemical, thermionic, and other parts, will be exhibited and their capabilities and limitations will be discussed. Current and proposed developments which are expected to overcome these limitations will be described.

Abstract No. 18

Application of Prefabricated Circuitry to Airborne Electronics Equipment

G. B. Way and N. R. Dunbar, North American Aviation, Inc., Downey, Calif

Mechanization of airborne electronic equipment is illustrated, using standardized, functional circuit elements. These transistorized circuit elements perform the necessary basic information transfer and modification required in an airborne analog flight control system. A design technique and packaging method is discussed wherein equipment using etched circuits, etched cabling, and automatic machine assembly can be produced with a minimum of design and engineering effort. Utilization of proper materials and processes enables the use of double-sided circuits and plated eyelets. The techniques provided a high circuit and component density per unit areas of etched circuit panels.

Abstract No. 19

Use of Shape as a Design Tool

R. K. Jenny, Westinghouse Electric Corp., Baltimore, Md.

Normally used methods for reduction of vibration amplification of phenolic boards at resonance have concomitant disadvantages. Some of these methods and their inherent disadvantages are: (*a*) backing the board with a damping media (sponge rubber, etc.) which introduces humidity and cooling problems; (*b*) stiffening structure or cutting size of boards which increases weight and uncertainty; (*c*) energy absorption device (dynamic absorber, etc.) which increases weight and causes self-excited vibration.

There are usable methods which have no inherent disadvantages. The one described in this paper is use of non-rectangular shapes.

Abstract No. 20

Quality Improvement in the Manufacture of Printed Wiring

E. J. Lorenz, International Business Machines Corp., Poughkeepsie, N. Y.

This paper outlines procedures and processes which have been found to improve the over-all quality of printed wiring cards or boards. Items to be covered include design and artwork, with their influence on the finished product, materials used for the finished product, methods and processes employed during the manufacturing cycle, and tests which are used to determine the quality of the finished product. The design in general is not discussed since the proper choice of materials and processing steps is felt to be the governing factor.

Abstract No. 21

An Approach for Meeting Future Needs of Electronic Components

A. A. Lawson, Melpar Inc., Alexandria, Va.

The purpose of this paper is to stimulate an interest in the future needs of electronic components. Construction and production techniques are considered, as are materials, smaller components, and the setting up of a program of standardization. Various factors which concern the "component user," the "component assemblers," and the "component manufacturer" are discussed. In conclusion, an approach to setting up pertinent factors for advance planning is presented.

ELECTRONICS—LUMINESCENCE

Abstract No. 22

Electroluminescent and Field Effects in Phosphors

H. F. Ivey, Research Lab., Lamp Div., Westinghouse Electric Corp., Bloomfield, N. J.

(No abstract received)

Abstract No. 23

Effect of Electron Traps on the Brightness Waveform of Electroluminescent ZnS:Cu

F. F. Morehead, Jr., Lamp Development Dept., Lamp Div., General Electric Co., Nela Park, Cleveland 12, Ohio

Experiments performed on ZnS:Cu electroluminescent powders embedded in a slightly conducting medium suggest that a field applied in one direction ionizes electrons from emission centers, displacing them to another part of the crystallite. Removal of the field permits only a small fraction of the displaced electrons to recombine (with light emission). Application of a field in the opposite direction accelerates the release of the displaced electrons from traps and their subsequent recombination. If the opposite field rises linearly with time (sawtooth), the resulting light emission rises to a maximum at a particular voltage and then falls as the supply of trapped electrons is exhausted. Variations of the voltage of the maximum with temperature and frequency gives values of trap depth and extension in space in good agreement with general theory if the traps are assumed to be coulombic rather than square wells.

Abstract No. 24

Field Enhancement of X-Ray Excited Luminescence in ZnS.CdS:Mn(Au)

Georges Destriau, Faculté des Sciences, Université de Paris, Paris, France; consultant, Lamp Div., Westinghouse Electric Corp., Bloomfield, N. J.

Electric fields enhance the x-ray excited luminescence of ZnS.CdS:Mn. It has been found that gold additions generally improve the enhancement ratio of such materials (the enhancement ratio is the ratio of the permanent brightness obtained with the field acting to that with the field removed). This action of gold depends on the firing temperature. Composition and firing temperature have been varied in order to obtain the maximum x-ray excited output with field acting.

Abstract No. 25

Characteristics of Electroluminescence at Audio Frequencies

R. M. Rulon and F. Koury, Sylvania Electric Products Inc., Salem, Mass.

Measurements have been made on electroluminescent lamps, in which the phosphor is imbedded in a ceramic dielectric, for voltages up to 1500 and for frequencies between 60 cycles and 10 kc/sec. The effect of various parameters on brightness, current, and wattage is reported.

Abstract No. 26

Electrocathodoluminescence

P. M. Jaffe, Research Dept., Westinghouse Electric Corp., Bloomfield, N. J.

The application of alternating electric fields to certain cathode ray excited ZnCdS:Mn phosphors causes the cathodoluminescence to be enhanced. Total light output (field plus cathode rays) exceeds the sum of the electroluminescence and the cathodoluminescence. Enhancement is a function of the strength and frequency of the applied field, the beam current density, and accelerating potential. There are indications that the cell thickness plays an important role in determining whether quenching is also present.

Abstract No. 27

AC Conductivity Measurements on CdS Crystals under Various Types of Illumination

S. Jaffe, H. Kallmann, B. Kramer, and G. M. Spruch, Physics Dept., New York University, Washington Square New York, N. Y.

Under strong illumination CdS crystals exhibit huge changes in capacitance and dissipation factor under various conditions of exciting radiation. They have been measured with impedance bridges and frequencies up to 100 kc under equilibrium and nonequilibrium conditions (rise and decay of photoconductivity). Two types of electrode arrangements were used in order to eliminate barrier layer effects: (*a*) transparent gold electrodes evaporated directly on the crystals, and (*b*) Mylar sheets (transparent, Al on one side) on each side of the crystal.

With gold electrodes, two classes of crystals are found. One group shows very little change in equivalent parallel capacitance as the conductivity increases, while the other shows a considerable capacitance increase with increasing conductivity. Using Mylar insulated crystals, as the exciting intensity is increased the measured capacitance increases monotonically, while the dissipation factor goes through a maximum. The equivalent parallel capacitance of the crystal itself can be calculated and is found to increase with increasing intensity.

The effect of additional infrared irradiation as well as the effect of the applied voltage is reported.

Abstract No. 28

Action of Temperature on the X-Ray Electroenhancement Effect

J. Mattler, Faculté des Sciences, Université de Paris, Paris, France

The sustained enhancement of luminescence of certain sulfide phosphors irradiated with x-rays and simultaneously submitted to alternating electric fields varies with temperature. For (Zn, Cd)S:Mn the enhancement factor increases regularly as the temperature increases from −155° to +120°C, slowly at low temperatures, strongly at high temperatures. Brightness waves obtained with pulsed x-rays and field enhancement show no modification with temperature. Temperature acts differently on the electroluminescence of the same sulfides; this suggests a different action of the field in the two phenomena.

Abstract No. 29

Thin Film Phosphors

L. R. Koller, Research Lab., General Electric Co., Schenectady, N. Y.

Thin transparent films of phosphors have been prepared by evaporation of commercial powder phosphors *in vacuo*. Luminescent Ag- and Cu-activated films were formed by a two-step process involving heat treatment in gaseous atmospheres subsequent to deposition. Mn-activated films were formed by a single-stage process and did not require any treatment subsequent to deposition. The brightness of these films under cathode ray excitation is about ⅓ of that of the powder from which they are made.

Abstract No. 30

Diffusion of Excitation in CdS Crystals

H. Kallmann, B. Kramer, and A. Orenstein, Physics Dept., New York University, Washington Square, New York, N. Y.

The large photoconductivity observed in CdS crystals is due to the motion of free electrons. If a long crystal with electrodes at one end is illuminated on a small area remote from the electrodes, strong photoconductivity is obtained even if the illuminated area is 1 cm away from the electrodes. Rise time at this distance, dependence of conductivity on distance, and wave length indicate that this conductivity comes about through a diffusion of excitation energy from the illuminated area rather than by reflected, scattered, or fluorescent radiation.

If infrared is added in the previous experiment on a small area, quenching is observed. The amount of quenching is almost independent of the position of the infrared illuminated area whether it is between the visible light and the electrodes or on the side away from the electrodes.

Abstract No. 31

Variations of the Fermi Level in ZnS Phosphors Contaminated with Iron Family Impurities

N. Arpiarian, Laboratoire de Luminescence de la Faculté des Sciences de Paris, Paris, France

Iron family impurities are generally considered as killers. However, in some conditions of concentration and temperature they can have an intensifier effect. This effect is described in ZnS(A, K), where A = Cu or Au, K = Fe, Ni, Co, and explained by introducing a variable Fermi Level in the forbidden band. The Fermi Level shows itself particularly in the ZnS(Au, Co) phosphors. It rises with decreasing temperature in any case, and with increasing Co concentration.

Abstract No. 32

Investigations in $CuGaS_2$-ZnS and $AgGaS_2$-ZnS Systems

E. F. Apple, Research Lab., General Electric Co., Schenectady, N. Y.

$CuGaS_2$ and $AgGaS_2$ have structures closely related to zinc-blende. $CuGaS_2$ and ZnS form a series of solid solutions over the entire range. Emission under 3650 Å excitation shifts from green to red with increase in $CuGaS_2$ concentration. Samples with more than 20 mole % $CuGaS_2$ do not emit at room temperature, whereas at −195°C, fairly bright luminescence is observed. $AgGaS_2$ is soluble in ZnS to about 5–10 mole %, above which separation of Ag_2S is observed. Emission under 3650 Å excitation shifts from the blue (0.01% $AgGaS_2$) to yellow (10% $AgGaS_2$).

Abstract No. 33

Energy Storage and Decay in Various Phosphors

H. Kallmann and E. Sucov, Physics Dept., New York University, Washington Square, New York, N. Y.

The rise curve method of Kallmann and Spruch has been applied to the determination of lifetime distribution of trapped electrons in various phosphors. Comparison of rise curve deficiency areas with areas under curves of decay of phosphorescence indicates that, for most phosphors, the recombination process is completely radiative. Comparison with areas under stimulation curves indicates that even when the phosphorescence decay process is completely radiative IR causes nonradiative transitions. A stimulable phosphor is distinguished from other phosphors not by the difference in the number of traps but by the fact that IR induces predominantly radiative recombinations of trapped electrons, while in other phosphors IR induces nonradiative transitions. Since substances with practically no phosphorescence or stimulation store large numbers of electrons for long periods of time, this lack of phosphorescence and stimulation is not due to lack of traps but to the overwhelming effect of nonradiative transitions.

Abstract No. 34

Luminescence of 'Self-Coactivated' ZnS:Cu

M. H. Aven and R. M. Potter, General Electric Co., Nela Park, Cleveland, Ohio

ZnS:Cu has been prepared which shows only a simple orange emission band. The results of others who found blue or yellow emission bands are ascribed to impurities. The effect of oxygenous impurities on ZnS:Cu was investigated. When ZnS:Cu was quenched to room temperature from 600°C or higher, an unstable green fluorescence was found in place of the normal orange. Also, ZnS:Cu fired under strongly reducing conditions was found to develop a stable green emission. Models for the orange and green centers are proposed which explain experimental results.

Abstract No. 35

Process of Light Stimulation in ZnS Phosphors

H. Kallmann, W. Schneider, and M. Sidran, Physics Dept., New York University, Washington Square, New York, N. Y.

Sucov has shown that stimulability is caused by the predominance of radiative over nonradiative recombinations produced by infrared. Decay of stimulated light, while IR is applied, is very similar to that of phosphorescent decay and follows a $C/(a + t)^n$ law with n close to one during the first part of the decay; later n approaches two. Such a smooth decay is observed only with newly excited samples; if the material is partially exhausted either by natural decay or by preceding IR irradiation, the decay of stimulation shows first an increase, goes through a maximum, and only thereafter decays as above. The more the sample is exhausted the later

the maximum occurs; the stronger the IR, the earlier it appears. Newly excited samples, even if their excitation is weak, show no maximum. A theory is presented which explains these features. It is based on the existence of two activators, one with very high radiation recombination probability, the other with a much smaller one. Thermal interactions and those produced by IR between these activators explain the above described effects.

Abstract No. 36
Energy Transfer and Sensitization in Single-Crystal Phosphors

R. Leach, Dept. of Physics, The University, Hull, U. K.

An experimental study is made of the luminescence characteristics of single crystals of fluorite activated by Ce^{3+} and Mn^{2+} ions, with particular reference to energy transfer between the two activators. Previous results of Ginther for such phosphors in powder form are confirmed, but new evidence on transfer processes is provided by quantitative measurements of absorption bands, yielding oscillator strengths, and of fluorescence life times. In addition, experiments are made on diffusion of activators into fluorite at relatively low temperatures, approximately 600°C. Results indicate association of activators rather than random dispersal as previously assumed.

Abstract No. 37
Some Aspects of Quenching of Fluorescence in Organic Liquids

M. Furst and H. Kallmann, Physics Dept., New York University, Washington Square, New York, N. Y.

The additivity of different solutes in producing self-quenching, and the ability of a solvent to transfer energy to a solute in fluorescent solutions are investigated. Solutes with different chemical structures but similar fluorescence efficiency and wave lengths of absorption and emission are found to behave independently in the solution so that no combined self-quenching occurs under high energy excitation. Mixtures of solutes with related chemical structures are also investigated. Experiments on characteristics of solvents which transfer energy efficiently or poorly are described. They show that higher levels of excitation are more easily quenched in solvents which transfer poorly.

Abstract No. 38
Infrared Photography with the Help of Various Inorganic Phosphors

H. Kallmann and J. Rennert, Physics Dept., Institute of Mathematical Sciences, New York University, Washington Square, New York, N.Y.

Inorganic phosphors are capable of storing excitation energy or electrons. These stored electrons can be released or made to recombine by IR irradiation. If a previously excited phosphor is illuminated with u.v., its fluorescence at the beginning is larger than that of the not pre-excited phosphor. To make IR pictures, the phosphor is pre-excited, then illuminated with the IR radiation to be depicted. The areas struck by IR radiation have less trapped electrons than the other areas. These areas can be made visible or permanently recorded by irradiating the sample after IR exposure with u.v. or with IR radiation (if it produces radiative recombinations). In this way it was possible to make IR pictures with IR radiation of 2.5 μ. Pre-irradiation can precede, and the radiation which makes the picture visible can follow the IR exposure by weeks.

Abstract No. 39
Time Constants of Alpha- and Electron-Produced Light Flashes

G. Brucker, Signal Corps, Camp Evans, N. J., and H. Kallmann, Physics Dept., New York University, Washington Square, New York, N. Y.

So-called time constants of various organic and inorganic materials are presented. They range from 3 to 100 $\times$ 10^{-9} sec. There is some correlation between strength of absorption for the organic materials and time-constants. The latter are the same for α and electron excitation. No indication of long time emission was observed; if such emission exists, it must be of small amplitude. The ratio of efficiencies for α and electron excitation is approximately the same for all investigated material in spite of the fact that they differ in time-constants and efficiencies tremendously. These findings indicate that quenching due to high density of excitation is a very fast process, faster than the shortest light emission process. A theory which explains these effects is presented; it is based on the migration of the excitation energy out of the excitation channel.

Abstract No. 40
Resolution of Thermoluminescence Curves

C. H. Haake, Research Dept., Westinghouse Electric Corp., Bloomfield, N. J.

The resolution of thermoluminescence curves is discussed analytically. With a given difference of trap depths, the only variable which may be used to change the resolution is the heating rate. The mathematical expression for the resolution with increasing heating rate shows two competing processes: (*a*) increasing separation of two neighboring glow peaks, and (*b*) increasing halfwidth of the peaks. The latter predominates in all cases and resolution can be enhanced only by decreasing heating rates.

Abstract No. 41
Potential Energy Curves for Phosphors

K. H. Butler, Sylvania Electric Products Inc., Salem, Mass.

A method of calculating potential energy curves of activator ions in phosphors from the emission and excitation spectra is described. Calculated curves for some alkali halide phosphors and for some orthophosphate phosphors are discussed.

Abstract No. 42
A Review of the Measurement of the Quantum Efficiency of Inorganic Phosphors

J. Tregellas-Williams, Research Lab., General Electric Co., Ltd., Wembley, England

Various methods of measuring the quantum efficiency of phosphors have been used in the past; these include absolute light measurement, a substitutional method, derivation from lamp efficiencies, and a calorimetric method. These are described and the results discussed and compared with those derived from original work on the lamp efficiency method and a modified microcalorimeter. A summary of published and unpublished values of quantum efficiency is appended.

Abstract No. 43
Temperature Characteristics of Phosphors for Use in High Pressure Mercury Vapor Lamps

A. H. McKeag, Research Labs., General Electric Co., Ltd., Wembley, England

This paper gives details of the preparation of improved barium strontium lithium silicate phosphors for use in high pressure mercury vapor (H.P.M.V.) lamps and shows that temperature characteristics of these phosphors are particularly sensitive to conditions of preparation. Color corrected H.P.M.V. lamps made with these improved phosphors show an appreciable improvement in color rendering properties. Other phosphors for use in H.P.M.V. lamps are also considered.

Abstract No. 44
Temperature Dependence of Fluorescence

R. W. Mooney, Sylvania Electric Products Inc., Towanda Pa.

Equipment for measuring the temperature dependence of fluorescence with excitation either by 2537 or 3600 Å radiation is described. Results on various phosphors including zinc-modified orthophosphates are discussed.

Abstract No. 45
Gray Discoloration in Calcium Halophosphates

W. L. Wanmaker and M. G. A. Tak, Philips Research Labs., N. V. Philips Gloeilampenfabrieken, Eindhoven, Netherlands

Calcium halophosphates can assume a light gray color when refired at 500°-600°C both in air and in a reducing atmosphere. The gray color due to oxidation is more pronounced in the presence of alkali, and occurs in practice during the baking process (removing of organic binder) of fluorescent lamps. The gray color due to reduction is observed during the evacuation of the fluorescent lamp coated with calcium halophosphate. The influence of the presence of Na and Al on the discolorations found is discussed and a theory of the observed phenomena is given.

Abstract No. 46
Cerium-Activated Halophosphate Phosphors

S. T. Henderson and P. W. Ranby, Thorn Electrical Industries Ltd., 52-56 Lawrence Rd., Tottenham, N. 15, England, and Great Cambridge Rd., Enfield, Middlesex, England, respectively

This paper describes the characteristics of a new group of alkaline earth halophosphate phosphors activated by Ce and Mn, and contrasts their behavior with that of halophosphates containing other primary activators. In their preparation, these Ce-activated materials show marked differences from other previously known halophosphates, but the luminescent properties are similar to those of the tin-activated system. The behavior and possible uses of these phosphors in fluorescent lamps are described.

Abstract No. 47

Luminescence of Tin-Activated Strontiumorthophosphate

H. Koelmans and A. P. M. Cox, Philips Research Labs., N. V. Philips' Gloeilampenfabrieken, Eindhoven, The Netherlands

The introduction of Al, Zn, Mg, Ca, or Cd in $Sr_3(PO_4)_2$ produces a new crystal phase which is probably isomorphous with $\beta Ca_3(PO_4)_2$. Activated with tin this Sr-orthophosphate gives a strong luminescence with a maximum at about 6300 Å under excitation with λ2537 Å.

Abstract No. 48

Zinc Modified Orthophosphate Phosphors

M. J. B. Thomas and K. H. Butler, Sylvania Electric Products Inc., Salem, Mass.

The preparation, properties, and uses of tin-activated calcium and strontium orthophosphate phosphors, modified by replacement of a portion of the alkaline earth metal by zinc, are described. The effect of varying composition on emission and excitation spectra is discussed.

Abstract No. 49

Transition Probability Ratios in KCl:Tl and KCl:In

F. E. Williams, P. D. Johnson, and B. Segall, Research Lab., General Electric Co., Schenectady, N. Y.

Transition probability ratios for the principal impurity absorption bands of KCl:Tl and KCl:In were calculated including the effect of crystal interactions. The excited states are assumed to have the character of $^1P_1^0$ and $^3P_1^0$ states of the sp configuration. In the formulation, the spin-orbit interaction is applied after the crystal interactions. Experimental transition energies for the crystal, rather than for the free ion, are used in the calculation. Satisfactory agreement with experiment is found.

Abstract No. 50

Shape of the F-Band in KCl

J. J. Markham and J. D. Konitzer, Zenith Radio Corp., Chicago, Ill.

In recent years detailed theories of the shape of optical absorption bands in solids have been developed. One has been unable to check these with experiments due to the lack of detailed data. The shape of the F-center in KCl at 300°K, 195°K, 78°K, and 5°K has been measured and a comparison has been made. Results are presented.

Abstract No. 51

Interaction of Color Centers in the Alkali Halides

W. D. Compton and John Lambe, U. S. Naval Research Lab., Washington, D. C.

A study of the interaction among various color centers of the alkali halides has been made. The following experimental observations have led the authors to postulate such an interaction: (*a*) If F-centers and M- or R_1-centers were present in the crystal, excitation in the F-band gave emission that was characteristic of the M- or R_1-centers but not of the F-center. (*b*) Excitation with polarized F-light gave polarized M- or R_1-emission. (*c*) Irradiation with polarized F-light produced dichroism in the F, M, R_1, and R_2-bands. (*d*) Excitation in the R_2-band of NaCl gave emission characteristic of the R_1-center.

Abstract No. 52

Luminescence of Color Centers

John Lambe and W. D. Compton, U. S. Naval Research Lab., Washington, D. C.

A study has been made of the luminescent properties of F-, M-, and R-centers in alkali halide crystals. Special emphasis was placed on the symmetry properties of these centers. In order to investigate this, the luminescent center is excited with polarized light and the resulting emission is analyzed for polarization. These measurements can then be used to determine some of the symmetry properties of the luminescent center. Results thus obtained were in good agreement with current theory for the F-center and M-center. In the case of R-centers results were more complex and a simple analysis was not applicable.

Abstract No. 53

Experiments on Color Center Production in KI:Tl

H. N. Hersh, Zenith Radio Corp., Chicago, Ill.

KI:Tl has been subjected to x-irradiation on electrolysis and rendered nonstoichiometric with excess K; absorption spectra have been measured. Measurements show that the addition of TlI to KI decreases the stability of the F-centers and results in more or less permanent coloration of the crystals. X-irradiation destroys the u.v. luminescence properties of the phosphor.

Abstract No. 54

Color Centers in Cadmium Fluoride

M. Rubenstein and E. Banks, Dept. of Chemistry, Polytechnic Institute of Brooklyn, Brooklyn 1, N. Y.

Single crystals of CdF_2, purified, and containing additions of NaF, CaF_2, and equimolar mixtures of NaF and CeF_3, were grown from the melt in carbon crucibles in a helium atmosphere. Transmission spectra were obtained before and after x-irradiation on slices about 1.5 mm thick, at 28°C, −78°C, and −190°C. Crystals containing 0.05–5 mole % NaF showed a radiation-induced absorption near the fundamental absorption edge, which is stable at room temperature, and an absorption stable at −190°C, which disappears between −190°C and −78°C. CdF_2, pure, or containing CeF_3 or NaF + CeF_3 in solid solution, all show only one absorption band, unstable above −10°C.

ELECTRONICS—SEMICONDUCTORS

Abstract No. 55

Compound Semiconductors

D. A. Jenny, RCA Labs., Princeton, N. J.

A review of the development and the present status of compound semiconductor research is presented followed by an outline of the practical implications. The study of compound semiconductors has contributed much to the basic understanding of semiconductors although many phenomena are still awaiting interpretation. New application areas are being opened up by the unusual properties of some recently discovered compounds, and at least one of the new compound materials is a potential competitor of Ge and Si.

Abstract No. 56

New Semiconductors

J. H. Wernick and K. E. Benson, Bell Telephone Labs., Murray Hill, N. J.

(No abstract received)

Abstract No. 57

Carrier Transport Phenomena in Germanium Bicrystals

H. F. Mataré and B. Reed, Research Lab., Tung-Sol Electric, Inc., 200 Bloomfield Ave., Bloomfield, N. J.

Medium angle grain boundaries (tilt angle between 5° and 25°) were grown from bicrystal seeds to study electrical properties of such interfaces. It is assumed that impurity diffusion or segregation at the interface is less important for these angles of misfit than the dangling bonds. Differential resistivity and lifetime of minority carriers show a strong influence of the sheet arrangement of dangling bonds with their energy level near the middle of the band gap.

Abstract No. 58

Photosensitivity of Ge Grain Boundaries

O. Weinreich and H. F. Mataré, Research Labs., Tung-Sol Electric, Inc., 200 Bloomfield Ave., Bloomfield, N. J.

Grain boundaries in Ge form a *P*-type region. One means of investigating potential jumps set up in grain boundaries consists of measuring the photovoltaic effect. If a light beam approaches the grain boundary, an increasing photovoltage is measured which then decreases and drops to zero when the position of the beam is approximately symmetric across the boundary. After crossing the boundary, the polarity of the emf is reversed. Results of the spectral response and temperature dependence are reported and will be discussed.

Abstract No. 59

Growth and Definition of Bicrystals

R. Wegener and H. F. Mataré, Research Lab., Tung-Sol Electric, Inc., 200 Bloomfield Ave., Bloomfield, N. J.

The investigation of electrical properties of grown boundaries gave impetus to the growth of the bicrystals to be discussed. The possible definition of bicrystals in terms of the lattice directions of one member and with respect to the grain boundary is discussed. For symmetrical configurations, the limiting range of unique combinations is given. Methods for seed orientation and preparation are described. Variations necessary in procedure to achieve desired precision limits of bicrystals are discussed.

Abstract No. 59A

Dissociation Pressure and Cohesive Energy of Indium-Phosphide

K. Weiser, RCA Labs., Princeton, N. J.

(No abstract received)

Abstract No. 60

Impurity Diffusion in Germanium and Silicon

M. Tanenbaum, Bell Telephone Labs., Inc., Murray Hill, N. J.

Studies of the diffusion coefficients of Group III and Group V impurities have shown that, for a wide range of concentrations of semiconductor interest,

diffusion coefficients of impurities are independent of concentration and have well-defined activation energies. Recent studies of these diffusion coefficients as a function of temperature are discussed and values obtained by various investigators are presented. Diffusion mechanisms are also discussed. Solutions of the diffusion equation for some of the boundary conditions of interest are to be presented. Selected device applications are discussed to demonstrate how the impurity distribution peculiar to diffusion processes affects device parameters.

Abstract No. 61

Effects of Heat Treatment on Silicon Diffusion-Created Devices

C. Levi and I. Weiman, Pacific Semiconductors Inc., 10451 W. Jefferson Blvd., Culver City, Calif.

This paper discusses the dependency of diffusion device characteristics on bulk lifetime with particular emphasis on lifetime changes occurring during the diffusion process heat treatment. Results of experimental work are correlated with theory. Diode parameters such as recovery time and forward currents are found to follow predicted relationships. Reverse saturation currents appear to be dependent on changes other than lifetime.

Abstract No. 62

Oxygen as Impurity in Transistor Grade Silicon

W. Kaiser and P. H. Keck (Present address: Sylvania Electric Products Inc., Bayside, N. Y.), Signal Corps Engineering Labs., Fort Monmouth, N. J.

The oxygen content of pulled Si crystals is correlated with the infrared absorption band at 9 μ. Diffusion of oxygen out of and into a liquid zone of Si was studied under a variety of experimental conditions. In vacuum, in a hydrogen or in an inert gas atmosphere, oxygen leaves the melt rapidly while an increased 9 μ absorption is found after the melt was kept in contact with an oxygen atmosphere or a SiO_2 surface for a short time.

Abstract No. 63

Ternary Distribution Coefficients in Silicon*

David Navon, Transitron Electronic Corp., 168-182 Albion St., Wakefield, Mass.

The doping effect of impurities introduced into Si by a carrier metal is of interest in producing alloy contacts. One can redefine the distribution coefficient to apply to these ternary systems. Values for this coefficient are presented for donor and acceptor impurities introduced into Si at different temperatures by a carrier metal. They are, in general, smaller than the normal coefficients for impurities such as Sb, As, and Ga.

* This work was supported by the U. S. Signal Corps under contract No. DA-36-039-sc-72714.

Abstract No. 64

Evaporation and Alloying of Metals to Silicon

J. M. Goldey, M. Tanenbaum, and N. Holonyak, Jr. (now on military leave with the U. S. Army Signal Corps), Bell Telephone Labs., Inc., Murray Hill, N. J.

A general discussion on the several aspects of evaporating and alloying of contacts to Si is presented. The Al-Si system is described in some detail. Preparation of materials and the degree of vacuum found satisfactory are mentioned. A brief discussion of outgassing of the Si substrate, masking and heating of the substrate, and evaporation on substrates at different temperatures is given. Procedure of alloying evaporated materials for Si is described.

Abstract No. 65

Transistor-Grade Silicon, I. Preparation of Ultrapure Silicon Tetraiodide

Bernard Rubin, G. H. Moates, and J. R. Weiner, Radiochemistry Section, Components and Techniques Lab., Air Force Cambridge Research Center, Air Research & Development Command, Bedford, Mass.

A stepwise method of preparing and purifying SiI_4 has been found, involving the direct combination of the elements, recrystallization of the product, followed by sublimation and zone purification steps. Values of the segregation coefficients of several impurity elements have been determined to concentrations of less than one part of impurity per billion parts of SiI_4 in 60 passes, using a 50 cm length charge.

Abstract No. 66

Transitor-Grade Silicon, II. Zone Purification of Silicon Tetraiodide

G. H. Moates and Bernard Rubin, Radiochemistry Section, Components & Techniques Lab., Air Force Cambridge Research Center, Air Research & Development Command, Bedford, Mass.

Effective segregation coefficients of various impurities determined from a study of zone melting of SiI_4 are given. The apparatus and technique employed are discussed, and limiting equilibrium conditions are defined. The significance of the results is illustrated by calculation of ultimate distribution profiles. Effects on the effective coefficient of velocity of crystallization, diffusion coefficient, and convection are discussed. Yield of purified SiI_4 is related to K_{eff}, charge length, zone length, and initial concentration.

Abstract No. 67

Paper withdrawn

Abstract No. 68

Contribution to the Floating Zone Technique for Refining Silicon

E. Buehler, Bell Telephone Labs., Inc., Murray Hill, N. J.

A recycling automatic floating zone apparatus for Si has been assembled. Features of this equipment such as the mechanical drive, the control panel, and a self-stabilizing r.f. heating circuit are described. Single-crystal Si of 16,000 ohm-cm and 1500 μsec lifetime has been produced in the apparatus. Results on the evaluation of raw material, lifetime degradation produced by heating, and the effects of the process variables during refining are described.

Abstract No. 69

Heat Treatment of Silicon Using Zone Heating Techniques

H. C. Theuerer, J. M. Whelan, H. E. Bridgers, and E. Buehler, Bell Telephone Labs., Inc., Murray Hill, N. J.

New insight into the mechanism for changes in Si with solid-state heat treatment has been obtained with the aid of the floating zone apparatus normally used to refine Si. Through the use of this technique, it has been established that contaminants left on the Si surface even after careful etching and washing procedures are a controlling factor in the observed heat treating effects.

Abstract No. 70

Optical Measurement of Film Growth on Silicon and Germanium Surfaces in Room Air

R. J. Archer, Bell Telephone Labs., Inc., Murray Hill, N. J.

The rate of growth of films, presumably oxide films, on polished Si and Ge surfaces in room air following a HF rinse was determined by measuring the ellipticity of reflected polarized light. Film thickness vs. log time plots are linear after about 10^4 sec with slopes of 6.8Å/decade (Si) and 8.1Å/decade (Ge). Immediately after the HF rinse the films are 10–15Å thick. After one day in air they are 25–30Å thick.

Abstract No. 71

Bonding Material for Making Contacts to Etched *P*-Type Silicon

D. R. Mason and J. C. Sarace (Present address: Dept. of Chemical and Metallurgical Engineering, University of Michigan, Ann Arbor, Mich.), Bell Telephone Labs., Inc., Murray Hill, N. J.

Mo clad on one side with Al has been used to form structurally sound ohmic contacts to etched p-type Si wafers containing p-n junctions. The desired Al-Si solid solution can be formed before a substantial amount of Al reacts irreversibly with the Mo. Coefficients of expansion are sufficiently well compensated so that the wafer does not crack during fabrication. Damaged wafers almost invariably result when structural sections of Al are used.

Abstract No. 72

Description of Electrochemical Jet Etching of Silicon

Albert Mark, Signal Corps Engineering Lab., Fort Monmouth, N. J.

Electrolytic jet etching of Si is described and factors effecting etching action are discussed. Geometry of cavity is approached from a fluid dynamic point of view. Cavities made with laminar flow and tubulent flow are shown to differ in terms of the velocity distribution of stream at moment of impact with a Si wafer. Extremely flat bottom cavities are made by employing the least distorted cross section of a flattened parabolic liquid stream. A new versatile laboratory jet apparatus is shown.

Abstract No. 73

Mechanism of Electrolytic Rectification

P. F. Schmidt, Research Div., Philco Corp., Philadelphia 34, Pa.

At voltages below forming voltage, the current in the anodic direction is

blocked by the space charge of electrons getting trapped in the oxide. At very high fields, avalanche breakdown occurs in localized spots. Essentially the same picture is true in the cathodic direction except that here protons penetrate into the oxide, neutralizing the negative space charge, and thus permitting continuous current flow. Experiments in electrolytes not containing protons support this view.

ELECTRONICS—THERMIONIC CATHODES

Abstract No. 74

Recent Work on Surface Properties of Oxide Semiconductors

J. J. Lander, Bell Telephone Labs., Inc., Murray Hill, N. J.

(No abstract received)

Abstract No. 75

Thermionic Emission Characteristics of Thoriated Rhenium*

W. E. Nexsen, Jr., and G. B. Gaines, Battelle Memorial Institute, Columbus, Ohio

Preliminary investigations show that thoriated rhenium behaves very similarly to thoriated tungsten as far as thermionic emission is concerned. Emission from the two, when put through a similar processing and activation schedule, is of the same order of magnitude, that is, many orders of magnitude larger than from the pure metal. Thoriated rhenium activates at a lower temperature than thoriated tungsten, indicating a larger diffusion coefficient for thorium through rhenium than for thorium through tungsten.

* Sponsored in part by The Air Force Cambridge Research Center.

Abstract No. 76

Thermionics and Evaporation Properties of Some Lanthanide Oxides

D. L. Schaefer, Power Tube Dept., General Electric Co., Schenectady, N. Y.

The following properties of lanthanum oxide, neodymium oxide, samarium oxide, and gadolinium oxide have been measured: (*a*) the thermionic work function and Richardson's constant for the oxides on tantalum base metal; (*b*) evaporation rates of the oxides and the activation energies for evaporation; (*c*) the minimum thermionic work function of the evaporant on a tungsten collector as well as the stable value which is reached when many times the minimum value has been collected.

Measured properties for each of the oxides are very similar, lanthanum oxide showing the greatest difference. Thermionic work functions are in the range of 2.9–3.2 e.v.; Richardson constants fall between 30 and 55, and activation energies for evaporation are between 6.8 and 7.4 e.v.

Abstract No. 77

Emission from Barium on Tantalum Carbide

J. E. White, Electronics Lab., General Electric Co., Syracuse, N. Y.

Refractory carbides have been used to a limited degree as emission-suppressing contings on grids in power tubes. Suppression of emission occurs because the monolayer of emissive material, such as Th or Ba, which ordinarily produces grid emission, dissolves into the carbide. The work to be described constitutes a systematic investigation of absorption and evaporation of Ba from one of the interesting carbides, and demonstrates that considerable thermionic densities can be obtained from TaC saturated with Ba.

Abstract No. 78

Preparation and Properties of the Magnesium Oxide Cold Cathode

Dietrich Dobischek, Evans Signal Lab., Fort Monmouth, N. J.

(No abstract received)

Abstract No. 79

Reactions of Oxide Cathodes with Gases at Low Pressures

R. J. Ruka and E. A. Gulbransen, Research Labs., Westinghouse Electric Corp., Pittsburgh, Pa.

Recent experimental work by Wagener and others has shown quantitatively that a relation exists between low pressures of certain gases and the electron emission in oxide cathode systems. A thermochemical analysis is made for the reactions of H_2O, O_2, CO, OH, SO_2, CO_2, and H_2 and compared with their reported action on the "poisoning" of "activation" of oxide coated cathodes. The possible role of negative ions is discussed.

Abstract No. 80

The Electron Microscopy of Alkaline Earth Carbonates*

C. F. Tufts, Research Labs., Sylvania Electric Products Inc., Bayside, N. Y.

An adaptation of the carbon replica technique has been developed which: (*a*) retains true specimen geometry by eliminating destructive dispersion manipulations during specimen preparation; (*b*) reveals size, shape, and surface geography to less than 100Å, permitting precise determination of both aggregate and single particle geometry; (*c*) furnishes a qualitative indication of the degree of crystal perfection for single particles; (*d*) serves as a monitor of interpretation for B.E.T. and Fisher Sub-Sieve size data.

* Supported in part by U. S. Navy Contract NO bs 8023.

Abstract No. 81

Relationship between Thermal Decomposition in Vacuum and Macrostructure of Alkaline Earth Carbonates*

B. Wolk and J. G. Buck, Research Labs., Sylvania Electric Products Inc., Kew Gardens, N. Y.

The control of quality in electronic tubes processed by production equipment depends on numerous factors. Among these factors are those involving time and temperature conditions for effective conversion of the cathode coating from the carbonate to the emitting oxide. A technique is described for evaluating relative thermal decomposition properties of different cathode carbonates under simulated tube processing conditions. Various observations on the relationship between the macrostructure of cathode carbonates and the thermal decomposition behavior are described.

* This work was supported by U. S. Navy Contracts NOBs 5369 and NOBs 8023.

Abstract No. 82

Study of the Interface Impedance Characteristics of Seven Commercial Cathode Nickel Alloys

C. D. Richard, Jr., and A. M. Bounds, Superior Tube Co., Norristown, Pa.

Measurements of interface impedance were made on 6BC8 tubes at several points during a 2000-hr accelerated life test. A comparison is made between heats of varying Si content from seven different commercial cathode Ni alloys. An attempt is made to show the variation between heats and to rate the alloys with respect to interface impedance buildup. A preliminary conclusion is that the tube structure and processing history are at least as important in the development of interface impedance as the composition of the cathode Ni alloy and its coating.

Abstract No. 83

Considerations of Oxide Cathode Interface Impedance

A. P. Haase, R. E. Holmes, and F. J. Schmidt, General Electric Co., Owensboro, Ky.

Interface-impedance effects have been observed under a number of operating conditions in a modern computer tube. A comparison of interface-impedance formation rates under these conditions is made and problems associated with the measurement of short time-constant interface impedances are discussed.

Also reported are typical interface-impedance formation characteristics of commonly used cathode alloys as measured in a triode-testing vehicle under varied operating conditions.

Abstract No. 84

A Study of the Molded Nickel Cathode

C. P. Hadley, W. G. Rudy, and A. J. Stoeckert, Tube Div., Radio Corp. of America, Lancaster, Pa.

Research work on the molded nickel cathode is described. Results are given regarding the effects on emission and life of variations in nickel powder, alkaline-earth-carbonates, reducing agents, sintering, and activation. Data on pulsed emission are presented and results are compared with those of previous workers.

Abstract No. 85

New Developments in the L-Cathode

C. A. M. van den Broek and A. Venema, Philips Research Labs., Eindhoven, Netherlands

A disadvantage of the original L-cathode with a (Ba, Sr)CO_3 filling is the generation of CO_2 during processing, which causes oxidation of the porous W. Also, in some cases a need exists for a lower evaporation rate of the alkaline earth metals and oxides.

With a filling of a pressed mixture of alkaline earth aluminates and a reducing agent (e.g., W) considerable improvement both in the gas production during processing and in the amount of evaporated material has been obtained.

ELECTRONICS—INSTRUMENTATION

Abstract No. 86

Equipment for the Autographic Determination of the Electrical Resistance of Metals at High Temperatures

G. A. Moore, National Bureau of Standards, Washington, D. C.

Recent extensions of metallurgical interests necessitate precise knowledge of numerous solid-state reactions not always conveniently observed by traditional methods. The change of electrical resistivity with temperature is both an important fundamental property and a valuable tool for observing certain reactions within metals.

The high sensitivity apparatus described autographically records the changing electrical resistances of a wide variety of metallic specimens while in vacuum or protective atmosphere and automatically carried through appropriate temperature cycles.

Abstract No. 87

Methods of Measuring High Resistances*

E. F. Turner, Jr., George Washington University, Washington, D. C.

A discussion is presented on basic methods of measuring resistance, pointing up the special problems encountered in the range of 10^{12}–10^{16} ohms. A continuous measuring instrumentation is described, and compared with the Wheatstone Bridge. Data on the resistivities of several commercial plastics obtained by the two methods are given.

* Work done at the Naval Research Laboratory, Washington, D. C.

Abstract No. 88

Calibration of Kinescope Test Sets for Color Balance and Light Output

G. P. Kirkpatrick and A. E. Hardy, Tube Div., Radio Corp. of America, Lancaster, Pa.

The routine calibration of color kinescope test sets for color balance and light output is achieved by means of spectroradiometrically calibrated kinescopes. The operation of these kinescopes is checked by means of a three-filter colorimeter. Details of the calibration techniques are discussed.

Abstract No. 89

Interferometric Calibration of Kinescope Aliminum Film Thickness Meters

G. P. Kirkpatrick and T. A. Saulnier, Tube Div., Radio Corp. of America, Lancaster, Pa.

The application of multiple-beam interferometry to the calibration of aluminum-film-thickness meters used to monitor aluminized kinescope screens is discussed. Comparison of interferometrically observed and calculated values of aluminum thicknesses indicates that the calculations are reliable in the range of 1300 to 5000 A.U., provided care is exercised in the preparation of the calibration plates. The interferometric check is far superior to that obtainable by quantitative chemical analysis. Empirical data and suggestions for further applications are included.

Abstract No. 90

An Apparatus for Vacuum and Atmospheric Differential Thermal Analysis

J. G. Rabatin and C. S. Card, Lamp Wire and Phosphors Dept., General Electric Co., Cleveland, Ohio

Apparatus described is suitable for differential thermal analysis of substances from full vacuum to 400 psi in gases such as O_2, N_2, H_2, CO_2, SO_2, H_2S, and NH_3. The atmospheric chamber housing the furnace is large enough to fire samples up to 100 g. The furnace will operate up to 1350°C.

Performance characteristics and sensitivity of DTA apparatus are reported. Applications to analysis of various substances under various pressures and gases are described.

Abstract No. 91

Application of Lead Sulfide Detector to the Study of Luminescence in the Near Infrared Region

J. M. Goldstein, W. M. McNabb, and J. F. Hazel, Dept. of Chemistry, University of Pennsylvania, Philadelphia, Pa.

Conventional fluorometers and spectrofluorometers utilize photomultiplier tubes for maximum sensitivity. In the present work an attempt was made to study luminescence to the near IR region, where photomultipliers have no response, by the utilization of lead sulfide detectors.

In the present instrument the luminescent radiation is chopped at 60 cps, amplified by a conventional amplifier, and the signal is phased by a special phasing device so that it can be fed to a conventional d-c recorder without the customary signal rectification.

Abstract No. 92

Effect of Current Drains on Cadmium Standard Cells

G. D. Vincent, Standard Cell Dept., The Eppley Lab., Inc., Newport, R. I.

Various sizes of commercial unsaturated cadmium standard cells were subjected to current drains of from 0.5 to 12 μa (0.2–23 μa/cm^2). The terminal voltages of these cells were observed for several years. The relationship between change in voltage and time is not a linear one; an approximation of the decrease is 11 μv/coulomb of current passed per reciprocal centimeter squared of electrode area.

ELECTRONICS—SCREEN APPLICATION

Abstract No. 93

Wet and Dry Strengths of Cathode Ray Screens

R. W. Spencer, N. W. McCready, and Wm. Stericker, Philadelphia Quartz Co., Public Ledger Bldg., Philadelphia 6, Pa.

In the manufacture of cathode ray tubes the dry strength of the screen has become more important because of lacquer filming before aluminizing. A method has been developed for testing dry strength which is based on the same general principles as thosed used in determining wet strength. Strictly speaking, the new method tests rewet strength. It is more reproducible than air-stream methods.

Wet and dry strengths vary independently of each other with different concentrations of potassium silicate and reactants.

Abstract No. 94

Sedimentation Volumes of a Phosphor Powder in Potassium Silicate and Potassium Silicate-Barium Acetate Settling Media

J. F. Hazel and Louis Fiorito, Dept. of Chemistry, University of Pennsylvania, Philadelphia, Pa.

A zinc sulfide-zinc cadmium sulfide phosphor was settled through aqueous solutions used in the preparation of cathode ray screens under conditions where the volume of the settled powder could be measured. The volume was decreased by low concentration of potassium silicate. The volume passed through a minimum and then increased as the concentration of silicate was increased. The presence of barium acetate in mixtures with potassium silicate increased the volume. A correlation exists between the sedimentation volume and zeta potential of the particles.

Abstract No. 95

Surface Phenomena Associated with the Application of Organic Films to Phosphor Screens

R. W. Dudding, Research Labs., General Electric Co. Ltd., Wembley, Middlesex, England

The production of aluminized screens for cathode ray tubes involves the formation of a temporary organic barrier film on the phosphor coating upon which the Al may be deposited. Defects in this film produce undesirable blemishes on the finished screen. Certain inherent defects encountered when employing a "flow" filming technique are described and the fundamental factors governing their formation and prevention are considered.

Abstract No. 96

Photodeposition of Luminescent Screens

M. Sadowsky and D. Payne, Jr., Philco Corp., Lansdale, Pa.

A description of the processes employed by the Philco Corp. in photodepositing a striped phosphor screen for color television is given. Some theories of chemical mechanisms involved in this deposition are presented. The relative importance of various parameters in the deposition is discussed.

Abstract No. 97

Phosphor Slurry Process for Color Kinescope Screening

D. J. Donahue and T. A. Saulnier, Tube Div., Radio Corp. of America, Lancaster, Pa.

In the preparation of the screen for a shadow-mask color kinescope, phosphor powders are dispersed in a photosensitive binder to form slurries. The phosphor slurries are then applied to tube assemblies by means of a spinning technique. This paper outlines general methods of preparation of the photosensitive slurries, and discusses process steps from slurry application through exposure, development, and inspection.

ELECTROTHERMICS AND METALLURGY

Abstract No. 98
High Temperature Oxidation of High Purity Nickel between 750° and 1050°C

E. A. Gulbransen and K. F. Andrew, Westinghouse Research Labs., Churchill Borough, Pittsburgh 35, Pa.

Kinetic studies have been extended to 1050°C to determine the conditions and mechanism of breakdown of the metal in oxidation. Below 900°C the metal oxidizes in the normal manner and rate data fit in well with rate relationships already established. At 900°C and higher, parabolic rate law plots of the data show increasing values of the constants with time. At 1000°C and higher, the oxide cracks away from the metal. It is suggested that nickel fails in oxidation due to a breakdown in the adhesion at the oxide-metal interface.

Abstract No. 99
Ten-Gram Levitation Melted Ingots

G. Comenetz and J. W. Salatka, Westinghouse Research Labs., Churchill Borough, Pittsburgh 35, Pa.

An account is given of experience at levitation melting and casting ingots of a number of pure metals and alloys, weighing from 6 to 13 g. The apparatus is similar to that of Polonis, Butters, and Parr. The technique seems likely to become widely used.

Abstract No. 100
Growth of Whiskers by Reduction of Halogenides

H. Wiedersich, Westinghouse Research Labs., Churchill Borough, Pittsburgh 35, Pa.

Reduction of halogenides results in a variety of growth forms of the precipitated crystals. The main forms observed are roughly equiaxed crystals with low indexed faces and "whiskers", i.e., long, thin crystals. Thermodynamic and kinetic considerations are applied to the variables which could influence the growth forms and checked with experimental results. Strong indications are found that an adsorption phenomenon makes certain crystallographic faces growth-inactive and causes whisker growth.

Abstract No. 101
Zone Melting of Uranium

C. I. Whitman, V. Compton, and R. B. Holden, Atomic Energy Div., Sylvania Electric Products Inc., Bayside, N. Y.

A study was made of the possible application of the zone melting technique to the separation of U from fission products and other impurities. Bar specimens of U having various alloying elements were zone purified in thoria-coated alumina boats. Uranium bars previously irradiated in the Brookhaven pile were also zone melted. Although zone melting did not appear promising as a method of processing irradiated U because of slagging of fission products into the surface of the bar, this technique has potential application to removing such fission products as Zr, Nb, and Ru, and to purifying ordinary U from such impurities as B, Fe, Si, Ni, and Co.

Abstract No. 102
Molybdenum Plating Inside of Large Bore Tubes

P. L. Raymond, National Research Corp., Cambridge, Mass.

The high temperature reduction of molybdenum pentachloride by H was used to deposit high purity Mo plates inside of large bore tubes. A large number of plating runs were conducted to develop the equipment and procedures and to determine the optimum operating condition. Strong adherent plates of Mo 0.004 in. thick were deposited inside of tubes utilizing equipment constructed from common engineering materials and components.

Abstract No. 103
Influence of Crystal Face on Some Electrochemical Properties of Single Crystals of Copper

A. T. Gwathmey, Dept. of Chemistry, University of Virginia, Charlottesville, Va.

Single crystals of Cu were etched in solutions of copper sulfate-H_2SO, and it was found that etching characteristics of the different faces varied with the *p*H of the solution. Measurements were made of the electrochemical potentials of the different faces in solutions of copper sulfate, and the effect on the potentials of annealing the crystals, of the nature of the gas dissolved in the solution, and of the *p*H of the solution was investigated.

Abstract No. 104
Structural and Chemical Factors Associated with the Fracture of Metals

W. D. Robertson, Hammond Metallurgical Lab., Yale University, New Haven, Conn.

Different crystal and intercrystalline imperfections are considered with respect to their role in fracture. The chemical activity of the metallic structure in the vicinity of these imperfections is discussed with respect to its significance in initiating fracture at particular structural sites.

Abstract No. 105
Influence of Structural Factors on the Corrosion of Stainless Steel

N. A. Nielsen and M. A. Streicher, Engineering Research Lab., Engineering Dept., E. I. du Pont de Nemours and Co., Inc., Wilmington, Del.

As a group, stainless steels exhibit a wide variety of corrosion phenomena which are known to be structure-dependent. Passivity, intergranular corrosion, and pitting-corrosion behavior are discussed in terms of such factors as alloy grain size and orientation, cold work, secondary-phase distribution, corrosive medium, etc., which affect the type, intensity, and localization of corrosion. These effects are demonstrated by weight loss and corrosion-rate data as well as by micrographic studies of corroded stainless steel samples.

Abstract No. 106
Role of Metal and Oxide Structures in High Temperature Oxidation Processes

C. E. Birchenall, Forrestal Research Center, Princeton University, Princeton, N. J.

The course of high temperature oxidation reactions of metals and alloys depends on the inherent properties of the metal phase and the oxide products and also on the relative values of some properties for two or more phases. Although the relative properties are most clearly associated with the early stages, especially nucleation, they play an important role in determining the soundness of the oxide layer and the metal-oxide interface in later stages of the reaction.

Abstract No. 107
Effect of Dislocations in Oxide Films on Oxidation

N. Cabrera, Dept. of Physics, University of Virginia, Charlottesville, Va.

(No abstract received)

Abstract No. 108
Interaction of Oxide and Metal Crystal Structures*

J. T. Waber, Los Alamos Scientific Lab., University of California, Los Alamos, N. Mex.

The general problem of the epitaxy of oriented overgrowths and, in particular, the relation of oxide films to their parent metals is reviewed. Wilman's theory is used to explain the lack of an orientation relationship between UO_2 and U even though the UO_2 film has been demonstrated to be oriented with respect to the specimen surface. The scant evidence which suggests that the surface orientation may depend on external conditions during oxidation is presented.

* Work done under the auspices of the Atomic Energy Commission.

Abstract No. 109
The Element Columbium and Its Compounds

J. R. Darnell and L. F. Yntema, Fansteel Metallurgical Corp., 2200 Sheldon Rd., North Chicago, Ill.

Columbium, a member of Group V of the Periodic Table, is a high melting metal whose compounds are in general nonbasic in character. It forms refractory binary compounds with elements of Groups III, IV, and V. Its melting point and reactivity impose restrictions on methods of preparation. The metal is of particular interest as a high temperature material of construction because of its strength at high temperatures and its workability.

Abstract No. 110
Supplies of Columbium

K. B. Higbie, Bureau of Mines, U. S. Dept. of the Interior, Washington 25, D. C.

(No abstract received)

Abstract No. 111
Some Sources and Production Statistics for Columbium

H. P. Croft, Kennecott Sales Corp., 161 E. 42 St., New York 17, N. Y.

(No abstract received)

Abstract No. 112
Economic Aspects and Supply Situation for Columbium

R. L. Carmichael, Battelle Memorial Institute, Columbus 1, Ohio

(No abstract received)

Abstract No. 113
A Review of the Extractive Metallurgy of Niobium

M. E. Sibert, A. J. Kolk, and M. A. Steinberg, Horizons Inc., 2905 E. 79 St., Cleveland 4, Ohio

Preparation of Nb metal has been attempted by a number of chemical and electrochemical routes. The chemical reduction of Nb compounds such as Nb_2O_5, K_2NbOF_5, K_2NbF_7, and $NbCl_5$ has been conducted with varying degrees of success. The electrochemical reduction of Nb from aqueous baths has been attempted, but no aqueous bath has been found to produce bulk deposits of metal. The electrolysis of molten baths containing K_2NbOF_5 or K_2NbF_7 has produced Nb metal.

The more promising methods of preparation of Nb metal at the present time include the reaction of Nb_2O_5 and NbC or C, hydrogen reduction of $NbCl_5$, and electrolysis of K_2NbF_7-NaCl mixtures.

Abstract No. 114
Informal Comments on the ONR Program of Basic Research on Columbium

N. E. Promisel, Materials Branch, Bureau of Aeronautics, Navy Dept., Washington 25, D. C.

(No abstract received)

Abstract No. 115
Separation of Ta and Nb

J. L. Tews and S. L. May, Bureau of Mines, U. S. Dept. of the Interior, Albany, Ore.

(No abstract received)

Abstract No. 116
Preparation and Properties of High Purity Tantalum and Columbium

R. C. Bourke, J. M. Blocher, Jr., and I. E. Campbell, Battelle Memorial Institute, Columbus 1, Ohio

(No abstract received)

Abstract No. 117
Preparation of High Purity, Ductile Niobium Metal by Fusion Electrolysis

A. J. Kolk, M. E. Sibert, and M. A. Steinberg, Horizons Inc., 2905 E. 79 St., Cleveland 4, Ohio

Electrolysis of molten solutions of K_2NbF_7 in NaCl and in NaCl-KCl mixtures has been conducted on a laboratory scale. The investigation has been conducted in a range of compositions of 10–40 w/o K_2NbF_7. The temperature range which was investigated in the case of K_2NbF_7-NaCl mixtures was 785°–840°C. Electrolysis of solutions of K_2NbF_7 in NaCl-KCl mixtures was conducted in the range of 675°–740°C. High purity, ductile niobium metal was prepared by the electrolytic procedure throughout a wide range of operating conditions.

Abstract No. 118
Analysis of Certain Metallic Impurities in Niobium

J. F. Reed and A. H. Wolfe, Research Labs., Westinghouse Electric Corp., Beulah Rd., Churchill Borough, Pittsburgh 35, Pa.

Procedure, accuracy, and precision of methods for the determination of certain metallic impurities in niobium are discussed.

Abstract No. 119
Analysis of Oxygen and Nitrogen in Niobium

W. Harris, Research Labs., Westinghouse Electric Corp., Beulah Rd., Churchill Borough, Pittsburgh 35, Pa.

Procedure, accuracy, and precision of methods for the determination of oxygen and N in Nb are discussed.

Abstract No. 120
Hydrogen and Niobium—Reaction and Diffusion Kinetics

M. W. Mallett and W. M. Albrecht, Battelle Memorial Institute, Columbus 1, Ohio

The reaction of H with Nb has been studied at 200°–700°C principally at 1 atm pressure. The pressure dependency of the reaction was investigated. Diffusion and solubility data were also obtained in the same temperature range. A reaction mechanism is proposed.

Abstract No. 121
Tensile Properties of Niobium on the Basis of Purity and Prior Stress History

F. J. Anders, Jr., and W. I. Pollock, Pigments Dept., E. I. du Pont de Nemours & Co., Newport, Del.

Tensile tests on samples of pure Nb have been conducted at room temperature. Rolling textures for Nb sheet have also been investigated. A behavior similar to α-iron in both tensile tests and rolling texture is observed. The effect of impurities is demonstrated to some extent.

Abstract No. 122
Ductile-to-Brittle Transition in Niobium

E. T. Wessel and D. D. Lawthers, Research Labs., Westinghouse Electric Corp., Beulah Rd., Churchill Borough, Pittsburgh 35, Pa.

Flow and fracture characteristics of commercially pure Nb are determined for the case of simple tension. The influence of such variables as temperature, strain rate, chemistry, and microstructure on the transition behavior are described.

Abstract No 123
Effect of Rare Earth Additions on the Ductility of Arc-Melted Group V-A Metals

J. W. Semmel, Jr., Metallurgy and Ceramics Research Dept., General Electric Co., The Knolls, Schenectady, N. Y.

Semipure metals of Group V-A V, Nb, and Ta were arc melted with rare earth additions, producing relatively soft buttons which were cold rolled successfully. Under similar conditions, but without the rare earth addition, these metals were harder and could not be cold rolled. A hot forged and cold rolled Nb-Ce alloy had room temperature and 2000°F tensile properties comparable to those of commercial Nb, which is made ductile by vacuum sintering. It is difficult to obtain sound buttons and the best ductility in Nb on the first melting.

Abstract No. 124
Electroplating on Columbium

J. G. Beach, Battelle Memorial Institute, Columbus 1, Ohio

Electroplated metals on Cb are an aid to joining Cb to another metal. Cb can be electroplated with Fe with a fair degree of adhesion. Subsequent outgassing at 400°F and heat treatment at 1300°F results in excellent adherence of the Fe coating. This Fe coated Cb then can be plated with other metals or joined to other metals by conventional means.

Abstract No. 125
Oxidation of Niobium between 375° and 700°C

E. A. Gulbransen and K. F. Andrew, Research Labs., Westinghouse Electric Corp., Beulah Rd., Churchill Borough, Pittsburgh 35, Pa.

Nb has been found to oxidize in a complex manner. At 400°C and lower a slow rate of reaction is observed with the kinetics following the parabolic rate law. At a weight gain of 55–70 $\mu g/cm^2$ a transition in the kinetics occurs to a nearly linear rate law. Between 550° and 625°C the oxidation rate is nearly constant as a function of temperature, while above 625°C the oxidation rate again increases with the temperature. The adherence of the oxide is poor above the transition point.

Abstract No. 126
Development of Oxidation-Resistant Niobium Alloys

H. T. Kling, Atomic Energy Div., Sylvania Electric Products Inc., Bayside, N. Y.

The nature of the oxidation process in pure Nb in described. The effect of the addition of several alloying elements on the oxidation process is then discussed in detail.

Abstract No. 127
Effect of Alloy Additions on Oxidation Resistance of Niobium

F. J. Clauss and C. A. Barrett, NACA Lewis Flight Propulsion Lab., 21000 Brookpark Rd., Cleveland 11, Ohio

Selection of alloying elements for improving the oxidation resistance of Nb at elevated temperatures is discussed. Results are presented of an extensive survey to evaluate the effects of up to 25 at. % of various alloying additions on the oxidation behavior at 1000° and 1200°C.

Abstract No. 128
Oxidation of Niobium-Chromium Alloys at Elevated Temperatures

C. A. Barrett and F. J. Clauss, NACA Lewis Flight Propulsion Lab., 21000 Brookpark Rd., Cleveland 11, Ohio

Detailed studies of the kinetics and mechanisms of oxidation of Nb-Cr alloys are presented. Results include continuous oxidation curves, x-ray diffraction studies, microstructural examinations, and chemical analyses of the scales and alloys.

Abstract No. 129
Vacuum Reactions of Niobium during Sintering

W. D. Klopp, C. T. Sims, and R. I. Jaffee, Battelle Memorial Institute, Columbus 1, Ohio

(No abstract received)

INDUSTRIAL ELECTROLYTIC

Abstract No. 130

Electromagnetic Forces in a Large Aluminum Furnace

O. Chr. Böckman, Elektrokemisk A/S, Oslo, Norway, and J. Wleügel, A/S Norsk Aluminium Co., Oslo, Norway

Certain difficulties in the operation of large Al furnaces are known to be caused by electromagnetic forces set up in the molten cryolite and Al layers. The problem has been analyzed mathematically and by use of scale models. Results obtained by this analysis and possible ways of reducing the electromagnetic forces are surveyed.

Abstract No. 131

Electrical Conductivity of Molten Florides, I. Apparatus and Method

E. W. Yim and Morris Feinleib, Chemical Research Dept., Kaiser Aluminum & Chemical Corp., Permanente, Calif.

A method and apparatus have been developed for determining the electrical conductivity of cryolite-base melts and other fluorides. Hot-pressed BN is used to fabricate high-resistance cells with constants ranging from 17 to 39 cm^{-1}. Such cells must be used under an inert atmosphere. Furthermore, in order to correct for the conductance of the cell body proper, measurements have to be made with the cell immersed in melt as well as out of the melt. A furnace and apparatus for accomplishing these objectives are described. An a-c Wheatstone bridge is used for measurements. Although Inconel electrodes were employed, resistance values were found to be independent of frequency above 1000 cycles.

Abstract No. 132

Electrical Conductivity of Molten Fluorides, II. Conductance of Alkali Fluorides, Cryolites, and Cryolite-Base Melts

E. W. Yim and Morris Feinleib, Chemical Research Dept., Kaiser Aluminum & Chemical Corp., Permanente, Calif.

The electrical conductivities of molten LiF, NaF, KF, Li_3AlF_6, Na_3AlF_6, and K_3AlF_6 have been determined. Typical values are:

Salt	LiF	NaF	KF	Li_3AlF_6	Na_3AlF_6	K_3AlF_6
Temp, °C	900	1020	900	900	1020	1020
K, ohm^{-1} cm^{-1}	8.43	5.15	3.80	3.78	2.84	2.28

The effect of alumina, CaF_2, and $NaF:AlF_3$ ratio on the conductivity of cryolite-base melts has been studied. Molar and equivalent conductances have been calculated for several melts, and their significance is discussed.

Abstract No. 133

Uranium Metal Preparation by Electrolytic Reduction of Its Oxides

L. W. Niedrach and B. E. Dearing, Knolls Atomic Power Lab., General Electric Co., Schenectady, N. Y.

Background work is described for a new continuous process for production of U by electrolytic reduction of U oxides in fused salt electrolytes. Unlike past electrolytic processes for U production, the present one is operated at temperatures (1200°–1250°C) above the melting point of U. The effect of current, salt bath composition, and other variables on efficiency and cell operation are discussed. Advantages of the new process are outlined, and areas requiring additional development work are indicated.

Abstract No. 134

Chlor-Alkali Committee Report

J. C. Cole, Diamond Alkali Co., Union Commerce Bldg., Cleveland 14, Ohio

(No abstract received)

Abstract No. 135

Influence of Impurities in the Electrolyte in Chlorine-Caustic Electrolysis by the Mercury Cell Process, VI. Investigation of the Influence of Graphite Particles on Amalgam Decomposition and Cathodic Current Efficiency

Gösta Angel, Rolf Brännland, and Stig Dahlerus, Div. of Applied Electrochemistry, Royal Institute of Technology, Stockholm, Sweden

The influence of graphite particles on the Hg cell process for the production of Cl and caustic soda has been investigated by measuring decomposition rate of sodium amalgam in buffered NaCl solutions and by study of the current efficiency of a laboratory mercury cell. Quantities of graphite under 3 g/l have little effect on current efficiency with pure brine, but in the presence of Mg or Al the effect is appreciable. The simultaneous presence of graphite and either Fe, Ca, or small quantities of V (<0.1 mg/l) does not affect the electrolysis process. Silicates and stannates inhibit the action of the graphite particles.

Abstract No. 136

The Castner-Kellner Shunt Circuit for Mercury Chlor-Alkali Cells

M. Janes, National Carbon Research Labs., National Carbon Co., A Div. of Union Carbide and Carbon Corp., Cleveland, Ohio

Analysis of the Castner-Kellner shunt circuit by Kirchoff's laws shows that anodic concentration polarization in the amalgam decomposition cell is a result of the circuit arrangement, and not the primary cause, as has been stated, of the failure to attain appreciable utilization of the chemical energy of the decomposition reaction as electrical energy (voltage saving). The potential of the anode in the denuder cell determines the Na concentration in the Hg returned to the Cl cell. The variation of this potential with other operating factors is discussed. An estimate is made of the possible voltage saving if some expedient other than the shunt circuit were employed to maintain a Na balance.

Abstract No. 137

Electrolytic Production of Sodium Perchlorate Using Lead Dioxide Anodes

J. C. Schumacher, D. R. Stern, and P. R. Graham, American Potash & Chemical Corp., Whittier, Calif.

The purpose of this study was to investigate the use of lead dioxide anodes as a substitute for Pt in the production of $NaClO_4$. Rod shaped lead dioxide deposits were prepared by plating on wires. Lead dioxide anodes will produce $NaClO_4$ at high cumulative current efficiencies. One anode was used 3000 hr. $NaClO_3$ can be produced using various metallic cathodes. Energy results indicate that stainless steel and Ni are the best cathodic materials. NH_4ClO_4 prepared from the $NaClO_4$ produced in this investigation contained no significant metallic contamination.

THEORETICAL ELECTROCHEMISTRY

Abstract No. 138

Interpretation of Activity and Osmotic Coefficients

George Scatchard, Dept. of Chemistry, Massachusetts Institute of Technology, Cambridge, Mass.

The Debye discharge-transfer-charge process in continuous media gives a start toward interpreting the cumulative, and approximately additive, effects of the charge-charge, charge-molecule, and molecule-molecule interactions in electrolyte solutions. For noble gas-type ions in water, the latter two are approximately those of holes in the solvent. The next approximations include effects on deviations from additivity, "higher terms," structure of the solvent, and specific deviations from noble gas-type ions. The greatest difficulties arise from those effects which are also operative in aqueous solutions of nonpolar electrolytes.

Abstract No. 139

Electrolytic Solution Problem in Statistical Mechanics

J. E. Mayer, Enrico Fermi Institute for Nuclear Studies, University of Chicago, Chicago, Ill.

The treatment of liquid solutions by formal statistical mechanical methods is always plagued by the absence of a completely satisfactory treatment of even a pure liquid. However, to some extent this difficulty can be evaded by assuming a knowledge of the properties of the pure solvent at the outset of the treatment. Various tricks for doing this are available. For electrolytic solutions, a special problem, the long range of the forces and consequent nonconvergence of the ordinary methods, adds a complication. Again, methods of avoiding the difficulty are available.

Abstract No. 140

Successes and Limitations of the Theory of Debye and Hückel

E. A. Guggenheim, Dept. of Chemistry, University of Reading, Reading, England

Appraisal of the Debye-Hückel theory should distinguish between the model (complete ionization, rigid spherical ions) and the approximation ($z\,e\,\psi \ll kT$). For 2-2 electrolytes in water the model is valid, the approximation is not. A combination of Müller's more accurate solution with a modified form of Bjerrum's conventional definition of association leads to complete agreement between theory and experimental measurements of freezing points on six sulfates of bivalent metals which are shown to have effective mean diameters between 3.5 and 4.0 Å.

Abstract No. 141

Statistical Mechanical Theory of Plasmas and Liquid Metals

J. G. Kirkwood, Sterling Chemistry Lab., Yale University, New Haven, Conn.

The Fermi-Thomas statistical theory of the atom and the Debye-Hückel theory of strong electrolytes are combined to provide a statistical mechanical description of electroneutral systems of positive ions and electrons in thermodynamic equilibrium. Differential equations for the average electrostatic potentials in the neighborhood positive ions and electrons are formulated, and the electrostatic free energy and equation of state of a dilute plasma are calculated. A generalization of the theory to include liquid metals is outlined.

Abstract No. 142

Properties of Concentrated Solutions of Acids and Alkalies

R. P. Bell, Physical Chemical Labs., Balliol College, Oxford, England

Data are presented for the acidity functions of a number of acids in aqueous solution over a large concentration range. Some analogous results are given for concentrated solutions of alkalies. Suggestions are made as to the interpretation of these results with special reference to the structure of water and of the hydrogen ion and the possible polymerization of the acid anions.

Abstract No. 142A

Present State of the Electrolyte Problem

C. A. Kraus, Dept. of Chemistry, Brown University, Providence, R. I.

This paper is a summarizing outline of present electrolyte problems.

Abstract No. 143

Properties of Rare Earth Salts in Electrolytic Solutions

F. H. Spedding and Gordon Atkinson, Institute for Atomic Research, Iowa State College of Agriculture and Mechanic Arts, Ames, Iowa

For the past eight years, the Ames Lab. has had a program of studying the electrolytic properties of the rare earth salts. These studies cover solutions of the chlorides, bromides, nitrates, perchlorates, and sulfates of the rare earth series. Data on the activity coefficients, conductances, transference numbers, heats of solution, heats of dilution, partial molal volumes, and partial compressibilities have been assembled in one paper. These data are discussed with respect to the Debye-Hückel and Onsager theoretical predictions. Regularities which have been observed are emphasized.

Abstract No. 144

Nuclear Magnetic Resonance Studies of Aqueous Solutions*

H. S. Gutowsky, Noyes Chemical Lab., University of Illinois, Urbana, Ill.

Very small interactions produce readily detectable changes in the various characteristics of the nuclear magnetic resonance absorption of a sample. Therefore, it is to be expected that intermolecular or interionic interactions can be studied by observing their effects on absorption. The nmr principles involved are summarized. Earlier nmr studies of solutions are reviewed and some recent work at Illinois is described. These applications include: (*a*) chemical shifts and quadruple broadening which are associated with the structure of solutions; (*b*) the study of rate processes in solution under equilibrium conditions by spin-lattice relaxation time measurements and also by chemical shifts.

* Assisted in part by ONR.

Abstract No. 145

Raman Spectral Studies of Ionic Equilibria in Solutions of Strong Electrolytes

T. F. Young, Dept. of Chemistry, University of Chicago, Chicago, Ill.

Some electrolytes emit Raman spectra sufficiently intense and simple to permit accurate (photoelectric) determinations of ion concentration. Measurements of intensities combined with studies of other properties, e.g., nuclear magnetic resonance and conductance, yield equilibrium constants covering temperature ranges so wide (150°–300°C) that $\Delta\bar{C}_p^0$ can be estimated. Values for the dissociation of strong acids are similar to those for typical weak acid (−35 to −40 cal mole^{-1} deg^{-1}).

Several nonaqueous solutions have been studied. Of particular interest are mixtures of fused salts, e.g., KCl and $CdCl_2$, in which complexes similar to those in aqueous media are observed.

Abstract No. 146

Melting Mechanisms of Ionic Crystals

A. R. Ubbelohde, Dept. of Chemical Engineering, Imperial College of Science and Technology, London, England

Mechanisms of melting which involve primarily positional disorder of the ions are reviewed. Normally these are not accompanied by extensive premelting in the solid state; some interesting exceptions are considered. Other melting mechanisms may accompany positional disorder in certain ionic salts. For polyatomic ions, formation of association complexes on melting can make important contributions to the total entropy of fusion, and can lead to abnormally low melting points.

Abstract No. 147

Influence of Complex Ions on Structure and Reactivity of Fused Salts

E. R. VanArtsdalen, Oak Ridge National Lab., Oak Ridge, Tenn., and National Carbon Research Labs., Cleveland, Ohio

Evidence for the existence of various types of complex ions in fused salts is presented and reviewed for both single salts and mixtures. Certain important structural concepts are considered. Methods and results are discussed which have been obtained by measurement of such properties as freezing point depression, entropy of fusion, viscosity, electrical conductance, x-ray diffraction, and reaction rate. Examples are given to illustrate ways in which the kinetics of chemical reactions, including electrode processes, can be influenced by the presence of complexing agents in a melt.

Abstract No. 148

A Point of View on Ion Clouds; A Suggested Explanation of an Activity Anomaly in Dilute Aqueous LiCl Solutions

H. S. Frank and P. T. Thompson, Dept. of Chemistry, University of Pittsburgh, Pittsburgh, Pa.

The log $\gamma - m^{1/2}$ curve for aqueous LiCl has a break near 0.001M which is so sharp that some cooperative phenomenon seems to be involved. It is suggested that in addition to a special ion-water structure effect there is a quasi-transition from the Debye-Hückel type ion cloud to a "diffuse lattice" type, in keeping with the accurate $m^{1/2}$ dependence of log γ from 0.001M to 0.05M. Theoretical considerations and the shapes of many activity, conductance, and diffusion curves suggest that such a lattice cloud occurs rather generally.

Abstract No. 149

Incomplete Dissociation in Aqueous Salt Solutions

C. W. Davies, Edward Davies Chemical Labs., University College of Wales, Aberystwyth, Wales, Great Britain

Development of methods for estimating the proportion of free ions in an aqueous electrolyte solution is described. Some of the results obtained are reviewed with reference to Bjerrum's ion-association hypothesis and to ionic hydration theories.

Abstract No. 150

Hydration and Association in Aqueous Electrolyte Solutions

E. Glueckauf, Atomic Energy Research Establishment, Harwell, Berks., England

Various approaches to effects of ionic hydration, hydrated ion size, and ionic association are examined critically. For weak ion pair formation, effectively linear terms result which cannot be separated from other terms. However, from strong associations (e.g., 2:2 electrolytes) nonlinear functions arise. Thus for $MgSO_4$ solutions Brown and Prue have shown that osmotic data up to 0.03M indicate formation of the undissociated ion pair. This paper shows that, up to 1M, data are consistent with additional formation of the triplet ion $Mg(SO_4)_2^{2-}$, but not with the complex $Mg(SO_4)_2$. This seems to apply to all 2:2 electrolytes.

Abstract No. 151

Hydrogen Bond Structures, Hydration of Protons, and Proton Transfer in Aqueous Solutions

M. Eigen, Max-Planck Institute for Physical Chemistry, University of Göttingen, Göttingen, Germany

From thermodynamic and kinetic data a defined model for hydration of the proton in aqueous solution has been derived. According to this model the proton exists as H_3O^+ ion connected to at least three additional H_2O molecules by H bonds, forming a complex with a proton of excessive mobility. Relaxation measurements in pure water and ice result in a half-life of about 10^{-13}–10^{-14} sec for the individual H_3O^+. Measurements with a new "stationary field method" yield an appreciably higher protonic mobility in ice than in water. Such proton-conducting H-bond systems which are also of biological interest show certain parallels to electronic semiconductors.

Abstract No. 152

Quantitative Measurements of Ionic Vibration Potentials*

E. Yeager, J. Booker, and F. Hovorka, Ultrasonic Research Lab., Western Reserve University, Cleveland, Ohio

When ultrasonic waves are introduced into an electrolytic solution, alternating potential differences are produced within the solution. This effect was proposed by Debye in 1933 for the study of ionic hydration. Apparatus involving pulse-modulated waves has been developed specifically for the investigation of this effect. Data with an estimated accuracy of ±10% will be presented and interpreted for several electrolytes at frequencies in the range 10^5 to 10^6 cps.

* Based on research supported by the Office of Naval Research.

Abstract No. 153

A Physical Theory of Ion Solvation

M. Balkanski, Corrosion Lab., Massachusetts Institute of Technology, Cambridge, Mass.

An attempt is made to calculate heat of solvation based on electrostatic considerations. The ion is assumed to be a spherical conductor with a uniform surface charge density enveloped by water molecules of volume v_1. The electrostatic energy accummulated in this volume is calculated, neglecting action of the electrical field of the ion outside the limits of the solvated complex, and expresses variation of solvation energy in which water polarization is assumed due only to dipole orientation. Here, the polarization is given by the Langevin function. Variation of energy is given by integration of this function between the crystallographic radius of the ion and the experimentally determined radius of the complex. The heat of solvation is calculated for certain cases.

Abstract No. 154

Aquo-ions and Ion Pairs

J. F. Duncan and D. L. Kepert, Chemistry Dept., University of Melbourne, Victoria, Australia

The electrostatic model of chemical bonding is discussed in relation to the structure of aquo-ions, complex ions, and ion pairs. Systematic relations between (*a*) the standard thermodynamic quantities of formation, (*b*) those of the components, and (*c*) the ionic radii are interpreted. The evidence on the nature of ion pairs obtainable from spectra is considered with reference to the crystal field theory.

Abstract No. 155

Ionization of the Bisulfate Ion; Notes on the Electromotive Force Method of Determining Ionization Constants

W. J. Hamer, National Bureau of Standards, Washington 25, D. C.

The ionization constant of the bisulfate ion determined by emf and spectrophotometric methods differs by 16% at 25°C. Harned and Owen in their book state "A reexamination of the methods of computing K_{2A} from the electromotive forces may remove this discrepancy." In 1952 Davies appeared to have removed the discrepancy by taking Na_2SO_4 as incompletely dissociated.

This paper gives a re-examination of emf data. Whereas the limiting Debye-Hückel equation was originally used, "ion sizes" were incorporated with resultant nonconvergence at infinite dilution. This is general for the emf method; nonconvergence is progressively higher with lower *p*Ks. Surprisingly, however, convergence is obtained when salt-free solutions, as employed by Davies, are used.

Abstract No. 156

Heats of Dilution of Very Dilute Solutions of Weak and Strong Electrolytes

E. Lange, Institute of Physical Chemistry, University of Erlangen, Erlangen, Germany

Heats of dilution of dilute aqueous solutions of electrolytes may be caused by interionic forces between dissolved ions and/or by heats of dissociation of dissolved molecules. Very dilute solutions of strong electrolytes show practically only exothermic interionic effects corresponding to their ionic valence type. Weak electrolytes and nonelectrolytes are exothermic or endothermic; in some cases they cause heats of dissociation. In dilute solutions, salts of weak bases or acids show heats of hydrolysis.

Abstract No. 157

Anion Exchange Studies of Metal Complexes

K. A. Kraus, Chemistry Div., Oak Ridge National Lab., Oak Ridge, Tenn.

Anion exchange of metal complexes is a general tool for investigation of complexing properties of metals. The method is of the thermodynamic type and is a supplement to other methods. With a large amount of anion exchange information available, conclusions may be drawn on a comparative basis. In favorable cases, equilibrium quotients for complex equilibria and information regarding the pertinent coefficient ratios may be obtained. The method is relatively simple for dilute electrolyte solutions, and reasonably firm for concentrated electrolyte solutions.

Abstract No. 158

Electrophoresis and Conductivity in Solutions Containing Polyelectrolytes

J. J. Hermans, Lab. for Inorganic and Physical Chemistry, Rijks University, Leiden, The Netherlands

According to a simple theory, the electrophoretic mobility U of charged chain molecules should be independent of the molecular weight when the ionic strength μ of the solution is high. At lower μ-values, U may increase and eventually reach a maximum. Some data appear to confirm this. It is more difficult to predict the conductivity κ. Experiments show that κ sometimes decreases in cases where the simple theory indicated above predicts an increase. An attempt to explain this behavior in terms of relaxation effects will be discussed.

Abstract No. 159

Normal and Abnormal Ionic Mobilities in Anhydrous Hydrofluoric Acid and Hydrogen Peroxide-Water Systems

Martin Kilpatrick, Dept. of Chemistry, Illinois Institute of Technology, Chicago, Ill.

Abnormal conductances of cations and anions of solvents water and H_2SO_4, and of cations of solvents methyl and ethyl alcohol, have been reported. In liquid ammonia neither the solvent cation nor anion shows abnormal conductance. This paper reports that the cation of anhydrous HF shows no abnormal conductance, but the anion has a higher mobility than other anions.

When H_2O_2 replaces water in a solution of $HClO_4$ the mobility of the cation decreases, and at 99% H_2O_2 the mobility is about the same as that of potassium ion. As H_2O_2 replaces water in a solution of KOH the ratio of the conductance to that of $KClO_4$ first decreases, then passes through a minimum, and increases beyond 25% H_2O_2. This result is interpreted to mean that the hydroperoxide ion has a greater mobility than the hydroxide ion. The problem is also considered for other solvent-water mixtures, and the importance of the nature and structure of the solvent stressed.

Abstract No. 160

Mobilities of Ions and Uncharged Molecules in Solutions in Relation to Viscosity

R. H. Stokes, Dept. of Chemistry, University of New England, Armidale, N.S.W., Australia

The rapid progress being made in the theoretical treatment of interionic effects on the motion of ions in relatively concentrated solutions emphasizes the poorness of our present understanding of the relation of viscosity to mobility in such solutions. Data are presented for (*a*) tracer diffusion of iodide in concentrated halide solutions, (*b*) ion mobilities in solutions of aqueous nonelectrolytes, and (*c*) conductances of concentrated electrolytes in water. Attempts are made to correlate the observations with viscosity data.

Abstract No. 161

Conductance Equations of Robinson-Stokes and Wishaw-Stokes Applied to the Regions of Dilute and of Concentrated Solutions, Respectively

A. N. Campbell, Dept. of Chemistry, University of Manitoba, Winnipeg, Man., Canada

This paper deals with the following subjects: the equation of Robinson and Stokes applied to conductance in the region of moderate dilution; limiting conductance of salts which hydrolyze; physical significance of å, the distance of closest approach of the ions; the hydrated ion in aqueous and mixed solvents; application of the Wishaw-Stokes equation to the conductance of concentrated solutions; viscosity correction.

Abstract No. 162

A Redetermination of the Value of the Faraday with the Iodine Coulometer

D. A. MacInnes and A. R. Pray, Rockefeller Institute for Medical Research, New York, N. Y.

Since the most accurate method for determining the charge e on the electron depends on $\mathbf{F} = N\,e$, the precise value of **F** takes on new importance, especially as e is related to most other physical constants. Aside from recent research by Craig and Hoffman on the oxalate coulometer, work on evaluation of the Faraday is over 40 years old.

The research described is a return to the iodine coulometer, but using modern techniques. Experimentally, this method depends on finding the amount of iodine released or absorbed during passage of a known current for an accurately measured time. A constant current apparatus

has been developed which regulates to at least 1 ppm. The time is obtained from Bureau of Standards broadcasts. Iodine is determined by differential electrometric titration, with a precision of 1 ppm; titrating fluid is calibrated using iodine tested by activation analysis and other methods.

Abstract No. 163

Diffusion and Activity Coefficients of Electrolytes in Dilute Aqueous Solutions

H. S. Harned, Sterling Chemistry Lab., Yale University, New Haven, Conn.

The theory of diffusion coefficients of electrolytes in dilute solutions leads to the expression

$$D = \nu 1000RT(\bar{M}/C)\left(1 + C\,\frac{\partial \ln y_{\pm}}{\partial C^{-}}\right)$$

where $\bar{M}/C$ is a mobility term, and the parenthesis containing the activity coefficient, $y_{\pm}$, is a thermodynamic term. It has been shown by a conductometric method that diffusion coefficients of many electrolytes of different valence types at concentrations below 0.01M conform to the theory. The small variation of the mobility term with concentration, caused by electrophoresis, appears to be of the right sign and magnitude.

Assuming that this mobility term is correct, activity coefficients in dilute solutions can be computed from diffusion data. This method is described and applied to solutions of 15 electrolytes.

Abstract No. 164

Thermal Diffusion and Related Effects in Solutions of Electrolytes

J. N. Agar, Dept. of Physical Chemistry, Cambridge University, Cambridge, England

The thermodynamic treatment of nonisothermal systems is summarized, and the significance of the entropy of transport and "transported entropy" outlined. Two recently developed methods of measuring Soret coefficients are described; they utilize (*a*) changes in emf of a nonisothermal cell, and (*b*) changes in conductance of the solution. The latter appears promising as a general method for dilute solutions of electrolytes. Soret coefficients (or entropies of transport) of aqueous ions are strongly temperature dependent and do not appear to be correlated in any simple manner with other ionic properties.

Abstract No. 165

Temperature Dependence of the Thermal Diffusion of Aqueous KCl

J. G. Longsworth, Rockefeller Institute for Medical Research, New York, N. Y.

Soret coefficients of 1,2,3, and 4*M* solutions of aqueous KCl have been determined over the temperature interval from 10° to 50° in 10° steps. Except at the highest temperature, T, and concentration, m, the magnitude of the coefficient increases as both T and m increase, the salt migrating to the cold plate in each instance. Concentration profiles have been determined *in situ* with the aid of a two-channel cell, filled with solution and solvent, respectively, and Rayleigh interferometry. Results are considered in relation to other methods for the measurement of thermal diffusion in liquids and the emf of electrolytic thermal cells.

Abstract No. 166

Data for the Concentration Dependence of the Four Diffusion Coefficients of the System NaCl-KCl-H_2O at 25°

I. J. O'Donnell and L. J. Gosting, University of Wisconsin, Madison, Wis.

Solute flows J_1 and J_2 in a 3-component system may be related to concentration gradients by the equations

$$J_1 = -D_{11}\frac{\partial C_1}{\partial x} - D_{12}\frac{\partial C_2}{\partial x}$$

$$J_2 = -D_{21}\frac{\partial C_1}{\partial x} - D_{22}\frac{\partial C_2}{\partial x}$$

In general, diffusion coefficients defined by these relations vary with both solute concentrations. Using the Gouy diffusiometer to study the refractive index curves for free diffusion, values have been obtained for the four diffusion coefficients of the system NaCl-KCl-H_2O. Results are reported for the four combinations of the two salt concentrations used, these concentrations being 0.25 and 0.5 mole/l. To evaluate diffusion coefficients for each combination of concentrations, four experiments were performed with different refractive fractions of NaCl. The Gouy fringe deviation graphs, used in evaluation of the diffusion coefficients, give on inspection direct information about flow interactions.

Abstract No. 167

Thermodynamic Functions of Single Ionic Species in Solutions

Pierre Van Rysselberghe, Dept. of Chemistry, Stanford University, Stanford, Calif.

Current conventions concerning the assignment of absolute values to the free enthalpies, enthalpies and entropies of single ionic species in solutions are critically re-examined. Expressions for absolute electrode potentials and electromotive forces of cells and for their temperature coefficients are written explicitly before conventions are introduced. The treatment, based mostly on a logical elaboration of the original convention concerning the standard hydrogen electrode, avoids contradictions, and is presented as a fundamental adjunct to theories of electrolytes.

Abstract No. 168

Some Thermodynamic Properties of Solutions of Salts of Bivalent Metals

J. M. Austin, R. A. Matheson, and H. N. Parton, Chemistry Dept., University of Otago, Dunedin, New Zealand

The heats of mixing of lead perchlorate and potassium halide solutions have been measured in a microcalorimeter, and the heats of formation of PbX^+ ions derived. Association constants of the ions $CdBr^+$, CdI^+, $Pb(SCN)^+$, $Hg(NO_3)^+$ have been measured spectrophotometrically. The optical method suggests that the ions $Cd(NO_3)^+$, $Cd(SCN)^+$, $Zn(SCN)^+$, PbF^+ do not exist in significant amounts in the solutions studied. The thermodynamics of ion association is discussed.

Abstract No. 169

Ionization Constants of Weak Acids from Spectrophotometric Measurements

R. A. Robinson, Dept. of Chemistry, University of Malaya, Singapore, Malaya

Many acids (including acids of the anilinium ion type) have markedly different u.v. absorption in solutions of low and high *p*H, and, from the variation of optical density with *p*H at a given wavelength, the degree of dissociation and the ionization constant of the acid can be determined. At least three measurements at different *p*H values are needed for a monobasic acid and at least five for a dibasic acid with overlapping dissociation. Recent work on substituted anilines, phenols, and barbituric acids will be discussed with relation to Hammett's Rule.

Abstract No. 170

Conductance and *p*H Measurements in Methanol-Water Mixtures

Theodore Shedlovsky, Rockefeller Institute for Medical Research, York Ave. & 66 St., New York, N. Y.

The electrical conductances of dilute solutions of salts and of strong and weak acids in water-methanol solvent mixtures are compared over the entire range of solvent composition at 25°C. The weak acid ionization constants are computed from these data. They are used for interpreting *p*H types of emf measurements obtained with glass electrodes on buffer solutions in these solvent mixtures.

Abstract No. 171

Ionization Equilibria in Ammonia-Water Solutions from 5° to 55° as Obtained from High Field Conductance Measurements

Emil Arnold, Harlow Freitag, and Andrew Patterson, Jr., Sterling Chemistry Lab., Yale University, New Haven, Conn.

High field conductance measurements on a series of ammonia-water solutions are reported. A temperature range of 5°–55° was covered. High field conductance results are treated so as to obtain ionization equilibrium constants for the several temperatures. Equilibrium constants (in contrast with those obtained from emf measurements) exhibit a minimum at about 30°, where the constant has the value 8.5×10^{-5}. The significance of these results and the possible ionization equilibria in water-ammonia solutions are discussed.

Abstract No. 172

An Isopiestic Unit for High Temperature Studies

B. A. Soldano, R. J. Fox, and R. W. Stoughton, Chemistry Div., Oak Ridge National Lab., operated by Union Carbide Nuclear Co., Oak Ridge, Tenn.

An isopiestic unit has been constructed for aqueous solution work at elevated temperatures up to 150° or higher. Periodic weighing of sample dishes is accomplished inside the vaccum-tight, pressurized, stainless steel equilibration vessel by means of a specially constructed Ti magnetic balance. The unit has been found to operate satisfactorily and to respond more rapidly although less accurately at the higher temperatures. Comparative osmotic coefficients are presented.

Abstract No. 173

Thermodynamics of Hydrogen Chloride in Ethyl Alcohol from EMF Measurements

G. J. Janz and Harry Taniguchi, Dept. of Chemistry, Rensselaer Polytechnic Institute, Troy, N. Y.

EMF measurements of the cell without liquid junction: Pt, H_2(1 atm)| HCl in Ethanol (m)|AgCl-Ag have been carried out at 25°C over a concentration range from 0.0048 to 0.12*M*. New experimental techniques were devised, and the latest computational methods were employed to obtain the standard electrode potential of the Ag, AgCl electrode in anhydrous ethanol and the activity coefficients of HCl in ethanolic solutions at 25°C.

Abstract No. 174

Kinetics of Bromoacetate-Thiosulfate Ionic Reaction

Gerald Corsaro and H. L. Stephens, Dept. of Chemistry, University of Akron, Akron 4, Ohio

Reported results on the kinetics of ionic reactions as between bromoacetate and thiosulfate ions implies a breakdown of the Debye-Hückel theory embodied in the Bronsted-Christonson-Scatchard equations relating salt effects to such reactions. A re-interpretation of the published data with further experimental results suggests a mechanism for ionic reactions conforming with theory. Ion association and the influence of the dielectric constant of the solvent media on ion association are demonstrated.

Abstract No. 175

Zinc Standard Potential in Water-Organic Mixtures

Gerald Corsaro and H. L. Stephens, Dept. of Chemistry, University of Akron, Akron 4, Ohio

Cell emf measurements with $ZnCl_2$ in EtOH, meOH, and 1,4-dioxane-water mixtures provide extended tests of the Debye-Hückel theory, particularly as it concerns the measured cell potential and the dielectric constant of the solvent. Activity coefficients from observed data compare favorably with those calculated from theory. The measured value for the zinc standard electrode potential is confirmed from the potential-dielectric constant relationship.

Abstract No. 176

Uncommon Valency Ions and the Difference Effect

M. E. Straumanis, Dept. of Metallurgical Engineering, University of Missouri School of Mines and Metallurgy, Rolla, Mo.

The appearance of uncommon ions (on the basis of Faraday's law) in anodic electrolytic processes is sometimes reported in the literature. It is shown that the possibility of formation of such ions could be assumed because the difference effect, the essence of which is explained briefly, was disregarded. Only when the influence of the effect is taken into account, can conclusions be drawn concerning the appearance of uncommon valency ions in anodic processes.

Abstract No. 177

Streaming Potentials in Spherical-Grain Sands

C. E. Bleil (Present address: Research Staff, General Motors Corp., Detroit, Mich.) and Wm. Schriever, Dept. of Physics, University of Oklahoma, Norman, Okla.

Streaming potentials were observed in spherical-grain sands. Water and four concentrations each of NaI, Na_2SO_4, $MgSO_4$, and $MgCl_2$ were used. The streaming potential per unit pressure V/P was observed to deviate from existing theory and satisfy the following equation

$$V/P = (V/P)_\infty \, (1 + k/d + k^2/d^2) \exp(-k/d)$$

where $(V/P)_\infty$ is the value for large grain diameter d, and k is a constant.

Abstract No. 178

EDL Capacities at Solid Metal-Solution Interfaces

J. J. McMullen and Norman Hackerman, Dept. of Chemistry, University of Texas, Austin 12, Texas

An electric analog of the metal-solution interface was assumed, and E vs. t changes were deduced mathematically for application of a square wave voltage. Analysis was verified using actual electric components, and it was demonstrated that the component of capacity could be measured readily. The method was then applied with some success to each of the following metals in 1*N* Na_2SO_4: Hg, Pt, Ag, Cu, Al, and Ta.

Abstract No. 179

Impedence at Polarized Platinum Electrodes in Various Electrolytes

J. N. Sarmousakis and M. J. Prager, William H. Nichols Chemical Lab., New York University, University Heights, New York 53, N. Y.

Results of alternating current bridge measurements of the impedances of bright platinum in contact with 1*N* aqueous solutions of potassium chloride, potassium bromide, and potassium iodide as functions of polarizing voltage and alternating current frequency are presented. Data may be interpreted in a manner similar to that for experiments with acid solutions. A model is offered to explain, in a qualitative way, the dependence of impedance on frequency for the electrical double layer at rough surfaces.

Abstract No. 180

Catalytic Activity and Electronic Structure

Sigmund Schuldiner and J. P. Hoare, Electrochemistry Branch, Chemistry Div., Naval Research Lab., Washington 25, D. C.

Catalytic activity of α- and β-Pd and Au-Pd alloys for hydrogen-producing reactions in solution was determined. A relationship exists between this catalytic activity and heat of adsorption of atomic H. When the atomic combination step is rate-determining, catalytic activity increases as heat of adsorption of atomic H decreases. However, when the slow discharge step is rate-determining, catalytic activity increases as heat of adsorption of atomic H increases. An explanation is given for virtual independence of overvoltage on current density for the H/Pd $\sim$ 1 alloy. Catalytic activity of Au-Pd alloys decreases as Au/Pd atomic ratio increases, indicating that heat of adsorption of atomic H on Au is greater than on β-Pd.

Abstract No. 181

Mechanism of Hydrogen Producing Reactions on Palladium, IV. Electrochemical Kinetics of the α-Palladium-Hydrogen System in Acid Solutions

J. P. Hoare and Sigmund Schuldiner, Electrochemistry Branch, Chemistry Div., Naval Research Lab., Washington 25, D. C.

An experimental investigation of the electrochemical kinetics of the α-palladium-hydrogen system was made by means of a palladium bi-electrode. The *p*H effect on the anodic and cathodic polarization behavior was determined and related to bi-electrode mechanisms. Thickness of the bi-electrode had no significant effect. It was found that catalytic activity for the hydrogen-producing reactions on α-Pd was definitely less than that on β-Pd. The transference number of protons in the bi-electrode was determined. A comparison with a platinum bi-electrode was made.

Abstract No. 182

A Tentative Theory of Inhibitions of Aqueous Kolbe Electrolyses

G. W. Thiessen, Chemistry Dept., Monmouth College, Monmouth, Ill.

Three well-recognized structural interferences exist for the discharge of the ion $R.COO^-$ at bright Pt anodes in water. They are: (*a*) ethenoid, (*b*) cyclohexanoid, and (*c*) benzenoid, caused by vinyl, cyclohexyl, and phenyl residues in R. Ethenoid inhibition can be correlated with aqueous ionization constants but the others cannot. Ethenoid inhibition appears due to a chain-transmitted electrostatic induction. The others are assumed due to steric hindrance from close carboxylate-ring association at all chain lengths.

Abstract No. 183

Electrochemical Polarization, II. Ferrous-Ferric Electrode Kinetics on Stainless Steel

Milton Stern, Metals Research Lab., Electro Metallurgical Co., a Div. of Union Carbide and Carbon Corp., Niagara Falls, N. Y.

The oxidation-reduction kinetics of the ferrous-ferric sulfate system have been measured on a stainless steel surface. The data completely support theoretical equations which describe the potential-current relationships for such a system. The analysis applies to reversible electrodes and to corroding electrodes where the potential is determined by two intersecting activation overvoltage functions. Also, the analysis permits calculation of a number of electrochemical constants with a minimum number of experimental observations. The possibility of determining anode-to-cathode area ratios for corroding metals is discussed.

Abstract No. 184

Relation between Pitting Corrosion and the Ferrous-Ferric Oxidation-Reduction Kinetics on Passive Surfaces

Milton Stern, Metal Research Lab., Electro Metallurgical Co., a Div. of Union Carbide and Carbon Corp., Niagara Falls, N. Y.

Ferrous-ferric electrode kinetics have been studied on a variety of passive alloys. Activation polarization parameters are not markedly different for all the surfaces studied except for Ti where the exchange current is an order of magnitude smaller. The local anodic polarization curve for solution of metal under passive conditions was found to be extremely steep. This is suggested as typical behavior for the passive condition.

Abstract No. 185

Potential of an Electrode of a Voltaic Cell. A New Definition with Justification for the Use of Two Sign Conventions

J. B. Ramsey, Dept. of Chemistry, University of California, Los Angeles 24, Calif.

A definition of the potential of an electrode, basically different from that of G. N. Lewis and J. Willard Gibbs, is developed on the basis of a thermodynamic analysis of the conditions existing in an electrode system at equilibrium. The value of this potential, so defined, is shown to be (*a*) invariant in sign, and (*b*) equal in magnitude and opposite in sign to that of the Gibbs potential. A justification for two sign conventions is presented.

Abstract No. 186

The Silver and Thallium Oxide Coulometer

W. T. Foley, Chemistry Dept., St. Francis Xavier University, Antigonish, Nova Scotia

A simple and precise coulometer makes use of a dilute solution of silver and thallium salts buffered to a *p*H of about 9.5 with ammonium nitrate and ammonium hydroxide. The anode deposit is an oxide of thallium and the cathode deposit is an accurate measure of the quantity of electricity used.

Abstract No. 187

Voltammetric Studies at Constant Current in Fused Chlorides

J. M. Wood, Jr., Research and Engineering Dept., Ethyl Corp., P. O. Box 341, Baton Rouge 1, La.

Techniques have been developed for extending the methods of constant current voltammetry to fused chloride solvents at 600°C, and characteristic measurements have been made on several ions. New developments include a new reference electrode, a unique method of separating anode, cathode, and reference compartments, and the development of electrolytic methods for determining hydrogen and oxygen bearing materials in fused halides.

Abstract No. 188

Rates of Oxidation of Titanium in Fused Salt Baths

M. E. Straumanis and Ch. Chiou, Dept. of Metallurgical Engineering, University of Missouri School of Mines and Metallurgy, Rolla, Mo.

Under a layer of molten NaCl, metallic Ti corrodes quickly in the presence of air. It could be shown that the process observed is an oxidation with oxidation products formed of the approximate composition $TiO_{0.2}$. The weight loss-time as well as the rate-temperature relationship was linear, which occurs when oxygen (through the liquid salt layer) and cracks in the Ti-O solid solution coating have free access to the reaction surface. A steady breakdown of the TiO_x solid solution from the surface of Ti was observed, explaining the high rate of oxidation or corrosion. Activation energies of the process were calculated and some conclusions will be drawn in the light of Eyring's theory of rate processes.

Abstract No. 189

Cathode Potentials during the Electrodeposition of Molybdenum Alloys from Aqueous Solutions

D. W. Ernst and M. L. Holt, Dept. of Chemistry, University of Wisconsin, Madison 6, Wis.

Cathode potential measurements were used in an attempt to explain cathode reactions that result in electrodeposition of Mo alloys. Potentials were obtained by the direct method during electrolysis of aqueous ammoniacal citrate solutions containing sodium molybdate, and the sulfate of the codepositing metal, Fe, Ni, or Co. Results indicate that reduction of molybdate ion in presence of a codepositing metal is not accomplished in one step with 6 electrons, but with 1, 2, or 3 electrons depending on the co-metal and its oxidation state. It was also concluded that hydrogen is involved in molybdate reduction. A two-step mechanism for reduction of molybdate ion in presence of a co-metal is proposed and an explanation of why the co-metal must be Fe, Co, or Ni rather than such metals as Cr, Mn, Cu, or Zn is presented.

Abstract No. 190

Electrodeposition of Iron-Molybdenum Alloys

Albertine Krohn and L. O. Case, University of Michigan Ann Arbor, Mich., and N. W. Hovey, University of Toledo, Toledo 6, Ohio

Preliminary experiments indicated that the best Fe-Mo alloy deposits were obtained from solutions containing sodium molybdate, ferric chloride, and sodium pyrophosphate buffered with excess sodium bicarbonate. Efficiency was increased by rotating the cylindrical cathode between rubber wiper blades. A complete study of the variables showed it possible to electrodeposit Fe-Mo alloys which are bright and adherent in thicknesses of a few hundredths of a millimeter. No theoretical treatment is yet available to completely explain this type of codeposition.

FALL MEETING

at the

STATLER HOTEL

Buffalo, N. Y.

October 6, 7, 8, 9, and 10, 1957

Sessions will be scheduled on

Batteries
Corrosion
Electrodeposition (symposium on "Metal Powders")
Electrodeposition — Corrosion (Joint Symposium on "Corrosion of Electrodeposited Metals")
Electronics—Semiconductors
Electro-Organics
Electrothermics and Metallurgy

Abstracts for the Fall Meeting (*not exceeding 75 words in length*) must reach the Secretary's Office, 216 West 102nd Street, New York 25, N. Y., *not later than June 1, 1957* in order to be included in the program.

Indicate on abstract for which Division's symposium the paper is to be scheduled.

INDEX TO AUTHORS

(The number in the right hand column is the abstract number used in the Technical Program and in the Abstracts.)

	Abstract No.
Agar, J. N.	164
Albrecht, W. M.	120
Anders, F. J., Jr.	121
Andrew, K. F.	98, 125
Angel, Gösta	135
Apple, E. F.	32
Archer, R. J.	70
Arledter, H. F.	3
Arnold, Emil	171
Arpiarian, N	31
Atkinson, Gordon	143
Austin, J. M.	168
Aven, M. H.	34
Balkanski, M.	153
Banks, E.	54
Barrett, C. A.	127, 128
Beach, J. G	124
Bell, R. P.	142
Benson, K. E	56
Berberich, L. J.	5
Birchenall, C. E	106
Bleil, C. E	177
Blocher, J. M., Jr	116
Böckman, O. Chr	130
Booker, J.	152
Bounds, A. M.	82

	Abstract No.
Bourke, R. C.	116
Brännland, Rolf	135
Bridgers, H. E.	69
Brucker, G.	39
Buck, J. G.	81
Buehler, E.	68, 69
Butler, K. H.	41, 48
Cabrera, N.	107
Callinan, T. D.	1, 2
Campbell, A. N.	161
Campbell, I. E.	116
Card, C. S.	90
Carmichael, R. L.	112
Case, L. O.	190
Chapman, J. J.	4
Chiou, Ch	188
Clauss, F. J.	127, 128
Cole, J. C.	134
Comenetz, G.	99
Compton, V.	101
Compton, W. D.	51, 52
Connor, J. A.	12
Corsaro, Gerald	174, 175
Cox, A. P. M.	47
Croft, H. P.	111
Dahlerus, Stig	135
Dakin, T. W.	6
Darnell, J. R.	109
Davidson, J. H.	11
Davies, C. W.	149
Dearing, B. E.	133
Destriau, Georges	24
Dexter, J. F.	8
Dobischek, Dietrich	78
Donahue, D. J.	97
Duddling, R. W.	95
Dunbar, N. R.	18
Duncan, J. F.	154
Eigen, M.	151
Ernst, D. W.	189
Feinleib, Morris	131, 132
Fiorito, Louis	94
Foley, W. T.	186
Fox, R. J.	172
Frank, H. S.	148
Frankel, H. C.	17
Freitag, Harlow	171
Frisco, L. J.	4
Furst, M.	37
Gaines, G. B.	75
Glueckauf, E.	150
Goldey, J. M.	64
Goldstein, J. M.	91
Gosting, L. J.	166
Graham, P. R.	137
Gross, Wilbur	17
Guggenheim, E. A.	140
Gulbransen, E. A.	79, 98, 125
Gutowsky, H. S.	144
Gwathmey, A. T.	103
Haake, C. H.	40
Haase, A. P.	83
Hackerman, Norman	178
Hadley, C. P.	84
Hamer, W. J.	155
Hardy, A. E.	88
Harned, H. S.	163
Harris, W.	119
Hazel, J. F.	91, 94
Henderson, S. T.	46
Hermans, J. J.	158
Hersh, H. N.	53
Higbie, K. B.	110
Hoare, J. P.	180, 181
Holden, R. B.	101
Holmes, R. E.	83
Holonyak, N., Jr.	64
Holt, M. L.	189
Horton, W. E.	10
Hovey, N. W.	190
Hovorka, F.	152
Ivey, H. F.	22
Jaffe, P. M.	26
Jaffe, S.	27
Jaffee, R. I.	129
Janes, M.	136
Janz, G. J.	173
Jenny, D. A.	55
Jenny, R. K.	19
Johnson, P. D.	49
Kaiser, W.	62
Kallmann, H.	27, 30, 33, 35, 37, 38, 39
Keck, P. H.	62
Kepert, D. L.	154
Kilpatrick, Martin	159
Kirkpatrick, G. P.	88, 89
Kirkwood, J. G.	141
Klein, P. H.	14
Kling, H. T.	126
Klopp, W. D.	129
Knickerbocker, G. G.	9
Koelmans, H.	47
Kolk, A. J.	113, 117
Koller, L. R.	29
Konitzer, J. D.	50
Koury, F.	25
Kouwenhoven, W. B.	9
Kramer, B.	27, 30
Kraus, C. A.	142A
Kraus, K. A.	157
Krohn, Albertine	190
Lambe, John	51, 52
Lander, J. J.	74
Lange, E.	156
Lawson, A. A.	21
Lawthers, D.D.	122
Leach, R.	36
Levi, C.	61
Liao, T. W.	13
Longsworth, L. G.	165
Lorenz, E. J.	20
MacInnes, D. A.	162
Mallett, M. W.	120
Mark, A.	72
Markham, J. J.	50
Mason, D. R.	71
Mataré, H. F.	57, 58, 59
Mathes, K. N.	7
Matheson, R. A.	168
Mattler, J.	28
May, S. L.	114
Mayer, J. E.	139
McCready, N. W.	93
McKeag, A. H.	43
McMullen, J. J.	178
McNabb, W. M.	91
Moates, G. H.	65, 66
Mooney, R. W.	44
Moore, G. A.	86
Morehead, F. F., Jr.	23
Morone, J. P.	15
Navon, David	63
Nexsen, W. E., Jr.	75
Niedrach, L. W.	133
Nielsen, N. A.	105
O'Donnell, I. J.	166
Orenstein, A.	30
Parton, H. N.	168
Patrick, M. F.	16
Patterson, Andrew, Jr.	171
Payne, D., Jr.	96
Pollock, W. I.	121
Potter, R. M.	34
Prager, M. J.	179
Pray, A. R.	162
Promisel, N. E.	114
Rabatin, J. G.	90
Ramsey, J. B.	185
Ranby, P. W.	46
Raymond, P. L.	102
Reed, B.	57
Reed, J. F.	118
Rennert, J.	38
Richard, C. D., Jr.	82
Robertson, W. D.	104
Robinson, R. A.	169
Romans, J. B.	1, 2
Rubenstein, M.	54
Rubin, B.	65, 66
Rudy, W. G.	84
Ruka, R. J.	79
Rulon, R. M.	25
Sadowsky, M.	96
Salatka, J. W.	99
Sarace, J. C.	71
Sarmousakis, J. N.	179
Saulnier, T. A.	89, 97
Scatchard, George	138
Schaefer, D. L.	76
Schmidt, F. J.	83
Schmidt, P.	73
Schneider, W. F.	35
Schriever, Wm.	177
Schuldiner, Sigmund	180, 181
Schumacher, J. C.	137
Segall, B.	49
Semmel, J. W., Jr.	123
Shedlovsky, Theodore	170
Sibert, M. E.	113, 117
Sidran, M.	35
Sims, C. T.	129
Soldano, B. A.	172
Spedding, F. H.	143
Spencer, R. W.	93
Spruch, G. M.	27
Steinberg, M. A.	113, 117
Stephens, H. L.	174, 175
Stericker, Wm.	93
Stern, D. R.	137
Stern, Milton	183, 184
Stoeckert, A. J.	84
Stokes, R. H.	160
Stoughton, R. W.	172
Straumanis, M. E.	176, 188
Streicher, M. A.	105
Sucov, E.	33
Tak, M. G. A.	45
Tanenbaum, M.	60, 64
Taniguchi, Harry	173
Tews, J. L.	115
Theuerer, H. C.	69
Thiessen, G. W.	182
Thomas, M. J. B.	48
Thompson, P. T.	148
Tregellas-Williams, J.	42
Troxel, D. I.	12
Tufts, C. F.	80
Turner, E. F., Jr.	87
Ubbelohde, A. R.	146
VanArtsdalen, E. R.	147
van den Broek, C. A. M.	85
Van Rysselberghe, Pierre	167
Venema, A.	85
Vincent, G. D.	92
Waber, J. T.	108
Wanmaker, W. L.	45
Way, G. B.	18
Wegener, R.	59
Weiman, I.	61
Weiner, J. R.	65
Weinreich, O.	58
Weiser, K.	59A
Wernick, J. H.	56
Wessel, E. T.	122
Whelan, J. M.	69
White, J. E.	77
Whitman, C. I.	101
Wiedersich, H.	100
Williams, F. E.	49
Wleügel, J.	130
Wolfe, A. H.	118
Wolk, B.	81
Wood, J. M., Jr.	187
Yeager, E.	152
Yim, E. W.	131, 132
Yntema, L. F.	109
Young, T. F.	145

Current Affairs

DIVISION NEWS

Electrodeposition Division Symposia

The Electrodeposition Division is planning two symposia for the 1957 Fall Meeting of the Society in Buffalo.

Dr. Cloyd Snavely, Battelle Memorial Institute, Columbus, Ohio, is arranging for a series of papers on "Metal Powders," covering the production, use, and properties of electrolytic powders.

"Corrosion of Electrodeposited Metals" is being organized by Dr. F. A. Lowenheim, Metal & Thermit Corp., P. O. Box 471, Rahway, N. J., and Dr. Harry Copson, International Nickel Co., P. O. Box U, Bergen Point Station, Bayonne, N. J., as a joint symposium with the Corrosion Division.

Authors who wish to present papers on either or both subjects are invited to contact the respective chairmen promptly. Abstracts (*not exceeding 75 words in length*) must be submitted to the Society Headquarters Office *not later than June 1, 1957.*

Electronics Division

The Nominating Committee (C. W. Jerome, Chairman, F. J. Biondi, and H. C. Froelich) has selected the following nominees for officers during the 1957–59 term (2 years).

Chairman—H. Bandes, Sylvania Electric Products Inc., Woburn, Mass.

Vice-Chairman (Luminescence)—R. J. Ginther, Naval Research Lab., Washington, D. C.

Vice-Chairman (General Electronics)—C. T. Lattimer, RCA Tube Div., Chemical & Physical Lab., Marion, Ind.

Vice-Chairman (Semiconductors)—J. W. Faust, Jr., Westinghouse Research Labs., Pittsburgh, Pa.

Secretary Treasurer—M. F. Quaely, Lamp Div., Research Dept., Westinghouse Electric Corp., Bloomfield, N. J.

Although the term of office of the Secretary-Treasurer had one more year to run he has agreed to have his term end at the next business meeting of the Division, so as to permit the terms of all elective officers to begin and end together.

Each nominee has given assurance of his willingness to serve if elected.

The Bylaws of the Division provide that additional nominations may be made by petition signed by five members of the Division. Such petitions must be in the hands of the Chairman of the Nominating Committee before the election, and the nominees must have given assurance of their willingness to serve if elected.

The election will be held at the business meeting of the Electronics Division during the Spring Meeting of the Society in Washington, D. C., May 12–16, 1957.

M. F. Quaely, *Secretary-Treasurer*

Semiconductor Mailing List

The mailing list for the Semiconductor Symposia is being revised. Persons who are not already on the list but would like to be are requested to send their names and addresses to Dr. J. W. Faust, Jr., Westinghouse Research Labs., Beulah Rd., Churchill Boro., Pittsburgh 35, Pa.

E & M Division Columbium Symposium

The spotlight of technical inquiry is to be turned on columbium (niobium), a refractory metal of increasing economic importance, during the four sessions of a symposium arranged by the Electrothermics and Metallurgy Division for the Washington Spring Meeting of the Society.

In former years an addition to stainless steel and stainless welding rod, columbium now has several new and important applications. Among these are its use in nuclear reactors as a material of construction, as a major constituent of new high-temperature alloys, and in fabrication of special corrosion-resistant equipment. Discovery of a number of substantial ore bodies in recent years has assured an adequate future supply of this metal which, in nature, usually is found keeping company with tantalum, a metal it resembles greatly in chemical properties.

Papers describing the supply situation, extraction of the metal from its ores, preparation in a state of high purity, its mechanical, chemical, and physical properties, and its alloys and their characteristics are to be discussed. If sufficient interest develops, it is probable that the proceedings of this symposium will be published.

Originally suggested as a symposium subject by Dr. I. E. Campbell, Chief, Div. of Inorganic Chemistry and Chemical Engineering, Battelle Memorial Institute, the columbium program was formulated by Drs. Campbell and B. W. Gonser, Technical Director, and E. M. Sherwood, Assistant Chief, Div. of Inorganic Chemistry and Chemical Engineering, all of Battelle.

Notice to Members

According to the Constitution of the Society, Article III, Section 9, "Any member delinquent in dues after April 1 of each year shall no longer receive the Society's publication. . . ." Such delinquents will not receive the May issue of the JOURNAL. A reminder notice was mailed to delinquents about the middle of February and a final notice will be mailed about the middle of March.

SECTION NEWS

Boston Section

The fourth meeting of the Boston Section was held November 15, 1956 in the Graduate House and Main Building of Massachusetts Institute of Technology.

Having reported on the affairs of the Society, President Hans Thurnauer, Central Research Dept., Minnesota Mining & Manufacturing Co., presented a paper on "The High Temperature Materials Problem."

He stated that better weapons and the development of more efficient energy sources require the availability of materials which will withstand high temperatures, the stresses of supersonic flight, and are more abrasion resistant and oxidation resistant.

The stability and strength of ceramic materials under high temperature con-

ditions appears especially promising, if their undesirable properties of brittleness, poor ductility, and sensitivity to thermal shock can be circumvented.

It has been demonstrated that certain electronic components, made chiefly of ceramics, can operate satisfactorily above 500°C. Such components are micro-miniature ceramic vacuum tubes, hermetically sealed resistors, also capacitors and transformers. Even motors with ceramic insulation can operate at 500°C and higher.

Our help to under-developed countries may consist of supplying them with economical atomic energy. Since present-day power reactor designs are neither cheap nor efficient, we may think of raising efficiency by operating atomic reactors at higher temperatures, provided we can find suitable ceramic reactor materials.

The technical program of the Boston Section meeting scheduled for March 21, 1957 will offer "New Sources of Electrical Energy, I. The Bell Solar Battery."

CHARLES LEVY, *Secretary*

Extended Abstracts Booklets

The Electronics Division will again publish an "Enlarged Abstracts" booklet for the Spring 1957 convention of the Society at Washington. The booklet will have 1000-word abstracts of the papers to be presented before the Electronics Division in its symposia on

Luminescence
Semiconductors
Instrumentation
Thermionic Cathodes
Screen Application

The abstracts will contain pertinent information and experimental data given in the papers, and will provide these details before publication, thus aiding workers in the field. The abstracts will be "printed but not published."

The booklets should be available by about April 15; the price will be $2.00.

Copies of the 1956 "Enlarged Abstracts" booklet of the San Francisco Meeting are still available at $2.00 per copy.

Checks should be made payable to: Electronics Division, The Electrochemical Society.

Orders should be sent to:

Martin F. Quaely
℅ Westinghouse Electric Corp.
Research Dept., Lamp Div.
Bloomfield, N. J.

* * *

The Theoretical Electrochemistry Division is making available extended abstracts of the symposium sponsored by the Division and the National Science Foundation on the Structure of Electrolytic Solutions (Electrolytes), as well as the two general symposia, for the Spring 1957 Washington Meeting.

Copies of the booklet can be obtained, at $3.00 each, from

Dr. Ralph Roberts
3308 Camalier Drive
Washington 15, D. C.

Philadelphia Section

The January 10 meeting of the Philadelphia Section was held in Harrison Lab., with Dr. Erik Blomgren as the speaker. He opened his talk with greetings from the electrochemists of Sweden, where, he said, the JOURNAL of The Electrochemical Society is well known and respected. He then gave a brief history of electrochemistry in Sweden, including some of the contributions from the University of Uppsala, where he has been doing research work for the past ten years.

In the technical portion of his talk, Dr. Blomgren discussed the use of electronic instrumentation in electrochemistry. The development of negative feedback circuits made possible the precise measurement and control of both voltage and current. They have been applied to many precise electronic instruments, such as continuous reading *p*H meters, polarographs, automatic titrating apparatus, and other more specialized techniques used in electrochemical research.

The cathode ray oscillographic polarograph can make a complete chemical analysis in less than 1 sec. Such an instrument was developed by Dr. Blomgren and is now being manufactured in Sweden. The oscillograph has also greatly aided the study of overvoltage. Since activation, concentration, and ohmic overvoltage all have different rates of decay, a single cathode ray oscillographic tracing of a decaying electrode potential can yield the magnitude of each of these components.

H. C. MILLER

Washington-Baltimore Section

At the November 1956 meeting the Section had the pleasure of having Hans Thurnauer, President of The Electrochemical Society, as guest speaker. He began by discussing the organization of the national Society. His technical speech was entitled "The High Temperature Materials Problems."

Mr. Thurnauer described how a solar heated boiler would solve many problems in India. He said that the development of small reactors would be a useful source of power in the undeveloped areas of the world. To accomplish these goals a radiation-resistant material must be found which

Battery Life Symposium Papers

The life of lead-acid batteries was discussed at the 1956 Cleveland Meeting in a symposium sponsored by the Battery Division. A booklet, "Life Testing of Automobile Batteries and Related Subjects," has been prepared containing the complete text and illustrations along with a summary of the discussion which followed.

This booklet can be obtained by sending $2.00 to E. J. Ritchie, Secretary, Battery Division, Eagle Picher Co., Joplin, Mo.

Papers included in this 96-page booklet are:

"Appearance of Battery Components at the End of Life Under Laboratory Test" by B. Agruss

"Effect of Normal Car Service on the Intermediate and Final Periods of Lead Storage Battery Performance" by D. Haskell

"The Correlation of Laboratory Life Tests with Automotive Service Tests of Lead-Acid Batteries" by J. F. Schaefer

"The Effect of Temperature on the Cycling Life of Lead-Acid Storage Batteries" by J. F. Macholl and A. G. Koch

"The Effect of Arsenic and Silver in Grid Alloy on Storage Battery Life in Field Tests and Fleet Service" by Howard Stoertz

"Pulse Maintaining of Storage Batteries" by J. B. Godshalk

"Positive Post Corrosion in Lead-Acid Cells" by Otto H. Bauer

can stand temperatures up to 1200°C. Ceramics may replace beryllium, uranium, and zirconium metals now used in reactors. Mr. Thurnauer also mentioned the use of diamond transistors at these high temperatures.

At the December meeting of the Section, D. T. Ferrell, Jr., announced his resignation as Chairman because he is leaving Washington to accept a position with the American Machine and Foundry Co. in Raleigh, N. C. Jeanne Burbank will serve as Chairman for the remainder of the year.

T. H. Orem, National Bureau of Standards, spoke on "Corrosion of Aluminum Single Crystals." When monocrystalline aluminum is corroded by a 15% sodium hydroxide solution, the attack is fastest in a direction normal to the cubic planes and slowest in a direction normal to the octahedral planes. The reverse is true when the corrosive medium was aqua regia containing a small amount of HF.

J. B. Romans, Naval Research Lab., spoke on "The Electrical Properties of Some Partially Fluorinated Esters" and "A New Dielectric Liquid for Impregnating Fixed Paper Capacitors." The electric moments of six partially fluorinated esters were reported. The materials studied were liquids at room temperature and were known to be chemically inert and thermally stable. All six esters were found to be highly polar compounds exhibiting marked tendencies to associate molecularly; they possessed dipole moments of the order of 2.8 to 3.8 $\times 10^{-18}$ esu-cm.

Fixed capacitors, using kraft paper as the solid dielectric and bis (1H,1H,7H-dodecafluoroheptyl) 3-methylglutarate (PFE-774) as the impregnant, have capacitance to volume ratios higher than similar capacitors impregnated with pentachlorodiphenyl. Furthermore, the change in capacitance with temperature is less than 4% within the range −55° to 85°C. Such capacitors have passed military specification MIL-C-25A for accelerated aging by withstanding 85°C and 130% rated voltage for 250 hr. Because the impregnant is unusually flame resistant, thermally stable, of low viscosity, and does not irritate the skin or cause rubber and plastics to swell and become tacky, this partially fluorinated ester is considered to be worthy of commercial development.

GWENDOLYN B. WOOD, *Secretary*

NEW MEMBERS

In January 1957 the following were approved for membership in The Electrochemical Society by the Admissions Committee:

Active Members Sponsored by a Patron or Sustaining Member

WILLIAM H. AILOR, JR., Reynolds Metals Co., Richmond 19, Va. (Corrosion)

FRANK CHRENCIK, Diamond Alkali Co., 300 Union Commerce Bldg., Cleveland 14, Ohio (Industrial Electrolytic)

THOMAS W. CLAPPER, American Potash & Chemical Corp., Box 55, Henderson, Nev. (Battery)

NELSON J. EHLERS, Columbia Southern Chemical Corp., No. 1 Gateway, Pittsburgh 22, Pa. (Industrial Electrolytic)

ERWIN C. HANDWERK, American Metal Co., Ltd., 61 Broadway, New York 6, N. Y. (Electrothermics & Metallurgy)

ROBERT W. KRAFT, Aluminum Co. of Canada, Ltd., P. O. Box 375, Kitimat, B. C., Canada (Industrial Electrolytic)

GEORGE W. WARD, Research Dept., Bethlehem Steel Corp., Bethlehem, Pa. (Electrodeposition)

GEORGE M. YOUNG, Aluminum Co. of Canada, Ltd., 1700 Sun Life Bldg., Montreal 2 Que., Canada (Electrothermics & Metallurgy)

Active Members

ROGER G. BATES, National Bureau of Standards, Washington 25, D. C. (Theoretical Electrochemistry)

HUBERT F. BAUMAN, Armour Research Foundation, Technology Center, Chicago 16, Ill. (Battery)

VINCENT E. BOWER, National Bureau of Standards, Washington 25, D. C. (Theoretical Electrochemistry)

MARTIN S. FRANT, AMP Incorporated, Eisenhower Blvd., Harrisburg, Pa. (Corrosion)

HARRY GILMAN, General Aniline Works; Mail add: 17 Post Lane, Levittown, Pa. (Corrosion)

THEO HEUMANN, Institut fur Physikalische Chemie der Universitat Munster; Mail add: Schloss platz 4, Munster, i.W., Germany (Corrosion, Theoretical Electrochemistry)

ALPHONSE M. HEUNINCKX, Gould-National Batteries, Inc., 35 Neoga St., Depew, N. Y. (Battery, Electrodeposition, Theoretical Electrochemistry)

WILLIAM E. ISHLER, Dept. #433, General Electric Co., Nela Park, Cleveland 12, Ohio (Electronics)

HERMAN A. JOHANSEN, Westinghouse Research Labs., Pittsburgh 35, Pa. (Electrothermics & Metallurgy)

JOSHYO KINOSHITA, Kaiser Aluminum & Chemical Corp.; Mail add: 1168 Cherry, San Jose, Calif. (Electrothermics & Metallurgy, Industrial Electrolytic)

EDWARD M. KLOPP, General Dry Batteries; Mail add: "Ty-Llawydd," R.D. 2, Medina, Ohio

ERICH LANGE, Institut fur Physikalische Chemie der Universitat Erlangen, Schuhstrasse 19, Fernruf 3061, Germany (Theoretical Electrochemistry)

WILLIAM B. MASSON, General Motors of Canada, Oshawa, Ont., Canada

ROBERT S. I. MCLAREN, Shawinigan Chemicals Ltd., Shawinigan Falls, Que., Canada (Electrothermics & Metallurgy)

WILLARD R. SCOTT, JR., Crest Research Labs., Inc.; Mail add: 1421 West 9 St., Santa Ana, Calif. (Corrosion)

THEODORE SHEDLOVSKY, Rockefeller Institute for Medical Research, York Ave. & 66 St., New York 21, N. Y. (Theoretical Electrochemistry)

ARTHUR R. SLOMAN, Associated Pulp & Paper Mills Ltd., P. O. Box 201, Burnie, Tasmania, Australia (Industrial Electrolytic)

JOHN R. SMITH, Weirton Steel Co., Quality Control Bldg., Weirton, W. Va. (Corrosion, Electrodeposition)

FRED STEVENS, Lancy Lab.; Mail add: Mounted Route 7, Ellwood City, Pa. (Electrodeposition)

LEWIS F. URRY, National Carbon Research Lab.; Mail add: 5491 Stumph Rd., Parma, Ohio (Battery)

ERNEST W. YIM, Kaiser Aluminum & Chemical Corp.; Mail add: 744 Camphor Way, Palo Alto, Calif. (Industrial Electrolytic, Theoretical Electrochemistry)

Associate Member

JEANNE R. PISCHEL, General Dry Batteries; Mail add: 13355 Carrington Ave., Cleveland 11, Ohio (Battery, Corrosion)

By action of the Board of Directors of the Society commencing January 1, 1956, all prospective members must include first year's dues with their applications for membership.

Also, please note that, if sponsors sign the application form itself processing can be expedited considerably.

Reinstatements to Active Membership

JACK M. NOY, Quebec Iron & Titanium Corp., P. O. Box 40, Sorel, Que., Canada (Electrothermics & Metallurgy)

WILLIAM F. SEYER, University of California; Mail add: 474 Halvern Dr., Los Angeles 49, Calif. (Corrosion, Theoretical Electrochemistry)

Transfer from Student Associate to Active Membership

RICHARD A. STREHLOW, Oak Ridge National Lab., Y-12 Plant, Oak Ridge, Tenn. (Electro-Organic)

Transfers from Associate to Active Membership

EDWARD A. KURE, Automotive Div., Electric Storage Battery Co., 246 E. 131 St. (Box 6266), Cleveland 1, Ohio

FRANK W. MARTIN, Raytheon Mfg. Co.; Mail add: 30 So. Central Ave., Wollaston, Mass. (Electrodeposition, Electronics)

WILLIAM N. REDANZ, Union Carbide & Carbon Corp.; Mail add: 1319 Linwood Ave., Niagara Falls, N. Y. (Electrothermics & Metallurgy, Industrial Electrolytic, Theoretical Electrochemistry)

Deceased Reported during December 1956

CHARLES F. RAMSEYER, New York, N. Y.

PERSONALS

THOMAS D. PARKS has been elected Vice-President—Research of Clorox Chemical Co., Oakland, Calif. Prior to joining the organization as Director of Research in 1955, Dr. Parks was Chairman of the Dept. of Chemistry and Assistant Director of the Physical Sciences Div. of Stanford Research Institute.

H. S. NEWHALL has been named to the post of Chief Development Engineer in the Engineering and Construction Dept. of Electro Metallurgical Co., A Div. of Union Carbide and Carbon Corp., in Niagara Falls, N. Y. Mr. Newhall will be responsible for the supervision of the development and service engineering of the department.

PAUL H. KECK has been appointed Manager of the solid state physics branch of the Research Labs. of Sylvania Electric Products Inc., Bayside, N. Y. He is assuming responsibility for research in semiconductors, luminescence, and other solid state materials and devices. Previously he was Deputy Chief of the Chemical Physics Branch, Army Signal Corps Engineering Labs., Fort Monmouth, N. J.

WILLIAM J. ROSENBLOOM has been appointed Director of Engineering for the Chemical Construction Corp., New York City, a subsidiary of Electric Bond and Share Co. He developed the electrolytic hydrogen cell and the atmospheric ammonium sulfate process used in many of the plants designed and engineered by Chemico.

T. D. CALLINAN has left the Naval Research Lab., Washington, D. C., to accept a position with I.B.M. at Poughkeepsie, N. Y.

D. T. FERRELL, JR., has joined the American Machine and Foundry Co., Raleigh, N. C. Formerly he had been with the Naval Ordnance Lab. in Washington, D. C.

WILBERT A. TAEBEL has been appointed Engineering Manager of the lamp parts department of the Westinghouse Lamp Div., Bloomfield, N. J. In his new position he will be responsible for engineering and development work on lamp parts including lamp bases, tungsten and molybdenum including powder, wire, sheet, and rod, chemicals, phosphor, glass tubing, nickel iron wire, and argon gas.

ERWIN F. LOWRY

Dr. Erwin F. Lowry, one of the nation's leading authorities on lighting and manager of the research engineering laboratories of the Lighting Div. of Sylvania Electric Products Inc. at Salem, Mass., died suddenly at his home on January 2. He was 65 years old.

He was born in Ridgeway, Mich., on January 22, 1891. He studied at Ohio Wesleyan University, receiving his A.B. degree in 1914 and his A.M. two years later. In 1923 he received his Ph.D. in physics from Ohio State University. From 1914 to 1925 he taught physics at Ohio Wesleyan, the University of Pittsburgh, and Ohio State, respectively.

Before joining Sylvania Dr. Lowry had been director of research at Flexolite Co. and Continental Electric Co. and from 1925 to 1938 was a research engineer with Westinghouse Electric Corp.

He joined Sylvania in 1940 as a senior engineer in the fluorescent engineering department of the company's Boston St., Salem, lighting facility. Progressing through engineering and management posts he became manager of fluorescent engineering three years later, and manager of the research laboratories in 1949.

Long a leader in lighting research Dr. Lowry in 1954 was awarded the highest honor in the field of illumination, the Gold Medal of the Illuminating Engineering Society. He was the first physicist engaged in light source research chosen to receive the medal. He had pioneered in three phases of lighting—cathode research, fluorescent lighting, and the new light source, electroluminescence.

He had 30 patents to his credit, almost all related to gaseous discharge devices, especially cathodes. Several others still are pending on fluorescent lamps and in electroluminescence.

Dr. Lowry was a past chairman of the Luminescence Group of the Electronics Division of The Electrochemical Society. He was also a Fellow of the Illuminating Engineering Society, and a member of the American Physical Society, the American Institute of Electrical Engineers, the U. S. National Commission on Illumination, the Societe Francaise de Ingenieurs Techniciens du Vide, and other scientific societies.

He is survived by his wife, Emily; a daughter, Mrs. Barbara Louise Johns of California; and two brothers, Earl M. of Rochester, N. Y., and Raymond F. of Michigan.

NEWS ITEMS

New Sustaining Member

The Chemical Research Dept., Kaiser Aluminum & Chemical Corp., Permanente, Calif., recently became a Sustaining Member of The Electrochemical Society.

Dielectrics Section Established at N.B.S.

The Dielectrics Section, a new unit for fundamental investigations of the dielectric properties of matter, has been established at the National Bureau of Standards. Part of the Electricity and Electronics Div., the new section will be headed by Dr. John D. Hoffman. A

(*Continued on page 83C*)

The books...

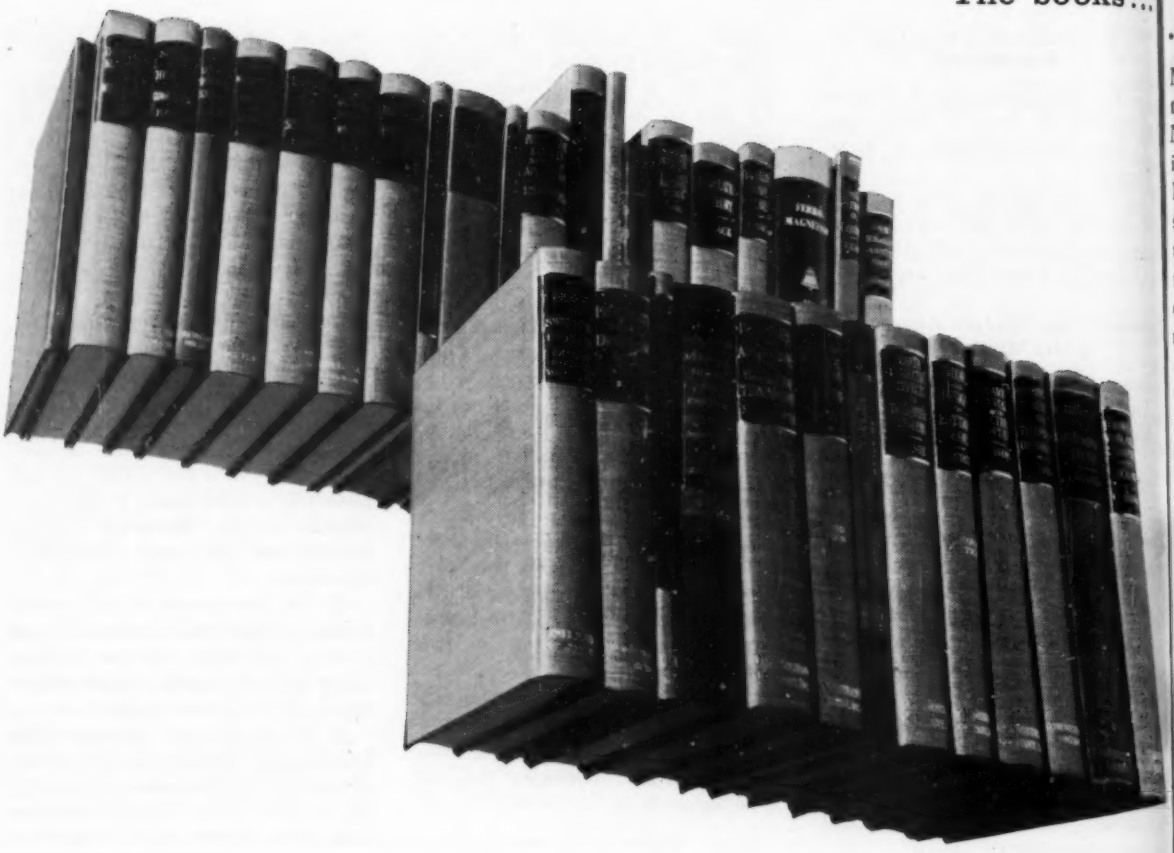

How the scientific world shares in fruits of the telephone art

In their work to improve telephony the scientists and engineers of Bell Telephone Laboratories make important findings in many sciences. They thoroughly report these findings in professional journals and magazines. But sometimes, as knowledge accumulates in a vital field, a "treatment in depth" is prepared in book form.

Bell Laboratories authors have written 36 books to date and others are in preparation. Many have become classics in the Laboratories' primary field of communications. Many have become standard works of wide application because they provide a fundamental guide for technologies in other fields. For example, the design of automatic switching systems is of primary importance in computers; statistical quality control provides the indispensable basis for economical manufacture. Through their books these scientists and engineers and the Laboratories attempt to repay benefits they receive from the published works of others.

The pictures on the opposite page show some Bell Laboratories authors of technical books. A complete listing of titles may be obtained by sending in this coupon.

Publication Department, Dept. 23
BELL TELEPHONE LABORATORIES
463 West Street, New York 14, N. Y.
Gentlemen:
Please send me a listing of titles, authors and publishers of books written by Bell Telephone Laboratories authors.

Name.....

Street.....

City.....State.....

BELL TELEPHONE LABORATORIES
World center of communications research and development

...the authors

Most of the books written by Laboratories authors are published by D. Van Nostrand Company. Other publishers include John Wiley & Sons and McGraw-Hill. Subjects include speech and hearing, mathematics, transmission and switching circuits, networks and wave filters, quality control, transducers, servomechanisms, quartz crystals, capacitors, visible speech, earth conduction, radar, electron beams, microwaves, waveguides, antennas, traveling-wave tubes, semiconductors, ferromagnetism.

Harold S. Black, B.S. in E.E., Worcester Polytechnic Inst., author of "Modulation Theory."

John R. Pierce, Ph.D., California Inst. of Tech., author of "Traveling-Wave Tubes."

Richard M. Bozorth, Ph.D., California Inst. of Tech., author of "Ferromagnetism."

W. Thornton Read, M.S., Brown University, author of "Dislocations in Crystals."

Hendrik W. Bode, Ph.D., Columbia University, author of "Network Analysis and Feedback Amplifier Design."

Walter A. Shewhart, Ph.D., University of California, author of "Economic Control of Quality of Manufactured Product."

(*Continued from page 81C*)

member of the American Physical Society, American Chemical Society, Washington Academy of Sciences, and Sigma Xi, Dr. Hoffman has written a number of papers in his field and is the holder of a patent for a process of recovering alumina from clay.

The primary purpose of the new section will be to augment the present knowledge in the field of dielectrics by conducting experimental and theoretical studies on substances which act as electrical insulators.

Union Carbide Research Institute Formed

The formation of the Union Carbide Research Institute to engage in basic scientific research has been announced by Morse G. Dial, President of Union Carbide and Carbon Corp. It will be located on the corporation's Westchester property near Tarrytown, N. Y.

The Institute will be under the administration of Dr. Augustus Kinzel, Vice-President—Research of Union Carbide. Dr. E. R. Jette, formerly head of the Chemistry and Metallurgy Div. at Los Alamos Scientific Lab., New Mexico, has been appointed the Director of the Institute. His assistants are: Dr. S. R. Aspinall, formerly with the U. S. Office of Naval Research, and Dr. A. J. Stosick, formerly Division Chief of the Rockets and Material Div. of the Jet Propulsion Labs. at the California Institute of Technology.

A major purpose of the new Research Institute will be to contribute to the store of fundamental knowledge by studying the physical and chemical behavior of matter under ordinary as well as extreme conditions of pressure and temperature. This work at the Institute will complement and extend the basic research now being carried on in the existing research laboratories of Union Carbide and Carbon Corp.

Enrico Fermi Professorship to be Established at University of Chicago

Plans to endow an Enrico Fermi Distinguished Service Professorship at the University of Chicago in memory of the world-renowned nuclear physicist were announced recently by Dr. M. J. Kelly, President of Bell Telephone Labs.

Dr. Kelly will serve as Chairman of a national committee to establish the Professorship.

The Professorship, to be established at the University's Institute of Nuclear Studies, is designed to perpetuate and memorialize Dr. Fermi's scientific contributions. He was both teaching and conducting research at the Institute at the time of his death in 1954.

Serving with Dr. Kelly will be Walker L. Cisler, President of Detroit Edison Co.; Dr. Crawford H. Greenewalt, President, E. I. du Pont de Nemours and Co.; and Admiral Lewis Strauss, Chairman of the United States Atomic Energy Commission.

Honorary members are The Honorable Clare Boothe Luce, former American Ambassador to Italy, and His Excellency Dr. Manlio Brosio, Italian Ambassador to the United States. In addition, an extensive Advisory Sub-Committee will be formed.

Porosity Detection in Plated Coatings

Recently, the National Bureau of Standards has developed a nondestructive procedure for ascertaining both the size and position of pores in electrodeposited coatings.[1] The method involves photographing an electroplated specimen exposed to radiation.

The present work was carried out for the American Electroplaters' Society by F. Ogburn of the Bureau staff and Margaret Hilkert of the Society's research fellowship at the Bureau.

In determining the location and size of pores, the specimen, a flat sheet of plated metal a few thousandths of an inch thick, is placed on a photographic film with the coating against the film emulsion. The assembly is held in a cardboard cassette, and the basis-metal side of the specimen is exposed to x-rays or radiation from a radioactive material. To insure good contrast, the x-radiation used must be soft. This requirement of low-energy x-rays limits the thickness of the basis material to several thousandths of an inch, since thicker metal absorbs too much of the x-ray beam and requires too long an exposure time. Radioactive iron, nickel, or cobalt held against the plated specimen in a cassette are also adequate sources of radiation.

After a suitable exposure time the film is removed and developed, satisfactory radiographs result from a 3- or 4-min exposure to an x-ray machine, and from a 24-hr exposure to 1μc of radioactivity. Wherever a pore existed in the coating, a black spot appears on the developed film. A fine-grain in-

[1] F. Ogburn and M. Hilkert, *Ann. Proc. Tech. Sessions Am. Electroplaters' Soc.*, p. 256 (1956).

dustrial x-ray film gives the most readable radiograph.

This radiographic method detects pits, voids, and inclusions in the coating to the order of 0.001 in. in diameter. Discontinuities in the basis metal may also be determined by radiographing the metal before plating.

BOOK REVIEWS

ELECTROCHEMICAL AFFINITY. STUDIES IN ELECTROCHEMICAL THERMODYNAMICS AND KINETICS by Pierre Van Rysselberghe. Published by Hermann & Cie., Paris, 1955. 109 pages. Price, 1250 F.F.

This monograph is an abridgement of the 1936 "Affinity" by De Donder and Van Rysselberghe, but now, as its title indicates, it is devoted to Electrochemistry.

It has been written because, "The majority of textbooks and treatises of Physical Chemistry and Electrochemistry are incomplete, oversimplified and often strangely silent concerning some of the most fundamental points of the subject"; further, "a rational treatment requires the use of the thermodynamics of irreversible processes. The few presentations from this point of view [Prigogine (1947), de Groot (1951)] are still fragmentary and some of them suffer perhaps from the defects of being too formal and of not providing the practical electrochemist with a sufficiently clear link with what he observes and measures. Remarks and criticisms of electrochemists are invited so that they may contribute toward the establishment of a more definitive treatment."

With this ambitious introduction the author proceeds to give a detailed exposition of electrochemical processes and definitions. The affinity of a process is measured by the maximum useful work the process can perform. It amounts to the decrease in the Helmholtz or Gibbs' Free Energy functions, depending upon whether or not volume or pressure is held constant under the important restriction of constant temperature.

By introducing the concept of the degree of advancement of a reaction, De Donder and Van Rysselberghe emphasized that these functions may then be considered as valid and existing at any instantaneous stage in the progress of the reaction. This treatment is an advance over that of Gibbs, who considered only the initial and final states and not the succession of quasi-equilibrium states of the process. Van Rysselberghe has also pointed out that this concept leads to a clearer understanding of the meaning of the operation designated by Δ in the Lewis and Randall system. Modern Thermodynamics is indebted to these authors for these clarifications.

However, once the physical meaning of Δ has been clarified, it hardly seems necessary to continually burden the presentation with the complicated mathematical notations which this development involves.

The present reviewer believes that i is this involved mathematical characte of the writings of the Belgian Schoo which has prevented an earlier and more general acceptance of the good points of their system. Although the present monograph exhibits some improvement of presentation, nevertheless mathematical prolixity still persists in the all too frequent repetition and display of equations which differ only in the obvious sign of an inequality or an equality.

The author recognizes that the "uncompensated heat" of Clausius and the corresponding time derivative which was introduced in the monograph of 1936, as the term "power of irreversibility," constitutes *perhaps* an unfortunate terminology which has not been clearly understood.

"Subsequently, Prigogine (1947) emphasized the importance of the concept of *entropy production* and showed that this more suggestive and concrete concept replaces the uncompensated heat in the second law and its various consequences." Entropy production is accordingly employed in the present monograph *as an additional means* of expressing the dissipation of energy in irreversible processes. This reviewer would suggest that readers of this monograph might perhaps understand better the author's meaning and be more receptive to the consequences if he did not leave them with the impression that "entropy production" as a means of elucidating the gist of the second law has been the exclusive development of the Belgian School. Entropy production is an improvement in presentation that should be credited to many authors prior to 1947, beginning with R. C. Tolman (1922); Tolman and Fine (1948); P. S. Epstein, "Thermodynamics" (1937); J. N. Brønsted (1936–46), *see Phil. Mag.* (1940) and *Roy. Dan. Acad.* (1941); C. Eckart (1940); and others.

The real reason that entropy production, $\delta S''$, is preferable to the uncompensated heat of Clausius, $\delta Q'' = T\,\delta S''$, is not, as the author says, that the concept of entropy is "more concrete" than that of "heat," but rather that entropy is the simpler of the two concepts. $\delta Q''$ is the product of $\delta S''$, an extensive quantity, and the *final temperature* T, an intensive property, of the reservoir to which all of the entropy production at the varying temperatures involved in the complex process of heat conduction, is ultimately transferred and collected in a nonisothermal process.

1956 Directory

The 1956 Directory of Members of the Electrochemical Society is now available. The Directory contains an alphabetical and geographical list of members of the Society as of March 1, 1956, and a list of Patron and Sustaining Members, Past Presidents, and winners of Society prizes and awards.

Members who wish to receive the Directory are requested to fill in and return the order form below, accompanied by check, to Society Headquarters, 216 West 102 St., New York 25, N. Y.

Please send_____copy(ies) of the 1956 Membership Directory to:

Name_____

Company_____

Street_____

City_____ Zone____ State_____

Attached is check for $_____ for Directory. (Single copies cost $2.00.)

Although this monograph is restricted primarily to isothermal processes, in which case heat and entropy differ only by the simple constant factor of proportionality, T, the last chapters attempt a treatment of the nonisothermal processes occurring in thermal cells (pp. 99–109). Part I (pp. 15–44) deals with reversible galvanic and electrolytic cells and with irreversibility arising solely from the creation of Joule heat from internal and external resistances. It is not until we reach Part II (pp. 45–76) that we encounter irreversibility at the electrodes as exhibited by polarization and overpotentials that require the development of equations of more recent vintage. The closing paragraphs on applications to corrosion problems are interesting.

Parts III and IV deal with simultaneous half cell reactions at the same electrode and their chemical kinetics. Here Tafel's relation between overpotential and current density is introduced. Good use is then made of the Onsager reciprocity relations (1931) which are responsible for most of the progress that has been made recently in the field of irreversible processes. A study of this chapter should be profitable for any electrochemist, but the reviewer advises the reader to study and compare with De Groot. Part V is devoted to nonisothermal processes as noted above. It is obvious that much remains to be done in this field of irreversible processes.

The author has performed a useful service in writing this monograph because all electrochemists should profit from reading it, if only to clarify their own thoughts by seeing familiar equations developed along somewhat different paths. The focusing of attention upon the irreversible character of most electrochemical processes is commendable, even if the treatment is incomplete.

VICTOR K. LA MER

TRANSPORT AND ACCUMULATION IN BIOLOGICAL SYSTEMS by E. J. Harris. Published by Academic Press Inc., New York, 1956. ix + 291 pages, $7.80.

Although quite incidental to Dr. Harris' main theme, his book will be a revelation to those that may yet picture biologists as people who, armed with collecting nets, stalk flitting butterflies in a sun-drenched meadow. For the author beautifully exemplifies in this monograph the great difference in, as well as the fruitfulness of, the approach to the solution of certain problems of life when based on physics and physical chemistry. The problem of interest here is permeability: "the rate, and mechanism, of passage of chemical substances through any boundary, be it cell wall or sheet of cells." And this is presented in a text that fairly bristles with rigorous and elegant applications of theories of thermodynamics, diffusion, and electrochemistry, and their special mathematical elaborations, that are essential to the proper exposition of the subject. Though very involved in the theoretical aspects, the author also gives thorough attention to the purely experimental work of his field, which is based on a wide variety of techniques, ranging from the relatively simple methods for determining osmotic pressure, to the use of radioactivity for the measure of the flux of tagged substances across membranes (much used by the author himself in numerous research articles).

The text critically discusses all the important most recent work dealing with the transport of both ions and nonelectrolytes across membranes of many different types such as found in yeast and egg cells, mitochondria, gastric and kidney mucosa, and muscle and nerve fibers in a state of excitation as well as at rest. The reader will be impressed by the fact that there are so many evidently qualitatively different permeability mechanisms, some of them cell-specific. Dr. Harris, however, always stresses fundamentals insofar as present evidence permits. Very impressive is the meticulous analysis of the theory of all the possible electrochemical mechanisms of the electrolytic heterogeneous systems that serve as models of the complex processes involved in the transport of ions across biological membranes. Detailed evidence, however, is discussed which proves in certain cases, e.g., the transport of Na^+ in many cells, that movement of substances can take place in a direction against their electrochemical gradients, and that therefore there must be a dependence on metabolically released energy to drive such uphill processes. Though ignorance prevails regarding actual mechanisms of such activity, Dr. Harris' perspicacious analyses of cases of this sort define the nature of our ignorance and highlight the need for further research on the coupling of energy released in an exergonic chemical reaction with the transport of a particle. Advances in the solution of this general problem will be of fundamental importance in biology and they will also

MANUSCRIPTS AND ABSTRACTS FOR FALL MEETING

Papers are now being solicited for the Fall Meeting of the Society, to be held at the Statler Hotel in Buffalo, N. Y., October 6, 7, 8, 9, and 10, 1957. Technical Sessions will be scheduled on Batteries, Corrosion, Electrodeposition (symposium on "Metal Powders"), Electrodeposition—Corrosion (Joint Symposium on "Corrosion of Electrodeposited Metals"), Electronics (Semiconductors), Electro-Organics, and Electrothermics and Metallurgy.

To be considered for this meeting, triplicate copies of abstracts (*not to exceed 75 words in length*) must be received at Society Headquarters, 216 West 102nd St., New York 25, N. Y., *not later than June 1, 1957. Please indicate on abstract for which Division's symposium the paper is to be scheduled.* Complete manuscripts should be sent in triplicate to the Managing Editor of the JOURNAL at the same address.

* * *

The Spring 1958 Meeting will be held in New York City, April 27, 28, 29, 30, and May 1, 1958, at the Statler Hotel. Sessions will be announced in a later issue.

provide new mechanisms of great interest to basic electrochemistry.

ALEXANDER SANDOW

ANNOUNCEMENTS FROM PUBLISHERS

SPECTROGRAPHIC METHODS FOR ANALYZING ZIRCONIUM HYDRIDE, ZIRCONIUM METAL, ZIRCONIUM-NICKEL ALLOYS, S. Weisberger, Samuel Feltman Ammunition Labs., for Army Ordnance Corps, July 1955. Report PB 111842,* 26 pages, 75 cents.

EVALUATION OF THIN IRON FILMS AS SENSITIVE CORROSION INDICATORS, D. Roller, Wright Air Development Center, June 1956. Report PB 121536,* 38 pages, $1.00.

DEVELOPMENT OF A CASE LINER FOR LONG-TERM OUTDOOR STORAGE, C. E. Hrubesky, R. A. Aubey, and A. Hyttinen, Forest Products Lab., U. S. Dept. of Agriculture, for U. S. Army Ordnance Corps, May 1955. Report PB 111916,* 33 pages, $1.00.

THE DEVELOPMENT OF A PROTECTIVE COATING RESISTANT TO NITRIC ACID AND HYDROCARBONS, D. F. Siddall, E. Hillier, R. Garling, and M. Gunther, the United States Stoneware Co., for Wright Air Development Center, June 1956. Report PB 121217S,* 116 pages, $3.00.

U. S. GOVERNMENT RESEARCH REPORTS; TECHNICAL REPORTS NEWSLETTER. To keep science and industry advised of new material released through OTS, the office issues news releases to the trade, business, and technical press, and publishes two monthly periodicals. *U. S. Government Research Reports*, a bibliography, describes 300 to 600 new reports in each issue. *Technical Reports Newsletter* reviews 15 to 20 of the most widely useable reports collected by OTS each month. These publications may be ordered from Superintendent of Documents, U. S. Government Printing Office, Washington 25, D. C., at $6.00 a year for the *USGRR* and $1.00 a year for *Technical Reports Newsletter*.

* Order from Office of Technical Services, U. S. Dept. of Commerce, Washington 25, D. C.

TABLES OF CHEMICAL KINETICS, HOMOGENEOUS REACTIONS, National Bureau of Standards Circular 510, Supplement 1, issued Nov. 14, 1956. 472 pages, $3.25. (Order from the Superintendent of Documents, U. S. Government Printing Office, Washington 25, D. C.)

UNIONIZATION AMONG AMERICAN ENGINEERS, 72-page report released by the National Industrial Conference Board, Inc., 460 Park Ave., New York, N. Y. This report gives details of a study of the extent and reasons for unionization among the nation's 500,000 engineers.

EMPLOYMENT SITUATIONS

Please address replies to box shown, c/o The Electrochemical Society, Inc., 216 W. 102nd St., New York 25, N. Y.

Positions Available

METALLURGIST. Company engaged in extractive and pyrometallurgy requires a man for production and development, preferably with experience in one or more of the following: smelting and refining, steelmaking, or electric furnace operation. Excellent opportunities for qualified man. All replies strictly confidential. Submit detailed resume, including educational and employment backgrounds, as well as salary requirements, to *Box A-269*.

ELECTRONIC SCIENTISTS, METALLURGISTS, PHYSICISTS, TECHNOLOGISTS, AND ENGINEERS (Aeronautical, Electrical, Electronic, Industrial, General, Mechanical, and Power Plant). The Naval Air Material Center, Philadelphia 12, Pa., has an urgent need for qualified engineering and scientific personnel to fill vacancies in the above positions. The Center is currently engaged in an extensive program of aeronautical research, development, experimentation, and test operations for the advancement of Naval aviation. Starting salaries range from $4480 to $7570 per annum. Application for Federal Employment, Standard Form 57, should be filed with the Industrial Relations Dept., Naval Air Material Center, Naval Base, Philadelphia 12, Pa. Applications may be obtained from the above address or information as to where they are available may be obtained from any first second or class post office.

Position Wanted

BATTERY ENGINEER, 37–17 years' experience in lead acid batteries. Capable of setting up and operating battery testing laboratory for production, research, and military test programs. Experienced in all types of Government and special purpose batteries, including aircraft. Knowledge of latest production methods of dry charging, formation, and oxide manufacture, mixing, and pasting. Complete resume will be supplied on request. *Reply to Box 360*.

ADVERTISERS' INDEX

Baker & Adamson Products, General Chemical Division, Allied Chemical & Dye Corporation 51C
Bell Telephone Laboratories, Inc. 82C–83C
Enthone, Incorporated ... Cover 4
Great Lakes Carbon Corporation ..... Cover 2
E. H. Sargent & Company 52C

JUNE 1957 DISCUSSION SECTION

A Discussion Section, covering papers published in the July–December 1956 JOURNALS, is scheduled for publication in the June 1957 issue. Any discussion which did not reach the Editor in time for inclusion in the December 1956 Discussion Section will be included in the June 1957 issue.